Tyrocidines, cyclic decapeptides produced by soil bacilli, as potent inhibitors of fungal pathogens

by

Anscha Mari Troskie

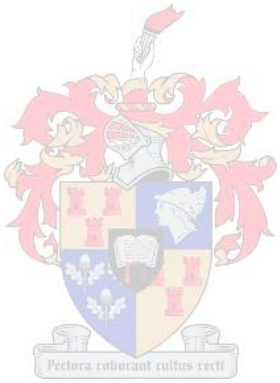

Dissertation approved for the degree

Doctor of Philosophy (Biochemistry)

in the

Faculty of Science

at the

University of Stellenbosch

Promoter: Prof. Marina Rautenbach

Department of Biochemistry

University of Stellenbosch

April 2014

Declaration

I, Anscha Mari Troskie, hereby declare that the entirety of the work contained in this thesis is my own original work and that I have not previously in its entirety or in part submitted it for obtaining any qualification at any university.

…… ……

Anscha Mari Troskie Date

Summary

The global rise in microbial resistance, ranging from the agricultural industry to the medical sector, has created the urgent need for novel or supplementary antibiotics. Antimicrobial peptides or "nature's antibiotics" may be the answer to this major problem. In this study a group of antimicrobial peptides, cyclic decapeptides named tyrocidines, produced by the soil bacterium *Bacillus aneurinolyticus*, was investigated for their antifungal activity, possible mode of antifungal action and potential applications.

The study illustrated that the tyrocidines have significant antifungal activity against a range of phytopathogens, including *Fusarium solani* and *Botrytis cinerea*, as well as the human pathogen *Candida albicans*. The activity of the tyrocidines is influenced by the identity of both the target organism and the media environment. Further evidence was obtained in support of the hypothesis that the tyrocidines are extremely sensitive to their environmental conditions and that they tend to self-assemble to form oligomers. The assessment of a small tyrocidine library and analogues, comprised of eight peptides, revealed no overt structure-activity relationships against fungal pathogens, except for the importance of a tyrosine residue. This indicated an important role for the conserved sequence of the tyrocidines, NQYVOLfP, together with the tendency of the tyrocidines to oligomerise into higher-order active structures in their antifungal activity.

The tyrocidines were found to be membrane active toward the fungal pathogens. However, supporting evidence was also obtained for additional mode(s) of antifungal action for the tyrocidines which *inter alia* induces morphological abnormalities in filamentous fungal target cells. Furthermore, the results also indicated that the membrane activity of the tyrocidines may be influenced by additional factors to that of the composition of the target cell membrane, for instance components of the fungal cell wall.

This investigation also indicated the significant potential of the tyrocidines to be developed for the commercial sector. The potent activity of the tyrocidines against agronomically important phytopathogens (significantly higher than the commercial fungicide bifonazole) together with their relative salt stability bodes well for their development as bio-fungicides for the agricultural sector. The tyrocidines also exhibited an overt sinergistic effect on the *in vitro* candidacidal activity of two key antifungal drugs, caspofungin and amphotericin B. Furthermore, tyrocidine A and caspofungin exhibited synergistic activity *in vivo* which had a significant positive effect on the survival of *C. albicans* infected *Caenorhabditis elegans*. Latter results highlighted their potential to serve as candidates for combinatorial treatment in the medical industry.

.

Opsomming

Die globale verskynsel van mikrobiese weerstand, wat strek vanaf die landbou sektor tot in die mediese bedryf, het ’n dringende behoefte vir die ontwikkeling van nuwe antmikrobiese middels geskep. Antimikrobiese peptiede of “die natuur se antibiotika”, kan moontlik die antwoord op hierdie ernstige problem wees. Tydens hierdie studie is ‘n groep sikliese antimikrobiese peptiede, naamlik die tirosidiene wat deur die grondbakterium *Bacillus aneurinolyticus* geproduseer word, vir hulle antifungiese aktiwiteit, hulle moontlike meganisme(s) van antifungiese werking en hulle potensiële aanwendings bestudeer.

Hierdie studie het getoon dat die tirosidiene uitsonderlike antifungiese aktiwiteit teen ‘n reeks fitopatogene, insluitend *Fusarium solani* en *Botrytis cinerea*, asook teen die mens patogeen *Candida albicans* het. Die aktiwiteit van die tirosidiene is deur beide die identiteit van die teikenorganisme sowel as die mediumomgewing beïnvloed. Daar is ook verdere bewyse verkry wat die hipotese dat tirosidiene uiters sensitief is tot hulle omgewing en dat hulle neig om te oligomeriseer, ondersteun. Die studie van die klein tirosidien-biblioteek, saamgestel uit agt tirosidiene en analoë, het geen ooglopende struktuur-aktiwiteit verwantskappe opgelewer nie, behalwe vir die oënskynlike invloed van die tirosien-residu. Laasgenoemde het die belangrikheid van die gekonserveerde aminosuurvolgorde van die tirosidiene, NQYVOLfP, asook die neiging van tirosidiene om hoë-orde aktiewe strukture te vorm deur self-verpakking, beklemtoon.

Tydens die studie is daar gevind dat die tirosidiene membraan-aktiewiteit toon teenoor fungiese patogene. Daar is egter ook goeie bewyse vir alternatiewe meganisme(s) van antifungiese werking, wat ondermeer tot morfologiese abnormaliteite in filamentagtige fungi-teikenselle lei, vir die tirosidiene verkry. Die resultate het verder ook daarop gewys dat die membraan-aktiwiteit

van die tirosidiene ook deur ander faktore, soos deur komponente van die fungiese selwand, en nie net deur die samestelling van die fungiese membraan beïnvloed word nie.

Hierdie ondersoek het ook die aansienlike potensiaal van die tirosidiene vir kommersiële ontwikkeling en gebruik uitgelig. Die merkwaardige aktiwiteit van die tirosidiene teen fitopatogene van agronomiese belang (wat selfs beter as diè van die kommersiële swamdoder bifonazole was) tesame met die relatiewe sout stabiliteit van die tirosidiene, is belowende tekens om die tirosidiene as bio-swamdoders vir die landbou sektor te ontwikkel. Die tirosidiene het ook ‘n uitgesproke sinergistiese effek op die *in vitro* candidasidiese aktiwiteit van twee sleutel antifungiese middels, caspofungin en amphotericin B, getoon. Verder is daar *in vivo* sinergistiese aktiwiteit gewys deur die kombinasie van tirosidien A en caspofungin wat ’n beduidende positiewe effek op die oorlewing van *C. albicans* geïnfekteerde *Caenorhabditis elegans* gehad het. Laasgenoemde dui op die potensiaal van die tirosidiene om in die mediese bedryf as kandidate vir kombinasie-behandeling te dien.

Acknowledgements

I would like to express my thanks and gratitude to the following persons/institutions:

- Prof. Marina Rautenbach, my MSc supervisor and PhD promoter, for her guidance, motivation and advise throughout this project and preparation of my PhD dissertation;
- Dr. Abré de Beer (BIOPEP laboratory, Department of Biochemistry, University of Stellenbosch) for his advice and guidance in the culturing of fungi and experimental development;
- Dr. Marietjie Stander (Central Analytical Facility, University of Stellenbosch), for the mass spectrometry;
- Dr. Ben Loos and Mrs. Lize Engelbrecht (Central Analytical Facility, University of Stellenbosch), for assistance with the fluorescence microscopy;
- Prof. Bruno Cammue, Dr. Karin Thevissen and Mr. Nicolas Delattin (Centre of Microbial and Plant Genetics, KU Leuven, Belgium), for welcoming me into their research group and providing guidance and support regarding *Candida albicans* and its biofilms;
- Dr. Margitta Dathe (Peptide-Lipid Interaction, FMP, Berlin, Germany), for receiving me into her research group and providing guidance and assistance with the model membrane studies;
- Mrs. Gertrude Gerstner (BIOPEP laboratory, Department of Biochemistry, University of Stellenbosch), for her assistance and support;
- Christiaan, for his love, understanding and absolute belief that I am capable of achieving my goals;
- My parents, for their love, support and belief in me over the past 26 years;
- The National Research Foundation (NRF) for personal funding.

Table of Contents

List of Abbreviations and Acronyms

AA	Ascorbic acid
ACN	Acetonitrile
AIDS	Acquired immunodeficiency syndrome
AmB	Amphotericin B
AMP(s)	Antimicrobial peptide(s)
A. fumigates	*Aspergillus fumigates*
Aspergillus spp.	*Aspergillus* species
ATCC	American type culture collection
B. aneurinolyticus	*Bacillus aneurinolyticus*
B. cinerea	*Botrytis cinerea*
BEC_{50}	Peptide concentration that results in 50% biofilm eradication
BIC	Peptide concentration that results in ≥90% biofilm prevention
BIC_{50}	Peptide concentration that results in 50% biofilm prevention
B. parabrevis	*Bacillus parabrevis*
B. subtilis	*Bacillus subtilis*
C. albicans	*Candida albicans*
CAS	Caspofungin
C. elegans	*Caenorhabditis elegans*
DmAMP1	*Dahlia merckii* antimicrobial peptide
DMSO	Dimethyl sulfoxide
DNA	Deoxyribonucleic acid
5-DOX	1-palmitoyl-2-stearyl(5-doxyl)-*sn*-glycero-3-phosphatidylcholine
12-DOX	1-palmitoyl-2-stearyl(12-doxyl)-*sn*-glycero-3-phosphatidylcholine
EC_{50}	Peptide concentration that induces 50% leakage
E. coli	*Escherichia coli*
EDTA	Ethylenediaminetetraacetic acid
EPM	Exopolymeric matrix
Erg	Ergosterol
ESMS	Electrospray mass spectrometry
f	D-phenylalanine

F	Phenylalanine
FICI	Fractional inhibition concentration index
F. oxysporum	*Fusarium oxysporum*
F. solani	*Fusarium solani*
F. verticilliodes	*Fusarium verticilliodes*
GlcCer	Glucosylceramide
GM	Genetically manipulated
GS	Gramicidin S
HC_{50}	Peptide concentration leading to 50 % haemolysis
HNP	Human neutrophil
HPLC	High performance liquid chromatography
HSA	Human serum albumin
HsAFP1	*Heuchera sanguine* antifungal peptide
IC_{50}	Peptide concentration leading to 50 % growth inhibition
IC_{max}	Peptide concentration leading to total growth inhibition, parameter derived from dose-response curve
ITS	Internal transcriber spacer
K	Lysine
L	Leucine
LB	Lysogeny broth
LL-37	Human cathelicidin
L. monocytogenes	*Listeria monocytogenes*
Lys	Lysine
LUV	Large unilamellar vesicle
[M]	Molecular ion
MC_{50}	Peptide concentration leading to 50 % nematode death
mCRAMP	Mouse cathelicidin
$M(IP)_2C$	Mannosyldiinositolphosphorylceramide
MOA	Mode of action
M_r	Relative molecular mass
MS	Mass spectrometry
m/z	Mass over charge ratio

N	Asparagine
NB	Nutrient broth
NaD1	*Nicotiana alata* defensin
NO	Nitric oxide
NP	Rabbit neutrophil
O	Ornithine
OD	Optical density
Orn	Ornithine
P	Proline
PBS	Phosphate buffered saline
PCR	Polymerase chain reaction
PDA	Potato dextrose agarose
PDB	Potato dextrose broth
Penicillium spp.	*Penicillium* species
P. digitatum	*Penicillium digitatum*
P. expansum	*Penicillium expansum*
P. falciparum	*Plasmodium falciparum*
P. glabrum	*Penicillium glabrum*
PhcA	Phenycidine A
Phe	Phenylalanine
PI	Propidium iodide
POPC	Palmitoyloleylphosphatidylcholine
*Pv*D1	*Phaseolus vulgaris* defensin
Q	Glutamine
ROS	Reactive oxygen species
*Ps*d1	*Pisum sativum* defensin
R_t	Retention time
RP-HPLC	Reverse phase high performance liquid chromatography
RPM	Revolutions per minute
RsAFP2	*Raphanus sativus* antifungal peptide
SEM	Standard error of the mean
SOFI	State of Food Insecurity in the World

TAP	Tracheal antimicrobial peptide
TEMPO	1,2-dioleoyl-*sn*-glycero-3-phosphotempocholine
TFA	Trifluoroacetic acid
T. mineoluteus	*Talaromyces mineoluteus*
TOF-ESMS	Time-of-flight electrospray mass spectrometry
TpcB	Tryptocidine B
$TpcC_1$	Tryptocidine C_1
TpcC	Tryptocidine C
Tr. atroviride	*Trichoderma atroviride*
T. ramulosus	*Talaromyces ramulosus*
$TrcA_1$	Tyrocidine A_1
TrcA	Tyrocidine A
$TrcB_1$	Tyrocidine B_1
TrcB	Tyrocidine B
$TrcC_1$	Tyrocidine C_1
TrcC	Tyrocidine C
Trc mixture	Tyrocidine mixture
Tris	Tris(hydroxymethyl)aminomethane
Trp	Tryptophan
TSB	Tryptone soy broth
Tyr	Tyrosine
UN	United Nations
UPLC	Ultra performance liquid chromatography
UV	Ultraviolet
V	Valine
w	D-tryptophan
W	Tryptophan
Y	Tyrosine
YPD	Yeast extract peptone dextrose
YTSA	Yeast supplemented tryptone soy agar
YTSB	Yeast supplemented tryptone soy broth

Preface

In recent years the steady increase in resistance against conventional chemical fungicides has led to significant problems in both the agricultural and medical sector creating an urgent need for the development of novel antifungal compounds. Antimicrobial peptides, with their wide range of activity and swift antimicrobial action, may potentially serve as alternative and/or supplementary antifungals. Tyrocidines, a group of cyclic decapeptides produced by *Bacillus aneurinolyticus*, have been illustrated to have significant antibacterial and antiplasmodium activity; however, information regarding their antifungal activity is limited. The tyrocidines may therefore be potential candidates to be developed as novel antifungals.

The objective of this study was to increase our knowledge regarding the antifungal activity of the tyrocidines and to investigate their possible mode(s) of antifungal action. Furthermore, the potential of the tyrocidines to be developed into commercial bio-fungicides in the agricultural sector, as well as antifungal agents for the treatment of *Candida albicans* infections in the medical industry was explored.

An overview regarding the problem of microbial resistance in both the agricultural and medical sector as well as a summary on antimicrobial peptides, their characteristics and antimicrobial activity and their potential to be the answer to the problem of microbial resistance is given in Chapter 1. In the five experimental chapters (Chapters 2-6) we address some of these themes/challenges and in Chapter 7 the outcomes of this project is discussed with recommendations for future studies.

The goal of this study was therefore to determine the antifungal activity of the tyrocidines, the structural and environmental modulators of tyrocidine antifungal activity and possible mode(s) of tyrocidine antifungal action. The aims to meet this goal were:

1. The purification and analysis of tyrocidines from the tyrothricin complex of *Bacillus aneurinolyticus* and the culture medium of *Brevibacillus parabrevis* ATCC 8185 (study presented in Chapter 2);
2. Development and optimisation of antifungal assays for optimum tyrocidine activity (study presented in Chapter 3);
3. Determine the antifungal activity of the tyrocidines against a range of phytopathogens and the influence of environmental composition on their antifungal activity (study presented in Chapter 4);
4. Investigate the possible mode(s) of antifungal action employed by the tyrocidines (study presented in Chapter 5); and
5. Investigate the activity of the tyrocidines against *Candida albicans* and its biofilms (Chapter 6).

The experimental chapters 2-6 in this thesis were, to some extent, written as independent units so as to facilitate future publication. Although this led to some repetition, every attempt was made to keep this to a minimum.

Outputs of PhD study

Peer reviewed articles

- Troskie AM, Vlok NM, Rautenbach M*, (2012). A novel 96-well gel-based assay for determining antifungal activity against filamentous fungi. *Journal of Microbiological Methods*, 91, 551–558

Patents

- Rautenbach M., Troskie A. M., De Beer A., Vosloo J. A. Antimicrobial peptide formulations for plants, PCT Patent, Submission number 52495, Application number PCT/IB 2013/051457, Filing date 22 February 2013

- Rautenbach M., Troskie A. M., De Beer A. (2012) Antifungal peptide formulations containing tyrocidines for plant pathogens, Preliminary patent 2012/01316

- De Beer A. Troskie A. M. Rautenbach M. (2012) Antimicrobial peptide formulations containing Gramicidin S for plant pathogens, Preliminary patent 2012/01317

Conferences/Oral presentations

- Troskie AM, De Beer A, Rautenbach M (2010) Exploring the potential of tyrocidines, cyclic antibiotic peptides from *Bacillus aneurinolyticus*, to act as bio-control agents against fungi, BIO-10/SASBMB conference, Bloemfontein, Free State, SA

- Troskie AM, Rautenbach M (2012) Exploring the potential of tyrocidines, cyclic antibiotic peptides from *Bacillus aneurinolyticus*, to act as bio-control agents against fungi, BIO-10/SASBMB conference, Bloemfontein, Free State, SA

- Troskie AM, Rautenbach M (2012) The antifungal activity of tyrocidines, cyclic decapeptideses produced by *Bacillus aneurinolyticus*, SAMP (International Symposium on Antimicrobial Peptides), Lille, France

- Troskie AM (2011, 2012) Antifungal activity of tyrocidine peptides from *Bacillus aneurinolyticus* Biochemistry Forum, University of Stellenbosch, Oral presentation

- Troskie AM (2014) Tyrocidines, cyclic decapeptides produced by soil bacilli, as potent inhibitors of fungal pathogens. PhD Defence, Biochemistry Forum, University of Stellenbosch, Oral presentation

Expected outputs

- Troskie AM, Rautenbach M, Delattin N, Vosloo JA, Cammue BPA*, Thevissen K (2014) Tyrocidines, cyclic cationic decapeptides inhibit *Candida albicans*, its biofilm formation and potentiate the biofilm eradication activity of amphotericin B and caspofungin. Submitted to *Antimicrobial Agents and Chemotherapy* AAC02381-14

- Troskie AM, De Beer A, Rautenbach M* (2014). Inhibition of agronomically relevant fungal phytopathogens by tyrocidines, cyclic antimicrobial peptides isolated from *Bacillus aneurinolyticus*. In preparation for submission to *BBA Biomembranes*.

- Troskie AM, Dathe M, De Beer A, Rautenbach M* (2014) Tyrocidines, cyclic decapeptides isolated from *Bacillus aneurinolyticus*: a comparative study regarding their antifungal activity and mode of antifungal action. In preparation for submission to *BBA Biomembranes*

Chapter 1

Literature Review: Antifungal Peptides

1.1 Introduction

In recent years a disturbing trend of fungal pathogen resistance against conventional antifungal compounds has been observed. This phenomenon has been reported for both the agricultural (1, 2) and medical (3-6) industries. The agricultural sector is afflicted by various fungal plant pathogens that infect a wide spectrum of crops which ultimately leads to significant losses in annual food yields. The medical industry is also plagued by mainly opportunistic fungal pathogens, which target immune-compromised individuals. The widespread use of broad spectrum antibiotics is the main culprit behind the rise in microbial resistance (1, 2, 7, 8). The development of novel antimicrobials, with novel modes of action, is therefore essential in both the agricultural and medical sector.

A natural, bio-degradable group of antibiotics is omnipresent in nature. These antibiotics comprise predominantly of antimicrobial peptides (AMPs) which are produced in almost every organism and tissue providing first line of defence against various infections and competing microorganisms such as bacteria, fungi, parasites and viruses (9-11). The structures of AMPs are just as diverse as their origins: AMPs can be divided into linear peptides which form amphipathic and hydrophobic helices, β-sheet peptides, peptides with a mixture of α-helices and β-sheets, modified peptides, cyclic peptides, lipopeptides and peptides rich in certain amino acids (12). Even though membrane interaction is integral to antimicrobial activity, additional/alternative modes of action for microbial inhibition have been illustrated (13). With the escalating problem of microorganisms exhibiting resistance against conventional antibiotics, there is increasing interest in the potential of antimicrobial peptides to serve as novel antibiotics (12). As a result of the wide range of inhibitory mechanisms exhibited by AMPs, they have less

likelihood of inducing *de novo* resistance in target microorganisms (9). Their selectivity, rapid action and low likelihood of inducing resistance make AMPs ideal candidates for novel/templates for novel antimicrobials (14).

Bacillus aneurinolyticus produces a complex of potent antibiotic peptides called the tyrothricin complex. Tyrothricin was one of the first clinically utilised antibiotic preparations (15). Tyrothricin can be separated into two fractions. The one fraction contains neutral, linear pentapeptides the gramicidins (unrelated to the cyclic gramicidin S). The other fraction contains the tyrocidines, basic cyclic decapeptides (16, 17). Since their discovery in 1939 (18) the tyrocidines have been shown to be active against various microorganisms including bacteria (17-19) and the parasite responsible for malaria, *Plasmodium falciparum* (20). Except for one study that has been conducted on the activity of tyrothricin (the tyrocidine-gramicidin metabolite complex of *B. aneurinolyticus*) against *Candida albicans* (21) and one report on the activity of tyrocidines against *Neurospora crassa* (22) the antifungal activity of tyrocidines has not yet been fully explored.

1.2 Fungal pathogens

1.2.1 Fungal pathogens of fruits in agriculture

According to the United Nations (UN) Populations Division we have a population of around 7.16 billion people. In the UN Food and Agriculture Organisation's State of Food Insecurity in the World (SOFI) report of 2013 it was revealed that the basic income of 0.84 billion people lie under the breadline which in essence means that approximately 12 % of the world population is starving. Furthermore, around a third of the annual global food production is wasted (SOFI 2013). Microorganisms, including fungal pathogens, are partly responsible for this wastage causing a loss of up to 16 % of the annual food production (23).

Furthermore, some fungal species secrete mycotoxins which can be toxic, as well as mutagenic with long term exposure, when ingested by humans and animals (24, 25). For example, the mycotoxin ochratoxin A is a nephrotoxin and possibly also a human carcinogen with neurotoxic and genotoxic properties (26).

Various plant species, including vegetables and fruits, are affected by the necrotrophic fungus *Botrytis cinerea* (27). Grapes, one of South Africa's most prized commodities, are a well-known target of *B. cinerea* (28, 29). Various factors make the control of *B. cinerea* a challenge. *B. cinerea* has a diverse host range, mechanisms of attack and it also has an astonishing capacity for survival (27). *Penicillium* spp. (30-32) and *Aspergillus* spp. (33) are further examples of post-harvest fungal infections that are a big problem in especially the grape and fruit industry (34). *Aspergillus* and *Penicillium* strains are believed to be the main culprits in the production of ochratoxin A in especially wine and red grape juice (26).

Fusarium species are predominantly soil fungi. They can survive in various climates ranging from tropical to arctic regions (35). Accordingly they infect a wide range of crops, in some instances opportunistic human pathogens have even been isolated (36), and resultantly lead to significant losses in yields and concurrent economic damages (37). Fungal spores can survive in contaminated soil for years infecting plants through their roots and vascular wounds (38). *Fusarium* species also secrete harmful mycotoxins (39, 40). These fusaric acids have numerous pharmacological implications in that they influence the functioning of both the brain and pineal neurotransmitters and metabolites (41).

Cylindrocarpon species are another group of economically significant fungal pathogens. They induce black foot disease in grape vines that lead to necrotic root lesions and necrosis of wood tissue. These pathogens are notably a problem in grapevine nurseries and young vineyards (42). Black foot disease is responsible for the reduction or loss in yield and the decline or death of young infected vines. Stunting phenotype and an incapability to carry fruit are symptoms of

older vines that have been infected with black foot disease. The incapability of infected vines to deliver yields leaves farmers with no choice but to replant the vines which entail further financial and production loss. However, the chance of the new vines also being infected is substantial as the major source of the problem is contaminated nurseries. Less than 50% of the cultivated plant material from nurseries leads to the production of healthy replantable vines (43).

Conventionally these pathogens are controlled with chemical fungicides. However, this widespread, prolonged and frequently excessive use of chemical fungicides often results in the target pathogens developing resistance against the chemicals (1, 2, 44). For example, *B. cinerea* that infects cyclamen developed resistance to benomyl, methyl-thiophanate and furidazol (45). A study on *B. cinerea* isolated from vegetable crops showed 61.8% frequency resistance against bezimidazole, 18% against dicarboximide, 49.1% against pyrimethanil and 57.4% against cyprodinil (46). Grape isolates of *B. cinerea* also show resistance to fenhexamid (47, 48), anilinopyrimidines (48, 49), fludioxonil (48), hydoxyanilides and phenylpyrrole derivates (49). Resistant strains of *Fusarium* against benomyl and thiophanate-methyl have been isolated (50). Fungicide resistance in *Penicillium* strains have also been observed. For instance *Penicillium digitatum*, cause of citrus green mould, resistant to imazalil, thiabendazole and sodium ortho-phenylphenate have been isolated (44).

Of even greater concern is the increasing evidence of the detrimental effect these chemicals have on the biosphere (2, 51). Furthermore, regulatory standards are progressively decreasing the acceptable amount for chemical residues in/on crops and their products. Additionally, importing markets and consumers are also increasingly demanding products with lower pesticide levels (2). Therefore there is a growing need for novel fungicides which will not only protect precious agricultural produce, but which will also have reduced risks of inducing target cell resistance and, most important of all, will not have harmful effects on the environment and consumers.

1.2.2 Human fungal pathogens

An alarming escalation in fungal infections has been observed in the past two decades. Not only was there a rise in the frequency of infections, but also in variety of fungal isolates from infections (3). Furthermore, the widespread use of broad spectrum antibiotics (52) together with the growth in immune compromised individuals such as AIDS and cancer patients and recipients of organ transplants or medical devices (3-5, 52-54) immune-suppression, chemotherapy and radiotherapy (3, 6) has *inter alia* led to growing resistance against conventional antifungal drugs (3-6). *Aspergillus* spp. (55, 56), such as *A. terreus*, *A. niger*, *A. flavus* (55) and *A. fumigates*,- the most commonly isolated specie from aspergilloses (55, 56), are frequently the culprits behind these infections. Invasive *Aspergillus* infections, which usually result from solid organ transplants, are quite serious and are associated with a 100% mortality rate (7, 57). *Candida* spp., of which *C. parapsilosis* accounts for 20-40% (of all *Candida* specie infections), *C. tropicalis* (10-30%), *C. krusei* (10-35%) and *C. glabrata* (5-40%) (58) and *C. albicans* (50%) (7, 55), in particular lead to serious infections and is recognised as one of the major causative agents of nosocomial infections (59, 60) and, with a mortality rate of approximately 40%, invasive *Candida* infections, such infections are a serious medical concern (7, 52, 61, 62). In recent years there has also been a rise in *Fusarium* spp. as new opportunistic human pathogens (63). After *Aspergillus* spp., *Fusraium* spp. are the most frequent filamentous pathogens in high risk patients. *Fusarium solani* is the most commonly isolated from infections contributing to almost 50% of *Fusarium* infections. Other opportunistic *Fusarium* species include *F. oxysporum*, *F. moniliforme* and *F. verticilloides* (64).

The focus of this study will be on *Candida albicans* and its biofilms as human pathogen. *C. albicans* is the most commonly isolated species from *Candida* infections and is able to efficiently infect various sites in humans, from cutaneous sites such as the skin to deep tissue and organs (52, 65). The ability of *C. albicans* to form biofilms on especially medical implants and

indwelling medical devices increases the seriousness/significance of their infections (52, 66) and is usually the culprit behind the instigation of candidiasis (59, 67, 68).

The ability of fungi and bacteria to form biofilms, a microbial community embedded in a polymeric matrix (6, 59, 60, 69), increases their resistance to antibacterial treatments (66). The exopolymeric matrix (EPM) that are secreted and formed by biofilms acts as a protective barrier against antifungal compounds, host immune factors (70), phagocytosis (71) and physical disruptions (52). The composition of the EPM depends on the species involved, but polysaccharides, chitins and proteins have been identified as general constituents of EPM's (52, 72, 73). Planktonic cells are therefore more vulnerable to antifungal action than their biofilm counterparts. Although the degree of resistance vary among clinical isolates, *Candida* biofilms can be 30 to 2000 times more resistant than planktonic cells against antifungal compounds such as fluconazole, ketoconazole and amphotericin B (52). The increased resistance of biofilms has been ascribed to various factors including decreased growth and/or altered metabolic activity of biofilm cells, physical barriers preventing the penetration of antifungal compounds and the existence of persisters (52, 74). These microbial communities can grow on various surfaces from biotic (mammalian tissues) to abiotic (synthetic polymers and indwelling medical devices) (75-77). A mature biofilm can serve as an inexhaustible source of detaching yeast cells that can cause fungemia and systemic infection in an individual (52). Biofilms result in significant hygiene problems in both the food industry and medical field (78).

Treatment of fungal infections is complicated since among the currently available antimycotics some are associated with harmful side-effects, can only be administered intravenously and/or pathogens have developed resistance against them (7, 54). Azole-derived antifungals are predominantly used in the treatment of aspergilloses (79, 80). However, the first resistant strain was isolated in 1999 and since then of resistance has increased drastically. In a study of itraconazole resistant *A. fumigates* strains cross-resistance to voriconazole and posaconazole was

observed (79). In addition to azoles being used for the treatment of chronic aspergilloses and over long periods, they are also used in agriculture. Azole-resistant *Aspergillus* strains have been isolated azole naïve patients, in azole exposed patients and in the environment (80). Azole resistance and cross-resistance is therefore a growing concern in the treatment of aspergilloses (79). Azole resistance in *C. albicans* is also a major concern. Fluconazole, with relatively low toxicity and with bio- availability greater than 90% after oral administration, has also been used extensively to treat a wide range of *Candida* infections. However, resistance or total failure of fluconazole treatment has been reported on several occasions (81). Mechanisms for fluconazole resistance include multidrug efflux pumps (82) and changes in phospholipids and the membrane sterol composition (83). *C. albicans* resistance to amphotericin B is acquired through mutations in ERG3, which lowers the concentration of ergosterol in the cell membrane. This mutation can also confer resistance to azoles and vice versa (83, 84). Thus far limited clinical resistance to the echinocandins has been reported. This may either be the result of limited use to date, or that resistance events are rare. However, the echinocandin-resistant *C. albicans* isolates that have been isolated have point mutations in their (1,3)-β-glucan synthase subunit Gsc1p (84).

The seriousness of fungal resistance is augmented by the fact that there is a limited variety of antifungal drugs classes available for treatment (84). Unfortunately numerous attempts to identify and develop novel antifungal compounds have been impeded by the fact that the majority of compounds that exhibit antifungal activity concurrently exhibit toxicity to mammalian cells (85). It has also been observed that under certain circumstances antifungal compounds and biofilm-specific antibodies act antagonistically (86).

It is therefore crucial that novel antifungal compounds with especially anti-biofilm action and low mammalian toxicity, be developed.

1.3 Antifungal peptides

Within the large family of AMPs, there are peptides with the ability for antifungal activity. Antifungal peptides come from various sources, including humans, insects and bacteria, and have diverse structural motifs (Table 1.1). This trend of diversity continues through to the antifungal peptides' mode of action. Their activity may either be membrane active, disrupting the outer membrane, or they may bind to a specific intracellular target (87).

1.3.1 Sources of antifungal peptides

As is the case with AMPs as a group, antifungal peptides can be found in diverse sources which include mammals, amphibians, insects, plants, bacteria and other fungi. The iturin and bacillomycin families, produced by the soil bacterium *Bacillus subtilis,* were among the earliest antifungal peptides to be discovered (87, 88). Gramicidin S, a cyclic decapepide produced by *Brevibacillus brevis* and polymyxin B, produced by *Bacillus polymyxa*, were illustrated to have significant activity against *B. cinerea* (89). Another *Bacillus* specie, *B. licheniformis*, produces the chitin binding peptide CB-1 which exhibits activity against *F. oxysporum* (90). Members of the *Pseudomonas syringae* pv. *syringae* also produces small cyclic lipodepsipeptides known as syringomycins (87, 91). Other antifungal peptides produced by bacteria include the powerful nikkomycins produced by *Streptomyces tendae*, which inhibit chitin biosynthesis (87, 92), the cepacidines, glycopeptides from *Burkholderia cepacia* (87, 93) and surfactin, also produced by *B. subtilis* (94).

Antifungal peptides produced by fungi are some of the most potent fungicides. Unfortunately these peptides are predominantly haemolytic (87). Selected peptides produced by fungi have been chemically modified to decrease their harmful side-effects (95). Work has been done on the echinocandins, peptides produced by *A. nidulans* and *A. rugulosus*, and pneumocandins, peptides from *Zalerion arboicola*, in order to decrease their haemolytic effect and increase their fungicidal properties (87).

Table 1.1 Examples of antifungal peptides from various sources, their structures and their antifungal activity.

Producer/Source	Peptides	Structure	Selected target organisms	Mode of action
Bacterial peptides				
Bacillus subtilis	Iturin A	lipopeptide	*Saccharomyces cerevisiae*	lytic
	Bacillomycin F	lipopeptide	*Aspergillus niger*	lytic
Pseudomonas syringae	Syringomycin E	lipodepsipeptide	*Aspergillus fumigatus*, *A. niger*, *Fusarium moniliforme*, *F. oxysporum*	lytic
	Syringostatin A	lipodepsipeptide	*Candida albicans*, *A. fumigatus*	lytic
	Syringotoxin B	lipodepsipeptide	*Candida albicans*, *A. fumigatus*	lytic
Burkholderia cepacia	Cepacidines	glycopeptides	*A. niger*, *F. oxysporum*	unknown
Streptomyces tendae	Nikkomycin X	peptidyl nucleoside	*Coccidiodes immitis*, *Blastomyces dermatitidis*	chitin synthesis
	Nikkomycin Z	peptidyl nucleoside	*Coccidiodes immitis*, *Blastomyces dermatitidis*	chitin synthesis
Bacillus brevis	Gramicidin S	cyclodecapeptide	*C. albicans*	lytic
Lactococcus lactis	Nisin	lantibiotic		
	Mersacidin			
Fungal peptides				
Aspergillus rugulosus	Echinocandin B	cyclic lipopeptide	*C. albicans*	glucan synthesis
Zalerion arboicola	Pneumocandins	lipopeptide	*Pneumocystis carnii*	glucan synthesis
Aspergillus aculeatus	Aculeacin	lipopeptide	*C. albicans*	glucan synthesis
Aspergillus syndowi var. *mulundensis*	Mulundocandins	lipopeptides	*A. niger*	glycan synthesis
Coleophoma empetri	WF11899 A, B and C	lipopeptides	*C. albicans*	glucan synthesis
Aureobasidium pullulans	Aureobasidin A	cyclic depsipeptide	*C. albicans*	actin assembly
Plant peptides				
Zea mays	Zeamatin		*C. albicans*	membrane permeabilisation
Nicotiana alata	NaD1		*F. oxysporum*	unknown
Dahlia merckii	DmAMP1		*S. cerevisiae*	membrane
Raphanus sativus	RsAFP2		*C. albicans*	apoptosis
Pisum sativum	*Ps*d1		*Neurospora crassa*	cyclin F
Phaseolus vulgaris	*Pv*D_1		*C. albicans, F. oxysporum*	membrane, apoptosis

Producer/Source	Peptides	Structure	Selected target organisms	Mode of action
Insect peptides				
Hyalopora cecropia	Cecropin A and B	linear peptides	*F. oxysporum, A. fumigatus*	lytic
Drosophila melanogaster	Drosomycin	44 amino acid cysteine rich peptide	*F. oxysporum*	lytic
Podisus maculiveris	Thanatin	21 amino acid cysteine rich peptide	*F. oxysporum, A. fumigatus*	unknown
Bee	Melittin	α-helix	*C. albicans*	permeabilisation
Amphibian peptides				
Phyllomedusa sauvagii	Dermaseptins	β-sheet	*F. oxysporum, A. fumigatus*	lytic
Xenopus laevis	Magainin 2	α-helical	*C. albicans*	lytic
	Buforin, buforin II			
Mammalian peptides				
Human neutrophils	HNP-1	30 amino acid cysteine rich peptide	*C. albicans*	lytic
	HNP-2	29 amino acid cysteine rich peptide	*C. albicans*	lytic
	HNP-3	30 amino acid cysteine rich peptide	*C. albicans, C. neoformans*	lytic
Rabbit neutrophils	Np-1	33 amino acid cysteine rich peptide	*A. fumigatus*	lytic
	NP-2	33 amino acid cysteine rich peptide	*A. fumigatus*	lytic
	NP-3a	24 amino acid cysteine rich peptide	*A. fumigatus*	lytic
Bovine epithelial cells	Tracheal antimicrobial peptide	38 amino acid cysteine rich peptide	*C. albicans*	lytic
Chicken leukocytes	Gallinacin-1, gallinacin-1α	39 amino acid lysine and arginine rich peptide	*C. albicans*	lytic
Human	LL-37 (hCAP18)	α-helix	*C. albicans*	lytic
Bovine	BMAP-28			
Human	hBD-1			
	Brevinin-1	α-helix	*Batrachochytrium dendrobatidis*	lytic

V-echinocandin (LY303366), with a substitution of its cyclic peptide ring, and caspofungin (MK-0991), with a long akyl N-acyl substitution, have both undergone successful clinical trials and were effective against esophageal candidiasis (87).

Plants are also rich sources of antifungal peptides that inhibit both plant and human fungal pathogens (96). RsAFP2 and HsAFP1, respectively isolated from *Raphanus sativus* and *Heuchera sanguinea*, are both peptides active against *C. albicans* (97, 98). *Dahlia merckii* produces the plant defensin DmAMP1 which inhibits *Saccharomyces cerevisiae* (96). A potent plant defensin from the ornamental tobacco *Nicotiana alata*, NaD1, inhibits 50% of *Fusarium oxysporum* and *F. graminearum* growth at a concentration of 2.5 μM (99).

The mammalian immune system also produces potent antifungal peptides. The α-defensins are produced by neutrophils and intestinal Paneth's cells. HNP-1 and HNP-2, produced by human neutrophils (100), and NP-1, NP-2 and NP-3, produced by rabbit neutrophils (101), are deadly to *C. albicans*. Epithelial cells are mainly responsible for the production of β-defensins. Tracheal antimicrobial peptide (TAP), a cysteine rich β-defensin, were active against *C. albicans* (MIC of 25 μg/mL) (87). The epithelial cells, together with neutrophils and macrophages, also produce the cathelicidin peptides (102). The human cathelicidin LL-37 and mouse cathelicidin mCRAMP exhibited activity against *C. albicans* (103).

Antifungal peptides have also been isolated from insects and amphibians. The giant silk moth, *Hyalopora cecropia*, produces linear lytic peptides the cecropins (104). These cecropins were able to kill 95% of *F. oxysporum* and *Aspergillus fumigates* at concentrations of respectively 12 and 9.5 μg/mL (87). Brevinin-1BYa, a peptide isolated from the skin of the yellow-legged frog *Rana boylii*, exhibited significant activity against *C. albicans* characterised by a MIC of 3 μM. Unfortunately this peptide is also quite haemolytic (HC_{50} = 4 μM) (105).

1.3.2 Antifungal peptide activity

Previously antifungal peptides were divided into two broudgroups based on their effect on fungal morphology. If the peptides induce changes in the morphology, e.g. induce hyperbranching, they were classified as morphogenic, while non-morphogenic peptides do not lead to any significant morphological changes in the fungi even though they inhibit fungal growth (106). Although this classification is very broad it is still useful to classify new peptide candidates into one of the broad catogories.

The inhibition of fungal growth can be achieved *via* various mechanisms of action. There are three targets for AMP interaction with the target organism, namely external cell wall components/structures, the cell membrane and intracellular targets (2). The major or common mode of action for antifungal peptides is believed to be the disruption of the fungal membrane integrity resulting in the leakage of ions and other molecules (87). Various models have been proposed for the disruption of membrane integrity: the barrel-stave model, the aggregate model, the carpet model and the toroidal pore model (9, 14). There are also peptides that target specific non-membrane targets. They may influence the synthesis of important cellular components, such as cell wall synthesis or chitin synthesis, they can interact with the nuclear components (87) or induce depolymerisation of the actin cytoskeleton (11) or interfere with cell division (9). Certain AMPs may also utilise various modes of action instead of just one, thereby decreasing the possibility of inducing microbial resistance against them (2).

Iturins, the small cyclic peptidolipids produced by *Bacillus subtilis*, affects membrane surface tension, which leads to pore formation with resultant ion leakage and cell death (107). Lipids that are predominantly found in eukaryotic membranes are phosphoglycerolipids, glycoglycerolipids, sphingolipids and sterols (108). A family of lipopeptides, the iturins produced by *B. subtilis*, form ionic pores in target cell membranes. These pores are believed to be the result of the formation of lipopeptide-sterol aggregates (109). The syringomycins, cyclic peptides produced by *P. syringe*,

interact with ergosterol in the membranes of yeast cells (87). An antifungal plant defensin from *Dahlia merckii*, DmAMP1, was shown to interact with the sphingolipid mannosyldiinositolphosphorylceramide ($M(IP)_2C$) from *S. cerevisiae* and subsequently permeabilise the membrane. Mutant *S. cerevisiae,* lacking the gene that encodes for $M(IP)_2C$, were resistant to DmAMP1. The presence of ergosterol together with $M(IP)_2C$ enhanced DmAMP1 activity (96). RsAFP2, a defensin produced by the radish plant (*Raphanus sativus*), targets fungal sphingolipid glucosylceramide (GlcCer) as part of their action against *Pichia pastoris* and *S. cerevisiae* (110). Subsequent to initial interaction with GlcCer, downstream signalling pathways leads to the induction of reactive oxygen species (ROS) and cellular apoptosis (97, 111). The defensin from *Nicotiana alata*, NaD1, appears to use a cell wall dependant mechanism to enter fungal cells. Van der Weerden *et al.* (99) observed that NaD1 lost antifungal activity against proteinase K treated hyphae, pointing to the possibility that a cell wall protein is the target for NaD1 (99).

Pisum sativum defensin 1 (*Ps*d1) is an example of an antifungal peptide with an intracellular target. *Ps*d1 interacts with cyclin F of *Neurospora crassa*, a protein involved in cell cycle control. *Ps*d1 induces endo-reduplication, i.e. the conidial DNA increases in the presence of the antifungal peptide but the entire process of cell division is not completed (112).

The activity of certain antifungal peptides have been linked to the formation of ROS (10). Certain antifungal compounds, such as the plant defensin RsAFP2, have been shown to inhibit *C. albicans* through the induction of endogenous ROS. In the presence of the antioxidant ascorbic acid, a significant loss in fungicidal activity could be observed linking the involvement of ROS induction to their activity against *C. albicans* (7, 97).

The induction of ROS triggers programmed cell death in yeast (113) and therefore the accumulation of endogenous ROS in yeast cells is a phenotypical marker of the initiation of the apoptotic process (113, 114) and has been linked to fungicidal activity in *C. albicans* (114). *Pv*D_1, a defensin from

Phaseolus vulgaris, permeabilises fungal membranes and causes apoptosis in *C. albicans* and *F. oxysporum*. Disorganisation in the cytoplasm and plasma membrane of *C. albicans* were observed following treatment with *Pv*D_1. It was further illustrated that *Pv*D_1 induces the formation of ROS in *C. albicans* and *F. oxysporum,* and nitric oxide (NO) in *C. albicans* (115). The peptide histatin-5 leads to mitochondrion depletion in *C. albicans* and concurrent induction of ROS (116).

The cyclic depsipeptide aureobasidin A, produced by *Aureobasidium pullulans*, disrupt actin assembly and resulted in chitin delocalisation and loss of membrane integrity in *S. cerevisiae*. Inhibition of normal cell budding was also observed as a result of aureobasidin A action (117).

The action of certain antifungal peptides, previously classified as morpogenic, can lead to hyperbranching of filamentous hyphae. This is probably due to interruption/interference with the fungal cell's ability to germinate and propagate the normal growth of hyphae since similar symptoms of hyperbranching has been observed for fungal mutants with alterations in their ability to establish and maintain polar growth (118). Not every aspect of spore germination, hyphal elongation and lateral branching is known and understood. However, a few factors/regulators have been identified as probably being involved in these processes. The establishment of a polar axis, essential for asymmetrical growth during germination (119), is believed to be regulated by Rho-type GTPases (119) and cAMP signalling (120, 121). Subsequent to establishing the polar cite, hyphal elongation is controlled by various factors such as GTPases (119, 122), formins and septins (120, 122), the Spitzenkorper, the microtubule cytoskeleton (122, 123) as well as actin polymerisation (123). Likewise the process of hyphal branching is not completely understood, but this process is also believed to be similarly complex. There are two proposed models for how a branching site is formed in hyphae. The first model is associated with septa where the septum possibly acts as an indicator of the region where branch formation should advance. In the second model, the "random pattern" model, there is evidence that GTPases (122), localised spikes in calcium (124, 125), ROS, as well as localised nuclear division, plays a role in temporal and spatial regulation of branch

formation (122). The cell cycle also seems to have a regulatory influence in some fungi on branching (122, 126).

Retarded germination and hyperbranching as a result of AMP activity can be the result of interference with any one of the above mentioned processes or their regulators. For example Thevissen *et al.* (127) hypothesised that RsAFP2-induced septin mislocalisation results in altered morphology and hyperbranching of the filamentous fungus *Fusarium culmorum* (127). The peptide PAF26's activity on *Penicillium digitatum* results in altered polar growth, hyperbranching and abnormal chitin deposition (118).

1.3.3 The tyrocidines and analogues as potential antifungal peptides

The tyrocidines and analogues, β-sheet cyclic decapeptides produced by *B. aneurinolyticus* as part of its secondary metabolite complex namely tyrothricin (tyrocidine-gramicidin complex) are the focus of this study. (16, 17). The primary structure of 28 natural tyrocidines has been determined by Tang *et al.* (16) (Table 1.2). The tyrocidines that principally compose the tyrocidine mixture, tyrocidine A_1, A, B_1, B, C_1 and C, are referred to as the major tyrocidines. The tyrocidine analogues are those peptides that are present in lower quantities when naturally produced by *B. aneurinolyticus* (16). Phenycidine A (PhcA) and tryptocidine C (TpcC) are the two analogues selected for this study. The tyrocidines and their analogues are highly conserved in their amino acid sequence. With the basic sequence of *cyclo*[$f^1P^2X^3x^4N^5Q^6Y^7V^8X^9L^{10}$] the major tyrocidines relevant to this study only vary in the amino acid residue positions $Trp^{3,4}$/$Phe^{3,4}$ or Lys^9/Orn^9 and the analogues in the amino acid residue position Tyr^7/Phe^7/Trp^7 (also refer to Figure 1.1). Tyrocidine A has been illustrated to have an antiparallel β-sheet structure (128). Gramicidin S (GS), with the sequence *cyclo*[VOLfPVOLfP], share 50 % sequence homology with some of the tyrocidines. Similar to the tyrocidines, GS is a β-sheet cyclic decapeptide which assumes similar backbone conformations/molecular topologies to the tyrocidines (129). GS has been illustrated to

have significant antifungal activity (130-132) and also to disrupt the integrity of membranes (130, 133-135). GS was therefore also included in this study for comparison purposes.

Subsequent to the discovery of the tyrocidine containing tyrothricin more than 70 years ago, Dubos and Hotchkiss (17) demonstrated that the tyrocidines possess noteworthy antibacterial activity. Since then the tyrocidines have been illustrated to exhibit activity against various other organisms.

Spathelf and Rautenbach (19) explored tyrocidines' potential to serve as therapeutic agents and bio-preservatives. The six major tyrocidines, tyrocidine A_1, A, B_1, B, C_1 and C exhibited inhibitory and membranolytic activity toward the Gram-positive bacteria, *Micrococcus luteus* and *Listeria monocytogenes*. This significant activity was not, however, observed for *Escherichia coli*, the Gram-negative representative.

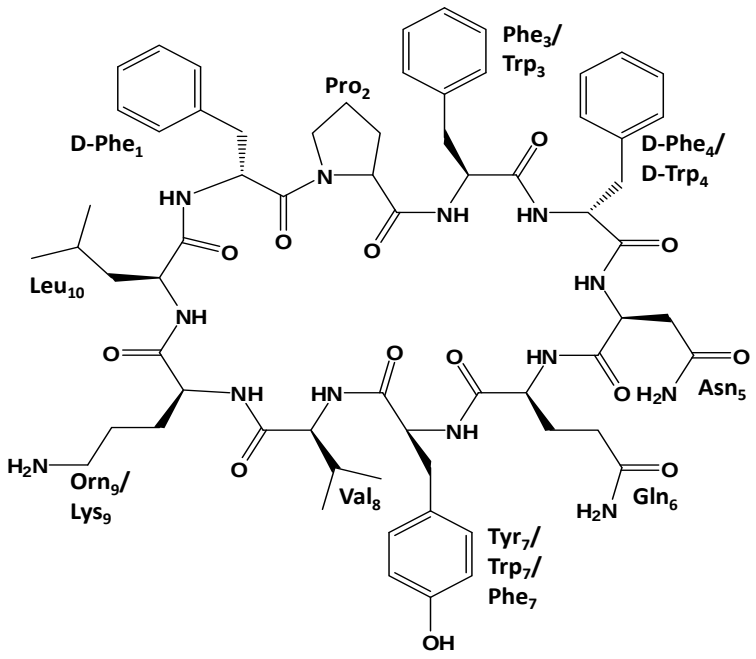

Figure 1.1: The primary structure of tyrocidine A (TrcA). The amino acid residues in variable positions 3, 4, 7 and 9 are indicated. Details on the primary structures of the different tyrocidines are given in Table 1.2.

Rautenbach *et al.* (20) established that the tyrocidines exhibit significant antimalarial activity. The six major tyrocidines also exhibited significant activity against *P. falciparum* with IC_{50}'s (peptide concentration resulting in 50% inhibition) < 500 nM. The concentrations where haemolysis was

observed were considerably higher and less variable than the IC_{50}'s. This high activity and selectivity of the tyrocidines make them potential templates for anti-malarial drug design (20).

Except for a study illustrating the ability of the tyrocidines to inhibit *Neurospora crassa* (22) and a study on the activity of tyrothricin (the tyrocidine-gramicidin complex produced by *B. aneurinolyticus*) against *C. albicans* (21), limited research has been conducted on the antifungal activity of the tyrocidines and their analogues.

Even though there is abundant evidence that the tyrocidines are membrane active (19, 136), there has also been results hinting/suggesting that the tyrocidines have additional/alternative mode(s) of action. Dubos (18) showed that even though the tyrocidines caused lysis of bacterial cells, this lysis was a secondary process as a result of a primary action, presumably inactivation of the glucose dehydrogenase system of the bacterial cell (18). Spathelf and Rautenbach (19) illustrated in 2009 that the antilisterial activity of the tyrocidines are, to a certain extent, as a result of a membranolytic mechanism of action. However, since the individual peptides had differing degrees of growth inhibition, even though their lytic rates were comparable, they proposed that there are additional factors(s) to membrane lysis that leads to cell death (19). This hypothesis is supported by the results of Spathelf (129) and Leussa (137) which indicates that the presence of Ca^{2+} promotes a non-lytic mode of antibacterial action in the tyrocidines. During their investigation of the tyrocidines' antimalarial activity, Rautenbach *et al.* (20) discovered, that despite their significant antimalarial activity, the tyrocidines did not induce noteworthy cell leakage. Nonetheless, prominent modifications/alterations of the parasite development could be observed after incubation with the tyrocidines. Definite conclusions on the mode of action employed by the tyrocidines against *P. falciparum* could not be made, but the investigators did suggest the disruption of the parasite cell-cycle development by the tyrocidines (20). Furthermore, the tyrocidines have also been shown to act as repressors of transcription through the interaction with the DNA of *B. brevis* (138-140) and to

inhibit β-galactosidase and acetylcholinesterase activity (141). Therefore the possibility exists that the tyrocidines may have additional/alternative mode(s) of action to that of membrane interaction.

Table 1.2: Structures and abundance of 28 tyrocidine and analogous peptides identified by Tang *et al*. (16).

Nr	Identity	Abbreviation	Sequence	M_r	Abundance
1	Tyrocidine D*	TrcD	VOLfPYwNQY	1324.7	2.1
2	Tyrocidine D_1*	$TrcD_1$	VKLfPYwNQY	1338.7	1.7
3	–	–	VOLyPWwNQY	1363.7	<1
4	Tyrocidine E'*	TrcE	VOLfPFyNQY	1285.7	<1
5	Tyrocidine E_1'*	$TrcE_1$	VKLfPFyNQY	1299.7	<1
6	Tyrocidine C	TrcC	VOLfPWwNQY	1347.7	100
7	Tyrocidine C_1	$TrcC_1$	VKLfPWwNQY	1361.7	30
8	Tryptocidine C	TpcC	VOLfPWwNQW	1370.7	23
9	Tryptocidine C_1*	$TpcC_1$	VKLfPWwNQW	1384.7	2.3
10	Tyrocidine B'*	TrcB'	VOLfPFwNQY	1308.7	14
11	Tyrocidine B_1'*	$TrcB_1$'	VKLfPFwNQY	1322.7	5.8
12	Tyrocidine B	TrcB	VOLfPWfNQY	1308.7	109
13	Tyrocidine B_1	$TrcB_1$	VKLfPWfNQY	1322.7	44
14	Tryptocidine B	TpcB	VOLfPWfNQW	1331.7	26
15	Tryptocidine B_1*	$TpcB_1$	VKLfPWfNQW	1345.7	13
16	Tyrocidine A	TrcA	VOLfPFfNQY	1269.7	88
17	Tyrocidine A_1	$TrcA_1$	VKLfPFfNQY	1283.7	39
18	Tryptocidine A	TpcA	VOLfPFfNQW	1292.7	15
19	Phenycidine A**	PhcA	VOLfPFfNQF	1253.7	3.1
20	Tyrocidine E*	TrcE	VOLfPYfNQY	1285.7	2.2
21	Tyrocidine E_1*	$TrcE_1$	VKLfPYfNQY	1299.7	1.1
22	–	–	VOLfPF(?)NQY	1336.7	4.5
23	–	–	VKLfPF(?)NQY	1350.7	9.4
24	Phenycidine B*	PhcB	VOLfPWfNQF	1292.7	3.7
25	–	–	(L/I)OLfPWfNQY	1322.7	1.9
26	–	–	(L/I)KLfPWfNQY	1336.7	2.6
27	–	–	VOLfP(L/I)fNQY	1325.7	1.2
28	–	–	VKLfP(L/I)fNQY	1249.7	<1

Conventional one letter abbreviations are used to depict peptide sequences [from Tang *et al.* (16)], except for ornithine that is represented by O. D-amino acid residues are indicated by lower case abbreviations.
The abundance of the tyrocidines is expressed relative to that of tyrocidine C.
Peptides marked with * were named by our group; ** renamed from tyrocidine E.

1.4 Factors influencing peptide activity

1.4.1 Target cell properties

As was mentioned in section 1.3.2, AMPs may have additional targets to that of membrane disruption or may even have multiple modes of action. However, these AMPs must still interact with the cell membrane and in some cases the cell wall, to gain access to the cell interior and to act on intracellular targets. AMPs have the ability, to some degree, to distinguish between different cells on the basis of differences in their cell membranes. For example, AMPs may be able to distinguish between differences in the membrane architecture and composition (142-146). Although all bio-membranes have the lipid bilayer as foundation, bio-membranes may differ extensively in their structure, composition and complexity. Different strains and growth conditions may also lead to diverse phospholipid compositions. Some of these membrane components may serve as targets for certain peptides (144-146) and can play part in microorganism specificity (144, 145, 147).

The interaction of cationic peptides with their target cells are influenced by *inter alia* the following characteristics:

- the lipid composition of, and the presence of sterols in, the target membrane (111, 148, 149);
- non-lipid components of target membrane, i.e. proteins (111);
- the metabolic state of the target cell (150), and
- the electrochemical potential of the membrane (151).

However, the complexity of the membrane makes the task of pinpointing peptide binding affinity to one component, and the effect on the membrane as a whole, a challenging task. Nevertheless, the importance of characteristic lipid composition of cell membranes for individual organisms are acknowledged (152). The preference some peptides have for certain membrane components could also influence their secondary structure (144-146).

Furthermore, the environment/culture conditions of the fungi may influence these target cell properties. The nutrient and oxygen availability can influence the metabolic state of the cell. The water potential and salt composition of their surroundings may influence the lipid composition of the fungal cell membrane and the electrochemical potential. Culture and assay conditions therefore influence the characteristics of the target cell and consequently peptide activity.

1.4.2 Environmental factors

AMP activity, selectivity and their modes of antimicrobial action are influenced by their environment (153-156). The presence of monovalent and divalent cations, proteases and polyvalent anions, such as glycosaminoglycans, influence peptide antimicrobial action (10). Cations, for example Na^{+}, Mg^{2+} and Ca^{2+}, decrease the activity of the majority of AMPs (100, 153, 157-163). Various reasons have been proposed for this phenomenon. The number of available active peptides may decrease as a result of peptide aggregation (160), or/and the electrostatic pull between negatively charged target membranes and cationic peptides can be hampered (158, 160). Another explanation for the decrease in AMP activity is that their mode(s) of action are dependant on cation concentrations or that the presence of cations interfere with their target interaction (164). For instance certain cell processes, such as hyphal elongation, are believed to be dependant on Ca^{2+} gradients and some AMPs are thought to interfere with this Ca^{2+} signalling as part of their antimicrobial action. Evidently the environment must be taken into account when determining the antimicrobial/antifungal action of a peptide.

Marques *et al.* (165) showed that the *in vitro* activity of TrcA, one of the cyclic antifungal peptides investigated in our studies, was decreased in the presence of calcium (165). However, our group observed that the critical concentration of 7.5 mM $CaCl_2$, increased the tyrocidines' activity against *L. monocytogenes*. The presence of Ca^{2+} not only increased the antilisterial activity of tyrocidines, but also changed the mode of action from lytic to an alternative non-lytic mode of action (129, 137).

It was proposed that in the presence of 7.5 mM $CaCl_2$ the tyrocidines form active/higher order structures which influences their degree of antilisterial activity as well as their mode of action (129).

1.5 Peptide application

1.5.1 Peptide application in the agricultural sector

Of late there has been a trend in agricultural research to use microorganisms as an eco-friendly method for controlling pathogens. Microorganisms that produce AMPs have been shown to successfully control plant diseases, for example *Bacillus subtilis* B-3 and *B. subtilis* RB14, that respectively produce iturin A and iturin A and surfactin, were successful in controlling *Monilinia fructicola* (166) and *Rhizoctonia solani* (167). *Bacillus cereus* UW85 cultures and culture extracts inhibits damping-off (caused by *Phytophthora medicaginis*) of alfalfa (168). *B. subtilis*, with trade name Kodiak (Gustafson Inc) is used, in combination with chemical fungicides, to control seedling and root diseases. Another biofungicide, MYCOSTOP®, was developed from the antibiotic producing *Streptomyces griseoviridis* for the protection of potatoes against scab (caused by *Streptomyces scabies*) (169). Products containing *Pseudomonas syringae* Van Hall that is active against *Botrytis*, *Penicillium*, *Mucor* and *Geotrichum* species; and *Candida oleophila* Montrocher, active against *Botrytis* and *Penicillium* spp., are also available (1). However, it is not always ideal to use live organisms. The growth conditions can be such that by the time the producer has reached the ideal growth condition for secreting AMPs, the pathogens could already have reached a growth state where they are strong enough to resist the AMPs and/or the pathogens have already caused a sufficient amount of harm to the crops. Furthermore, the inhibitory activity observed may not necessarily be the result of peptide production and release into the environment, but the result of other MOA including microbial competition (170, 171) and therefore not sufficiently reliable for consistent results. In addition, a live organism can change the character of the harvest and the products thereof (172). Another approach is to genetically modify plants to express antimicrobial peptides and thereby increasing their resistance against pathogens. However, consumers' resistance

to genetically manipulated (GM) products renders this strategy currently unfavourable. A solution to the problem is to utilise the naturally produced AMPs themselves. Cyclic peptides - primarily produced by ground dwelling bacteria - are, as a result of their stable nature, especially promising candidates. Even though they are bio-degradable, they have inherent resistance to degradation by proteases.

1.5.2 Peptide application in medicine

The pharmacologic application of AMPs has been hindered by various barriers. A large number of AMPs are unfortunately also toxic to human cells or they are haemolytic. Furthermore, as was discussed in section 1.4.2, AMP activity is influenced by their environment and therefore physiologic salt, pH and serum conditions may negatively influence their activity. The majority of peptides are also susceptible to proteolytic degradation *in vivo* (10, 14, 173). However, there is a large body of research being conducted on developing AMPs for medical/pharmaceutical applications with a number of peptides in advanced clinical trials and already approved for clinical use (Table 1.3).

One research approach is to modify the AMP structure in order to gain a molecule with more favourable properties. For example the lipopeptide echinocandin B produced by *A. nidulans* and *A. rugulosus* inhibits the synthesis of 1,3-β-glucan and has significant activity against *Candida* spp. (MIC of 0.20-0.35 μg/mL). Unfortunately echinocandin B is also quite haemolytic and could therefore not be developed as a clinical antifungal agent (174). Subsequent to modifications and numerous screenings, cilofungin (LY121019) was selected as an echinocandin analogue with significantly lower haemolysis activity, but retained activity against *Candida* spp. and *A. fumigates* (174, 175). Unfortunately, as a result of side effects, the clinical trials of cilofungin were discontinued (174, 176).

Table 1.3: Selected examples of antimicrobial peptides in development for clinical treatment

Company	Peptide	Source	Clinical trial stage	Application
AM-Pharma	hLF1-11 (based on Lactoferrin)	human	Phase IIa	Systemic; transplant infection
Migenix	Omiganan (MX-226/MBI-226) (based on indolicidin)	bovine	Phase III & II	Topical; prevention of catheter infections
Pacgen Biopharmaceuticals Corp.	PAC-113 (based on histatin)	human	Phase IIb	Oral; candidiasis, antifungal
Pfizer Pharmaceuticals	Anidulafungin (echinocandin B)	*Coleophoma empetri*	FDA and EMEA approved	Systemic; candidemia and candidiasis
Astellas Pharmaceuticals	Micafungin (FR901379)	*Aspergillus nidulans*	FDA and EMEA approved	Systemic; candidemia and candidiasis
Merck and Co	Caspofungin (pneumocandin B_0)	*Glarea lozoyensis*	FDA and EMEA approved	Systemic; candidemia and candidiasis
MacroChem	Pexiganan acetate (MSI-78) (based on magainin)	*Xenopus laevis*	Phase III	Topical; antibiotic
Zengen	CZEN-002 (based α-melanocyte-stimulating hormone)	human	Phase IIb	Topical; vulvovaginal candidiasis

An alternative tactic to increase the therapeutic applicability and systemic uptake of AMPs is to apply them in formulation or delivery substrate. AMPs in a lipid-based formulation have been shown to exhibit increased stability and solubility, increased plasma half-life and decreased toxicity. Furthermore the liposomal formulation allows for measured peptide release (173). Polymyxin E (177) and indolicidin (178) in a liposomal formulation exhibited significant reduced toxicity compared to unencapsulated peptides (177). Human serum albumin (HSA) has also been illustrated to be a successful carrier for AMPs, decreasing toxicity and increasing systemic distribution (173, 179).

Another approach is combinatorial treatment which is considered as a solution to the development of resistance against an individual compound. Other benefits from combinatorial treatment includes synergy, which not only makes lower drug dosage possible with concurrent decrease in toxicity, but also a wider range of activity and speedier antifungal effect (60).

Using the above mentioned research approaches there are a few success stories regarding AMP application in medicine. Micafungin (Mycamine, Astellas Pharmaceuticals), anidulafungin (Eraxis, Pfizer Pharmaceuticals) and caspofungin (Cancidas, Merck and Co.), semisynthetic cyclic lipopeptides based on echinocandins, have been clinically approved and are effective against *Candida* sp. and *Aspergillus* sp. infections (180).

1.6 References

1. **Spadaro D, Gullino ML.** 2004. State of the art and future prospects of the biological control of postharvest fruit diseases. Int. J.Food Micrbiol. **91:**185-194.

2. **Larrañaga P, Díaz-Dellavalle P, Cabrera A, Alem D, Leoni C, Almeida-Souza AL, Giovanni-De-Simone S, Dalla-Rizza M.** 2012. Activity of naturally derived antimicrobial peptides against filamentous fungi relevant for agriculture. Sustainable Agriculture Research. **1:**211-221.

3. **Letscher-Bru V, Herbrecht R.** 2003. Caspofungin: the first representative of a new antifungal class. J. Antimicrob. Chemother. **51:**513-521.

4. **Bink A, Vandenbosch D, Coenye T, Nelis H, Cammue BPA, Thevissen K.** 2011. Superoxide dismutases are involved in *Candida albicans* biofilm persistence against miconazole. Antimicrob. Agents Chemother. **55:**4033-4037.

5. **Tobudic S, Lassnigg A, Kratzer C, Graninger W, Presterl E.** 2010. Antifungal activity of amphotericin B, caspofungin and posaconazole on *Candida albicans* biofilms in intermediate and mature development phases. Mycoses. **53:**208-214.

6. **Ramage G, Mowat E, Jones B, Williams C, Lopez-Ribot J.** 2009. Our current understanding of fungal biofilms. Crit. Rev. Microbiol. **35:**340-355.

7. **François IE, Thevissen K, Pellens K, Meert EM, Heeres J, Freyne E, Coesemans E, Viellevoye M, Deroose F, Martinez Gonzalez S, Pastor J, Corens D, Meerpoel L, Borgers M, Ausma J, Dispersyn GD, Cammue BP.** 2009. Design and synthesis of a series of piperazine-1-carboxamidine derivatives with antifungal activity resulting from accumulation of endogenous reactive oxygen species. ChemMedChem. **4:**1714-1721.

8. **Ghannoum MA, Rice LB.** 1999. Antifungal agents: Mode of action, mechanisms of resistance, and correlation of these mechanisms with bacterial resistance. Clinical Microbiology Reviews. **12:**501–517.

9. **Yeung AY, Gellatly S, Hancock RW.** 2011. Multifunctional cationic host defence peptides and their clinical applications. Cellular and Molecular Life Sciences. **68:**2161-2176.

10. **Jenssen H, Hamill P, Hancock REW.** 2006. Peptide antimicrobial agents. Clinical Microbiology Reviews. **19:**491-511.

11. **Brandenburg L-O, Merres J, Albrecht L-J, Varoga D, Pufe T.** 2012. Antimicrobial peptides: multifunctional drugs for different applications. Polymers. **4:**539-560.

12. **Epand RM, Vogel HJ.** 1999. Diversity of antimicrobial peptides and their mechanisms of action. Biochimica et Biophysica Acta. **1462:**11-28.

13. **Wu M, Maier E, Benz R, Hancock REW.** 1999. Mechanism of interaction of different classes of cationic antimicrobial peptides with planar bilayers and with the cytoplasmic membrane of *Escherichia coli*. Biochemistry. **38:**7235-7242.

14. **Bradshaw JP.** 2003. Cationic antimicrobial peptides. Biodrugs. **17:**233-240.

15. **Van Epps HL.** 2006. René Dubos: unearthing antibiotics. J. Exp. Med. **203:**259.

16. **Tang X-J, Thibault P, Boyd RK.** 1992. Characterisation of the tyrocidine and gramicidin fractions of the tyrothricin complex from *Bacillus brevis* using liquid chromatography and mass spectrometry. Int. J. Mass Spectrom. Ion Processes. **122:**153-179.

17. **Hotchkiss RD, Dubos RJ.** 1941. The isolation of bactericidal substances from cultures of *Bacillus brevis*. J. Biol. Chem. **141:**155-162.

18. **Dubos RJ.** 1939. Studies on a bactericidal agent extracted from a soil *Bacillus*: I. Preparation of the agent. J. Exp. Med. **70:**1-10.

19. **Spathelf BM, Rautenbach M.** 2009. Anti-listerial activity and structure–activity relationships of the six major tyrocidines, cyclic decapeptides from *Bacillus aneurinolyticus*. Bioorg. Med. Chem. **17:**5541-5548.

20. **Rautenbach M, Vlok NM, Stander M, Hoppe HC.** 2007. Inhibition of malaria parasite blood stages by tyrocidines, membrane-active cyclic peptide antibiotics from *Bacillus brevis*. Biochim. Biophys. Acta. **1768:**1488-1497.

21. **Kretschmar M, Nichterlein T, Nebe CT, Hof H, Burger KJ.** 1996. Fungicidal effect of tyrothricin on *Candida albicans*. Mycoses. **39:**45-50.

22. **Mach B, Slayman CW.** 1966. Mode of action of tyrocidine on *Neurospora*. Biochim. Biophys. Acta. **124:**351-361.

23. **Chakraborty S, Newton AC.** 2011. Climate change, plant diseases and food security: an overview. Plant Pathol. **60:**2-14.

24. **Smith JE, Solomons G, Lewis C, Anderson JG.** 1995. Role of mycotoxins in human and animal nutrition and health. Nat. Toxins. **3:**187-192.

25. **Bennett JW, Klich M.** 2003. Mycotoxins. Clin. Microbiol. Rev. **16:**497-516.

26. **Battilani P, Pietri A.** 2002. Ochratoxin A in grapes and wine. European Journal of Plant Pathology. **108:**639-643.

27. **Williamson B, Tudzynski B, Tudzynski P, Van Kan JAL.** 2007. *Botrytis cinerea*: the cause of grey mould disease. Molecular Plant Pathology. **8:**561-580.

28. **Montero C, Cristescu SM, Jiménez JB, Orea JM, te Lintel Hekkert S, Harren FJM, González Ureña A.** 2003. Trans-resveratrol and grape disease resistance. A dynamical study by high-resolution laser-based techniques. Plant Physiology. **131:**129-138.

29. **Coertze S, Holz G.** 2002. Epidemiology of *Botrytis cinerea* on grape: wound infection by dry airborne conidia. South African Journal for Enology and Viticulture. **23:**72-77.

30. **Barkai-Golan R.** 1974. Species of *Penicillium* causing decay of stored fruits and vegetables in Israel. Mycopathologia et Mycologia Applicata. **54:**141-145.

31. **Macarisin D, Cohen L, Eick A, Rafael G, Belausov E, Wisniewski M, Droby S.** 2007. *Penicillium digitatum* suppresses production of hydrogen peroxide in host tissue during infection of citrus fruit. Phytopathology. **97:**1491-1500.

32. **Vilanova L, Viñas I, Torres R, Usall J, Jauset AM, Teixidó N.** 2012. Infection capacities in the orange-pathogen relationship: Compatible (*Penicillium digitatum*) and incompatible (*Penicillium expansum*) interactions. Food Microbiology. **29:**56-66.

33. **Kazi BA, Emmett RW, Nancarrow N, Partington DL.** 2008. Berry infection and the development of bunch rot in grapes caused by *Aspergillus carbonarius*. Plant Pathology. **57:**301-307.

34. **Lorenzini M, Azzolini M, Tosi E, Zapparoli G.** 2013. Postharvest grape infection of *Botrytis cinerea* and its interactions with other moulds under withering conditions to produce noble-rotten grapes. Journal of Applied Microbiology. **114:**762-770.

35. **Booth C.** 1971. The Genus Fusarium. Commonwealth Mycological institute, Kew, Surrey.

36. **Katiyar SK, Edlind TD.** 2009. Role for Fks1 in the intrinsic echinocandin resistance of *Fusarium solani* as evidenced by hybrid expression in *Saccharomyces cerevisiae*. Antimicrobial Agents and Chemotherapy. **53:**1772-1778.

37. **Correll JC.** 1991. The relationship between formae speciales, races and vegetative compatibility groups in *Fusarium oxysporum*. Phytopathology. **81:**1061-1067.

38. **Berrocal-Lobo M, Molina A.** 2008. Arabidopsis defense response against *Fusarium oxysporum*. Trends in Plant Science. **13:**145-150.

39. **Plattner RD.** 1999. HPLC/MS analysis of *Fusarium* mycotoxins, fumonisins and deoxynivalenol. Natural Toxins. **7:**365-370.

40. **Magan N, Aldred D.** 2007. Post-harvest control strategies: minimizing mycotoxins in the food chain. International Journal of Food Microbiology. **119:**131-139.

41. **Bacon CW, Porter JK, Norred WP, Leslie JF.** 1996. Production of fusaric acid by *Fusraium* species. Applied and Environmental Microbiology **62:**4039-4043.

42. **Alaniz S, León M, Vicent A, García-Jiménez J, Abad-Campos P, Armengol J.** 2007. Characterization of *Cylindrocarpon* species associated with black foot disease of grapevine in Spain. Plant Disease. **91:**1187-1193.

43. **Fourie PH, Halleen F.** 2004. Occurence of grapevine trunk disease pathogens in rootstock mother plants in South Africa. Australasian Plant Pathology. **33:**313-315.

44. **Kinay P, Mansour MF, Gabler FM, Margosan DA, Smilanick JL.** 2007. Characterization of fungicide-resistant isolates of *Penicillium digitatum* collected in California. Crop Protection. **26:**647-656.

45. **Bollen GJ, Scholten G.** 1971. Acquired resistance to benomyl and some other systemic fungicides in a strain of *Botrytis cinerea* in cyclamen. Netherlands Journal of Plant Pathology. **77:**83-90.

46. **Myresiotis CK, G. S. Karaoglanidis GS, Tzavella-Klonari K.** 2007. Resistance of Botrytis cinerea isolates from vegetable crops to anilinopyrimidine, phenylpyrrole, hydroxyanilide, benzimidazole, and dicarboximide fungicides. Plant Disease. **91:**407-413.

47. **Saito S, Cadle-Davidson L, Wilcox WF.** 2013. Selection, fitness, and control of grape isolates of Botrytis cinerea variably sensitive to fenhexamid. Plant Disease. **98:**233-240.

48. **De Miccolis Angelini RM, Rotolo C, Masiello M, Gerin D, Pollastro S, Faretra F.** 2014. Occurrence of fungicide resistance in populations of Botryotinia fuckeliana (Botrytis cinerea) on table grape and strawberry in southern Italy. Pest Management Science**:**n/a-n/a.

49. **Latorre BA, Torres R.** 2012. Prevalence of isolates of *Botrytis cinerea* resistant to multiple fungicides in Chilean vineyards. Crop Protection. **40:**49-52.

50. **Chung WH, Chung WC, Ting PF, Ru CC, Huang HC, Huang JW.** 2009. Nature of resistance to methyl benzimidazole carbamate fungicides in Fusarium oxysporum f.sp. lilii and F. oxysporum f.sp. gladioli in Taiwan. Journal of Phytopathology. **157:**742-747.

51. **Klich M, Arthur K, Lax A, Bland J.** 1994. Iturin A: A potential new fungicide for stored grains. Mycopathologia. **127:**123-127.

52. **Martinez L, Fries B.** 2010. Fungal biofilms: relevance in the setting of human disease. Current Fungal Infection Reports. **4:**266-275.

53. **Van Minnebruggen G, François IEJA, Cammue BPA, Thevissen K, Vroome V, Borgers M, Shroot B.** 2010. A general overview on past, present and future antimycotics. The Open Mycology Journal. **4:**22-32.

54. **White TC, Marr KA, Bowden RA.** 1998. Clinical, cellular, and molecular factors that contribute to antifungal drug resistance. Clinical Microbiology Reviews. **11:**382-402.

55. **Pappas PG, Alexander BD, Andes DR, Hadley S, Kauffman CA, Freifeld A, Anaissie EJ, Brumble LM, Herwaldt L, Ito J, Kontoyiannis DP, Lyon GM, Marr KA, Morrison VA, Park BJ, Patterson TF, Perl TM, Oster RA, Schuster MG, Walker R, Walsh TJ, Wannemuehler KA, Chiller TM.** 2010. Invasive fungal infections among organ transplant recipients: Results of the Transplant-Associated Infection Surveillance Network (TRANSNET). Clinical Infectious Diseases. **60:**1101-1111.

56. **Walsh TJ, Anaissie EJ, Denning DW, Herbrecht R, Kontoyiannis DP, Marr KA, Morrison VA, Segal BH, Steinbach WJ, Stevens DA, van Burik J-A, Wingard JR, Patterson TF.** 2008. Treatment of aspergillosis: Clinical practice guidelines of the Infectious Diseases Society of America. Clinical Infectious Diseases. **46:**327-360.

57. **Minari A, Husni R, Avery RK, Longworth DL, DeCamp M, Bertin M, Schilz R, Smedira N, Haug MT, Mehta A, Gordon SM.** 2002. The incidence of invasive

aspergillosis among solid organ transplant recipients and implications for prophylaxis in lung transplants. Transplant Infectious Disease. **4:**195-200.

58. **Krcmery V, Barnes AJ.** 2002. Non-albicans *Candida* spp. causing fungaemia: pathogenicity and antifungal resistance. The Journal of hospital infection. **50:**243-260.

59. **Ferreira JAG, Carr JH, Starling CEF, de Resende MA, Donlan RM.** 2009. Biofilm formation and effect of caspofungin on biofilm structure of *Candida* species bloodstream isolates. Antimicrob. Agents Chemother. **53:**4377-4384.

60. **Bink A, Pellens K, Cammue BPA, Thevissen K.** 2011. Anti-biofilm strategies: How to eradicate *Candida* biofilms? Open Mycol. J. **5:**29-38.

61. **Edmond MB, Wallace SE, McClish DK, Pfaller MA, Jones RN, Wenzel RP.** 1999. Nosocomial bloodstream infections in United States hospitals: a three-year analysis. Clinical Infectious Diseases. **29:**239-244.

62. **Ramage G, Martínez JP, López-Ribot JL.** 2006. *Candida* biofilms on implanted biomaterials: a clinically significant problem. FEMS Yeast Research. **6:**979-986.

63. **Boutati EI, Anaissie EJ.** 1997. Fusarium, a significant emerging pathogen in patients with hematologic malignancy: Ten years' experience at a cancer center and implications for management. Blood. **90:**999-1008.

64. **Roilides E, Dotis J, Katragkou A.** 2007. *Fusraium* and *Scedosporium*: Emerging fungal pathogens. *In* Kavanagh K (ed.), New insights in medical mycoclogy. Springer Netherlands, p. 267.

65. **Tournu H, Van Dijck P.** 2011. *Candida* biofilms and the host: Models and new concepts for eradication. International Journal of Microbiology. **2012**.

66. **Thevissen K, Pellens K, De Brucker K, François IEJA, Chow KK, Meert EMK, Meert W, Van Minnebruggen G, Borgers M, Vroome V, Levin J, De Vos D, Maes L, Cos P, Cammue BPA.** 2011. Novel fungicidal benzylsulfanyl-phenylguanidines. Bioorganic & Medicinal Chemistry Letters. **21:**3686-3692.

67. **Bachmann SP, VandeWalle K, Ramage G, Patterson TF, Wickes BL, Graybill JR, López-Ribot JL.** 2002. *In vitro* activity of caspofungin against *Candida albicans* biofilms. Antimicrob. Agents Chemother. **46:**3591-3596.

68. **Crump JA, Collignon PJ.** 2000. Intravascular catheter-associated infections. Eur. J. Clin. Microbiol. Infect. Dis. **19:**1-8.

69. **Chandra J, Kuhn DM, Mukherjee PK, Hoyer LL, McCormick T, Ghannoum MA.** 2001. Biofilm formation by the fungal pathogen *Candida albicans*: Development, architecture, and drug resistance. J. Bacteriol. **183:**5385-5394.

70. **Leid JG, Shirtliff ME, Costerton JW, Stoodley P.** 2002. Human leukocytes adhere to, penetrate, and respond to *Staphylococcus aureus* biofilms. Infection and Immunity. **70:**6339-6345.

71. **Leid JG, Willson CJ, Shirtliff ME, Hassett DJ, Parsek MR, Jeffers AK.** 2005. The exopolysaccharide alginate protects *Pseudomonas aeruginosa* biofilm bacteria from IFN-γ-mediated macrophage killing. The Journal of Immunology. **175:**7512-7518.

72. **Martinez LR, Casadevall A.** 2007. *Cryptococcus neoformans* biofilm formation depends on surface support and carbon source and reduces fungal cell susceptibility to heat, cold, and UV light. Applied and Environmental Microbiology. **73:**4592–4601.

73. **Al-Fattani MA, Douglas LJ.** 2006. Biofilm matrix of *Candida albicans* and *Candida tropicalis*: chemical composition and role in drug resistance. Journal of Medical Microbiology. **55:**999-1008.

74. **Hawser SP, Douglas LJ.** 1994. Biofilm formation by *Candida* species on the surface of catheter materials in vitro. Infection and Immunity. **62:**915-921.

75. **Dongari-Bagtzoglou A.** 2008. Pathogenesis of mucosal biofilm infections: challenges and progress. Expert Review of Anti-infective Therapy. **6:**201–208.

76. **Donlan RM.** 2002 Biofilms: microbial life on surfaces. Emerging Infectious Diseases. **8:**881–890.

77. **Davis LE, Cook G, Costerton JW.** 2002. Biofilm on ventriculo-peritoneal shunt tubing as a cause of treatment failure in *Coccidioidal meningitis*. Emerging Infectious Diseases. **8:**376-379.

78. **Meyer B.** 2003. Approaches to prevention, removal and killing of biofilms. International Biodeterioration & Biodegradation. **51:**249-253.

79. **Howard SJ, Cerar D, Anderson MJ, Albarrag A, Fisher MC, Pasqualotto A, Laverdiere M, Arendrup MC, Perlin DS, Denning DW.** 2009. Frequency and evolution of azole resistance in *Aspergillus fumigatus* associated with treatment failure. Emerging Infectious Diseases **15:**1068-1076.

80. **Howard SJ, Arendrup MC.** 2011. Acquired antifungal drug resistance in *Aspergillus fumigatus*: epidemiology and detection. Medical Mycology. **49:**S90-S95.

81. **Rex JH, Rinaldi MG, Pfaller MA.** 1995. Resistance of *Candida* species to fluconazole. Antimicrobial Agents and Chemotherapy. **39:**1-8.

82. **Ramage G, Bachmann S, Patterson TF, Wickes BL, López-Ribot JL.** 2002. Investigation of multidrug efflux pumps in relation to fluconazole resistance in *Candida albicans* biofilms. Journal of Antimicrobial Chemotherapy. **49:**973-980.

83. **Nolte FS, Parkinson T, Falconer DJ, Dix S, Williams J, Gilmore C, Geller R, Wingard J.** 1997. Isolation and characterization of fluconazole- and amphotericin B-resistant *Candida albicans* from blood of two patients with leukemia. Antimicrobial Agents and Chemotherapy. **44:**196-199.

84. **Cannon RD, Lamping E, Holmes AR, Niimi K, Tanabe K, Niimi M, Monk BC.** 2007. *Candida albicans* drug resistance – another way to cope with stress. Microbiology. **153:**3211-3217.

85. **Breger J, Fuchs BB, Aperis G, Moy TI, Ausubel FM, Mylonakis E.** 2007. Antifungal chemical compounds identified using a *C. elegans* pathogenicity assay. PLoS Pathog. **3:**e18.

86. **Martinez LR, Christaki E, Casadevall A.** 2006. Specific antibody to *Cryptococcus neoformans* glucurunoxylomannan antagonizes antifungal drug action against cryptococcal biofilms in vitro. Journal of Infectious Diseases. **194:**261-266.

87. **De Lucca AJ, Walsh TJ.** 1999. Antifungal peptides: Novel therapeutic compounds against emerging pathogens. Antimicrobial Agents and Chemotherapy. **43:**1-11.

88. **Moyne A-L, Shelby R, Cleveland TE, Tuzun S.** 2001. Bacillomycin D: an iturin with antifungal activity against *Aspergillus favus*. Journal of Applied Microbiology. **90:**622-629.

89. **Haggag WM.** 2008. Isolation of bioactive antibiotic peptides from *Bacillus brevis* and *Bacillus polymyxa* against *Botrytis* grey mould in strawberry. Archives Of Phytopathology And Plant Protection. **41:**477-491.

90. **Oita S, Horita M, Yanagi SO.** 1996. Purification and properties of a new chitin-binding antifungal CB-1 from *Bacillus licheniformis* M-4. Bioscience, Biotechnology, and Biochemistry. **60:**481–483.

91. **Segre A, Bachmann RC, Ballio A, Bossa F, Grgurina I, Iacobellis NS, Marino G, Pucci P, Simmaco M, Takemoto JY.** 1989. The structure of syringomycins A1, E, and G. . FEBS Letters. **255:**27-31.

92. **Li RK, Rinaldi MG.** 1999. In vitro antifungal activity of nikkomycin Z in combination with fluconazole or itraconazole. Antimicrobial Agents and Chemotherapy. **43:**1401-1405.

93. **Lee CH, Kim S, Hyun B, Suh JW, Yon C, Kim C, Lim Y, Kim C.** 1994 Cepacidine A, a novel antifungal antibiotic produced by *Pseudomonas cepacia*. I. Taxonomy, production, isolation and biological activity. The Journal of Antibiotics. **47:**1402-1405.

94. **Sandrin C, Peypoux F, Michel G.** 1990. Coproduction of surfactin and iturin A, lipopeptides with surfactant and antifungal properties, by *Bacillus subtilis*. Biotechnology and Applied Biochemistry. **12(4)::**370-375.

95. **Eschenauer G, DePestel DD, Carver PL.** 2007. Comparison of echinocandin antifungals. Therapeutics and Clinical Risk Management. **3:**71–97.

96. **Thevissen K, François IEJA, Takemoto JY, Ferket KKA, Meert EMK, Cammue BPA.** 2003. DmAMP1, an antifungal plant defensin from dahlia (*Dahlia merckii*), interacts with sphingolipids from *Saccharomyces cerevisiae*. FEMS Microbiology Letters. **226:**169-173.

97. **Aerts AM, François IEJA, Meert EMK, Li Q-t, Cammue BPA, Thevissen K.** 2007. The antifungal activity of RsAFP2, a plant defensin from *Raphanus sativus*, involves the induction of reactive oxygen species in *Candida albicans*. J. Mol. Microbiol. Biotechnol. **13:**243-247.

98. **Aerts AM, Bammens L, Govaert G, Carmona-Gutierrez D, Madeo F, Cammue BPA, Thevissen K.** 2011. The antifungal plant defensin HsAFP1 from *Heuchera sanguinea* induces apoptosis in *Candida albicans*. Frontiers in Microbiology. **2:**1-9.

99. **van der Weerden NL, Hancock REW, Anderson MA.** 2010. Permeabilization of fungal hyphae by the plant defensin NaD1 occurs through a cell wall-dependent process. Journal of Biological Chemistry. **285:**37513-37520.

100. **Lehrer R, Ganz T, Szklarek D, Selstedlt ME.** 1988. Modulation of the in vitro candidacidal activity of human neutrophil defensins by target cell metabolism and divalent cations. J. Clin. Invest. **81:**1829–1835.

101. **Selsted ME, Harwig SS, Ganz T, Schilling JW, Lehrer RI.** 1985. Primary structures of three human neutrophil defensins. The Journal of Clinical Investigation. **76:**1436-1439.

102. **Wang J, Wong ESW, Whitley JC, Li J, Stringer JM, Short KR, Renfree MB, Belov K, Cocks BG.** 2011. Ancient antimicrobial peptides kill antibiotic-resistant pathogens: Australian mammals provide new options. PLoS ONE **6:**e24030.

103. **López-García B, Lee PH, Yamasaki K, Gallo RL.** 2005. Anti-fungal activity of cathelicidins and their potential role in *Candida albicans* skin infection. The Journal of Investigative Dermatology. **125:**108-115.

104. **Christensen B, Fink J, Merrifield RB, Mauzerall D.** 1988. Channel-forming properties of cecropins and related model compounds incorporated into planar lipid membranes. Proceedings of the National Academy of Sciences USA. **85:**5072–5076.

105. **Conlon JM, Sonnevend A, Patel M, Davidson C, Nielsen PF, Pa T,´Rollins-Smith ILA.** 2003. Isolation of peptides of the brevinin-1 family with potent candidacidal activity from the skin secretions of the frog *Rana boylii*. The Journal of Peptide Research. **62:**207-213.

106. **Thevissen K, Ghazi A, De Samblanx GW, Brownlee C, Osborn RW, Broekaert WF.** 1996. Fungal membrane responses induced by plant defensins and thionins. J. Biol. Chem. **271:**15018-15025.

107. **Thimon L, Peypoux F, Maget-Dana R, Michel G.** 1992. Surface-active properties of antifungal lipopeptides produced by *Bacillus subtilis*. Journal of the American Oil Chemists' Society. **69:**92-93.

108. **Daum G, Lees ND, Bard M, Dickson R.** 1998. Biochemistry, cell biology and molecular biology of lipids of *Saccharomyces cerevisiae*. Yeast. **14:**1471-1510.

109. **Maget-Dana R, Peypoux F.** 1994. Iturins, a special class of pore-forming lipopeptides: biological and physicochemical properties. Toxicology. **87:**151-174.

110. **Thevissen K, Ferket KKA, François IEJA, Cammue BPA.** 2003. Interactions of antifungal plant defensins with fungal membrane components. Peptides. **24:**1705-1712.

111. **Wilmes M, Cammue BPA, Sahl H-G, Thevissen K.** 2011. Antibiotic activities of host defense peptides: more to it than lipid bilayer perturbation. Natural Product Reports. **28:**1350-1358.

112. **Lobo DS, Pereira IB, Fragel-Madeira L, Medeiros LN, Cabral LM, Faria J, Bellio M, Campos RC, Linden R, Kurtenbach E.** 2007. Antifungal *Pisum sativum* defensin 1 interacts with *Neurospora crassa* Cyclin F related to the cell cycle. Biochemistry. **46:**987-996.

113. **Madeo F, Carmona-Gutierrez D, Julia Ring J, Sabrina Büttner S, Tobias Eisenberg T, Guido Kroeme G.** 2009. Caspase-dependent and caspase-independent cell death pathways in yeast. Biochemical and Biophysical Research Communications. **382:**227–231.

114. **Bink A, Govaert G, François IEJA, Pellens K, Meerpoel L, Borgers M, Van Minnebruggen G, Vroome V, Cammue BPA, Thevissen K.** 2010. A fungicidal piperazine-1-carboxamidine induces mitochondrial fission-dependent apoptosis in yeast. FEMS Yeast Res. **10:**812-818.

115. **Mello E, Ribeiro SF, Carvalho A, Santos I, Cunha M, Santa-Catarina C, Gomes V.** 2011. Antifungal activity of PvD1 defensin involves plasma membrane permeabilization, inhibition of medium acidification, and induction of ROS in fungi cells. Current Microbiology. **62:**1209-1217.

116. **Helmerhorst EJ, Troxler RF, Oppenheim FG.** 2001. The human salivary peptide histatin 5 exerts its antifungal activity through the formation of reactive oxygen species. Proceedings of the National Academy of Sciences USA. **98:**14637–14642.

117. **Endo M, Takesako K, Kato I, Yamaguchi H.** 1997. Fungicidal action of aureobasidin A, a cyclic depsipeptide antifungal antibiotic, against *Saccharomyces cerevisiae*. Antimicrobial Agents and Chemotherapy. **41:**672–676.

118. **Muñoz A, López-García B, Marcos JF.** 2006. Studies on the mode of action of the antifungal hexapeptide PAF26. Antimicrobial Agents and Chemotherapy. **50:**3847-3855.

119. **Nesher I, Minz A, Kokkelink L, Tudzynski P, Sharon A.** 2011. Regulation of pathogenic spore germination by CgRac1 in the fungal plant pathogen *Colletotrichum gloeosporioides*. Eukaryotic Cell. **10:**1122-1130.

120. **Boyce KJ, Chang H, D'Souza CA, Kronstad JW.** 2005. An *Ustilago maydis* septin is required for filamentous growth in culture and for full symptom development on maize. Eukaryotic Cell. **4:**2044-2056.

121. **Fillinger S, Chaveroche M-K, Shimizu K, Keller N, D'Enfert C.** 2002. cAMP and Ras signalling independently control spore germination in the filamentous fungus *Aspergillus nidulans*. Molecular Microbiology. **44:**1001-1016.

122. **Harris SD.** 2008. Branching of fungal hyphae: regulation, mechanisms and comparison with other branching systems. Mycologia. **100:**823-832.

123. **Kaiserer L, Oberparleiter C, Weiler-Görz R, Burgstaller W, Leiter E, Marx F.** 2003. Characterization of the *Penicillium chrysogenum* antifungal protein PAF. Archives of Microbiology. **180:**204-210.

124. **Dicker JW, Turian G.** 1990. Calcium deficiencies and apical hyperbranching in wild-type and the "frost" and "spray" morphological mutants of *Neurospora crassa*. Journal of General Microbiology. **136:**1413-1420.

125. **Spelbrink RG, Dilmac N, Allen A, Smith TJ, Shah DM, Hockerman GH.** 2004. Differential antifungal and calcium channel-blocking activity among structurally related plant defensins. Plant Physiol. **135:**2055-2067.

126. **Binder U, Oberparleiter C, Meyer V, Marx F.** 2010. The antifungal protein PAF interferes with PKC/MPK and cAMP/PKA signalling of *Aspergillus nidulans*. Mol. Microbiol. **75:**294-307.

127. **Thevissen K, de Mello Tavares P, Xu D, Blankenship J, Vandenbosch D, Idkowiak-Baldys J, Govaert G, Bink A, Rozental S, de Groot PWJ, Davis TR, Kumamoto CA, Vargas G, Nimrichter L, Coenye T, Mitchell A, Roemer T, Hannun YA, Cammue BPA.** 2012. The plant defensin RsAFP2 induces cell wall stress, septin mislocalization and accumulation of ceramides in *Candida albicans*. Mol. Microbiol. **84:**166-180.

128. **Kuo M, Gibbons WA.** 1979. Total assignments, including four aromatic residues, and sequence confirmation of the decapeptide tyrocidine A using difference double resonance. Qualitative nuclear overhauser effect criteria for beta turn and antiparallel beta-pleated sheet conformations. J. Biol. Chem. **254:**6278-6287.

129. **Spathelf BM.** 2010. Qualitative structure-actvity relationships of the major tyrocidines, cyclic decapeptides from *Bacillus aneurinolyticus*. PhD Thesis, Department of Biochemistry, University of Stellenbosch, http://scholar.sun.ac.za/handle/10019.1/4001.

130. **Lee DL, Hodges RS.** 2003. Structure-activity relationships of de novo designed cyclic antimicrobial peptides based on gramicidin S. Peptide Science. **71:**28-48.

131. **Kondejewski LH, Farmer SW, Wishart DS, Kay CM, Hancock REW, Hodges RS.** 1996. Modulation of structure and antibacterial and hemolytic activity by ring size in cyclic gramicidin S analogs. Journal of Biological Chemistry. **271:**25261-25268.

132. **Murray T, Leighton FC, Seddon B.** 1986. Inhibition of fungal spore germination by gramicidin S and its potential use as a biocontrol against fungal plant pathogens. Letters in Applied Microbiology. **3:**5-7.

133. **Prenner EJ, Lewis RN, McElhaney RN.** 1999. The interaction of the antimicrobial peptide gramicidin S with lipid bilayer model and biological membranes. Biochimica et Biophysica Acta. **1462:**201-221.

134. **Prenner EJ, Lewis RNAH, Neuman KC, Gruner SM, Kondejewski LH, Hodges RS, McElhaney RN.** 1997. Nonlamellar phases induced by the interaction of gramicidin S with lipid bilayers. A possible relationship to membrane-disrupting activity. Biochemistry. **36:**7906-7916.

135. **Jelokhani-Niaraki M, Hodges RS, Meissner JE, Hassenstein UE, Wheaton L.** 2008. Interaction of gramicidin S and its aromatic amino-acid analog with phospholipid membranes. Biophysical Journal. **95:**3306-3321.

136. **Aranda FJ, de Kruijff B.** 1988. Interrelationships between tyrocidine and gramicidin A' in their interaction with phospholipids in model membranes. Biochim. Biophys. Acta. **937:**195-203.

137. **Leussa AN-N.** 2013. Characterisation of small cyclic peptides with antimalarial and antilisterial activity, Department of Biochemistry, University of Stellenbosch, PhD Thesis in progress, completion March 2014. Personal communication.

138. **Bohg A, Ristow H.** 1987. Tyrocidine-induced modulation of the DNA conformation in *Bacillus brevis*. European Journal of Biochemistry. **170:**253-258.

139. **Bohg A, Ristow H.** 1986. DNA-supercoiling is affected in vitro by the peptide antibiotics tyrocidine and gramicidin. European Journal of Biochemistry. **160:**587-591.

140. **Chakraborty T, Hansen J, Ristow H, Schazschneider B.** 1978. The DNA-tyrocidine complex and its dissociation in the presence of gramicidin D. European Journal of Biochemistry. **90:**261-270.

141. **Changeux J-P, Ryter A, Leuzinger W, Barrand P, Podleski T.** 1969. On the association of tyrocidine with acetylcholinesterase. Proceedings of the National Academy of Sciences USA. **62:**986–993.

142. **Yeaman MR, Yount NY.** 2003. Mechanisms of antimicrobial peptide action and resistance. Pharmacological Reviews. **55:**27-55.

143. **Dathe M, Schümann M, Wieprecht T, Winkler A, Beyermann M, Krause E, Matsuzaki K, Murase O, Bienert M.** 1996. Peptide helicity and membrane surface charge modulate the balance of electrostatic and hydrophobic interactions with lipid bilayers and biological membranes. Biochemistry. **35:**12612-12622.

144. **Matsuzaki K, Sugishita K-i, Harada M, Fujii N, Miyajima K.** 1997. Interactions of an antimicrobial peptide, magainin 2, with outer and inner membranes of Gram-negative bacteria. Biochimica et Biophysica Acta (BBA) - Biomembranes. **1327:**119-130.

145. **Sitaram N, Nagaraj R.** 1993. Interaction of the 47-residue antibacterial peptide seminalplasmin and its 13-residue fragment which has antibacterial and hemolytic activities with model membranes. Biochemistry. **32:**3124-3130.

146. **Choung S-Y, Kobayashi T, Takemoto K, Ishitsuka H, Inoue K.** 1988. Interaction of a cyclic peptide, Ro09-0198, with phosphatidylethanolamine in liposomal membranes. Biochimica et Biophysica Acta (BBA) - Biomembranes. **940:**180-187.

147. **Lohner K, Latal A, Lehrer RI, Ganz T.** 1997. Differential scanning microcalorimetry indicates that human defensin, HNP-2, interacts specifically with biomembrane mimetic systems. Biochemistry. **36:**1525-1531.

148. **Yount NY, Yeaman MR.** 2005. Immunocontinuum: Perspectives in antimicrobial peptide mechanisms of action and resistance. Protein and Peptide Letters. **12** 49-67.

149. **Jelokhani-Niaraki M, Prenner EJ, Kay CM, McElhaney RN, Hodges RS.** 2002. Conformation and interaction of the cyclic cationic antimicrobial peptides in lipid bilayers. The Journal of Peptide Research. **60:**23-36.

150. **Liang JF, Sun, Kim C.** 1999. Not only the nature of peptide but also the characteristics of cell membrane determine the antimicrobial mechanism of a peptide. The Journal of Peptide Research. **53:**518-522.

151. **Hancock REW, Lehrer R.** 1998. Cationic peptides: a new source of antibiotics. Trends in Biotechnology. **16:**82-88.

152. **Blondelle SE, Lohner K.** 2000. Combinatorial libraries: A tool to design antimicrobial and antifungal peptide analogues having lytic specificities for structure-activity relationships studies. Biopolymers. **55:**74-87.

153. **Hwang PM, Vogel HJ.** 1998. Structure-function relationships of antimicrobial peptides. Biochem. Cell Biol. **76:**235-246.

154. **Hof WVt, Veerman EC, Helmerhorst EJ, Amerongen AV.** 2001. Antimicrobial peptides: Properties and applicability. J. Biol. Chem. **382:**597-619.

155. **Zasloff M.** 2002. Antimicrobial peptides of multicellular organisms. Nature. **415:**389-395.

156. **Andreu D, Rivas L.** 1998. Animal antimicrobial peptides: An overview. J. Pept. Sci. **47:**415-433.

157. **Skerlavaj B, Romeo D, Gennaro R.** 1990. Rapid membrane permeabilization and inhibition of vital functions of Gram-negative bacteria by bactenecins. Infect. Immun. **58:**3724-3730.

158. **Montville TJ, Chen Y.** 1998. Mechanistic action of pediocin and nisin: recent progress and unresolved questions. Appl. Microbiol. Biotechnol. **50:**511-519.

159. **Bals R, Goldman MJ, Wilson JM.** 1998. Mouse β-Defensin 1 is a salt-sensitive antimicrobial peptide present in epithelia of the lung and urogenital tract. Infect. Immun. **66:**1225-1232.

160. **Cociancich S, Ghazi A, Hetru C, Hoffmann JA, Letellier L.** 1993. Insect defensin, an inducible antibacterial peptide, forms voltage-dependent channels in *Micrococcus luteus*. J. Biol. Chem. **268:**19239-19245.

161. **Yamauchi K, Tomita M, Giehl TJ, Ellison RT.** 1993. Antibacterial activity of lactoferrin and a pepsin-derived lactoferrin peptide fragment. Infection and Immunity. **61:**719-728.

162. **Broekaert WF, Terras FRG, Cammue BPA, Osborn RW.** 1995. Plant defensins: Novel antimicrobial peptides as components of the host defense system. Plant Physiol. **108:**1353-1358.

163. **Bowdish DME, Davidson DJ, Lau YE, Lee K, Scott MG, Hancock REW.** 2005. Impact of LL-37 on anti-infective immunity. Journal of Leukocyte Biology. **77:**451-459.

164. **Bowman SM, Free SJ.** 2006. The structure and synthesis of the fungal cell wall. BioEssays. **28:**799-808.

165. **Marques MA, Citron DM, Wang CC.** 2007. Development of tyrocidine A analogues with improved antibacterial activity. Bioorg. Med. Chem. **15:**6667-6677.

166. **Pusey PL.** 1989. Use of *Bacillus subtilis* and related organisms as biofungicides. Pesticide Science. **27:**133-140.

167. **Asaka O, Shoda M.** 1996. Biocontrol of *Rhizoctonia solani* damping-off of tomato with *Bacillus subtilis* RB14. Applied and Environmental Microbiology. **62:**4081-4085.

168. **Silo-Suh LA, Lethbridge BJ, Raffel SJ, He H, Clardy J, Handelsman J.** 1994. Biological activities of two fungistatic antibiotics produced by *Bacillus cereus* UW85. Applied and Environmental Microbiology. **60:**2023–2030.

169. **Sardi P, Saracchi M, Quaroni S, Petrolini B, Borgonovi GE, Merli S.** 1992. Isolation of endophytic *Streptomyces* strains from surface-sterilized roots. Applied and Environmental Microbiology. **58:**2691-2693.

170. **Papavizas GC, Lumsden RD.** 1980. Biological control of soilborne fungal propagules. Annual Review of Phytopathology. **18:**389-413.

171. **Ray RC, Swain MR.** 2013. Bio (bacterial) control of pre- andpostharvest disease of root and tuber crops. *In* Maheshwari DK (ed.), Bacteria in agrobiology: Disease management. Springer, p. 326-330.

172. **Sundaram S, Dwivedi P, Purwar S.** 2011. In vitro evaluation of antibacterial activities of crude extracts of *Withania somnifera* (Ashwagandha) to bacterial pathogens. Asian Journal of Biotechnology. **3:**194-199.

173. **Yount NY, Yeaman MR.** 2012. Emerging themes and therapeutic prospects for anti-infective peptides. Annual Review of Pharmacology and Toxicology. **52:**337-360.

174. **Matejuk A, Leng Q, Begum MD, Woodle MC, Scaria P, Chou S-T, Mixson AJ.** 2010. Peptide-based antifungal therapies against emerging infections. Drugs Future. **35:**197-231.

175. **Zambias RA, Hammond ML, Heck JV, Bartizal K, Trainor C, Abruzzo G, Schmatz DM, Nollstadt KM.** 1992. Preparation and structure-activity relationships of simplified analogues of the antifungal agent cilofungin: a total synthesis approach. Journal of Medicinal Chemistry. **35:**2843–2855.

176. **Gordee RS, Zeckner DJ, Howard LC, Alborn WEJ, Debono M.** 1988. Anti-Candida activity and toxicology of LY121019, a novel semisynthetic polypeptide antifungal antibiotic. Annals of the New York Academy of Sciences. **544:**294–309.

177. **Wang D, Kong L, Wang J, He X, Li X, Xiao Y.** 2009. Polymyxin E sulfate-loaded liposome for intravenous use: preparation, lyophilization, and toxicity assessment in vivo. PDA Journal of Pharmaceutical Science and Technology. **63:**159-167.

178. **Ahmad I, Perkins WR, Lupan DM, Selsted ME, Janoff AS.** 1995. Liposomal entrapment of the neutrophil-derived peptide indolicidin endows it with in vivo antifungal activity. Biochimica et Biophysica Acta. **1237:**109-114.

179. **Hussain R, Siligardi G.** 2010. Novel drug delivery system for lipophilic therapeutics of small molecule, peptide-based and protein drugs. Chirality. **22:**E44-E46.

180. **Smith L, Lu S-E.** 2010. Medical claims and current applications of the potent echinocandin antifungals. Recent Patents on Anti-Infective Drug Discovery. **5:**58-63.

Chapter 2

Purification and analysis of the six major tyrocidines and their analogues

2.1 Introduction

The steady increase in microbial resistance against conventional chemical fungicides has created an urgent need for the development of novel antifungal compounds. A group of antimicrobial peptides, the tyrocidines, have been illustrated to have significant antibacterial and antiplasmodium activity; however, information regarding their antifungal activity is limited. Therefore the aim of this study is to investigate the tyrocidines for potential antifungal activity and their potential to act as novel antifungal compounds.

The tyrocidines and analogues selected for this study are part of the secondary metabolite peptide complex, namely tyrothricin, produced by *Bacillus aneurinolyticus*. It must be noted that there is controversy surrounding the nomenclature of the tyrocidine producers. Upon their discovery the tyrocidine producers were originally referred to as the Dubos strain of *Bacillus brevis* (1). Afterwards it was illustrated that *B. aneurinolyticus* is a distinct group with comparable phenotype (2) and phylogenetics (3) to the *B. brevis* group. Since the taxonomical descriptions of *B. aneurinolyticus* relied on only few strains (4) the name was not included in the "Approved lists of bacterial names" (5). However, Shida *et al.* (6) have proposed a revival of the name *B. aneurinolyticus,* but later suggested that the *B. brevis* cluster of bacteria be referred to as *Brevibacillus* gen. nov. and that bacteria of the *B. aneurinolyticus* cluster be referred to as *Aneurinibacillus* gen. Nov (7). For simplicity the tyrothricin/tyrocidine producers will be referred to as *B. aneurinolyticus* during the rest of this study.

The tyrothricin complex, which is commercially available, consists of linear gramicidins and the cyclic tyrocidines. In order to purify the tyrocidines, they must be extracted from the tyrothricin complex and separated from each other, a challenging task as a result of their highly conserved sequences (8). Producer strains of *B. aneurinolyticus* (denoted by ATCC as *Brevibacillus parabrevis* 8185) can also be induced to produce tyrothricin (9).

Our group developed improved methods of culturing and supplementing the growth medium of *B. aneurinolyticus* to increase the peptide yield and also, depending on growth medium supplementation, to produce only selected tyrocidines of interest (10). These advanced methods greatly simplified the process of peptide purification.

In general compounds are separated from each other using their characteristic differences i.e. size, charge, physicochemical properties and hydrophobicity. An effective way of separating peptides from each other on the basis of their variances in hydrophobicity is through reverse-phase high-performance liquid chromatography (RP-HPLC). Even though RP-HPLC is one of the most efficient techniques for separating peptides, the similarity of some antimicrobial peptides in their amphipathicity and hydrophobicity may complicate their separation. Therefore all aspects of the RP-HPLC setup must be taken into account. With the characteristics of the peptides of interest in mind the matrix, column dimensions, eluant compositions, gradient profile and temperature must be fine-tuned in order to separate analogous peptides (11).

Subsequent to the production, extraction, separation and purification of the peptides, their identities and purities must be confirmed. Mass spectrometry is an effective analytical technique for determination of the identity, the elemental composition and purity of a sample based on molecular mass. Time-of-flight electrospray mass spectrometry (TOF-ESMS) is an extremely sensitive technique that has high accuracy in molecular mass determination by the generation and detection of multiply charged species. Ultra performance liquid chromatography (UPLC) is a powerful method with high resolution for separating most if not all the components in a sample.

UPLC-linked electrospray mass spectrometry (ESMS) provides a combination of these two powerful methods to determine the identity of a sample with high accuracy.

In order to evaluate the antifungal activity of the tyrocidines, to determine any structure-function relationships and to investigate possible modes of action, high purity peptide preparations are essential. An optimised high-performance liquid chromatography (HPLC) purification method, developed by our group (11, 12), was utilised to separate these highly analogue peptides. The purity of the obtained peptide fractions was subsequently determined with UPLC and ESMS.

2.1.1 Peptides of interest: Tyrocidines and analogues

The antimicrobial peptides relevant to this study are selected tyrocidines and two of their analogues. These cyclic decapeptides are produced by *Bacillus aneurinolyticus* as part of a complex of peptides, namely tyrothricin which can be separated into two fractions. The one fraction contains neutral, linear pentapeptides, namely the gramicidins. The other fraction contains the tyrocidines which are basic cyclic decapeptides (8, 13). Tang *et al.* identified and determined the structures of 28 natural tyrocidines (8). The major tyrocidines, tyrocidine A_1, A, B_1, B, C_1 and C, and the two analogues relevant to this study, phenycidine A (PhcA) and tryptocidine C (TpcC), are highly conserved in their amino acid sequence. With the basic sequence of *cyclo*[$f^1P^2X^3x^4N^5Q^6Y^7V^8X^9L^{10}$] the tyrocidines selected for this study only vary in the amino acid residue positions $Trp^{3,4}$/$Phe^{3,4}$, Lys^9/Orn^9 or Tyr^7/Phe^7/Trp^7 (Table 2.1). The physicochemical properties of the tyrocidine peptides are therefore very similar and consequently the separation of these peptides can be a challenging task.

Table 2.1: Summary of the peptides selected for this study

Identity	Abbreviation	Sequence[a]	Theoretical Monoisotopic M_r[b]
Major natural tyrocidines			
Tyrocidine C_1	$TrcC_1$	*Cyclo*-(VKLfPWwNQY)	1361.6921
Tyrocidine C	TrcC	*Cyclo*-(VOLfPWwNQY)	1347.6764
Tyrocidine B_1	$TrcB_1$	*Cyclo*-(VKLfPWfNQY)	1322.6812
Tyrocidine B	TrcB	*Cyclo*-(VOLfPWfNQY)	1308.6655
Tyrocidine A_1	$TrcA_1$	*Cyclo*-(VKLfPFfNQY)	1283.6703
Tyrocidine A	TrcA	*Cyclo*-(VOLfPFfNQY)	1269.6546
Natural tyrocidine analogues			
Tryptocidine C	TpcC	*Cyclo*-(VOLfPWwNQW)	1370.6924
Phenycidine A	PhcA	*Cyclo*-(VOLfPFfNQF)	1253.6597
Gramicidin S	GS	*Cyclo*-(VOLfPVOLfP)	1140.7059

[a]Conventional one-letter abbreviations are used for amino acid sequences [from Tang *et al.* (8)], except that O was used for Orn. Lower case one-letter abbreviations indicate D-amino acid residues. Identities were confirmed by our group (11, 12, 14).
[b]The theoretical monoisotopic Mr were calculated as the sum of the molecular weights of the constituent amino acids of the peptide.

2.2 Materials

Tyrothricin, gramicidin S (97.5 % purity according to manufacturers, 94% purity according to UPLC-MS, Table 2.5) the amino acids, Tyr, Phe and Trp, and trifluoroacetic acid (TFA, >98%) were supplied by Sigma (St Louis, USA). *Brevibacillus parabrevis* 8185 (referred to as *Bacillus aneurinolyticus* ATCC 8185 in this study) cultures were supplied by the American Type Culture Collection (Manassas, VA, USA). Lys was supplied by Merck (Darmstadt, Germany). The nutrient broth powder and tryptone were supplied by Oxoid (Basingstole, England) and the urea by ICN Biomedicals (Ohio, USA). For the TGYM medium Biolab (Wadeville, South Africa) supplied the peptone powder, agar powder and yeast extract. The glucose and skimmed milk powder were respectively supplied by Associated Chemical Enterprises (Glenvista, South Africa) and Clover (Roodepoort, South Africa). Merck Chemicals (Wadeville, South Africa) supplied the diethyl ether, acetone and sodium chloride. Acetonitrile (ACN) (HPLC-grade, far

UV cut-off) and methanol were obtained from Romil (Cambridge, England). The Nova-Pak® C18 (6 µm particle size, 60 Å pore size, 7.8mm × 300mm) semi-preparative and Nova-Pak® C18 (5 µm particle size, 60 Å pore size, 150mm × 3.9mm) analytical HPLC columns were supplied by Millipore (Milford, USA). Biotage (Uppsala, Sweden) provided the Isolute-XL C_8 column. Analytical grade water was prepared by filtering water from a reverse osmosis plant through a Millipore Milli-Q® water purification system (Milford, USA).

2.3 Methods

2.3.1 Purification of the tyrocidines from commercial tyrothricin

The mixture of tyrocidine peptides were isolated from a commercial tyrothricin complex using an adapted organic extraction method (13). The dry tyrothricin powder (520 mg) was washed three times with ether:acetone (1:1, *v/v*). The pellet, which was collected *via* centrifugation (5 minutes at 1.3 ×*g*) and dried under vacuum, contained a mixture of tyrocidines and their analogues (referred to as Trc mixture). In order to determine the purity of the Trc mixture – in terms of its tyrocidine content – the sample was analysed using semi-preparative RP-HPLC and UPLC linked to ESMS. With the aim of separating the individual tyrocidines from each other, the crude Trc mixture was dissolved in methanol:water (1:1, *v/v*) (10 mg/mL) and separated by semi-preparative RP-HPLC, using a Nova-Pak® C_{18} (6 µm particle size, 60 Å pore size, 7.8 mm × 300 mm) semi-preparative HPLC column. Two Waters 510 pumps, controlled by MAXIMA software, comprised the chromatographic system and the injections were controlled manually. Results were monitored with a Waters 440 detector at 254 nm. An eluant A (0.1% TFA in water, *v/v*) and eluant B (10% A in 90% acetonitrile, *v/v*) were used to create a gradient of decreasing polarity at 35˚C (Table 2.2) (12, 15). For the semi-preparative RP-HPLC the flow rate was 3 mL/min and the injection volume was 100 µL of 10 mg/mL crude tyrocidine mixture in methanol:water (1:1, *v/v*). Certain fractions required further purification on a reverse-phase analytical C_{18} Nova-Pak® column (5 µm particle size, 60 Å pore size, 150 mm × 3.9 mm). The

chromatographic system comprised of two Waters 510 pumps, a Waters 717 Plus Autosampler and a Waters 440 detector (set at 254 nm). The whole system was controlled by Millennium[32] software. Although the same solvent gradient (Table 2.2) and temperature was applied, the flow rate had to be decreased to 1 mL/min. The sample volume and concentration per run was also decreased to respectively 50 µL and 1 mg/mL in methanol:water (1:1, *v*/*v*).

Table 2.2: HPLC gradient program used for peptide purification and analysis

Time (min)	% Eluant A[a]	% Eluant B[b]	Curve type
0.0	50	50	
0.5/1.0[c]	50	50	6 (linear)
23.0	20	80	5 (curve)
24.0	0	100	6 (linear)
26.0	0	100	6 (linear)
28.0	–	–	–
30.0	50	50	6 (linear)
35.0	50	50	6 (linear)

[a]Eluant A was 0.1% TFA in water
[b]Eluant B was 10% A in acetonitrile
[c]0.5 min for semi-preparative RP-HPLC, 1.0 min for analytical RP-HPLC

2.3.2 Production of peptides through Brevibacillus aneurinolyticus *8185*

For the production and isolation of tyrocidines and their analogues from *B. aneurinolyticus* 8185 culture medium, *B. aneurinolyticus* 8185 was pre-cultured from lyophylised stocks in TGYM (0.5% tryptone, 0.1% glucose, 0.3% yeast extract, 0.05% methionine, pH 7.0), shaking at 220 rpm at 37˚C. After 24 hours this pre-culture medium was added to nutrient broth (NB, 0.1% meat extract, 0.2% yeast extract, 0.5% peptone, 0.8% sodium chloride) supplemented with urea and the relevant amino acids (Table 2.3) (10). Subsequent to a second incubation step of 36 hours shaking at a slant (220 RPM) at 37˚C, the medium was acidified to a pH of 4.7 and left for 24 hours at 37˚C. In order to isolate the tyrocidines, the media was centrifuged (2200×*g* at 4˚C), the precipitate washed three times with methanol and lastly dried with nitrogen gas. The crude samples were dissolved in 50% ACN to a concentration of 5 mg/mL and then eluted on an Isolute-XL C_8 column (500mg/10mL) (Biotage, Sweden) equilibrated in 50% ACN. After sample addition, the C_8 column was washed two times with 50% ACN to remove contaminants.

Thereafter eluant B (Table 2.2) was used to elute the peptides from the column. The peptides were then purified following the same protocol as for the commercial tyrocidines. Semi-preparative RP-HPLC on a Nova-Pak® C_{18} (6µm particle size, 60 Å pore size, 7.8 mm × 300 mm) semi-preparative HPLC column was performed with an identical solvent gradient program (Table 2.2). The injection volume and concentration of 100 µL of a 10 mg/mL solution (methanol:water, 1:1,*v/v*) also remained constant.

Table 2.3: Urea and amino acid supplementation of growth medium

Peptide of interest	Supplement				
	% Urea	% Lys	% Phe	% Tyr	% Trp
TrcA+PhcA	0.1	0.5	0.5		
	0.1		0.5		
TrcA	0.1		0.5	0.5	
TpcC	0.1				0.3

The nutrient broth for *Brevibacillus aneurinolyticus* 8185 was supplemented with urea and different amino acids so as to obtain the peptides of interest (10).

2.3.3 Analysis of the purified tyrocidines

With the purpose of confirming the identity and determining the purity of the peptide fractions, each fraction was analysed using UPLC and TOF-ESMS. Direct injection TOF-ESMS analyses were performed on a Waters Q-TOF Ultima mass spectrometer fitted with an electrospray ionisation source. The peptide samples (3 µL of 200 µg/mL in acetonitrile/water, 1:1, *v*/*v*) were injected into the ESMS and subjected to a capillary voltage of 3.0 kV. The source voltage was 15 V and the temperature 120˚C. Data was collected in the positive mode by scanning over an *m/z* range of 300-2000. For UPLC 3 µL peptide sample in water was chromatographed on an Acquity UPLC® BEH C_{18} column at a flow rate of 0.450 mL/min, using a 0.5 %[1] formic acid (A) to acetonitrile (B) gradient (100% A from 0 to 0.5 minutes, 0 to 58% B from 0.5 to 12 minutes and then 58 to 90% B from 12 to 13 minutes). In-line ESMS analysis of the analytes separated *via* UPLC was done with same settings as for the direct injection of peptide samples.

[1] 1.0% Formic acid for UPLC of $TrcB_1$ sample.

2.4 Results and Discussion

2.4.1 Tyrocidines purified from commercial tyrothricin

Tyrocidines C_1, C, B_1, B and A_1 were purified from the commercial tyrothricin complex. A yield of 67.3% (350 mg) was obtained for the crude mixture of tyrocidine peptides through organic extraction from the tyrothricin complex. This is consistent with the 40:60 ratio of gramicidin to tyrocidine found in literature for the tyrothricin complex (13). ESMS-linked UPLC analysis of the organically extracted Trc mixture indicated the presence of the six major tyrocidines and their tryptocidine analogues (Figures 2.1 and 2.2).

From Figure 2.2 A it is evident that the tyrocidines tend to oligomerise. The monomers, dimers, trimers and tetramers of the tyrocidines and their tryptocidine analogues can be observed. In the transformed mass spectrum of the monomeric peptides in the Trc mixture (Figure 2.2 B) the six major tyrocidines, TrcA (1269.6334), $TrcA_1$ (1283.6462), TrcB (1308.6412), $TrcB_1$ (1322.6578), TrcC (1347.6520) and $TrcC_1$ (1361.6631), as well as their tryptocidine analogues, TpcB (1331.6530), TpcC (1370.6663) and $TpcC_1$ (1384.6754), can be observed.

The purity of the Trc mixture, in terms of its tyrocidine content in mass, was analysed with semi-preparative RP-HPLC (Figure 2.3). The tyrocidine containing fraction (fraction B) and the fractions eluting before and after the tyrocidines (respectively fraction A and C) were collected and weighed analytically. Fraction B, the tyrocidine containing fraction, weighed 2.38 mg of the total 2.5 mg injected (Figure 2.3). Therefore the Trc mixture obtained through organic extraction from the commercial tyrothricin complex has a purity >95 %. Refer to table 2.4 for a summary of the composition and abundance of each peptide in the Trc mixture.

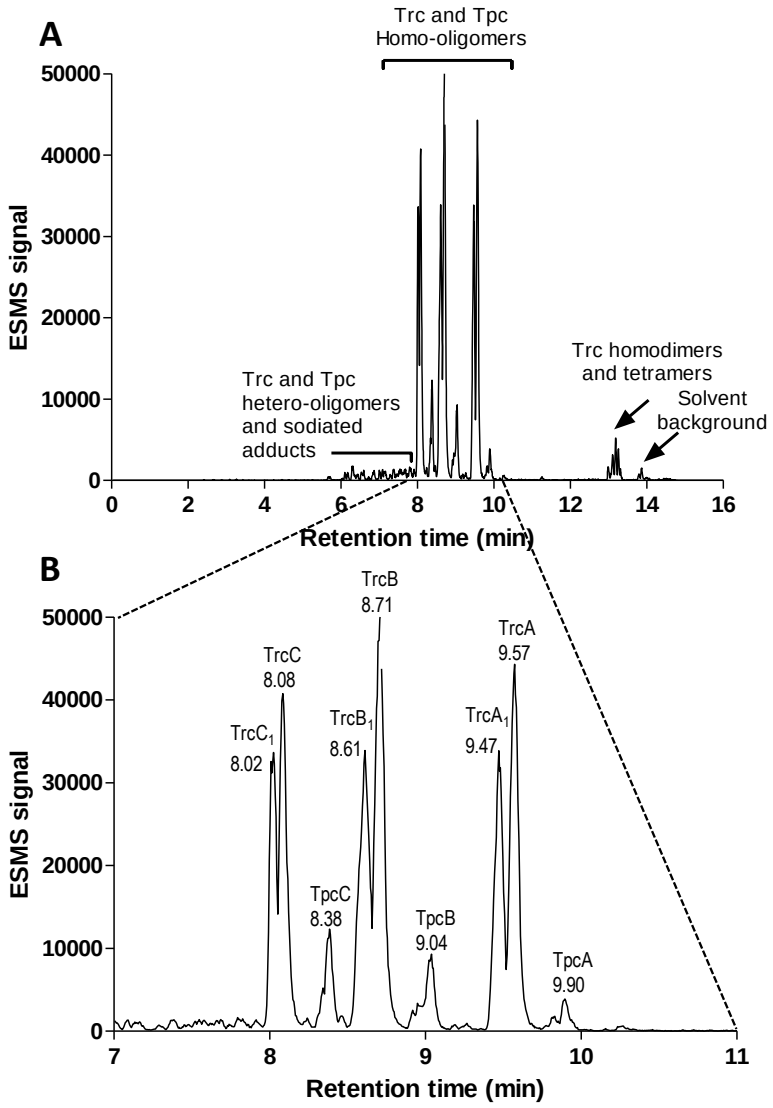

Figure 2.1: **A:** ESMS linked UPLC analysis of the Trc mixture organically extracted from the comercial tyrothricin complex.
B: Enlargement of the chromatogram to show the different peaks from the tyrocidines and analogues.

A C_{18} RP-HPLC semi-preparative column was used for the first round of peptide purification from the Trc mixture organically extracted from tyrothricin. Six fractions (denoted I-VI) were initially collected *via* semi-preparative RP-HPLC (Figure 2.4).

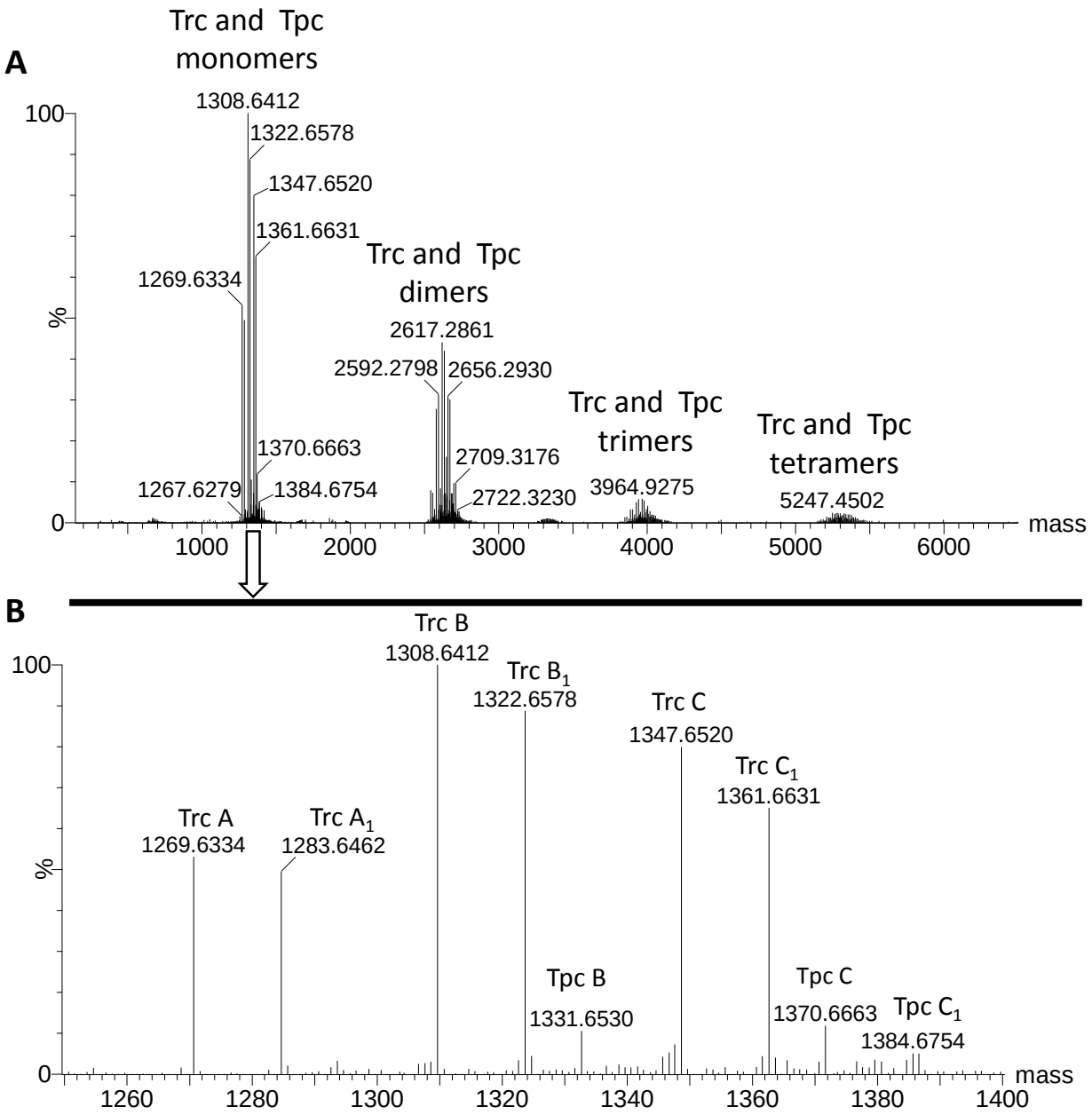

Figure 2.2: TOF-ESMS spectra of the Trc mixture extracted from tyrothricin.
A: The ESMS spectrum from *m*/*z* 300-2000 show the singly ($[M+H]^{+}$) and doubly ($[M+2H]^{2+}$) charged molecular species of the major tyrocidines for which monomers, dimers, trimers and tetramers were observed.
B: The transformed mass spectrum of the monomeric tyrocidines in the mixture.

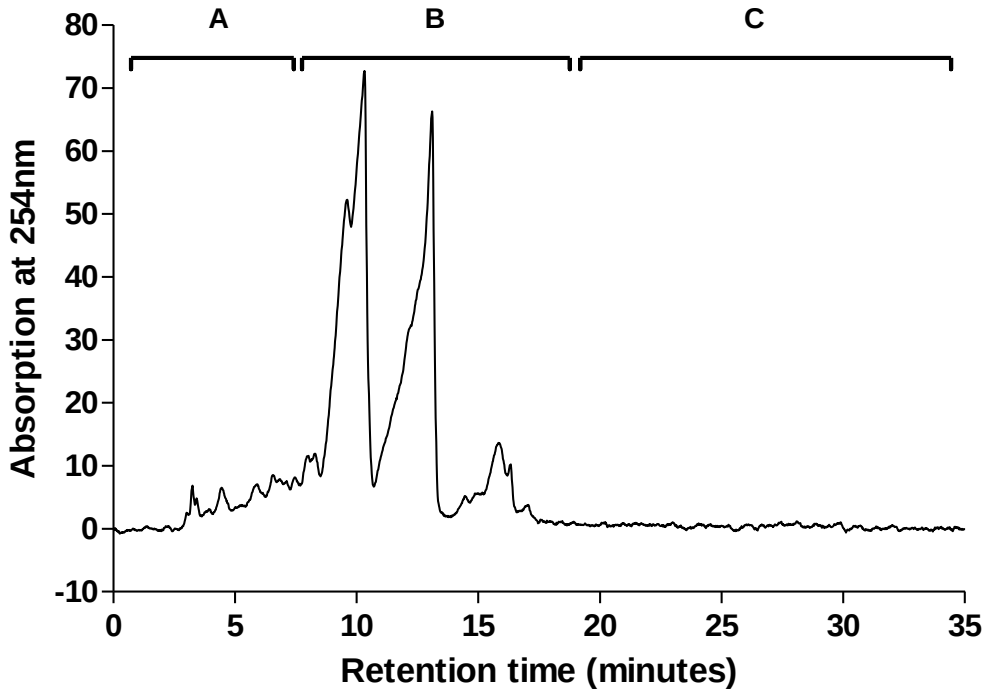

Figure 2.3: The Trc mixture, obtained through organic extraction from the tyrothricin complex, was subjected to preparative C_{18} HPLC. Fraction A, B and C were collected separately and weighed analytically.

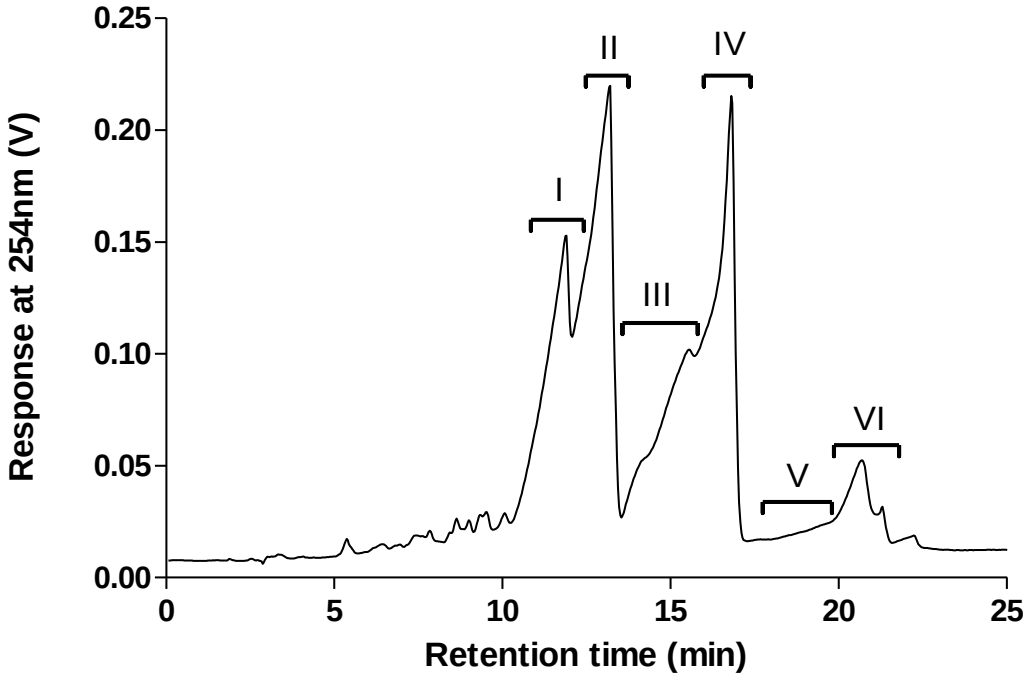

Figure 2.4: Semi-preparative RP-HPLC chromatogram of the tyrocidine mixture. The indicated six fractions (fractions I to VI) were isolated during the first round of semi-preparative RP-HPLC purification.

Table 2.4: Summary of analysis of Trc mixture extracted from commercial tyrothricin

Peptide	Abbr	Sequence[a]	Detected monoisotopic M*r* (theoretical M*r*)[b]	% Abundance in Trc mixture[c]	R_t (min)[d]	Fraction (Fig 2.4)
Tyrocidine C_1	$TrcC_1$	*Cyclo*-(VKLfPWwNQY)	1361.6781 (1361.6921)	10.3	8.02	I
Tyrocidine C	TrcC	*Cyclo*-(VOLfPWwNQY)	1347.6626 (1347.6764)	14.3	8.08	II
Tryptocidine C	TpcC	*Cyclo*-(VOLfPWwNQW)	1370.6792 (1370.6924)	3.5	8.38	-
Tyrocidine B_1	$TrcB_1$	*Cyclo*-(VKLfPWfNQY)	1322.6597 (13226812)	15.7	8.61[e]	III
Tyrocidine B	TrcB	*Cyclo*-(VOLfPWfNQY)	1308.6510 (1308.6655)	21.3	8.71	IV
Tryptocidine B	TpcB	*Cyclo*-(VOLfPWfNQW)	1331.6632 (1331.6815)	3.1	9.04	-
Tyrocidine A_1	$TrcA_1$	*Cyclo*-(VKLfPFfNQY)	1283.6500 (1283.6703)	13.2	9.47	V
Tyrocidine A	TrcA	*Cyclo*-(VOLfPFfNQY)	1269.6347 (1269.6538)	17.6	9.57	VI
Tryptocidine A	TpcA	*Cyclo*-(VOLfPFfNQW)	1292.6479 (1292.6706)	<1	9.90	-

[a]Conventional one-letter abbreviations are used for amino acid sequences [from Tang *et al.* (8)], except that O was used for Orn. Lower case one-letter abbreviations indicate D-amino acid residues.

[b]The theoretical monoisotopic M*r* were calculated as the sum of the molecular weights of the constituent amino acids of the peptide; and the detected monoisotopic M*r* determined from UPLC-MS.

[c]Abundances were calculated from the peak areas determined with ESMS-linked UPLC of the Trc mixture.

[d]The UPLC chromatogram of the Trc mixture supplied the retention times.

[e]While 0.5% Formic acid was used for the UPLC of the tyrocidines and analogues, 1.0 % Formic acid was used for $TrcB_1$, explaining the delayed retention of $TrcB_1$.

The first fraction (I) was analysed with UPLC and TOF-ESMS. The UPLC results showed that fraction I contained purified $TrcC_1$ (>90%), with a retention time (R_t) of 7.93 minutes (Figure 2.5 A). Direct TOF-ESMS analysis again revealed the tendency of the purified tyrocidines to oligomerise (aggregate) into dimers and trimers that are stable under ESMS conditions, as well as form adducts with cations such as sodium and hydrogen. In the TOF-ESMS spectra of Figure 2.5 BI, the $TrcC_1$ monomer and its dimers and trimers can be observed. In Figure 2.5 BII $TrcC_1$ (1361.6868) and its sodium adduct (1383.6722) can be observed. The minor impurities in the $TrcC_1$ sample were also revealed to be TrcC (1347.6727) and TpcC (1393.6807).

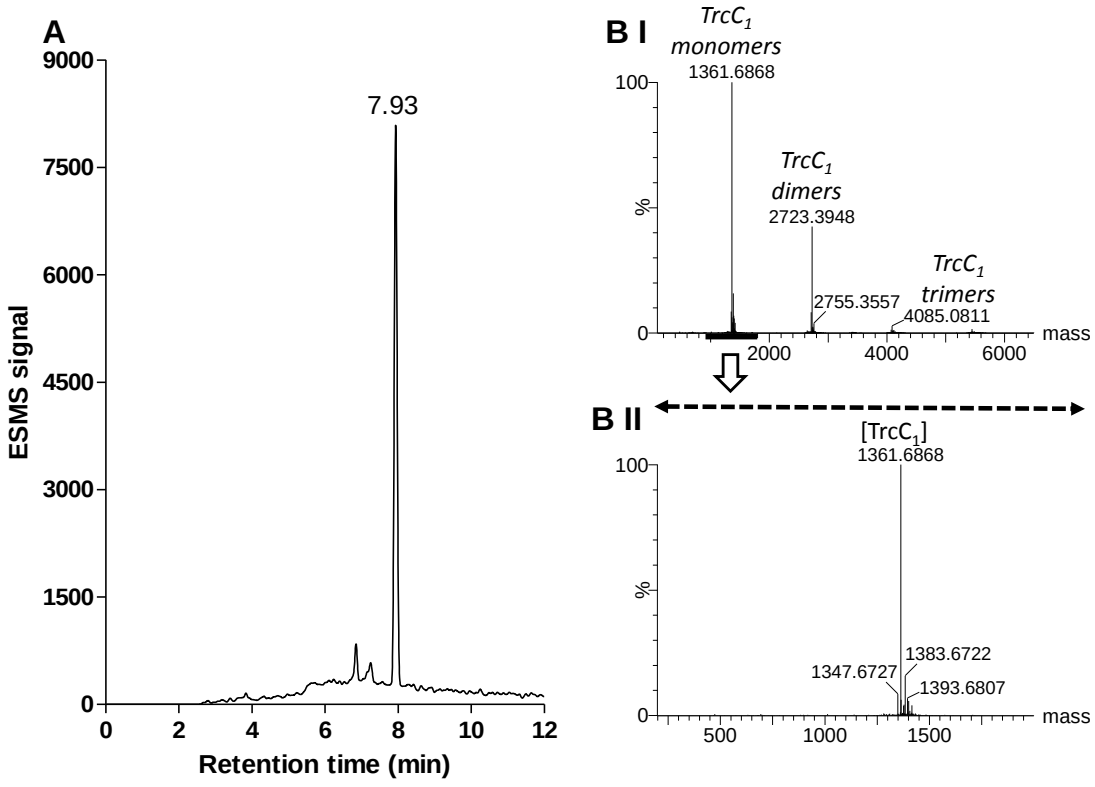

Figure 2.5: UPLC and TOF-ESMS analysis of purified $TrcC_1$
A: UPLC chromatogram of purified $TrcC_1$ (200 µg/mL, 3 µL injection volume) providing peptide identity and retention time (in minutes).
B: TOF-ESMS spectrum from *m*/*z* 300-2000 of purified $TrcC_1$ indicating the $TrcC_1$ monomers, dimers and trimers (I) and (II) the enlarged spectrum of the monomeric molecules present in the $TrcC_1$ sample. Details on peptide purity are given in Table 2.5.

Fraction II contained purified TrcC (>90%), with a UPLC R_t of 8.07 minutes (Figure 2.6 A). Similar to that of $TrcC_1$, TrcC also tended to oligomerise, as can be seen from the TOF-ESMS spectra in Figure 2.6 BI. Figure 6 BII shows the TrcC (1347.6713) and its sodium adduct (1369.6488).

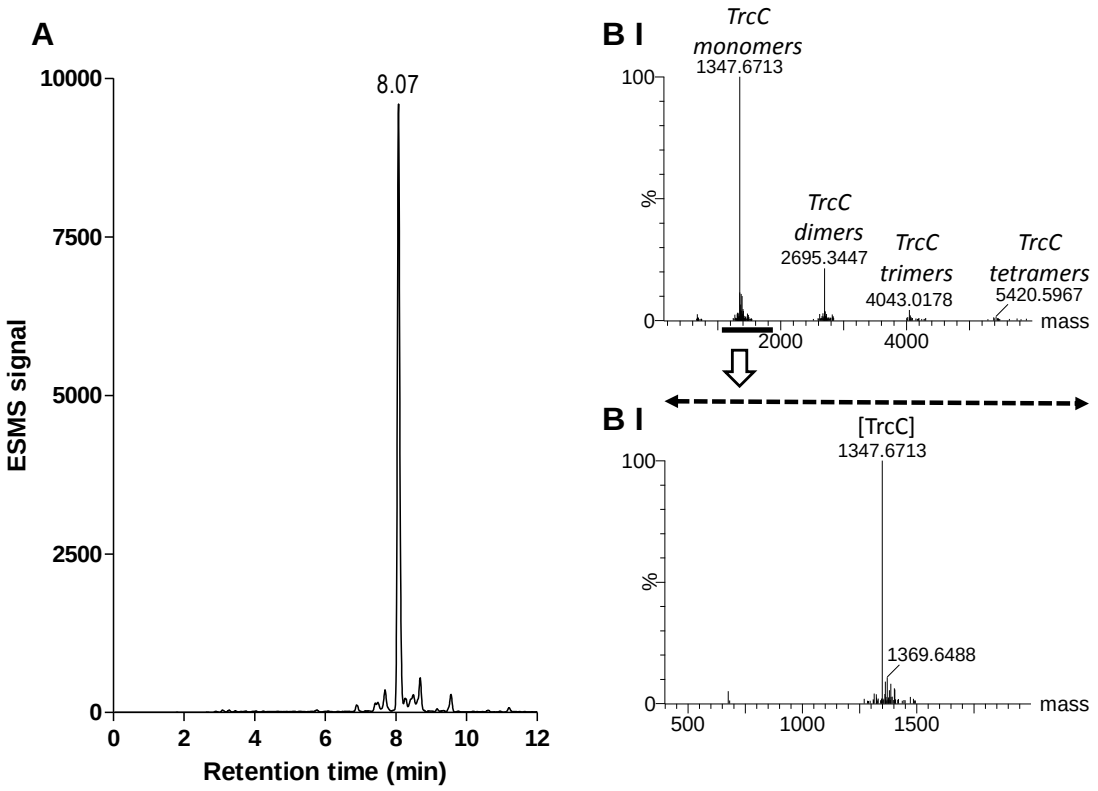

Figure 2.6: UPLC and TOF-ESMS analysis of purified TrcC
A: UPLC chromatogram of purified TrcC (200 µg/mL, 3 µL injection volume) providing peptide identity and retention time (in minutes).
B: TOF-ESMS spectrum from *m/z* 300-2000 of purified TrcC indicating the TrcC monomers, dimers, trimers and tetramers (I) and (II) the enlarged spectrum of the monomeric molecules present in the TrcC sample. Details on peptide purity are given in Table 2.5.

Analysis of fraction III indicated that it is a mixture of $TrcB_1$ and TrcB. A sample that went through multiple semi-preparative C_{18} RP-HPLC purifications showed that $TrcB_1$ was purified (>90%) with a R_t of 8.74 minutes (Figure 2.7 A). The TOF-ESMS indicates that $TrcB_1$ formed monomers, dimers, trimers and tetramers (Figure 2.7 BI) and the $TrcB_1$ monomer (1322.6730) with minor contamination from TrcB (1308.6589) (Figure 2.7 BII).

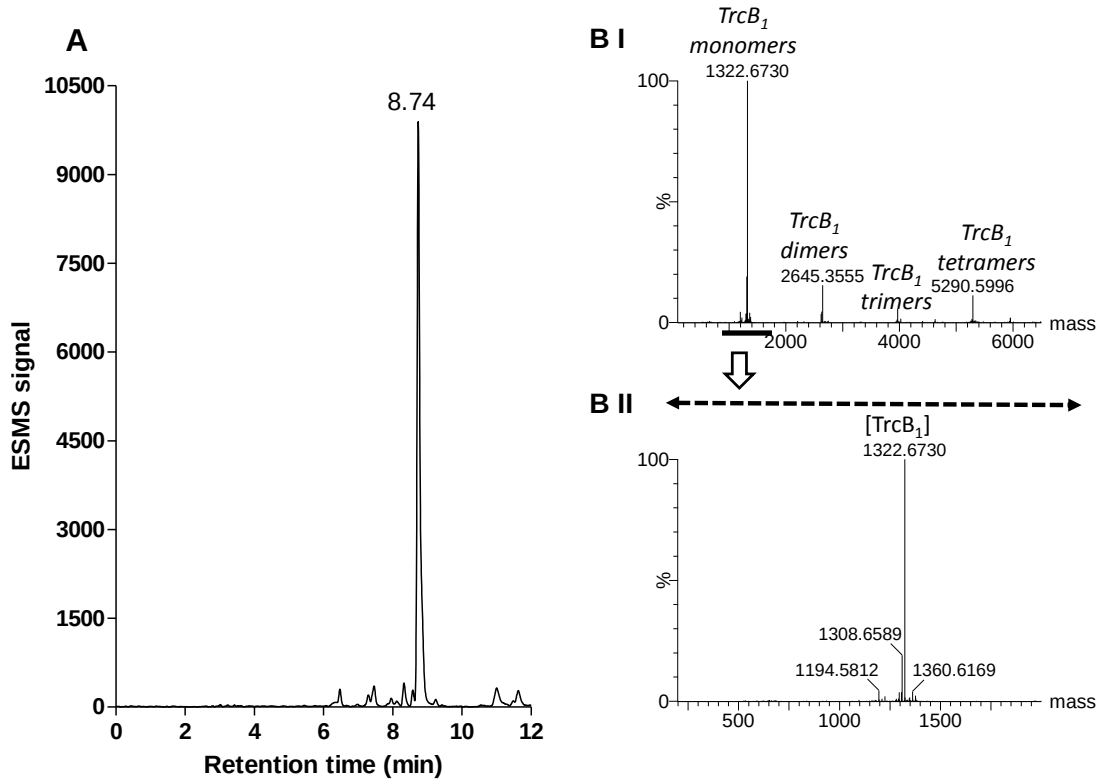

Figure 2.7: UPLC and TOF-ESMS analysis of purified $TrcB_1$
A: UPLC chromatogram of purified $TrcB_1$ (200 µg/mL, 3 µL injection volume) providing peptide identity and retention time (in minutes).
B: TOF-ESMS spectrum from *m/z* 300-2000 of purified $TrcB_1$ indicating the $TrcB_1$ monomers, dimers, trimers and tetramers (I) and (II) the enlarged spectrum of the monomeric molecules present in the $TrcB_1$ sample. Details on peptide purity are given in Table 2.5.

Fraction IV contained purified (>90%) TrcB with R_t of 8.41 minutes (Figure 2.8 A). As with the other tyrocidines and analogues, oligomers of TrcB were also detected. A minor impurity is due to the presence of $TrcB_1$ (1322.6772) in the sample (Figure 2.8 BI and BII).

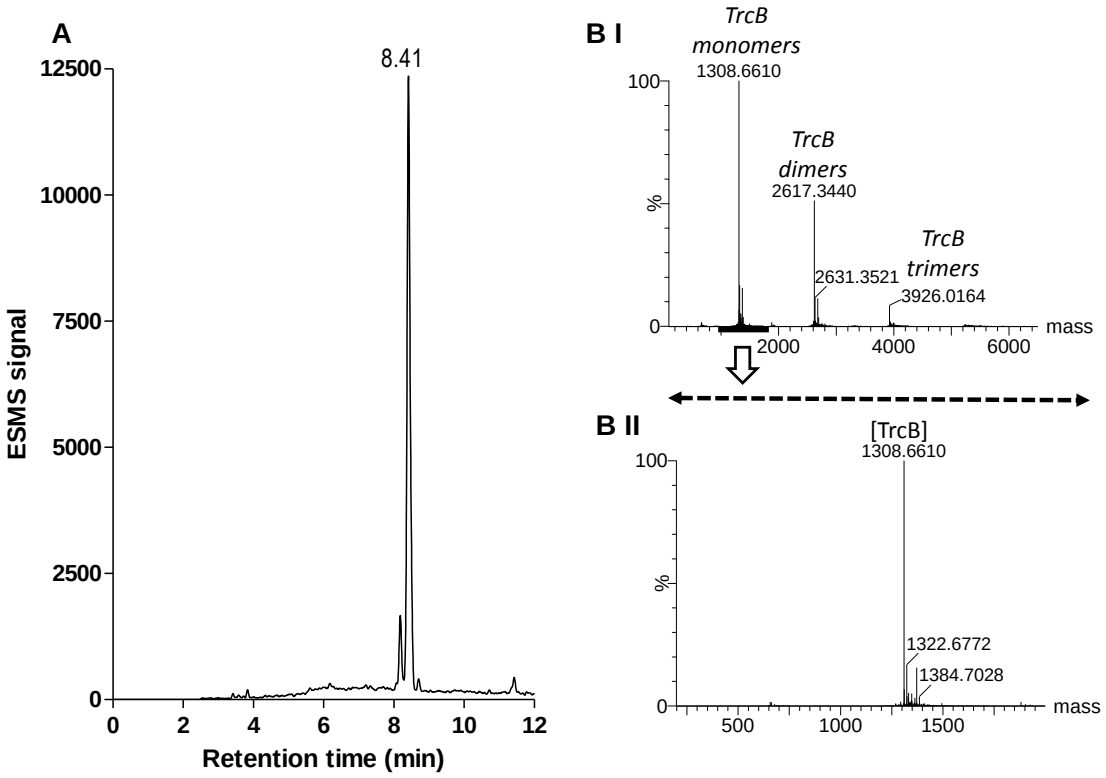

Figure 2.8: UPLC and TOF-ESMS analysis of purified TrcB
A: UPLC chromatogram of purified TrcB (200 µg/mL, 3 µL injection volume) providing peptide identity and retention time (in minutes).
B: TOF-ESMS spectrum from *m*/*z* 300-2000 of purified TrcB indicating the TrcB monomers, dimers and trimers (I) and (II) the enlarged spectrum of the monomeric molecules present in the TrcB sample. Details on peptide purity are given in Table 2.5.

Fraction V was found to contain both $TrcA_1$ and TrcA. Semi-preparative C_{18} RP-HPLC was not adequate for the separation of $TrcA_1$ and TrcA. Therefore an analytical C_{18} RP-HPLC method (12, 15) was used to successfully purify $TrcA_1$ to purity >95% from fraction V (R_t of 9.21 minutes) (Figure 2.9 A). $TrcA_1$ monomers (1283.6694) and dimers (2567.3562) can be observed in the TOF-ESMS spectra (Figure 2.9 BI). Its monomer, potassium and sodium adducts and minor contamination by TrcA can be seen in Figure 2.9 BII.

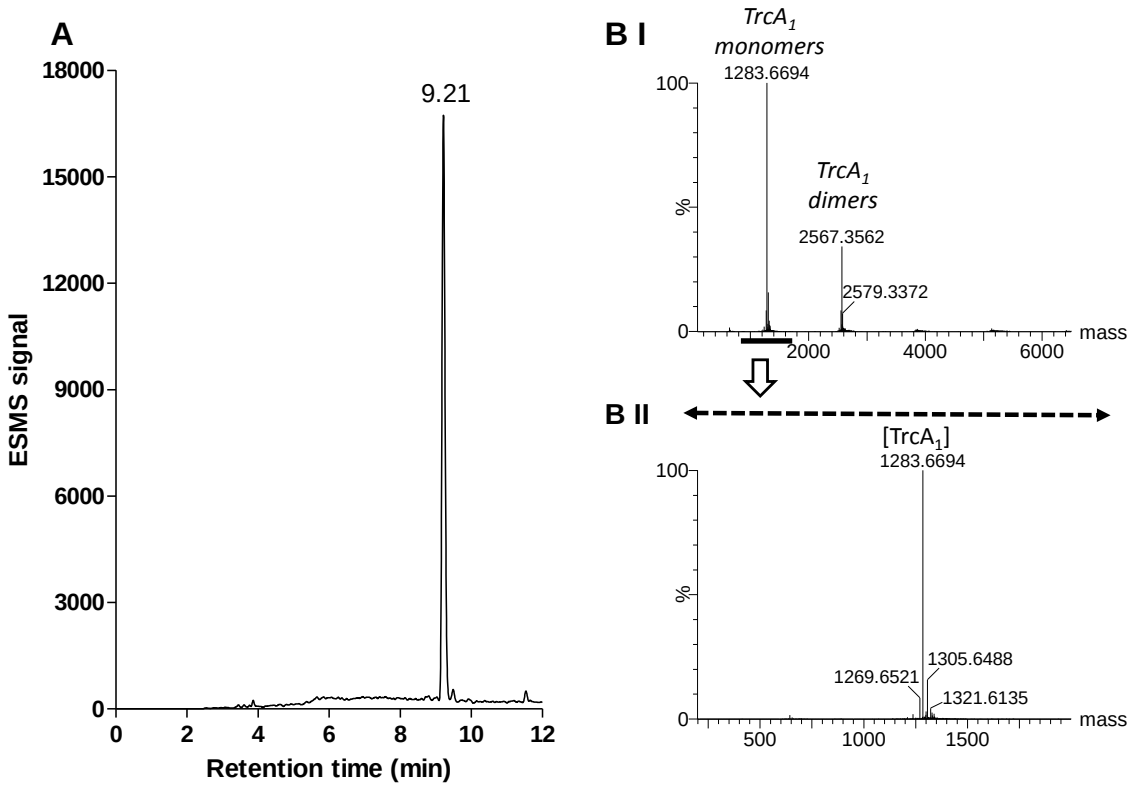

Figure 2.9: UPLC and TOF-ESMS analysis of purified $TrcA_1$
A: UPLC chromatogram of purified $TrcA_1$ (200 µg/mL, 3 µL injection volume) providing peptide identity and retention time (in minutes).
B: TOF-ESMS spectrum from *m/z* 300-2000 of purified $TrcA_1$ indicating the $TrcA_1$ monomers and dimers (I) and (II) the enlarged spectrum of the monomeric molecules present in the $TrcA_1$ sample. Details on peptide purity are given in Table 2.5.

The purification of TrcA to >90% purity from the Trc mixture, organically extracted from the commercial tyrothricin, proved to be quite difficult from fraction V and VI. Exhaustive analytical RP-HPLC of the isolated factions was not efficient for the purification of TrcA. Therefore the focus of obtaining pure peptides switched to the isolation of peptides from the cultures of the tyrothricin producer *B. aneurinolyticus* 8185.

2.4.2 Tyrocidines purified from the culture broth of B. aneurinolyticus

The culture medium of *B. aneurinolyticus* 8185 was supplemented with specific amino acids, in addition to urea, to obtain specific tyrocidine peptides/analogues (Table 2.3) (10). Initial analytical RP-HPLC analysis of the crude peptide extractions from culture medium indicated a large early eluting fraction containing a yellow pigment contaminating all of the tyrocidine extracts (Figure 2.10 A). In the process of refining the purification procedure, a C_8 matrix wash step was used to remove the contaminating pigment prior to further purification *via* preparative C_{18} RP-HPLC (Figure 2.10 B).

Supplementing the growth medium of *B. aneurinolyticus* 8185 with 0.5% Lys and 0.5% Phe produced peptide fractions that indicated two peaks with analytical C_{18} RP-HPLC analysis (Figure 2.11 A). TOF-ESMS analysis indicated that the larger peak (I) consisted of TrcA and the smaller peak (II) of PhcA.

Supplementation with 0.5% Phe again resulted in a peptide fraction with two peaks as indicated with analytical HPLC (Figure 2.11 B). However this time the majority of peptide produced was PhcA (IV) and TrcA (III) was present in smaller amounts. Only TrcA was produced when the medium was supplemented with 0.5% Phe and 0.5% Tyr (Figure 2.11 C). TpcC was almost exclusively produced in large amounts when the culture medium was supplemented with 0.3% Trp (Figure 2.10 B).

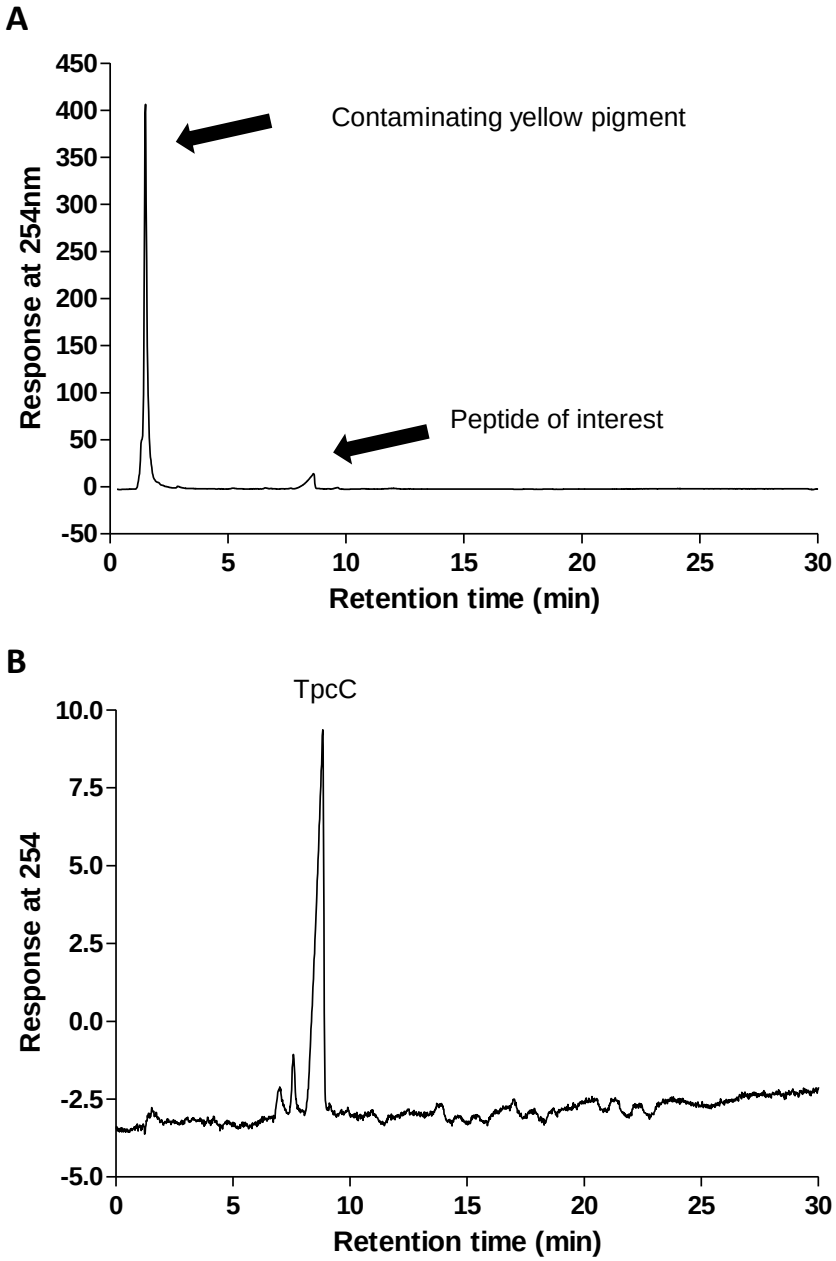

Figure 2.10: Analytical RP-HPLC analysis of *B. aneurinolyticus 8185* culture extract supplemented with 0.1 % urea and 0.3 % Trp.
A: Analytical RP-HPLC chromatogram of methanol extracted sample from *B. aneurinolyticus* 8185 culture medium.
B: Analytical RP-HPLC chromatogram of methanol extracted sample purified on an Isolute-XL C_8 column.

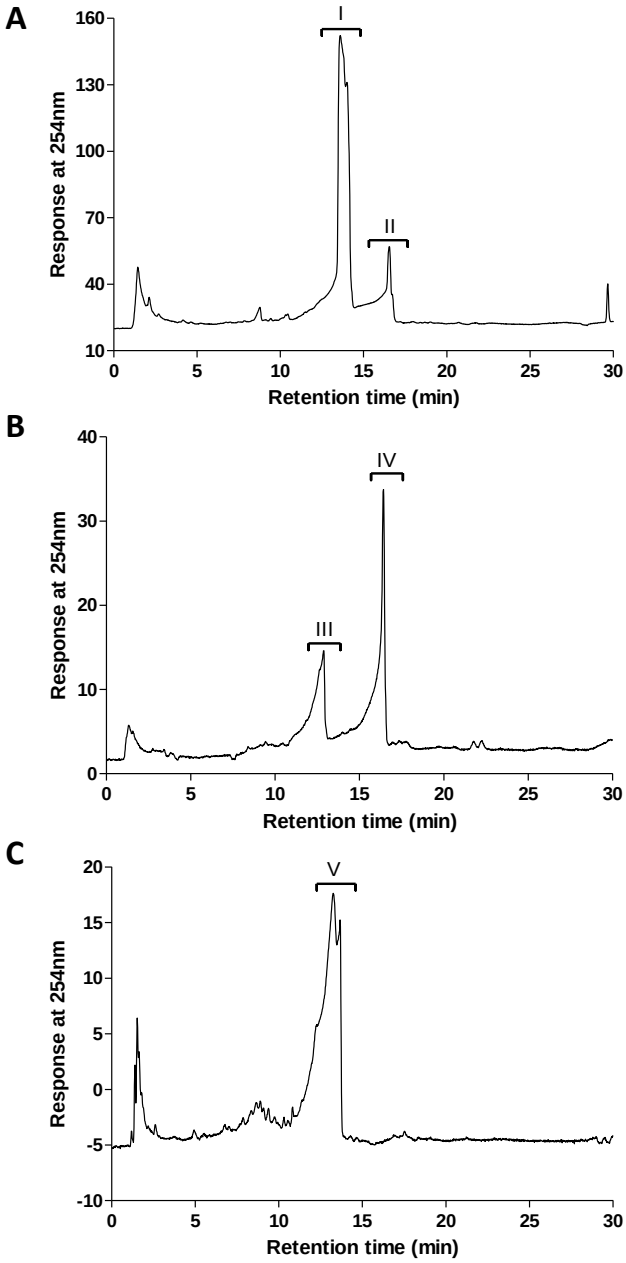

Figure 2.11: **A:** Analytical RP-HPLC analysis of *B. aneurinolyticus 8185* culture extract supplemented with 0.1 % urea, 0.5 % Lys and 0.5% Phe.
B: Analytical RP-HPLC analysis of *B. aneurinolyticus 8185* culture extract supplemented with 0.1 % urea and 0.5 % Phe.
C: Analytical RP-HPLC analysis of *B. aneurinolyticus 8185* culture extract supplemented with 0.1 % urea, 0.5 % Phe and 0.5% Tyr.

Peak fractions I to V - as depicted in Figure 2.11 - were further purified using semi-preparative C_{18} RP-HPLC. Fractions I, III and V yielded TrcA of >95% purity as indicated by UPLC-MS. TOF-ESMS spectra indicated the TrcA oligomers (Figure 2.12 BI) and monomeric TrcA (1269.6615) and its sodium adduct (1291.6343) (Figure 2.12 BII).

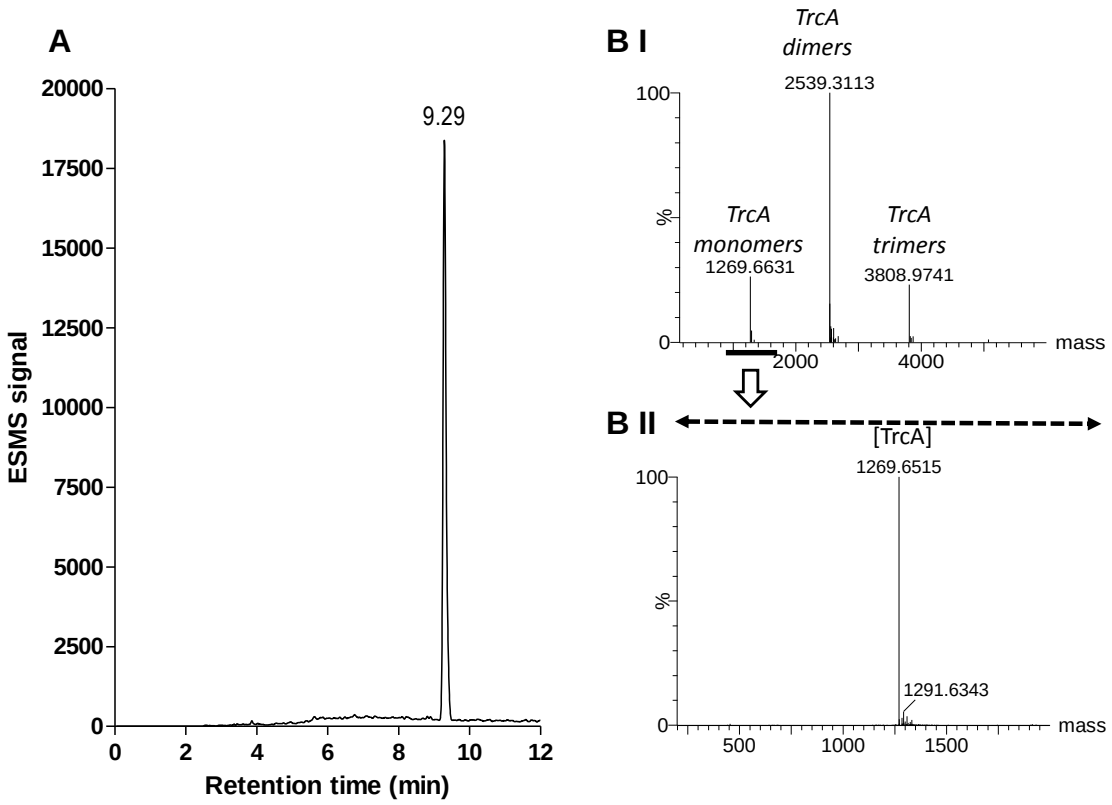

Figure 2.12: UPLC and TOF-ESMS analysis of purified TrcA
A: UPLC chromatogram of purified TrcA (200 µg/mL, 3 µL injection volume) providing peptide identity and retention time (in minutes).
B: TOF-ESMS spectrum from *m/z* 300-2000 of purified TrcA indicating the TrcA monomers, dimers and trimers (I) and (II) the enlarged spectrum of the monomeric molecules present in the TrcA sample. Details on peptide purity are given in Table 2.5.

PhcA, with high purity of >95%, was purified from fractions II and IV using semi-preparative C_{18} RP-HPLC (Figure 2.13 A). Again the tendency of the tyrocidines to oligomerise can be observed in the TOF-ESMS spectra of PhcA (Figure 2.13 BI). In Figure 2.13 BII the PhcA monomer (1254.6625) and its sodium adducts can be observed. Minor "contamination" from TpcA is also evident.

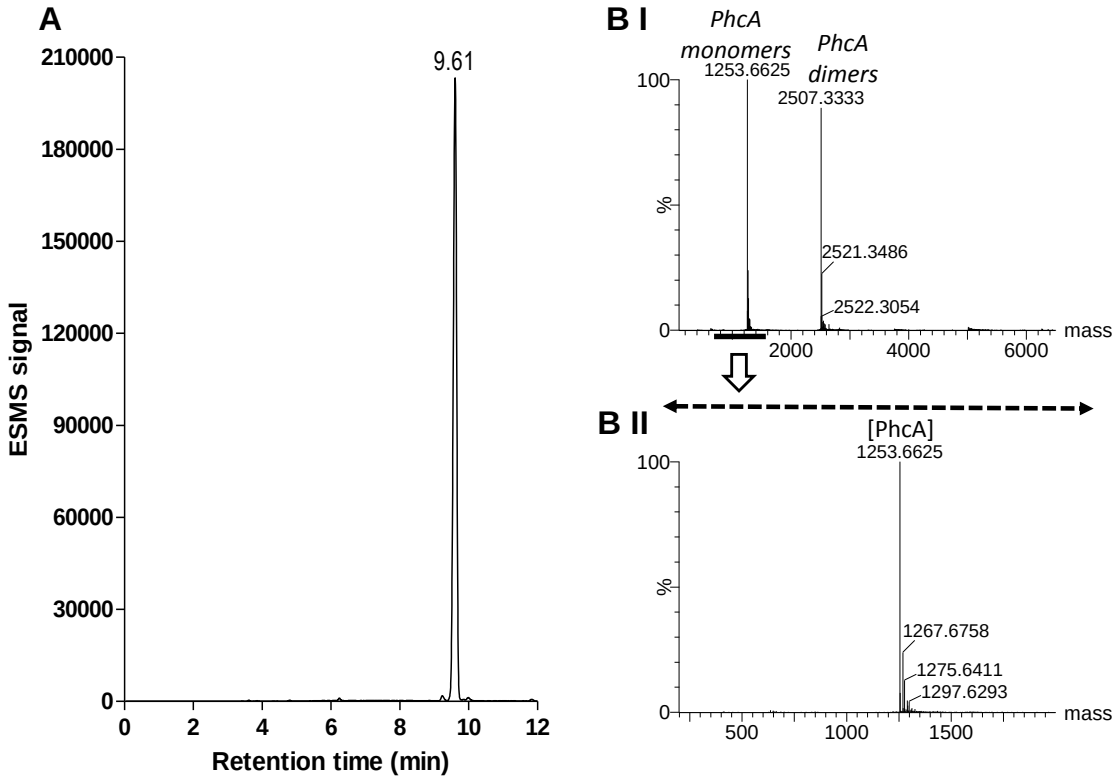

Figure 2.13: UPLC and TOF-ESMS analysis of purified PhcA
A: UPLC chromatogram of purified PhcA (200 µg/mL, 3 µL injection volume) providing peptide identity and retention time (in minutes).
B: TOF-ESMS spectrum from *m/z* 300-2000 of purified PhcA indicating the PhcA monomers and dimers (I) and (II) the enlarged spectrum of the monomeric molecules present in the PhcA sample. Details on peptide purity are given in Table 2.5.

After a preparative C_{18} RP-HPLC step of the crude TpcC sample (refer to Figure 2.10 B), UPLC analysis revealed a peptide fraction with two peak fractions (Figure 2.14 A). However, ESMS analysis of each peak revealed that they both consist of TpcC. The formation of the two peaks can be ascribed to peptide oligomerisation and protonation. A TpcC fraction of >95% purity was therefore obtained. This was confirmed by TOF-ESMS spectra of TpcC which indicated TpcC oligomers (Figure 2.14 BI), with the TpcC monomer (1370.6866) and its sodium adducts indicated in Figure 2.14 BII.

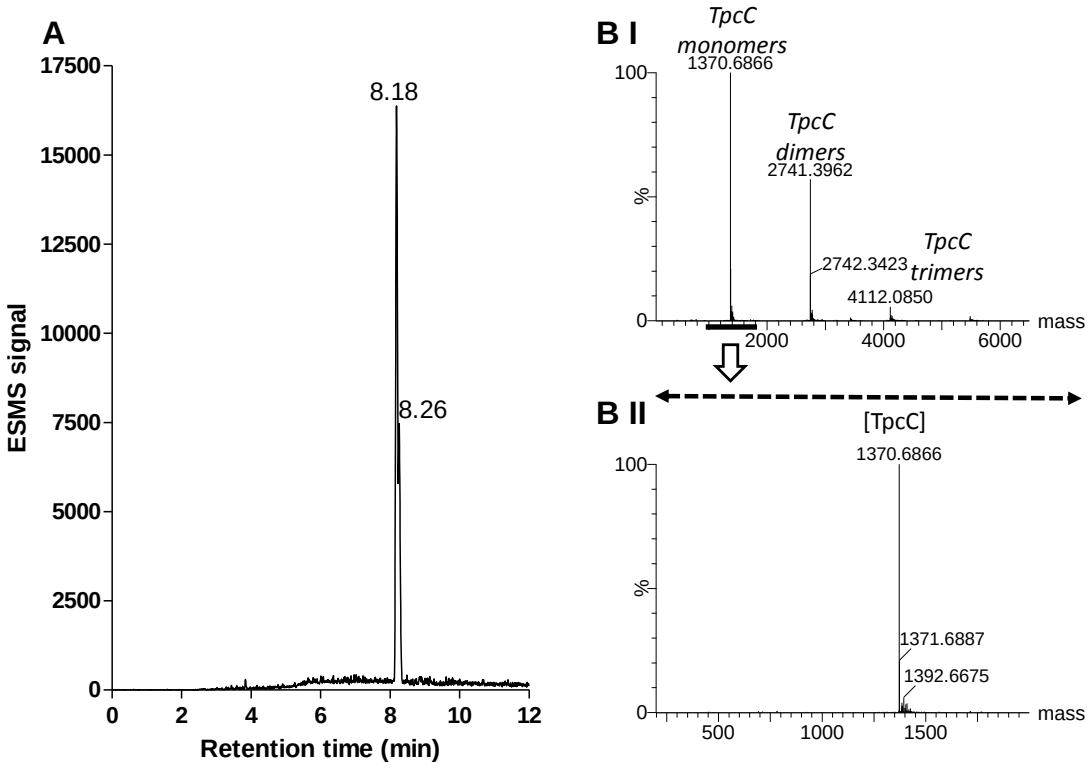

Figure 2.14: UPLC and TOF-ESMS analysis of purified TpcC
A: UPLC chromatogram of purified TpcC (200 µg/mL, 3 µL injection volume) providing peptide identity and retention time (in minutes).
B: TOF-ESMS spectrum from *m/z* 300-2000 of purified TpcC indicating the TpcC monomers, dimers and trimers (I) and (II) the enlarged spectrum of the monomeric molecules present in the TpcC sample. Details on peptide purity are given in Table 2.5.

The commercial GS was also analysed using UPLC and TOF-ESMS. UPLC analysis revealed that the purity of the GS sample is 94% (Figure 2.15 A). In contrast to the tyrocidines, TOF-ESMS spectra of GS did not reveal any tendencies of GS to oligomerise. In Figure 2.15 BI and BII the GS monomer (1140.7067) and its sodium and hydrogen adducts can be observed. Impurities can be ascribed to other gramicidin species.

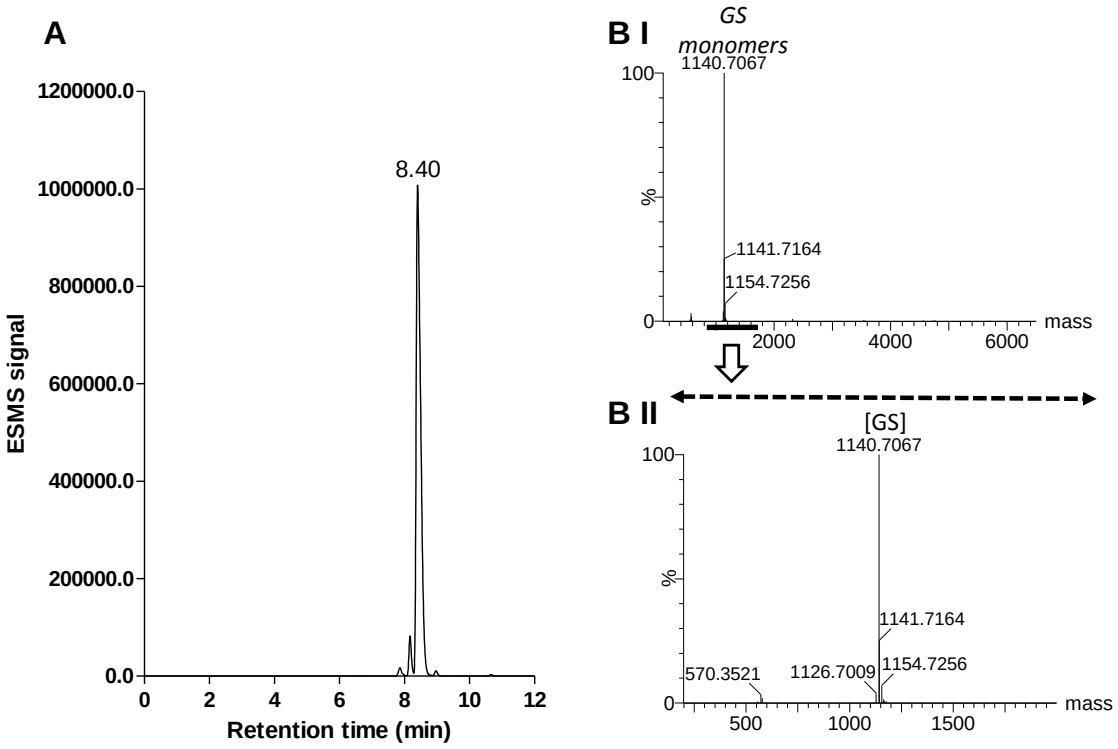

Figure 2.15: UPLC and TOF-ESMS analysis of GS
A: UPLC chromatogram of purified GS (200µg/mL, 3 µL injection volume) providing peptide identity and retention time (in minutes).
B: TOF-ESMS spectrum from *m*/*z* 300-2000 of purified GS indicating the GS monomer (I) and (II) the enlarged spectrum of the monomeric molecules present in the GS sample. Details on peptide purity are given in Table 2.5.

Table 2.5: Summary of the purification data

Peptide	Crude extract (mg)	% Yield (Yield, mg)	Theoretical Mr	TOF-ESMS M_r of ion signals	Peak identity	UPLC R_t	% Purity
Peptides purified from commercial tyrothricin complex							
Tyrocidine C_1	350	7.1 (24.8)	1361.6921	1347.6727	TrcC	7.93	93
				1361.6868	$TrcC_1$		
				1383.6722	$TrcC_1 + 2Na^+$		
				1393.6807	$TpcC + H^+ + 2Na^+$		
Tyrocidine C	350	10.1 (35.3)	1347.6764	**1347.6713**	TrcC	8.07	91
				1369.6488	$TrcC + 2Na^+$		
Tyrocidine B_1	350	2.1 (7.3)	1322.6812	1194.5812	unknown	8.74	93
				1308.6589	TrcB		
				1322.6730	$TrcB_1$		
				1360.6169	$TrcB_1 + K^+$		
Tyrocidine B	350	13.0 (45.4)	1308.6655	**1308.6610**	TrcB	8.41	90
				1322.6772	$TrcB_1$		
				1384.7028	$TpcC_1$		
Tyrocidine A_1	350	1.2 (4.3)	1283.6703	1269.6521	TrcA	9.21	94
				1283.6694	$TrcA_1$		
				1305.6488	$TrcA_1 + 2Na^+$		
				1321.6135	$TrcA_1 + K^+$		
Peptides purified from B. parabrevis *8185 culture extract*							
Tyrocidine A	300	2.9 (8.7)	1269.6546	**1269.6515**	TrcA	9.29	98
				1291.6343	$TrcA + 2Na^+$		
Phenycidine A	300	0.3 (0.8)	1253.6597	**1253.6625**	PhcA	9.61	98
				1267.6758	$PhcA_1$		
				1275.6411	$PhcA + 2Na^+$		
				1297.6293	$PhcA + 4Na^+$		
Tryptocidine C	200	1.1 (2.1)	1370.6924	**1370.6866**	TpcC	8.18	95
				1371.6887	$TpcC + H^+$		
				1392.6675	$TpcC + 2Na^+$		
Commercial peptide							
Gramicidin S	-	-	1140.7059	**570.3521**	$[GS]^{2+}$	8.40	93
				1126.7009	unknown		
				1140.7067	GS		
				1141.7164	$GS + H^+$		
				1154.7256	$GS + 2H^+ + Na^+$		

The UPLC chromatograms of the purified peptides supplied the UPLC retention times (in minutes) and were used to calculate their purity. The observed monoisotopic Mr were obtained from the TOF-ESMS spectra. The expected monoisotopic Mr were calculated as the sum of the molecular weights of the constituent amino acids. The percentage yield was calculated as the percentage of the mass of the crude commercial tyrocidine complex, or as the percentage of the mass of the crude extract from *B. parabrevis* 8185 culture medium.

2.5 Conclusions

A mixture of tyrocidine peptides (Trc mixture), of >95 % purity in terms of tyrocidine peptide content, was successfully extracted from the commercial tyrothricin. Using preparative and analytical RP-HPLC, TrcA_1, B_1, B, C_1 and C with purities >90%, were effectively purified from the Trc mixture. Supplementation of the culture broth of *B. aneurinolyticus 8185* with specific amino acids eased the process of peptide purification and made it possible to acquire sufficient amounts of pure rare peptides in order to perform studies on their bioactivity and physicochemical properties. It was especially a breakthrough in the case of PhcA and TpcC since the purification of these peptides in large amounts have not previously been possible from the commercial tyrothricin mixture. The optimised RP-HPLC purification methodology enabled the purification of the produced peptides, as well as tyrocidines from commercial tyrothricin, to >90% purity (Table 2.5). Any minor contamination was as a result of the presence of other tyrocidines or analogues. The identity, purity and chemical integrity of each fraction were confirmed with UPLC and TOF-ESMS analysis. The major tyrocidines (TrcC_1, C, B_1, B, A_1 and A) and two of their analogues, PhcA and TpcC, were successfully purified (Table 2.5) for the bioactivity and physicochemical studies reported in Chapters 3-6.

2.6 References

1. **Okuda K, Edwards GC, Winnick T.** 1963. Biosynthesis of gramicidin and tyrocidine in the dubos strain of Bacillus brevis: I . Experiments with growing cultures. Journal of bacteriology. **85:**329–338.

2. **Claus D, Berkeley RCW.** 1986. Genus Bacillus Cohn 1872, 174AL. *In* Sneath PHA, Mair NS, Sharpe ME, Holt JG (ed.), Bergey's manual of systematic bacteriology, vol. 2. Williams & Wilkins Co., Baltimore, p. 1105–1139.

3. **Farrow JA, Ash C, Wallbanks S, Collins MD.** 1992. Phylogenetic analysis of the genera Planococcus, Marinococcus and Sporosarcina and their relationships to members of the genus Bacillus. FEMS Microbiology letters. **72:**167–172.

4. **Aoyama S.** 1952. Studies on the thiamin-decomposing bacterium. I. Bacteriological researches of a new thiamin decomposing bacillus *Bacillus aneurinolyticus*. . Acta scholae medicinalis universitatis in Kioto. **30:**127–132.

5. **Skerman VBD, McGowan V, Sneath PHA.** 1989. Approved lists of bacterial names (amended). ASM Press, Washington (DC).

6. **Shida O, Takag H, Kadowaki K, Yan H.** 1994. Bacillus aneurinolyticus sp. nov., nom. rev. International journal of systematic bacteriology. **232:**143–150.

7. **Shida O, Takaghi H, Kadowaki K, Komagata K.** 1996. Proposal for two new genera, Brevibacillus gen. nov. and Aneurinibacillus gen. nov. International journal of systematic bacteriology. **46:**939–946.

8. **Tang X-J, Thibault P, Boyd RK.** 1992. Characterisation of the tyrocidine and gramicidin fractions of the tyrothricin complex from *Bacillus brevis* using liquid chromatography and mass spectrometry. Int. J. Mass Spectrom. Ion Processes. **122:**153-179.

9. **Baron AL.** 1949. Preparation of tyrothricin. US patent 2482832

10. **Leussa AN-N.** 2013. Characterisation of small cyclic peptides with antimalarial and antilisterial activity, Department of Biochemistry, University of Stellenbosch, PhD Thesis in progress, completion March 2014. Personal communication.

11. **Spathelf BM.** 2010. Qualitative structure-actvity relationships of the major tyrocidines, cyclic decapeptides from *Bacillus aneurinolyticus*. PhD Thesis, Department of Biochemistry, University of Stellenbosch, http://scholar.sun.ac.za/handle/10019.1/4001.

12. **Eyéghé-Bickong HA.** 2011. Role of surfactin from *Bacillus subtilis* in protection against antimicrobial peptides produced by other *Bacillus* species. PhD Thesis, Department of Biochemistry, University of Stellenbosch, http://scholar.sun.ac.za/handle/10019/6773.

13. **Hotchkiss RD, Dubos RJ.** 1941. The isolation of bactericidal substances from cultures of *Bacillus brevis*. J. Biol. Chem. **141:**155-162.

14. **Vosloo JA, Stander M, Leussa AN-N, Spathelf BM, Rautenbach M.** 2013. Manipulation of the tyrothricin production profile of *Bacillus aneurinolyticus*. Microbiology. **159:**2200-2211.

15. **Rautenbach M, Vlok NM, Stander M, Hoppe HC.** 2007. Inhibition of malaria parasite blood stages by tyrocidines, membrane-active cyclic peptide antibiotics from *Bacillus brevis*. Biochim. Biophys. Acta. **1768:**1488-1497.

Chapter 3

Development and optimisation of antifungal assays to determine tyrocidine activity

3.1 Introduction

In preparation for our research described in Chapters 4 and 5 and our article (Addendum Chapter 3, (1)) published on the gel-based antifungal assay in which the influence of culture conditions on antimicrobial peptide (AMP) activity and fungal growth were highlighted, antifungal assays were optimised in terms of two representative fungal pathogens, *Fusarium solani* and *Botrytis cinerea*, as well as for tyrocidine antifungal activity. The microtiter plate treatment and growth medium, as well as the percentage ethanol in the peptide solvent, were chosen for optimal fungal growth and maximum tyrocidine activity.

Tyrocidines, similar to the majority of AMPs, are very sensitive to their environment. Their environment influences the degree of tyrocidine aggregation and consequently their activity (2). The amphipathic tyrocidines have a tendency to aggregate in aqueous environments, forming complex structures (2-5). Ethanol in water dilution is used to solubilise the tyrocidines in order to perform dilution assays. The extent of their aggregation is influenced by initial concentration of the tyrocidine stock solution in addition to the percentage ethanol used to get the peptides into solution. However, Dantigny *et al.* (6) illustrated that, at a concentration range of 3% to 5%, ethanol kills various fungi species and reduces their growth rate at lower concentrations (6). As one of our aims is to determine the degree of antifungal activity of tyrocidines and their mode of action, any inhibitory effect observed must not be attributed solely to ethanol. In the course of assay development different concentrations of ethanol were assessed for their influence on fungal growth and peptide activity. Gramicidin S (GS), an analogue of the tyrocidines with 50%

sequence identity, was used as control peptide. It is soluble in water and does not tend to aggregate. GS was previously shown to have antifungal activity in both broth and agar media (7) and is known to be highly lytic to eukaryotic cells (8).

Since fungal species survive in various environments on earth (9), it follows that different species will prosper to varying degrees in different mediums. Therefore the growth of *F. solani* and *B. cinerea* was determined in different broth mediums as wel as on different agar mediums. During the course of assay development and optimisation, the influence of different mediums on the activity of the tyrocidine mixture was also assessed.

3.2 Materials

The fungal strains *Fusarium solani* STEU 6188 and *Botrytis cinerea* CKJ1731 were provided by the Department of Plant Pathology, University of Stellenbosch. The potato dextrose broth (PDB), potato dextrose agarose (PDA) and Tween 20® were obtained from Fluka (St. Louis, USA). Biolab (Wadeville, Gauteng) provided the tryptone soy broth (TSB), yeast extract and lysogeny broth (LB). Ethanol (99.9%) was obtained from Merck Chemicals (Pty) (Wadeville, Gauteng). The sterile polypropylene plates were provided by Nunc (Roskilde, Denmark), while Corning (Corning, USA) provided the sterile microtiter plates. Bovine milk casein was supplied by Fluka Chemicals (Buchs, Switzerland). The Na_2HPO_4 and KH_2PO_4 were supplied by Merck (Darmstadt, Germany). Capital Enterprises (Hillcrest, South Africa) supplied the KCl. Analytical quality water was prepared by passing water from a reverse osmoses plant through a Millipore (Milford, USA) Milli Q® water purification system.

The peptides, the mixture of tyrocidine peptides (Trc mixture), tyrocidine C (TrcC) and gramicidin S (GS), were purified and analysed as described in Chapter 2.

3.3 Methods

3.3.1 Growth and harvesting of fungi

F. solani was grown at 25 ˚C on PDA until sporulation (± 2 weeks). Spores were harvested with 3 mL 0.1 % Tween-analytical water. *B. cinerea* was grown in culture plates on sterile strawberry halves at 23-25 ˚C until sporulation (± 3 weeks). *B. cinerea* spores were harvested dry using vacuum. Subsequent to harvesting, spores were counted using a counting chamber. Standard practices to ensure sterility were followed.

3.3.2 Treatment of microtiter plates

Broth microdilution assays were performed in unblocked and casein blocked plates. Casein blocked plates were prepared using sterile 0.5% casein in Dulbecco's phosphate buffered saline (PBS) (10, 11). Spores of either *B. cinerea* or *F. solani* were suspended in half strength PDB to a concentration of 2.5×10^4 spores/mL (12). Of the broth-spore suspension 90 µL were added to the wells of either sterile unblocked 96-well microtiter plates or casein blocked microtiter plates. The Trc mixture was dissolved in ethanol (15 %) to a concentration of 1.00 mg/mL. Doubling dilution series were performed in polypropylene microtiter plates using ethanol (15 %). Thereafter 10 µL peptide was added to the broth-spore suspensions in the microtiter plates. Microtiter plates were incubated at 25 ˚C for 48 hours. Light dispersion of each well was spectrophotometrically determined at 595 nm using a BioRad microtiter plate reader.

3.3.3 Determining growth of fungi in different mediums

Growth of *F. solani* and *B. cinerea* in PDB, yeast supplemented TSB (YTSB, TSB containing 20% *m/v* yeast extract), LB, PDA and YTSA was determined using 96-well microtiter plates. The agar plates were prepared by pipetting 70 µL PDA/YTSA (65°C) into sterile microtiter plates using the reverse pipetting method (13) and letting it cool before the addition of spore-containing broth suspensions. Broth suspensions consisted of half strength PDB, YTSB or LB and either *F. solani* or *B. cinerea* spores at a concentration of 2.5×10^4 spores/mL (broth media)

or 1.0×10^5 spores/mL (agar media) of which 100 µL was added to microtiter plates for growth determination in the broth media and 30 µL was added onto prepared PDA/YTSA plates for growth determination on agar media. Plates were incubated at 23-25 ˚C and growth measured every 24 hours for 96 hours. Light dispersion of each well was spectrophotometrically determined at 595 nm using a BioRad microtiter plate reader.

3.3.4 Determining growth of fungi in different concentrations of ethanol

The influence of respectively 1.0%, 1.5% and 2.0% ethanol on the growth of *F. solani* and *B. cinerea* was determined using broth assays in 96-well microtiter plates. Of the broth suspensions, which consisted of half strength PDB, YTSB or LB and spores at a concentration of 2×10^4/mL (12) and final ethanol concentrations of 0%, 1.0%, 1.5% or 2.0%, 100 µL was added to each well. Plates were incubated at 25 ˚C and growth measured every 24 hours for 96 hours (*B. cinerea*) or 72 hours (*F. solani*). Light dispersion of each well was spectrophotometrically determined at 595 nm using a BioRad microtiter plate reader.

3.3.5 Different ethanol concentrations for peptide preparation

Broth microdilution assays with *B. cinerea* were used to assess different ethanol concentrations for peptide preparation. *B. cinerea* spores were suspended in half strength PDB to a concentration of 2.5×10^4 spores/mL (12). The peptides were dissolved in an ethanol:water solution of either 10% or 15% to a concentration of 1.00 mg/mL. Doubling dilution series were made in polypropylene microtiter plates using ethanol:water solutions of respectively 10% and 15%. Into each well 90 µL of the broth suspension was added followed by 10 µL peptide. Peptide treated and growth controls had a final ethanol concentration of either 1.0% or 1.5%.

3.3.6 Determining tyrocidine activity in PDB, YTSB, PDA and YTSA

The activities of the Trc mixture and GS in PDB, YTSB, PDA and YTSA were compared using broth and agar microdilution assays (1, 12, 13). The agar plates were prepared by pipetting 70 µL PDA/YTSA (65°C) into sterile microtiter plates using the reverse pipetting method (13) and

letting it cool before the addition of spore-containing broth suspensions. Broth suspensions consisted of half strength PDB or YTSB and either *F. solani* or *B. cinerea* spores at a concentration of 2.5×10^4 spores/mL (broth assays) or 1.0×10^5 spores/mL (agar assays) (12). The Trc mixture was dissolved in ethanol (15 %) to a concentration of 1.00 mg/mL. Doubling dilution series were made in polypropylene microtiter plates using ethanol (15 %). Into each well 90 µL (broth assays) or 20 µL (agar assays) of the broth suspension was added followed by 10 µL peptide. Growth control received 10 µL of 15 % ethanol in water solution instead of peptide. Sterility control was a combination of PDB or YTSB analytical water and 1.5 % ethanol. All wells had a final volume of 100 µL. Subsequent to peptide addition the microtiter plates were incubated at 23-25 ˚C for 48 hours. Light dispersion of each well was spectrophotometrically determined at 595 nm using a BioRad microtiter plate reader.

3.3.7 Data and Statistical analysis

In order to calculate the percentage growth inhibition the light dispersion at each concentration was used as described by Rautenbach *et al*. (14). GraphPad Prism® 4.03 (GraphPad Software, San Diego, USA) was used to plot the dose response curves. Non-linear regression and sigmoidal curves (with a slope default setting at <7) were fitted for dose response analysis (14). The point halfway between top and bottom (IC_{50}) represents the concentration necessary to cause 50% growth inhibition. The minimum inhibition concentration (MIC), calculated as the x-value at the intercept between the slope and the top plateau of a full dose-response curve, was denoted as IC_{max} (14) to make the distinction with MIC values obtained from visual inspection of a dose-response result.

GraphPad Prism® was also used for the statistical analysis of data. Analysis included 95% confidence levels, absolute sum of squares, standard error of the mean, Bonferroni's post test and Newman-Keuls multiple comparison test.

3.4 Results and Discussion

3.4.1 Influence of treatment of microtiter plates on peptide activity

During previous studies the 96-well microtiter plates for broth assays were blocked with casein in PBS to decrease non-specific binding and consequently increase peptide activity (10, 11). However, when we compared the activities of the tyrocidines between blocked and unblocked plates, we found that the tyrocidines exhibited higher activity in the unblocked low protein binding plates (Figure 3.1).

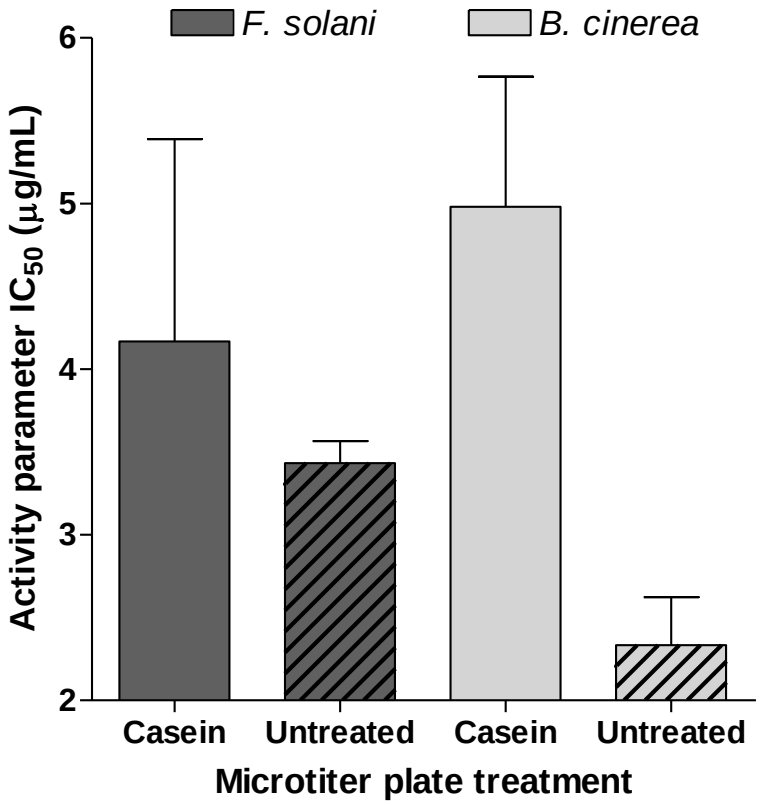

Figure 3.1: Treatment of microtiter plates with casein. The activity of the Trc mixture is compared, in terms of its IC_{50} values for *B. cinerea* and *F. solani*, when using casein blocked microtiter plates or unblocked microtiter plates. Each activity determination is the mean of at least three biological repeats (three technical repeats per assay) ± standard error of the mean (SEM).

Casein has been shown to bind Ca^{2+} (15) and the tyrocidines to form complexes with Ca^{2+} whereupon they either change in their degree of activity or type of activity (2). Therefore the decrease in activity in the blocked plates can be the result of the tyrocidines associating with Ca^{2+} which on its turn binds to casein and resultantly there is a decrease in available active peptides. At high tyrocidine concentrations peptide aggregation was also a probable cause of activity loss in the casein-blocked microtiter plates. In the reported studies we used unblocked low protein binding 96-well plates.

3.4.2 Growth of B. cinerea *and* F. solani *in different mediums*

Different species of fungi can be found in different niches on earth. *Fusarium* species, for instance, survives from arctic regions through to tropical regions (9). It follows therefore that various fungal species will prosper in varying degrees in different mediums (Table 3.1). Our results confirmed this premise. *F. solani* prospered in YTSB and LB and its growth was much faster in these two mediums than in PDB (Figure 3.2 A). *B. cinerea*, on the other hand, exhibited faster growth in PDB than in YTSB and LB (Figure 3.2 B). Both *B. cinerea* and *F. solani* grew faster on the gelatinous YTSA and PDA than in the YTSB, PDB and LB broths (Figure 3.3). Nevertheless, the growth of *F. solani* was faster on YTSA than on PDA (Figure 3.3 A) and the growth of *B. cinerea* faster on PDA than YTSA (Figure 3.3 B). Statistical analysis confirmed that these differences are significant. The growth of *F. solani* in PDB was significantly ($P<0.001$) lower than its growth in YTSB, LB, PDA and YTSA (Figure 3.4). Even though there was no significant difference in *F. solani* growth between YTSB and LB, the growth in these two mediums was significantly ($P<0.001$) lower than on the two agar mediums PDA and YTSA. Furthermore, the growth of *F. solani* on YTSA was significantly higher than on PDA.

Table 3.1: Summary of characteristics of different mediums

Medium	Abbreviation	Common use	% Nitrogen	% Fermentable sugars	Vitamins	Salt	Composition
Potato dextrose broth	PDB	Primarily for fungal growth	**	***	**	**	83% glucose, 17% potato extract, 9.5-10.5% N, <20% NaCl
Tryptone soy broth	TSB	Versatile medium	****	**	***	***	50% tryptone, 16.7% soy-peptone, 16.7% NaCl, 8.3% P_2HPO_4, 8.3% dextrose
Yeast extract tryptone soy broth	YTSB	Novel medium	****	**	****	****	20% tryptone, 6.7% soy-peptone, 46.7% NaCl, 3.3 % P_2HPO_4, 3.3% dextrose, 20% yeast extract
Lysogeny broth	LB	Primarily for bacterial growth	***	*	*** (Vit B)	****	40% tryptone, 20% yeast extract, 40% NaCl

* = low, ** = medium, *** = high, **** = very high

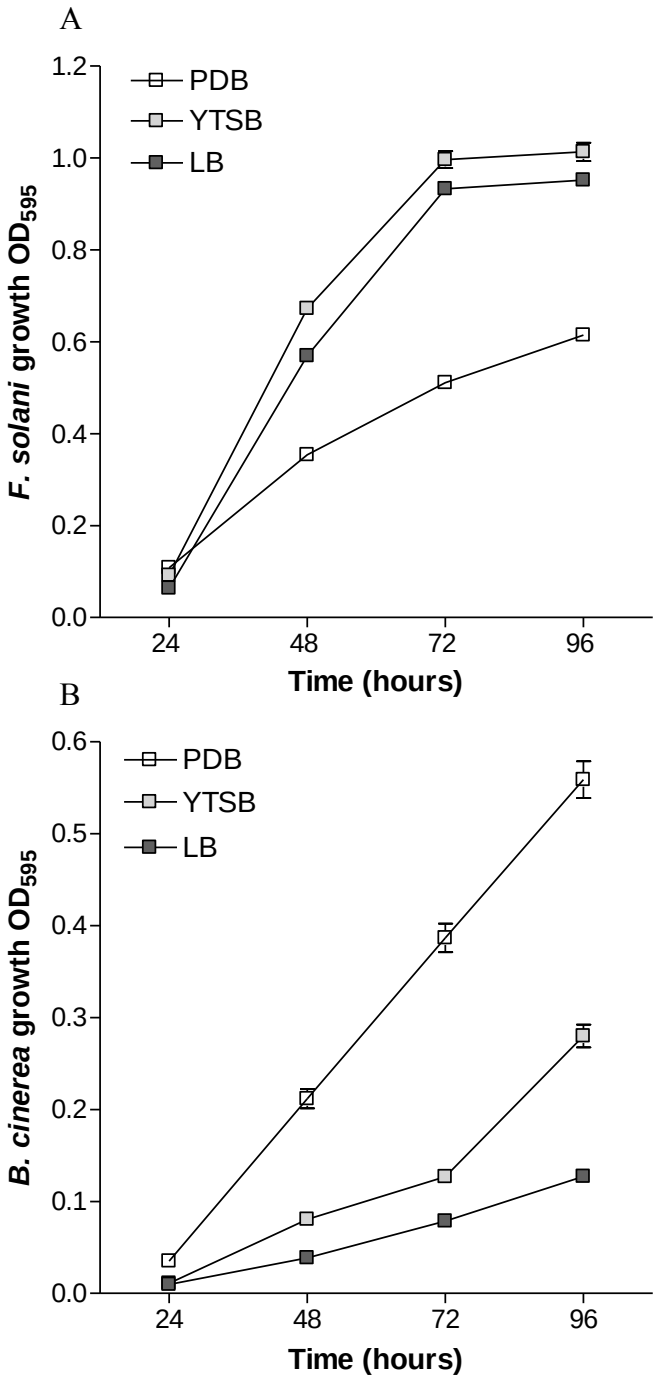

Figure 3.2: Growth of *F. solani* (**A**) and *B. cinerea* (**B**) in PDB, YTSB and LB media over a period of 96 hours. Each data point is the mean of at least 8 repeats with SEM.

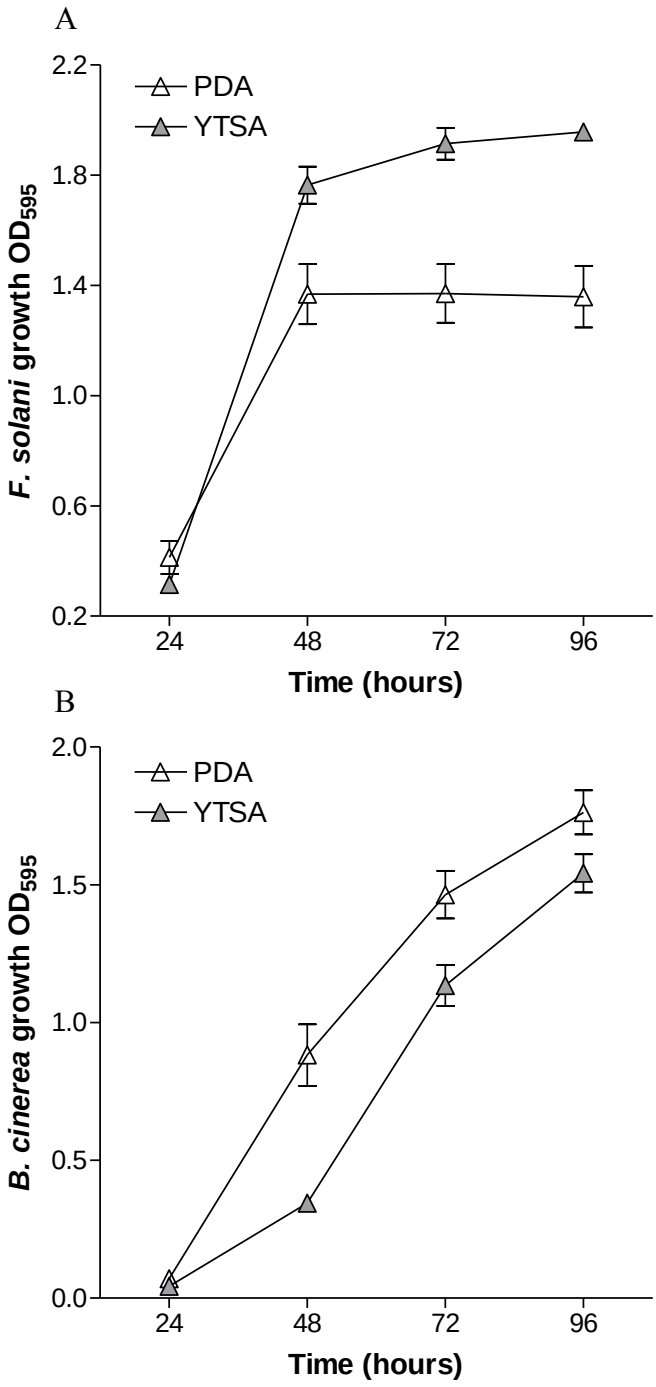

Figure 3.3: Growth of *F. solani* (**A**) and *B. cinerea* (**B**) on PDA and YTSA media over a period of 96 hours. Each data point is the mean of at least 8 repeats ± SEM.

For *B. cinerea* the growth results are quite different (Figure 3.5). *B. cinerea* growth in LB and YTSB was significantly ($P<0.001$) lower than the growth in PDB. The growth on the two agar mediums, PDA and YTSA, was significantly ($P<0.001$) higher than the growth in the broth

mediums. Furthermore, in contrast to *F. solani*, the growth of *B. cinerea* was significantly higher on PDA than on YTSA.

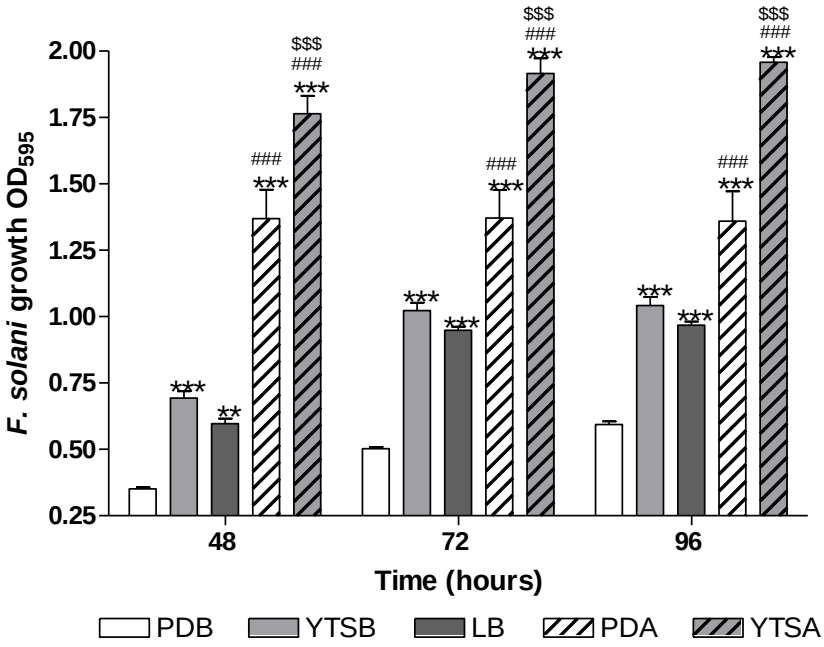

Figure 3.4: Comparison of growth of *F. solani* in PDB, YTSB, LB, PDA and YTSA over a period of 96 hours. According to the Newman-Keuls multiple comparison test *F. solani* growth in PDB is significantly lower than growth in YTSB, LB, PDA and YTSA (**P<0.01, ***P<0.001); growth in LB and YTSB are significantly lower than on PDA and YTSA ($^{###}$P<0.001) and the growth on PDA significantly lower than the growth on YTSA ($^{\$\$\$}$P<0.001). Each growth measurement is the mean of at least 8 repeats ± SEM.

In terms of nutrient composition *F. solani* prospered in the nitrogen and salt rich YTSB and YTSA mediums while *B. cinerea* preferred the less complex PDB and PDA mediums (Table 3.1). To accurately determine growth inhibition the optical density (OD_{595}) reading must at least have a value between 0.2-0.3 and *B. cinerea* only reached that growth density after 96 hours in YTSB (Figure 3.3 B and 3.5). Consequently broth assays performed in YTSB with *B. cinerea* were evaluated after a period of 96 hours. The variance in the growth of fungi from liquid broths to solid agar mediums may have an influence on peptide activity. Therefore one can only get a comprehensive view of peptide activity if their activity is evaluated in/on both liquid broth and solid agar mediums.

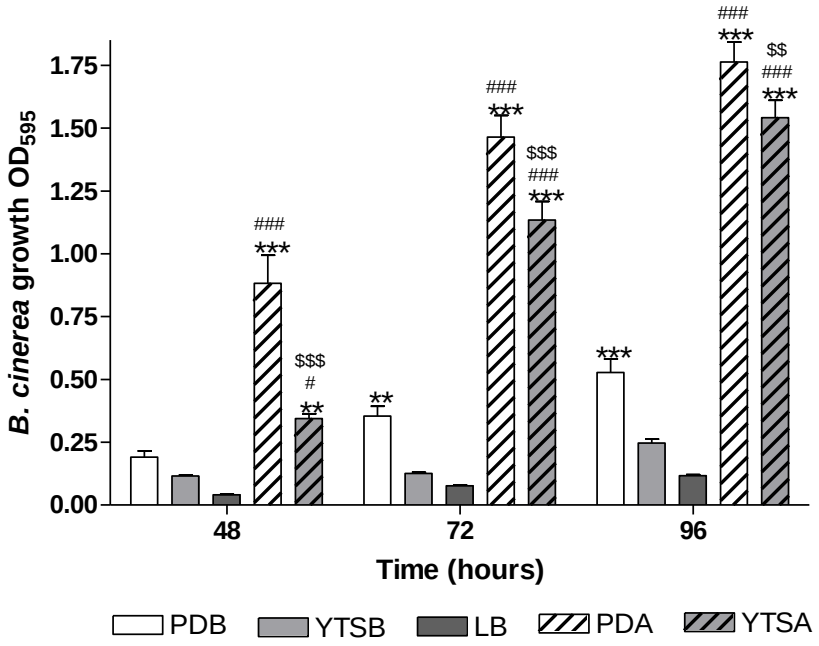

Figure 3.5: Comparison of growth of *B. cinerea* in PDB, YTSB, LB, PDA and YTSA over a period of 96 hours. According to the Newman-Keuls multiple comparison test *B. cinerea* growth in LB and YTSB are significantly lower than growth in PDB, PDA and YTSA (**P<0.01, ***P<0.001); growth in PDB are significantly lower than on PDA and YTSA ($^{\#}$P<0.05, $^{\#\#\#}$P<0.001) and the growth on YTSA significantly lower than the growth on PDA ($^{\$\$}$P<0.01, $^{\$\$\$}$P<0.001). Each growth measurement is the mean of at least 8 repeats ± SEM.

3.4.3 Growth of fungi in different concentrations of ethanol

As previously stated the tyrocidines tend to aggregate in aqueous environments forming complex structures which may influence their activity (3, 16). Since it is difficult to recover peptides from solvents such as dimethyl sulfoxide (DMSO), an ethanol/water mixture was generally used to solubilise the tyrocidines, but ethanol is a universal sterilising agent. It was therefore important to determine that the inhibitory effect observed is as a result of the tyrocidine action and not due to ethanol. The same percentage ethanol was therefore used throughout, from the initial peptide preparation through to the dilution series and in the growth control. Tyrocidines are soluble at about 1-2 mg/mL in ethanol concentrations of 10-20% (*v/v*). For dose-response assays we generally dilute the peptides 10 times on the assay medium which yields a final ethanol concentration of 1-2%. In order to assess the influence of the residual ethanol on fungal growth, *F. solani* and *B. cinerea* were cultured in YTSB, PDB and LB at final ethanol concentrations of 1.0%, 1.5% and 2.0%.

In Figure 3.6 the growth of *F. solani* and *B. cinerea* is illustrated in the different media at the various ethanol concentrations. Since we previously established that *B. cinerea* only reaches an adequate OD in YTSB subsequent to 96 hours of incubation (Figure 3.2 B and 3.5), *B. cinerea*'s growth at different ethanol concentrations in YTSB was measured up to 96 hours. As expected the growth of both fungal species were affected by increasing concentrations of ethanol (Figure 3.6). The effect was more pronounced in YTSB (Figure 3.6 AI and BI) and LB (Figure 3.6 AIII and BIII) than in PDB (Figure 3.6 AII and BII). Furthermore, *F. solani* (Figure 3.6 A) growth was more stable in the various ethanol concentrations than that of *B. cinerea* (Figure 3.6 B).

In Figure 3.7 the growth of *F. solani* at the various ethanol concentrations and in the different mediums is statistically compared. According to the Newman-Keuls multiple comparison test *F. solani* growth in YTSB medium is significantly ($P<0.001$) lower at ethanol concentrations of 1.5% and 2.0% compared to growth at 1.0% ethanol; and the growth in LB and PDB significantly ($P<0.001$) lower at 2.0% ethanol compared to the growth in 1.0% and 1.5% ethanol. When the growth in the three different mediums at a specific ethanol concentration is compared, the percentage growth in YTSB at 1.5% ethanol is significantly ($P<0.001$) lower than the growth in PDB and LB; and at 2.0% ethanol the growth in YTSB and LB is significantly lower than the growth in PDB ($P<0.001$). *B. cinerea* growth at the various ethanol concentrations in YTSB, PDB and LB is statistically compared in Figure 3.8. Since the growth of *B. cinerea* in YTSB and LB is relatively slow compared to PDB, growth after 48 and 96 hours is compared. Except for *B. cinerea* growth at 2.0% ethanol in LB, there is no significant difference in the growth of *B. cinerea* after 48 hours in each medium at the different ethanol concentrations. After 96 hours the growth in both LB and YTSB at 2.0% ethanol is significantly lower than the growth at 1.0% and 1.5% ethanol. Similar to *F. solani*, the growth of *B. cinerea* was also more stable in PDB. After 48 hours (Figure 3.8 A), at a concentration of 1.0% ethanol, the growth in YTSB ($P<0.01$) and LB ($P<0.001$) is significantly lower than in PDB. This variance in growth increases with increasing ethanol concentrations.

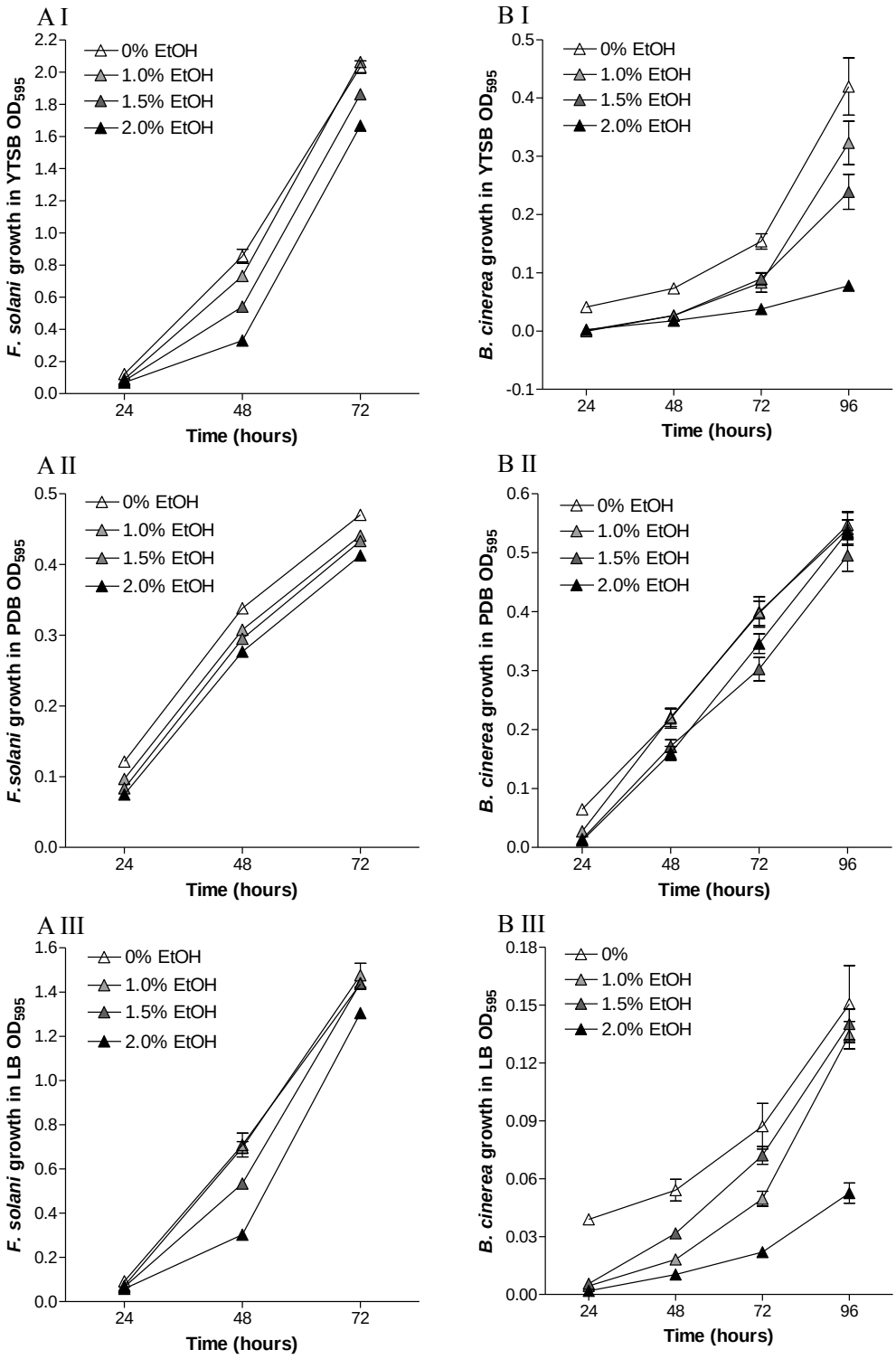

Figure 3.6: Growth of *F. solani* (**A**) and *B. cinerea* (**B**) in YTSB (I), PDB (II) and LB (III) at ethanol concentrations of 1.0%, 1.5% and 2.0%. Each data point represents the mean of at least 8 repeats ± SEM.

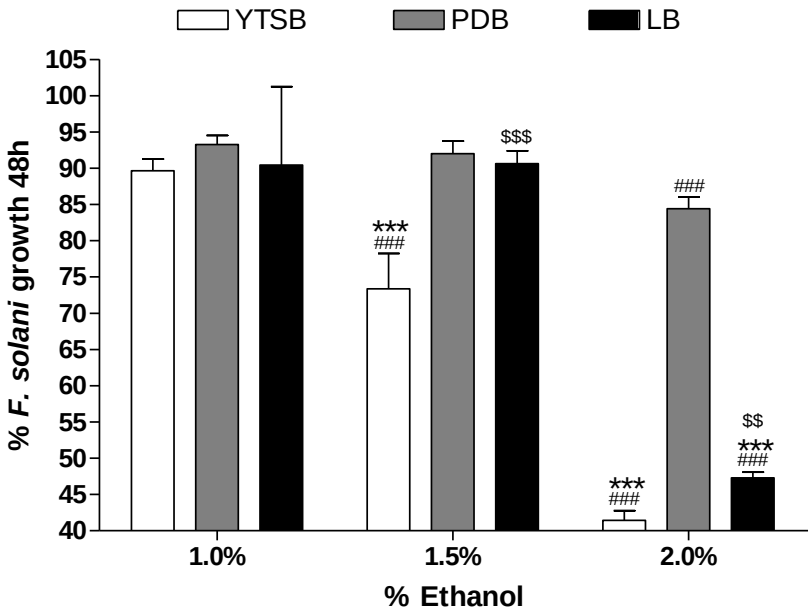

Figure 3.7: Percentage growth of *F. solani* after 48 hours in YTSB, PDB and LB media at ethanol concentration of 1.0%, 1.5% and 2.0%. According to the Newman-Keuls multiple comparison test there is significant difference between the growth of *F. solani* in the different ethanol concentrations in each medium ($^{###}$P<0.001). The growth in YTSB and LB is also significantly lower than the growth in PDB (***P<0.001); and the growth in YTSB lower than the growth in LB ($^{\$\$}$P<0.01, $^{\$\$\$}$P<0.001) at the various ethanol concentrations. Each data point represents the mean of 12 repeats ± SEM.

After 96 hours (Figure 3.8 B), as was expected, there is less variance between the different mediums. However, at an ethanol concentration of 2.0% the growth in YTSB and LB is significantly (P<0.001) lower than at concentrations of 1.0% and 1.5% and the growth in PDB is still significantly (P<0.001) higher than the growth in YTSB and LB. From these results it is evident that increasing concentrations of ethanol effects the growth of both *F. solani* and *B. cinerea*, especially at an ethanol concentration of 2.0%. Therefore a final ethanol concentration of 2.0% would not be advisable for peptide activity determination.

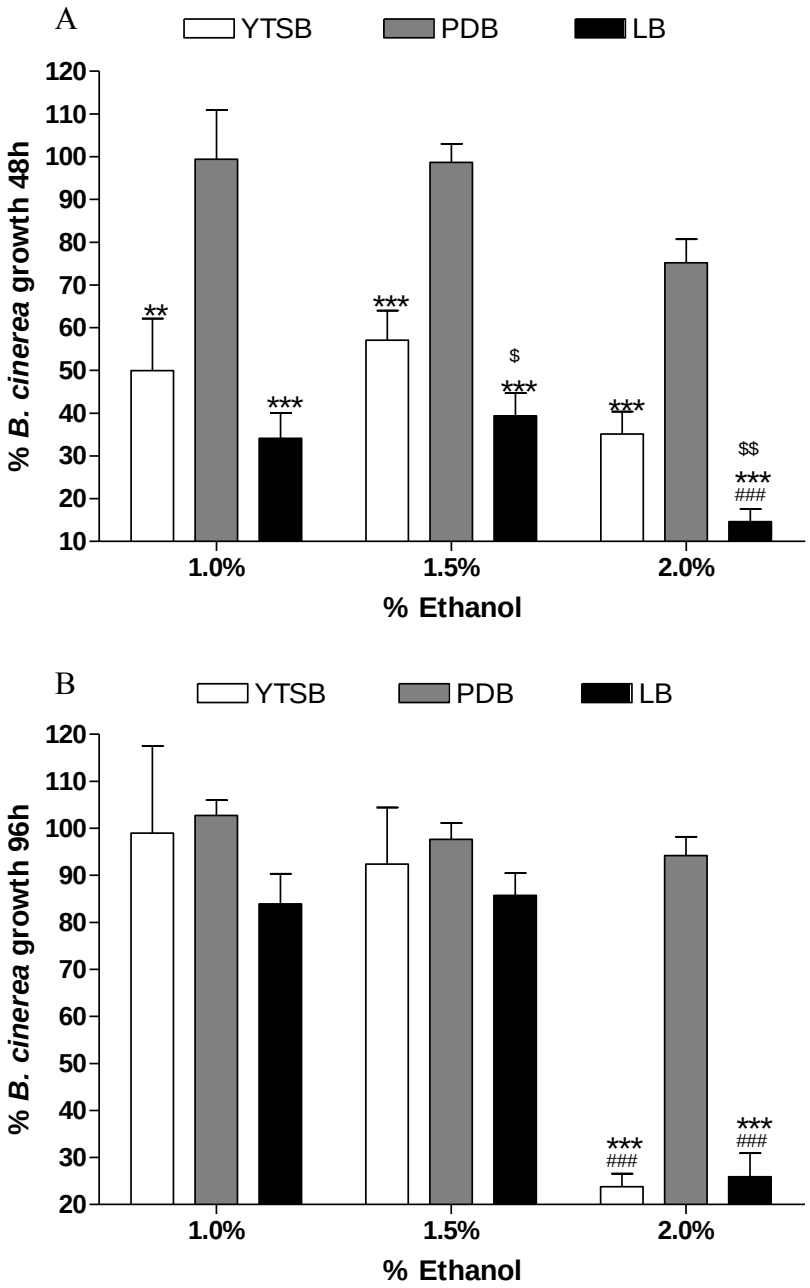

Figure 3.8: Percentage growth of *B. cinerea* after 48 hours (**A**) and 96 hours (**B**) in YTSB, PDB and LB media at ethanol concentration of 1.0%, 1.5% and 2.0%. According to the Newman-Keuls multiple comparison test there is significant difference between the growth of *B. cinerea* in 1.0 - 1.5% and 2.0% ethanol concentrations in each medium ($^{###}P<0.001$). The growth in YTSB and LB is also significantly lower than the growth in PDB ($^{**}P<0.01$, $^{***}P<0.001$); and the growth in LB lower than the growth in YTSB ($^{\$}P<0.05$, $^{\$\$}P<0.01$) at the various ethanol concentrations. Each data point represent the mean of 12 repeats ± SEM.

Furthermore, the growth of both the fungal species was relatively unaffected in PDB medium and there was no significant difference for both *F. solani* and *B. cinerea* between 1.0% and 1.5% ethanol. This is interesting since *F. solani* growth was much faster in YTSB and LB than in PDB (Figure 3.2 A and 3.4), but more affected by ethanol. Therefore the activity of the tyrocidines diluted in 10% and 15% ethanol (final concentrations of 1.0% and 1.5%) was compared in PDB.

3.4.4 Different ethanol concentrations for peptide preparation

Tyrocidines are amphipathic (17) cyclic decapeptides (18) with a β-sheet conformation that have a tendency to aggregate in aqueous environments, forming complex structures (3-5, 19). Their activity may be dependant on, or may vary in efficacy, depending on the degree of their aggregation. An ethanol in water solution is used to get the tyrocidines into solution in order to perform dilution assays. The extent of peptide aggregation, and therefore activity, will be determined by the percentage ethanol used. The higher the percentage ethanol, the lower the predilection to aggregate will be, but also the lower the fungal growth (as illustrated in section 3.4.3). Tyrocidines are soluble in ethanol concentrations of 10-20% (*v/v*) which in an assay environment gives final concentrations of 1-2% ethanol. We determined in section 3.4.3 that ethanol concentrations of 2.0% significantly decreases the growth of *B. cinerea* and *F. solani*. Such high ethanol concentrations may mask or synergise with peptide activity. Furthermore, *B. cinerea* and *F. solani* were more susceptible to increases in ethanol concentrations in YTSB and LB media. Consequently the activities of the Trc mixture, TrcC and GS were compared when prepared in either a 10% or 15% ethanol concentration (final concentrations of 1.0% and 1.5% ethanol) in PDB (Figure 3.9).

According to the Newman-Keuls multiple comparison test the activities of the Trc mixture, TrcC and GS were significantly higher when prepared in a 15% ethanol solution than a 10% ethanol solution. Therefore in order to obtain maximum peptide activity, without simultaneously causing

a significant inhibitory effect from ethanol, an ethanol concentration of 15% (to give a final concentration of 1.5%) were chosen as standard to dissolve and dilute peptides.

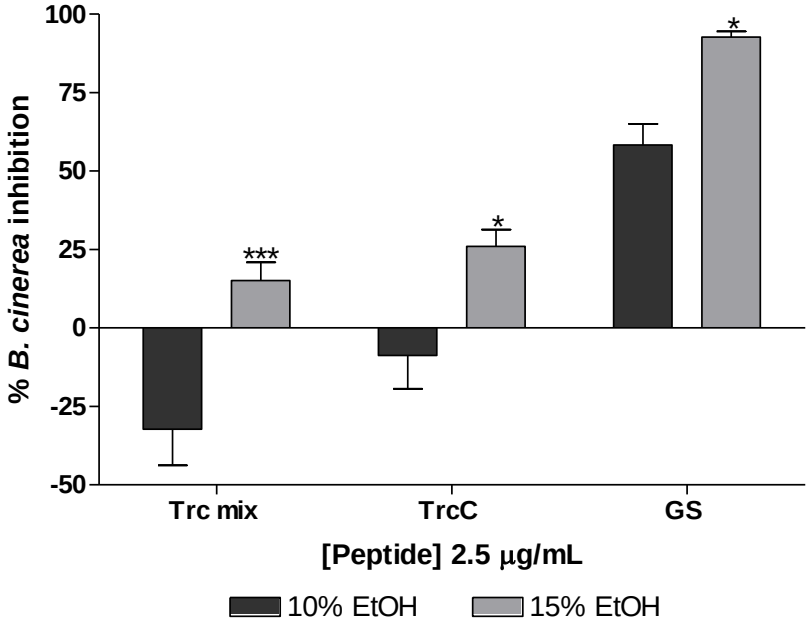

Figure 3.9: Comparison between the activity of the Trc mixture, TrcC and GS prepared either in 10% or 15% ethanol (EtOH) against *B. cinerea* grown in PDB. Antifungal activities of the Trc mixture, TrcC and GS were determined at 2.5 µg/mL prepared in either 10% or 15% ethanol, final ethanol concentrations in assay culture 1.0 % and 1.5%. According to the Newman-Keuls multiple comparison test the activity of the Trc mixture, TrcC and GS prepared in 15% ethanol is higher than that of peptides prepared in 10% ethanol (* P <0.05, ** P <0.01, *** P <0.001). The average of 18 repeats ± SEM is shown.

3.4.5 Antifungal activity of tyrocidines and gramicidin S in PDB, PDA, YTSB, and YTSA.

Various investigators in our group found that the tyrocidines' activities against a variety of target cells is influenced by their environment. If the peptides are in an aqueous or organic environment, or if monovalent and divalent ions are present, their conformation and degree of self-assembly could be influenced (2). Different conformations and levels of self-assembly affect the type and/or degree of peptide activity (20, 21). Mediums with various compositions will therefore influence tyrocidine activity in varying degrees.

Since *F. solani* exhibited the most rapid growth in YTSB (Figure 3.2 A) and *B. cinerea* in PDB (Figure 3.2 B), microdilution assays were used to compare the activities of the Trc mixture and

GS in PDB and YTSB liquid media; and on PDA and YTSA agar medium against *F. solani* and *B. cinerea* (Figure 3.10). In terms of the inhibition of *F. solani* the Trc mixture's antifungal activity was higher in YTSB than in PDB (Figure 3.10 A). The tyrocidines' activity decreased significantly on the agar mediums, especially PDA. For both PDA and YTSA 100 % inhibition of *F. solani* could not be reached at a concentration of 100 µg/mL. The activity of GS was more consistent in the various mediums. There was a slight decrease of activity on the agar medium, but not as significant as that for the Trc mixture. The variance in activity may either be ascribed to different growth forms of *F. solani* in the various mediums, differences in peptide conformation that may influence their activity or the shielding/masking of the peptide target in one or more of the mediums.

The influence of medium composition on the activity of the Trc mixture and GS against *B. cinerea* was also determined (Figure 3.10 B). Inhibition of *B. cinerea* in PDB could be determined after 48 hours. However, as was illustrated in section 3.4.2, growth of *B. cinerea* is slow in YTSB and therefore inhibition determinations could only be performed after a period of 96 hours. The activity of the Trc mixture was much more consistent against *B. cinerea* in the different mediums. A decrease in activity was again observed on the agar mediums, but was not as noteworthy. *B. cinerea* growth could still be inhibited at concentrations below 16 µg/mL. GS's activity was again relatively consistent in/on all four mediums with slightly lower activity on the YTSA medium.

The Trc mixture's, and to a lesser extent GS's, activities are influenced by the activity test environment. The degree whereby their activities differed was also affected by the target organism. The activity against *B. cinerea* in the different mediums does not seem to fluctuate as significantly as the activity against *F. solani*. Evidently the composition of the environment does not only have an influence on the growth of fungi, but also on the activity of the tyrocidines and GS.

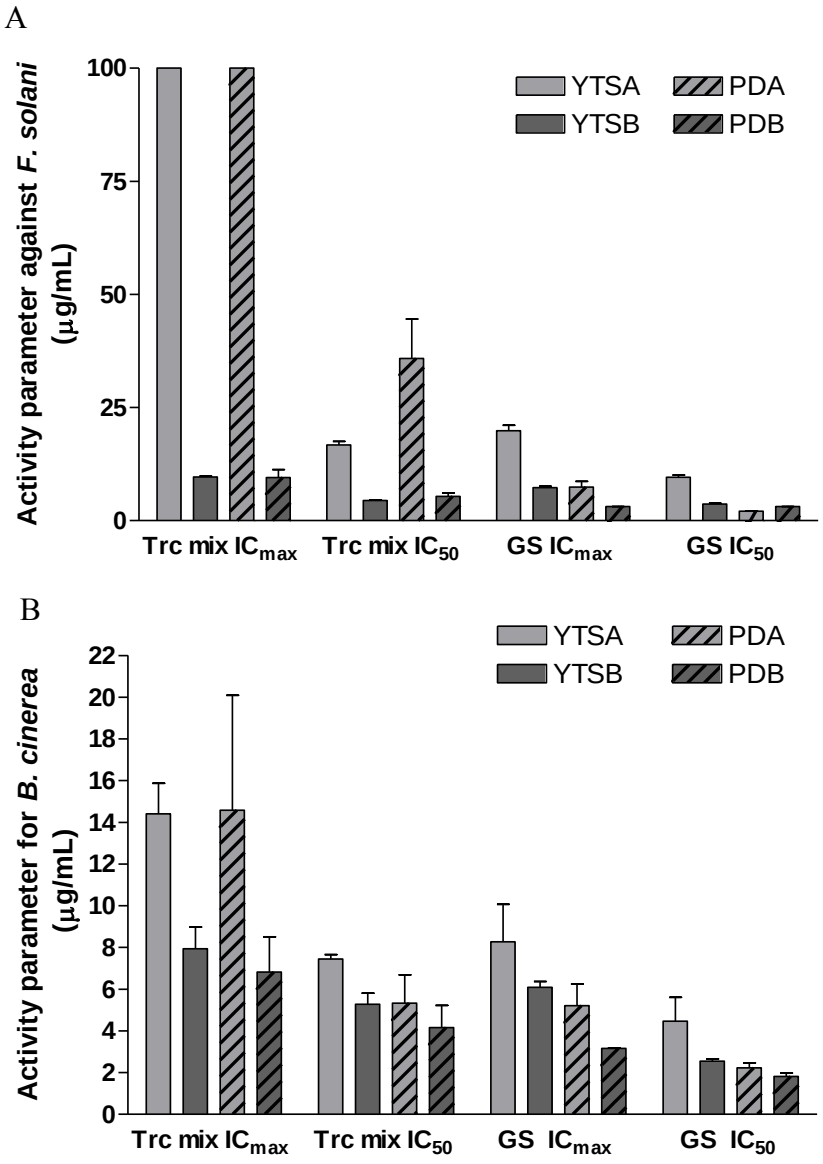

Figure 3.10: Activity parameters for the Trc mixture and GS for inhibition of *F. solani* (**A**) and *B. cinerea* (**B**) in YTSA, YTSB, PDA and PDB. Activity determinations were performed in triplicate with triplicate technical repeats per assay ± SEM.

3.5 Conclusion

The tyrocidines were found to exhibit an increase in activity when higher percentages ethanol was used for the dissolving and dilution of peptides. However, at higher concentrations ethanol, fungal growth was inhibited. The growth of both *F. solani* and *B. cinerea* was unaffected at concentrations ≤1.5% ethanol and therefore ≤15% ethanol in peptide solvent must preferably be used to avoid any inhibitory effect as a result of ethanol, but to still retain tyrocidine activity. A concentration of 15 % ethanol was chosen as standard for peptide solvent and PDB was chosen as standard assay medium, especially for mode of action studies (Chapters 4-6). Furthermore, a final ethanol concentration of 1.5% was included in growth controls to normalise any influence ethanol may have on the results. All assays reported in Chapters 4-5 were performed in unblocked low protein binding microtiter plates. Since the growth of fungi, in this case *F. solani* and *B. cinerea* were clearly influenced by their environment, as well as the activities of the tyrocidine mixture and to a lesser extent GS, activity tests on PDA and in YTSB medium were also included in Chapters 4-5 to obtain a more accurate understanding of the tyrocidines antifungal action.

3.6 References

1. **Troskie AM, Vlok NM, Rautenbach M.** 2012. A novel 96-well gel-based assay for determining antifungal activity against filamentous fungi. J. Microbiol. Methods. **91:**551-558.

2. **Spathelf BM.** 2010. Qualitative structure-actvity relationships of the major tyrocidines, cyclic decapeptides from *Bacillus aneurinolyticus*. PhD Thesis, Department of Biochemistry, University of Stellenbosch, http://scholar.sun.ac.za/handle/10019.1/4001.

3. **Yount NY, Yeaman MR.** 2005. Immunocontinuum: Perspectives in antimicrobial peptide mechanisms of action and resistance. Protein and Peptide Letters. **12** 49-67.

4. **Ruttenberg MA, King TP, Craig LC.** 1965. The use of the tyrocidines for the study of conformation and aggregation behavior. J. Am. Chem. Soc. **87:**4196-4198.

5. **Ruttenberg MA, King TP, Craig LC.** 1966. The chemistry of tyrocidine. VII. Studies on association behavior and implications regarding conformation. Biochemistry. **5:**2857-2864.

6. **Dantigny P, Guilmart A, Radoi F, Bensoussan M, Zwietering M.** 2005. Modelling the effect of ethanol on growth rate of food spoilage moulds. International Journal of Food Microbiology. **98:**261-269.

7. **Vlok NM.** 2005. Investigation of complexation and antimicrobial activity of gramicidin S in the presence of lipopeptides from *Bacillus subtilis*. PhD Thesis, Department of Biochemistry, University of Stellenbosch.

8. **Rautenbach M, Vlok NM, Stander M, Hoppe HC.** 2007. Inhibition of malaria parasite blood stages by tyrocidines, membrane-active cyclic peptide antibiotics from *Bacillus brevis*. Biochim. Biophys. Acta. **1768:**1488-1497.

9. **Mule G, Gonzalez-Jean MT, Hornok L, Nicholson P, Waalwijk C.** 2005. Advances in molecular diagnosis of toxigenic Fusarium species: A review. Food Additives and Contaminants. **22:**316–323.

10. **Spathelf BM, Rautenbach M.** 2009. Anti-listerial activity and structure–activity relationships of the six major tyrocidines, cyclic decapeptides from *Bacillus aneurinolyticus*. Bioorg. Med. Chem. **17:**5541-5548.

11. **Dulbecco R, Vogt M.** 1954. Plaque formation and isolation of pure lines with Poliomyelitis viruses. The Journal of Experimental Medicine. **99:**167-182.

12. **Broekaert WF, Terras FRG, Cammue BPA, Vanderleyden J.** 1990. An automated quantitative assay for fungal growth inhibition. FEMS Microbiol. Lett. **69:**55-59.

13. **du Toit EA, Rautenbach M.** 2000. A sensitive standardised micro-gel well diffusion assay for the determination of antimicrobial activity. Journal of microbiological methods. **42:**159-165.

14. **Rautenbach M, Gerstner GD, Vlok NM, Kulenkampff J, Westerhoff HV.** 2006. Analyses of dose-response curves to compare the antimicrobial activity of model cationic α-helical peptides highlights the necessity for a minimum of two activity parameters. Anal. Biochem. **350:**81-90.

15. **Zittle CA, Della MES, Rudd RK, Custer JH.** 1958. Binding of calcium to casein: Influence of pH and calcium and phosphate concentrations. Archives of Biochemistry and Biophysics. **76:**342-353.

16. **Munyuki G, Jackson GE, Venter GA, Kövér KE, Szilágyi L, Rautenbach M, Spathelf BM, Bhattacharya B, Van der Spoel D.** 2013. β-Sheet structures and dimer models of two major tyrocidines, antimicrobial peptides from *Bacillus aneurinolyticus*. Biochemistry. **52:**7798-7806.

17. **Marques MA, Citron DM, Wang CC.** 2007. Development of tyrocidine A analogues with improved antibacterial activity. Bioorg. Med. Chem. **15:**6667-6677.

18. **Tang X-J, Thibault P, Boyd RK.** 1992. Characterisation of the tyrocidine and gramicidin fractions of the tyrothricin complex from *Bacillus brevis* using liquid chromatography and mass spectrometry. Int. J. Mass Spectrom. Ion Processes. **122:**153-179.

19. **Paradies HH.** 1979. Aggregation of tyrocidine in aqueous solutions. Biochemical and Biophysical Research Communications. **88:**810-817.

20. **Jelokhani-Niaraki M, Prenner EJ, Kay CM, McElhaney RN, Hodges RS.** 2002. Conformation and interaction of the cyclic cationic antimicrobial peptides in lipid bilayers. The Journal of Peptide Research. **60:**23-36.

21. **Jelokhani-Niaraki M, Prenner EJ, Kay CM, McElhaney RN, Hodges RS, Kondejewski LH.** 2001. Conformation and other biophysical properties of cyclic antimicrobial peptides in aqueous solutions. The Journal of Peptide Research. **58:**293-306.

Addendum (Chapter 3)

A novel 96-well gel-based assay for determining antifungal activity against filamentous fungi

In the course of the development and optimisation of the antifungal assays, the significant effect of the assay environment on activity test results was observed. Furthermore, it was noticed that the morphogenic effect of the peptides (i.e. hyperbranching) influenced the accuracy of the assay results. Consequently an activity test was developed which will allow activity determination on an alternative medium to that of broth; and which will also minimise the inaccuracy experienced with assay tests that rely on spectrophotometric analysis of results.

The Addendum to Chapter 3 has been published in *Journal of Microbiological Methods*, Volume 91, September 2012, pages 551-558; first author A. M. Troskie (all experimental work, data analysis, writing of article, co-authors N. M. Vlok (initial experimental work) and M. Rautenbach (co-writer and editing, critical evaluation of study and data). This article, as published, is included as Addendum Chapter 3 of this thesis.

~

A novel 96-well gel-based assay for determining antifungal activity against filamentous fungi

Anscha Mari Troskie, Nicolas Maré Vlok and Marina Rautenbach*

BIOPEP Peptide Group, Department of Biochemistry,
University of Stellenbosch, Private Bag X1, Matieland 7600, South Africa

*Communicating author:

Marina Rautenbach

BIOPEP Peptide Group
Department of Biochemistry
University of Stellenbosch
Private Bag X1, Matieland 7602
Republic of South Africa
Tel: +27-21-8085872/8
Fax: +27-21-8085863
E-mail: mra@sun.ac.za

Keywords:

Filamentous fungi, hyperbranching, micro-gel antifungal assay

Abstract

In recent years the global rise in antibiotic resistance and environmental consciousness lead to a renewed fervour to find and develop novel antibiotics, including antifungals. However, the influence of the environment on antifungal activity is often disregarded and many *in vitro* assays may cause the activity of certain antifungals to be overestimated or underestimated. The general antifungal test assays that are economically accessible to the majority of scientists primarily rely on visual examination or on spectrophotometric analysis. The effect of certain morphogenic antifungals, which may lead to hyperbranching of filamentous fungi, unfortunately renders these methods unreliable. To minimise the difficulties experienced as a result of hyperbranching, we developed a straightforward, economical 96-well gel-based method, independent of spectrophotometric analysis, for highly repeatable determination of antifungal activity. For the calculation of inhibition parameters, this method relies on the visualisation of assay results by digitisation. The antifungal activity results from our novel micro-gel dilution assay are comparable to that of the micro-broth dilution assay used as standard reference test of The Clinical and Laboratory Standard Institute. Furthermore, our economical assay is multifunctional as it permits microscopic analysis of the preserved assay results, as well as retendering highly reliable data.

1. Introduction

The upsurge in antimicrobial resistance in recent years, together with the detrimental impact of conventional antibiotics on the environment, necessitates the search for novel antimicrobials (Hancock, 2001; Hancock, 1997; Steinstraesser et al., 2009). However, to assess the activity of potential antifungals, a standardised accurate quantitative test is vital. Various antifungal growth assays have been developed, each with their own advantages and disadvantages (Broekaert et al., 1990). The disc-plate diffusion assay, where substance saturated paper discs are placed on the top/at the edge of an emerging fungal lawn (Franrich et al.; 1983, Mauch et al. 1988, Roberts and Selitrennikoff, 1986), is a commonly utilised method (Broekaert et al., 1990). However, since the extent of fungal growth inhibition can merely be evaluated on arbitrary scores and the *in situ* concentrations cannot be accurately determined, the disc plate diffusion assay and analogous spot and radial assays are only semi-quantitative tests (Broekaert et al., 1990). Furthermore, diffusion tests require an appreciable amount of the test substance and are not readily adapted for high throughput analyses. Methods that permit more accurate quantification of inhibition are procedures where the length of the fungal hyphae is measured (Broekaert et al., 1988) or were the dry mycelia weight is measured (Odebode et al., 2006). These methods are still not ideal as they are arduous and hyphi measurement can only be applied to young fungal germlings (Broekaert et al., 1990). Methods that are not based on light absorption distinguish between live and dead cells by either metabolic measurement (Broekaert et al., 1990) or flow cytometry (Green et al., 1994). However, the fungal development stage in one culture and thus metabolism is unfortunately not always uniform (Damir, 2006; Rautio et al., 2006) and it has also been observed that some organisms increase their metabolic rate when experiencing stress (Fehri et al., 2005; Hilpert et al., 2010; Tzeng et al., 2005). Consequently tests based on the measurement of metabolic components are not recommended for the evaluation of fungal

growth inhibition (Broekaert et al., 1990). With the purpose of eliminating the complications in fungal growth inhibition tests, Broekaert et al. (1990) developed a quantitative broth dilution assay based on the absorbance at 595 nm that was set as the standard reference test (M38-A2) for antifungal activity by The Clinical and Laboratory Standard Institute (CLSI) (previously known as The National Committee for Clinical Laboratory Standards, United States of America) (CLSI, 2008).

As the broth assays could be adapted to be done in 96-well microplates, this assay could be used for high through put analyses. However the broth assay is highly dependent on spectrophotometric analysis. Moreover, fungi can be found in diverse niches on earth and do not always grow well in liquid environments. They can be surface pathogens on for instance grapes (Cotoras and Silva, 2005) and potatoes (El-Banna et al., 1984), or they can develop in the soil (Vakalounakis and Chalkias, 2004) or the xylem (Alaniz et al., 2007) of plants. Different fungi will therefore thrive in varying extents in various environments and consequently also in different experimental mediums and/or settings. Also fungi have different growth stages that generally differ in sensitivity to fungicides. It is therefore advisable that substances evaluated for its ability to inhibit fungal growth be tested in or on more than one growth medium and growth stage. Broth dilution assay only assess antibiotics on their ability to inhibit the fungi in a liquid environment.

The broth dilution inhibition test assays, based on spectrophotometric measurements, are better suited to the more homogenous bacterial growth in suspension than heterogeneous fungal growth. The growth of bacteria increases the optical density of the medium uniformly giving a generally consistent increase in spectrophotometric measurements. However, antibiotics inhibiting fungal growth could have morphogenic and non-morphogenic activity on fungal growth of filamentous fungi. Morphogenic antifungals will alter the morphology of fungi while non-morphogenic antifungals, although inhibiting fungal growth, won't lead to

any alterations in morphology. One of the effects of morphogenic antifungals is hyperbranching of filamentous fungi: natural hyphal elongation is inhibited and multiple germination tubes and hyphi form, leading to high density growth in one small area. The variable influence on fungal growth will therefore influence the detected changes in optical density; therefore assays based on spectrophotometric measurements could lead to variance in determination of inhibition parameters of filamentous fungi.

Du Toit and Rautenbach (2000) developed a quantitative micro-gel well diffusion assay which adapted the traditional radial diffusion test for bacteria so that it can be performed in microtiter plates. This test has the advantage that a larger scale experiment can be executed with a smaller amount of test substance than is used for the conventional radial diffusion assays (du Toit and Rautenbach, 2000). The dose response results could also be enhanced using Coomassie blue staining and preserved using formaldehyde for future analyses. It has been suggested that gel-based methods are better able to assist in exposing antimicrobial resistance (Pfaller et al., 2001). Using this gel-based assay as basis, our aim was to develop an economical, practical gel-based antifungal assay, comparable to broth-based assays that will eliminate the complications experienced using conventional methods for determining filamentous fungal inhibition. We modified the method of Du Toit and Rautenbach (2000) for determination of fungal growth inhibition on solid environments. To limit or eliminate the variance of visual and spectrophotometric measurements as a result of hyperbranching, we utilised Coomassie blue to enhance the visualisation of fungal growth/inhibition, which was determined by simple digitisation of the dose-response result.

2. Materials

The fungal strains *Fusarium solani* and *Botrytis cinerea* was provided by the Department of Plant Pathology, University of Stellenbosch. The potato dextrose broth (PDB), potato

dextrose agarose (PDA) and Tween 20® were obtained from Fluka (St. Louis, USA). Ethanol (99.9%) and sodium chloride were obtained from Merck Chemicals (Pty) (Wadeville, Gauteng). The yeast extract powder, tryptone soy broth and agar agar powder for the yeast extract tryptone soy broth (YTSB) and yeast extract tryptone agarose were from Biolab Merck (Wadeville, Gauteng). Strawberry halves were used for *B. cinerea* growth. The sterile polypropylene plates were provided by Nunc (Denmark). Sterile culture dishes and microtiter plates where obtained from Corning Incorporated (USA) and sterile petri dishes from Lasec (Cape Town, South Africa). Analytical quality water was prepared by passing water from a reverse osmoses plant through a Millipore (Milford, USA) Milli Q® water purification system.

3. Methods

3.1 Growth and harvesting of fungi

Fusarium solani were grown at 23-25 ˚C on PDA until sporulation (± 2 weeks). Spores were harvested with 3 mL of 0.1 % Tween-analytical water. *Botrytis cinerea* were grown on sterilised strawberry halves in culture dishes at 23-25 ˚C until sporulation (± 3 weeks). Spores were harvested dry, using vacuum. Spores were then counted using a counting chamber. Standard practices to ensure sterility were followed throughout these procedures.

3.2 Determining growth in different mediums

Growth of *F. solani* and *B. cinerea* in PDB and YTSB was determined using 96-well microtiter plates (Refer to Table 1 for media compositions). The suspensions for the broths consisted of half strength PDB or YTSB, together with fungal spores so that in the end, each well had a total of 2000 spores (Broekaert et al., 1990) and a volume of 100 µL. Plates were incubated at 23-25 ˚C and growth measured every 24 hours for 96 hours. Light dispersion of

each well was spectrophotometrically determined at 595 nm using a Biorad microtiter plate reader.

3.3 Micro-broth dilution antifungal assay

The activities of gramicidin S and bifonazole were determined against *F. solani* and *B. cinerea* using micro-broth dilution assays (Broekaert et al., 1990; du Toit and Rautenbach, 2000). All procedures were performed so as to ensure sterility. The broth dilution assays were performed in sterile 96-well microtiter plates. The broth suspension consisted of fungal spores suspended in half strength PDB whereof 90 µL were added to the wells so that each well had a total of 2000 spores (Broekaert et al., 1990). Gramicidin S was dissolved in 15 % ethanol to a concentration of 1.00 mg/mL. Doubling dilution series were made in polypropylene microtiter plates using 15% ethanol. Bifonazole was diluted in 20% ethanol to a concentration of 1.00 mg/mL and doubling dilution series were made with half strength PDB. Antibiotic (10 µL) were then added to the wells containing broth suspension. Growth control received 10 µL of 15% ethanol instead of antibiotic. Sterility control was a combination of half strength PDB and a final ethanol concentration of 1.5%. All wells had a final volume of 100 µL. Subsequent to antibiotic addition the microtiter plates were covered tightly with tinfoil, sealed with parafilm and incubated at 23-25 ˚C for 48 hours. Light dispersion of each well was spectrophotometrically determined at 595 nm using a Biorad microtiter plate reader.

3.4 Micro-gel antifungal assay

The PDA (65 ˚C) was pipetted into sterile microtiter plates using the reverse pipetting method (du Toit and Rautenbach, 2000) so that each well contained 70 µL. On the cooled/set plates 20 µL of spore-half strength PDB solution was added so that each well had 2000 spores. Gramicidin S and bifonazole were respectively dissolved in 15% and 20% ethanol to a

concentration of 1.00 mg/mL. Doubling dilution series were made in polypropylene microtiter plates using either 15% ethanol (gramicidin S) or half strength PDB (bifonazole). After the spores had time to settle on the PDA, a 10 µL of fungicide dilution was added. Growth control received 10 µL of 15% ethanol in water solution. Sterility control was a combination of 20 µL half strength PDB and 10 µL 15% ethanol. The microtiter plates were incubated at 23-25 ˚C for 48 hours. Light dispersion of each well was spectrophotometrically determined at 595 nm using a Biorad microtiter plate reader.

Table 1

Summary of characteristics of different mediums for fungal cultures

Medium	Abbr.	Common use	Nitrogen	Ferment-able sugars	Vita-mins	Salt	Composition
Potato dextrose broth/ agar	PDB/ PDA*	Primarily for fungal growth	average	high	average	average	83% glucose, 17% potato extract, 9.5-10.5% N, <20% NaCl *includes 1% agar
Yeast extract tryptone soy broth/ agar	YTSB/ YTSA*	Novel medium	Very high	average	Very high	Very high	20% tryptone, 6.7% soy-peptone, 46.7% NaCl, 3.3 % hydrogen phosphate, 3.3% dextrose, 20% yeast extract *includes 1% agar

3.5 Staining and destaining

The PDA plates were stained with Coomassie blue stain (0.063% Coomassie blue R-250, 50% methanol, 10% acetic acid) for one hour. Subsequent to gently shaking out the stain, the plates were destained (12.5% isopropanol, 10% acetic acid) for 72 hours, changing the destain three times. The results were captured with a Canon 600D camera.

3.6 Digitisation of results

For the digitisation of the results from the stained PDA plates, high resolution (18 mega pixels) photographs of the plates were analysed as gels, converted to grey scale, in UN-

SCAN-IT *gel*™, version 6.1 from Silk Scientific Corporation. The average pixel count for each well was used to calculate the growth or growth inhibition of *B. cinerea* and *F. solani* by gramicidin S and bifonazole.

3.7 Data processing

In order to calculate the percentage growth inhibition the light dispersion or average pixel count at each concentration was used (Eq. 3.7.1) (Rautenbach et al., 2005).

$$\% \text{ growth inhibition} = 100 - \frac{(A_{595} \text{ of well - Average } A_{595} \text{ of background})}{\text{Average } A_{595} \text{ of growth wells - Average } A_{595} \text{ of background}} \qquad 3.7.1$$

GraphPad Prism® 4.00 (GraphPad Software, San Diego, USA) were used to plot the growth and dose response curves. Non-linear regression and sigmoidal curves (with a slope <7) were fitted (Eq. 3.7.2) (Rautenbach et al., 2005) for dose response analysis.

$$Y = \frac{bottom + (top - bottom)}{1 + 10^{\log IC_{50} \times Activity\ \ slope}} \qquad 3.7.2$$

Top represents growth at high fungicide concentration and bottom growth in the absence of fungicide. The point halfway between top and bottom (IC_{50}) represents the concentration necessary to cause 50% growth inhibition. The activity slope, related to the Hill slope, defines the slope of the curve. The IC_{max} represents the x-value at the intercept between the slope and the top plateau. The IC_{max} is therefore the calculated concentration of minimum inhibition (MIC) (Rautenbach et al., 2005). For determining the lethal concentration (LC) values we used the first fungicide concentration where no growth is both visually and microscopically observable in a well.

GraphPad Prism® was also used for the statistical analysis of data. Analysis included 95% confidence levels, absolute sum of squares, standard error of the mean and Newman-Keuls multiple comparison test.

4. Results and Discussion

4.1 Growth of fungi in different environments

Different species of fungi can be found in different niches on earth. It follows therefore that various fungal species will prosper in varying degrees in different mediums. We tested this hypothesis by monitoring the growth of *F. solani* and *B. cinerea* in/on different mediums (Refer to Table 1 for composition of media).

Both *B. cinerea* and *F. solani* grew faster on the gelatinous YTSA and PDA than in the aqueous YTSB and PDB (Figure 1). In terms of nutrient composition *F. solani* prospered in the nitrogen and salt rich YTSB and YTSA mediums, while *B. cinerea* preferred the less complex PDB and PDA mediums (Figure 1). However, to more reliably determine growth inhibition the OD_{595} measurement must at least have a value >0.10 (OD reading reliable at two significant digits). *B. cinerea* only reached such growth density after 96 hours in YTSB/YTSA and consequently any broth assays performed in YTSA/YTSA with *B. cinerea* can only be evaluated after a period of 96 hours. Hence it was decided that micro-broth dilution assays, as well as a novel micro-gel assay using PDB and PDA respectively as growth media, will be utilised for development of our micro-gel assay and comparison of the antifungal activity of the commercial fungicide, bifonazole, and the broad spectrum antimicrobial and lytic peptide, gramicidin S.

4.2 Antifungal assays

Broth dilution assays will support fungal growth form and/or species that prosper in environments with high water and low oxygen levels. The variation in fungal growth on the different mediums suggest that the fungi will be more susceptible to fungicidal action in certain mediums than in other and thus the growth medium could have an influence on the

activity of the antifungal compounds tested. The use of only broth dilution assays is consequently not adequate in determining the scope of antifungal activity of a substance. Therefore, to better assess the activity of a potential fungicide, it is necessary to evaluate their activity both in liquid broth and on solid/gel media.

We confirmed the antifungal activity of a known fungicide, bifonazole and a broad spectrum antimicrobial peptide, gramicidin S using a standard the micro-broth dilution antifungal assay accepted by the CLSI (CLSI, 2008), The two antifungal compounds exhibited micromolar liquid phase activity towards both *B. cinerea* and *F. solani*, the two selected filamentous fungal species (Table 2).

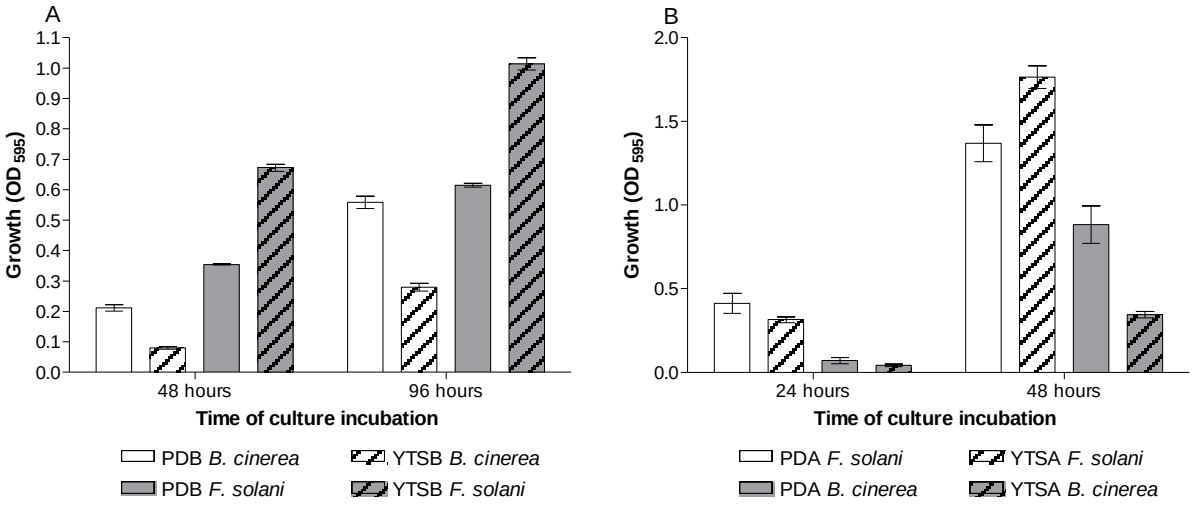

Fig. 1. Growth of *F. solani* and *B. cinerea* in PDB and YTSB (A) on PDA and YTSA (B). The growth progression of the fungi in/on the various media was evaluated over a period of 96 hours. Each growth measurement is the mean of at least 8 repeats ± SEM. Growth was determined spectrophotometrically.

Table 2
Summary of the activity parameters obtained for bifonazole and gramicidin S against *B. cinerea* and *F. solani*.

Growth Medium	Fungal target	Bifonazole		Gramicidin S	
		IC_{50}±SEM (*n*)	IC_{max}±SEM (*n*)	IC_{50}±SEM (*n*)	IC_{max}±SEM (*n*)
PDB	*B. cinerea*	7.7 ± 1.6 (5)	16 ± 2.3 (5)	1.8 ± 0.3 (4)	2.7 ± 0.7 (4)
	F. solani	14 ± 1.7 (5)	53 ± 9.0 (5)	2.6 ± 0.2 (4)	5.3 ± 1.8 (4)
PDA	*B. cinerea*	9.6 ± 0.5 (4)	20 ± 0.3 (4)	2.2 ± 0.2 (4)	4.1 ± 0.2 (4)
	F. solani	25 ± 2.4 (5)	71 ± 8.7 (5)	6.1 ± 0.1 (7)	8.3 ± 0.3 (7)

The inhibition parameter values of gramicidin S and bifonazole are given in µM. Each value represents the mean of *n* biological repeats, with 4 technical repeats per assay ± SEM.

4.3 Development of a 96-well gel-based antifungal assay

We adapted the micro-gel diffusion assay described by du Toit and Rautenbach (2000) to be suitable for antifungal activity determination. For example, PDA was used as solid growth medium, fungal spores were place on top of the gel and we introduced a novel data visualisation method using digitisation.

Spectrophotometer light absorption readings of the micro-gel dilution assays were initially used to assess the activity of gramicidin S and bifonazole. Hyperbranching can influence results to over- or underestimate antifungal activity. Due to the hyperbranching and uneven growth, the readings were comparable, but slightly more error prone to that of the micro-broth antifungal assay (results not shown). Optimisation of the data visualisation was therefore very important. Although most of the problems associated with the determination of antifungal activity in different environments are addressed by doing both the broth and micro-gel dilution assays, one problem still remains: hyperbranching of filamentous fungi induced by morphogenic antifungals. Hyperbranching leads to very dense growth of fungi on one spot and there is no hyphal elongation. Therefore the fungal growth is not uniform in a well and will lead to false readings, as most microtiter plate readers only determine the light absorption or dispersion through the middle of the plate's well. A method where the growth

of the entire well can be determined will therefore be ideal, as well as having the option to determine mode of action and survival microscopically in the same assay.

In our novel micro-gel assays, performed on PDA, the fungi in each well were stained with Coomassie blue (so as to be able to distinguish more accurately between areas of no growth and growth), photographed or scanned and analysed by digitisation software (UN-SCAN-IT *gel*™, version 6.1). The PDA plates stained satisfactorily and clear visual distinction could be made between growth and well with medium or no growth (Figure 2). Because the fungi were fixed and stained the result is preserved for further analysis, such as microscopy. In Figure 3, microscopy photographs of the fungal growth in some of the wells are shown and it is clear that the observed *F. solani* growth was due to hyperbranching in the presence of the antifungal compound. Furthermore, the staining process accentuates the morphology of the fungi which allows for enhanced microscopic photography (Figure 3). The ability to discern fungal morphology and colonies is enhanced. Therefore one is better able to detect any alterations induced by antibiotic action and, if the initial spore concentration is known, the inhibition of fungal germination/growth at a certain concentration of antibiotic can be determined through colony counting.

Staining the PDA plates not only assisted in improving the microscopic visualisation, including hyperbranching, but also facilitated the preservation of the PDA plates (Figure 2). By digitally capturing the enhanced assay results and digitising it (specifically measuring the pixel intensity in each well) the well in its entirety is taken into account and a small patch of growth won't be missed, or alternatively, seen as high/dense growth. The digitized data showed that our assays were highly repeatable with the standard error of the mean (SEM) for percentage inhibition at each concentration at less than 2%.

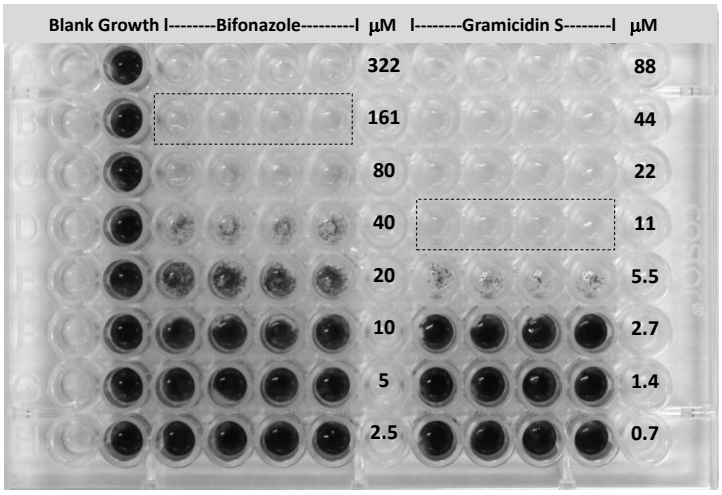

Fig. 2. A representative 96-well PDA plate with Coomassie blue stained *F. solani*. The dose response of bifonazole (columns 3-6) and gramicidin S (columns 8-11) towards *F. solani* are visualised by die blue stained fungi. The growth controls (Gr) are shown in column 2 and blank/sterility (Bl) controls in column 1. LC values are indicated with the dotted line.

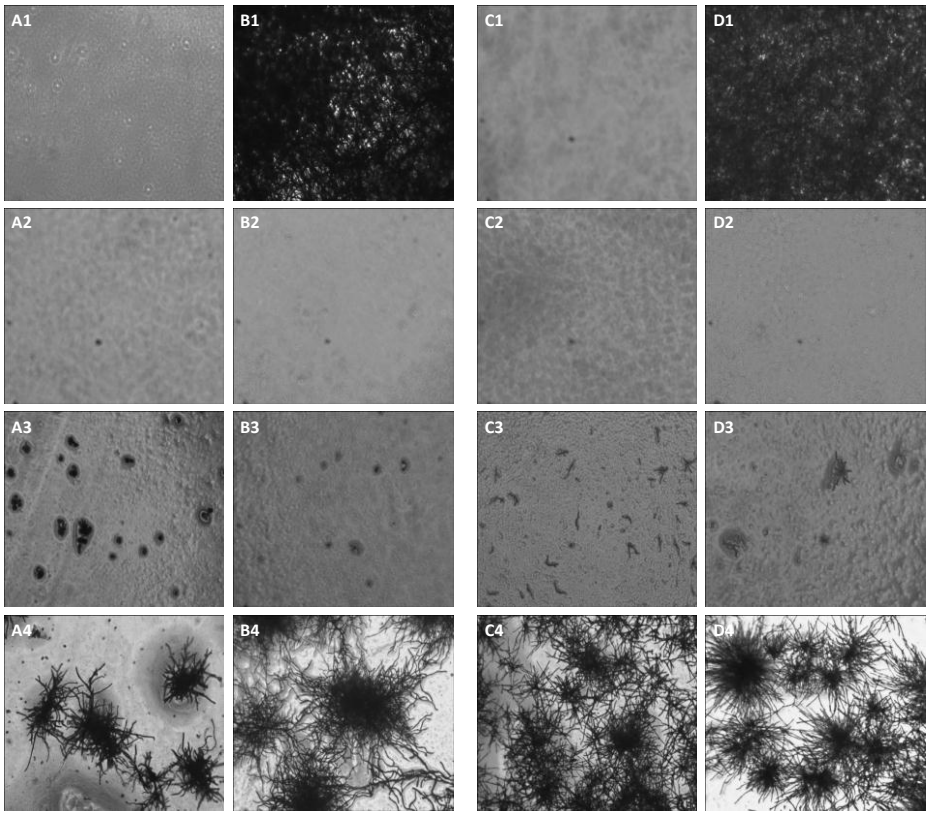

Fig. 3. Microscopic visualisation of the activity of gramicidin S and bifonazole against *B. cinerea* and *F. solani* cultured on PDA after Coomassie blue staining. Bifonazole (A2 80µM; A3 40µM; A4 20µM) and gramicidin S (B2 22µM; B3 11µM; B4 2.7µM) treated *B. cinerea* spores are compared to growth control (B1) and sterility control (A1). *F. solani* growth control (D1, C1 is sterility control) is compared to *F. solani* treated with bifonazole (C2 322µM; C3 161µM; C4 40µM) and gramicidin S (D2 22µM; D3 11µM; D4 5.5µM). Images were captured using a Leica light microscope coupled to a DCM 510 digital camera.

4.4 Comparison of inhibition parameters determined on agar gel and in broth media

Comparing the dose response curves obtained from the broth assay with digitised assay results for the two fungicides towards *F. solani* and *B. cinerea*, a marked increase in repeatability and prediction accuracy is visible (Figure 4). In terms of the repeatability for the individual antibiotic concentrations, the error (95% confidence interval) is less for the digitised gel-based assay results than for the broth assay results. Evaluating the dose response as a whole, the 95% prediction interval for the sigmoidal fits for the digitised gel-based assay results are narrower/closer to the fitted sigmoidal line, than for the broth dilutions assays. In our hands we found more consistent repeats for the individual fungicide concentrations and a better sigmoidal fit to the data points obtained for the digitised gel-based assay results than for the broth dilution assays. Especially for *B. cinerea*, a culture that exhibits significant hyperbranching and resultantly gave more variation between experimental repeats using spectrophotometric measurements, a more reliable sigmoidal fit could be obtained for the experimental repeats for the digitised gel-based assay than for the broth-based assay repeats. In terms of the repeatability for the determination of activity parameter against the two filamentous fungi, the 96-well gel-based assay consistently delivered more accurate parameter results with regard to standard error of the mean (Table 2, Figures 5 and 6).

Gramicidin S and, to a lesser extent, bifonazole inhibited the growth of both *B. cinerea* and *F. solani* during PDB assays and PDA assays (Table 2). However, some variance in the activity parameters obtained for gramicidin S and bifonazole could be observed between the results from the PDB assays and the digitised PDA assays. A small, but non-significant increase was observed in the activity parameters for bifonazole against *B. cinerea* with the IC_{50} value increasing from 7.7 µM in PDB assay to 9.6 µM for the digitised assay (Figure 6). The IC_{max} value increased from 16 µM to 20 µM, with some hyperbranching visible at 20 µM. (Table

2). The same LC for bifonazole was found in both types of assays (indicated with arrow in Figure 5). The activity parameters for gramicidin S against *B. cinerea* also remained relatively constant, only increasing slightly from 1.8 µM to 2.2 µM for the IC_{50} value, 2.7 µM to 4.1 µM for the IC_{max} value, but giving the same LC in both assays (indicated with arrow in Figure 5). Extensive hyperbranching was visible at 2.7 µM.

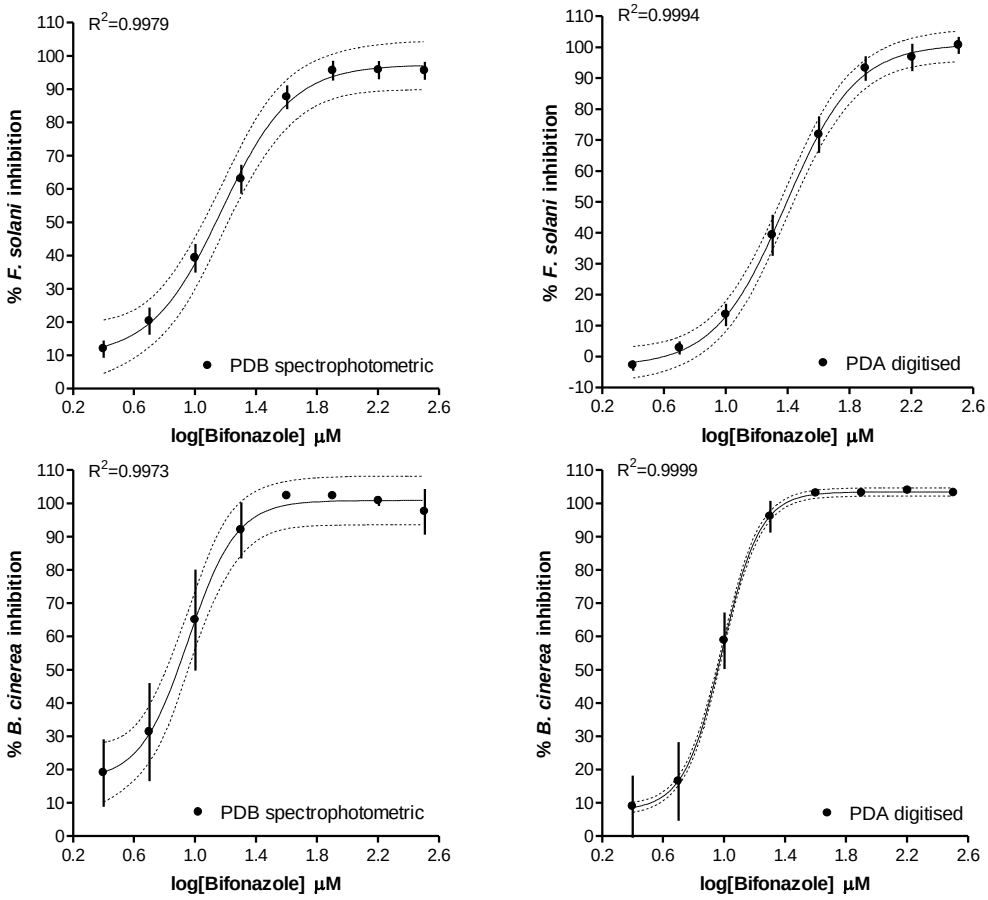

Fig. 4. Representative dose response curves of bifonazole against *F. solani* (top two graphs) and *B. cinerea* (bottom two graphs) in PDB (left hand graphs) and PDA (right hand graphs). The solid line in each graph represents the sigmoidal fit to the data points. The dotted lines represent the 95% prediction interval for the sigmoidal line fit to the data. Each data point is the mean of at least 16 determinations and the error bar represents the 95% confidence interval of the data point.

A significant change was observed in the activity parameters for both bifonazole and gramicidin S against *F. solani* from the PDB assay results to the digitised PDA assay results (Figures 5 and 6). An increase in the IC_{50} value of bifonazole of almost two fold (14 µM to

25 µM) was observed and the IC_{max} value increased from 53 µM to 71 µM, by a factor of 1.3. We also observed that the bifonazole LC value doubled (indicated with arrows in Figure 5), which may be an overestimation as extensive hyperbranching was detected at 40 µM (Figure 3).

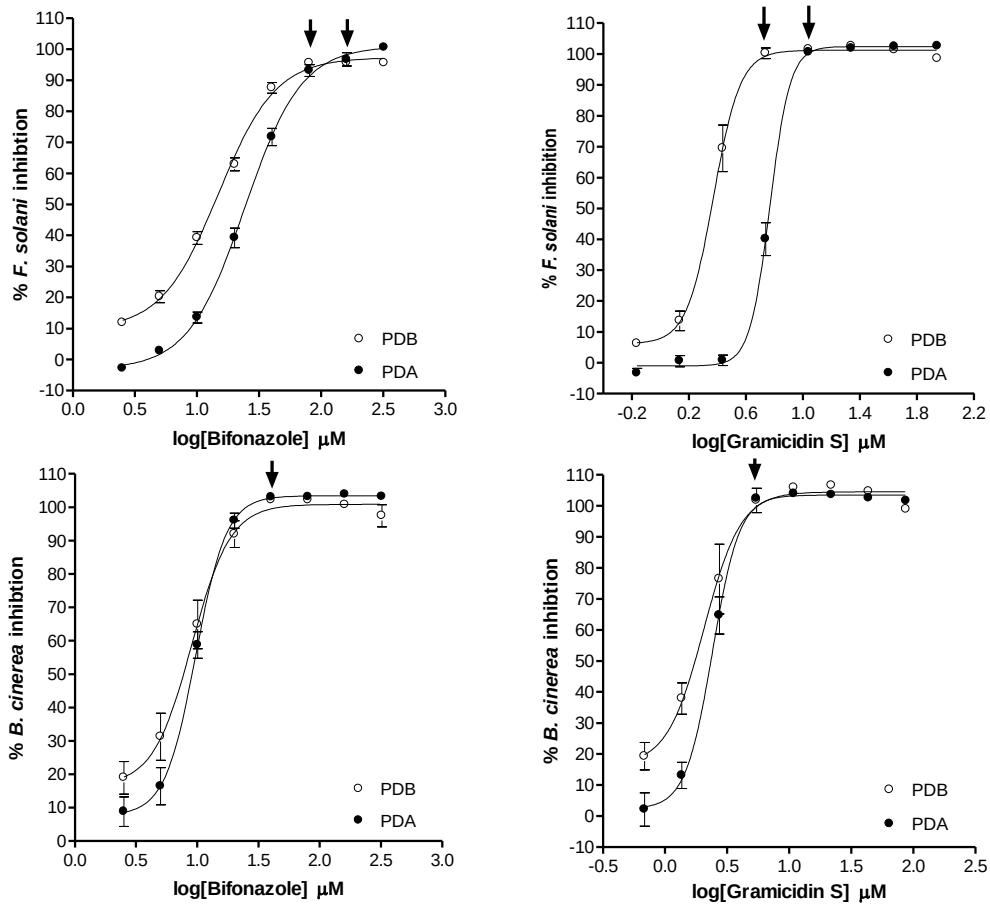

Fig. 5. Representative dose response curves illustrating the activity of bifonazole against *F. solani* (A) and *B. cinerea* (C), and gramicidin S against *F. solani* (B) and *B. cinerea* (D) in PDB and on PDA. The arrows indicate the lethal concentrations where no growth was observed. Each data point represents the mean of at least quadruplicate biological repeats ± SEM, with quadruplicate technical repeats per assay. R^2>0.997 was found for the sigmoidal fit of all the curves to the means of the data points.

Similarly a significant increase in the IC_{50} value (2.6 µM to 6.1 µM) from PDB assay results to the digitised PDA assay results was also observed for gramicidin S (Figure 6). This correlated with the increased IC_{max} value from 5.3 µM to 8.3 µM (Table 2) and doubling of the LC value for gramicidin S (indicated with arrows on Figure 5), which may again be related to hyperbranching (Figure 3).

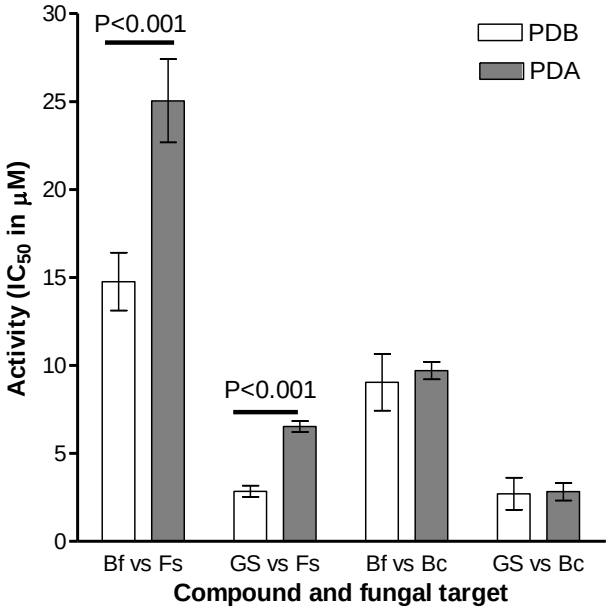

Fig. 6. Comparison of IC_{50} values obtained using results from PDB and digitised PDA assays. The average IC_{50} values ± SEM of gramicidin S (GS) against *B. cinerea* (Bc) and *F. solani* (Fs) and of bifonazole (Bf) against *B. cinerea* and *F. solani* are shown. One way ANOVA with Newman-Keuls multiple comparison test was used for the statistical analysis of at least quadruplicate biological repeats with quadruplicate technical repeats per assay.

The observed decrease in activity of bifonazole and gramicidin S from broth to agar gel medium could be the result of an overestimation of the activity of bifonazole and gramicidin S against *F. solani* in the micro-broth assays. However, the decrease in activity may also be the result of variances in growth of fungal species in different environments, and a resultant increase in their ability to resist fungicide action in certain environments. The observed variance in activity may also be explained by differences in the mode of action employed by the antibiotics in/on different environments and that the specific mechanism of action of the antibiotics permits for better activity in a liquid environment. A liquid environment may also allow for better/uniform distribution of the antibiotic and resultantly higher antifungal activity is observed. However, the fact that both the activities of gramicidin S and bifonazole decreased significantly against only *F. solani* supports the idea that it is the growth of *F. solani* that is altered from the aqueous PDB environment to the gelatinous PDA environment, rendering *F. solani* less susceptible to fungicide action. This argument is supported by the

results depicted in Figure 1 that illustrates the enhanced growth of *F. solani* on PDA compared to that in PDB.

Our results are comparable with that of Llop *et al.* (Llop et al., 1999) and Fernandez-Torres et al. (2003) who found that fungicide activity is dependent on the chosen medium. Evidently the "environmental factors" of the chosen activity test must be taken into account when assessing a novel anti-fungal and that more than one environmental condition must be included in the evaluations.

5. Conclusions

The digitised micro-gel assay method developed through this research decreases the difficulties experienced as a result of hyperbranching. Digitisation of results allows measuring of growth in the entire well in contrast to spectrophotometric results which usually only give a representation of the middle of the well. Therefore, the growth inhibition results obtained from the digitised micro-gel assays give a more realistic portrayal of growth/no growth in the entire well with a smaller error margin and higher repeatability (Figure 4). Our novel gel-based activity assay also provides additional benefits for the user. The staining process not only allows for the digitisation of results, but also improves the microscopic visualization of fungal morphology. This opens up doors for additional analysis of fungal inhibition that includes the study of the retardation/prevention of germination and any alterations in fungal morphology induced by the antifungal action (Figure 3). Furthermore, the staining process also allows for the preservation of the results. The minor downside of the gel-based method is that it is slightly more time consuming than the broth-based method. However, the multi-functionality and reliability of our novel 96-well gel-based antifungal assay renders it a straightforward useful method for determining antifungal activity against filamentous fungi.

References

Alaniz, S., León, M., Vicent, A., García-Jiménez, J., Abad-Campos, P., Armengol, J., 2007. Characterization of *Cylindrocarpon* species associated with black foot disease of grapevine in spain. Plant Dis. 91, 1187-1193.

Broekaert, W.F., Terras, F.R.G., Cammue, B.P.A., Vanderleyden, J., 1990. An automated quantitative assay for fungal growth inhibition. FEMS Microbiol. Lett. 69, 55-60.

Broekaert, W.F., Van Parijs, J., Allen, J., Peumans, W.J., 1988. Comparison of some molecular, enzymatic and antifungal properties of chitinases from thorn-apple, tobacco and wheat. Physiol. Plant Pathol. 33, 319-331.

CLSI, 2008. Reference method for broth dilution antifungal susceptibility testing for filamentous fungi; approved standard-second edition. CLSI document M38-A2. The Clinical and Laboratory Standard Institite, Wayne, Pennsylvania.

Cotoras, M., Silva, E., 2005. Differences in the initial events of infection of *Botrytis cinerea* strains isolated from tomato and grape. Mycologia 97, 485-492.

Damir, M.E., 2006. Variation in germination, virulence and conidial production of single spore isolates of entomopathogenic fungi in response to environmental heterogeneity. J. Biol. Sci. 6, 305-315.

du Toit, E.A., Rautenbach, M., 2000. A sensitive standardised micro-gel well diffusion assay for the determination of antimicrobial activity. J. Microbiol. Meth. 42, 159-165.

El-Banna, A.A., Scott, P.M., Lau, P., Sakuma, T., Platt, H.W., Campbell, V., 1984. Formation of trichothecenes by *Fusarium solani* var. *coeruleum* and *Fusarium sambucinum* in potaoes. Appl. Environ. Microb. 47, 1169-1171.

Fehri, L.F., Sirand-Pugnet, P., Gourgues, G., Jan, G., Wroblewski, H., Blanchard, A., 2005. Resistance to antimicrobial peptides and stress response in *Mycoplasma pulmonis*. Antimicrob. Agents Chemother. 49, 4154-4165.

Fernandez-Torres, B., Carrillo-Munoz, A., Ortoneda, M., Pujol, I., Pastor, F.J., Guarro, J., 2003. Interlaboratory evaluation of the Etest for anti-fungal susceptibility testing of dermatophytes. Med. Mycol. 41, 125-130.

Franrich, R.A., Gaogil, P.D., Shain, L., 1983. Fungistatic effects of *Pinus radiata* needle epicuticular fatty and resin acids on *Dothistroma pini*. Physiol. Plant Pathol. 23, 183-195.

Green, L., Petersen, B., Steimel, L., Haeber, P., Current, W., 1994. Rapid determination of antifungal activity by flow cytometry. J. Clin. Microbiol. 32, 1088-1091.

Hancock, R.E., 2001. Cationic peptides: Effectors in innate immunity and novel antimicrobials. Lancet Infect. Dis. 1, 156-164.

Hancock, R.E.W., 1997. Peptide antibiotics. The Lancet 349, 418-422.

Hilpert, K., McLeod, B., Yu, J., Elliott, M.R., Rautenbach, M., Ruden, S., Burck, J., Muhle-Goll, C., Ulrich, A.S., Keller, S., Hancock, R.E.W., 2010. Short cationic antimicrobial peptides interact with ATP. Antimicrob. Agents Chemother. 54, 4480-4483.

Llop, C., Sala, J., Riba, M.D., Guarro, J., 1999. Antimicrobial susceptibility testing of dematiaceous filamentous fungi: effect of medium composition at different temperatures and times of reading. Mycopathologia 148, 25-31.

Mauch, F., Mauch-Mani, B., Boller, T., 1988. Antifungal Hydrolases in Pea Tissue: II. Inhibition of Fungal Growth by Combinations of Chitinase and β-1,3-Glucanase. Plant Physiol. 88, 936-942.

Odebode, A.C., Jonker, S.A., Joseph, C.C., Wachira, S.W., 2006. Anti-fungal activities of constituents from *Uvaria scheffleri* and *Artabotrys brachypetalus*. J. Agric. Sci. 51, 79-86.

Pfaller, M.A., Messer, S.A., Mills, K., Bolmstrom, A., Jones, R.N., 2001. Evaluation of Etest Method for determining caspofungin (MK-0991) susceptibilities of 726 clinical isolates of *Candida* species. J. Clin. Microbiol. 39, 4387-4389.

Rautenbach, M., Gerstner, G.D., Vlok, N.M., Kulenkampff, J., Westerhoff, H.V., 2005. Analysis of dose-response curves to compare the antimicrobial activity of model cationic α-helical peptides highlights the necessity for a minimum of two activity parameters. Anal. Biochem. 350, 81-90.

Rautio, J.J., Smit, B.A., Wiebe, M., Penttila, M., Saloheimo, M., 2006. Transcriptional monitoring of steady state and effects of anaerobic phases in chemostat cultures of the filamentous fungus *Trichoderma reesei*. BMC Genomics 7, 247.

Roberts, W.K., Selitrennikoff, C.P., 1986. Isolation and partial characterization of two antifungal proteins from barley. Biochim. Biophys. Acta 880, 161-170.

Steinstraesser, L., Kraneburg, U.M., Hirsch, T., Kesting, M., Steinau, H., Jacobsen, F., Al-Benna, S., 2009. Host defense peptides as effector molecules of the innate immune response: A sledgehammer for drug resistance? Int. J. Mol. Sci. 10, 3951-3970.

Tzeng, Y., Ambrose, K.D., Zughaier, S., Zhou, X., Miller, Y.K., Shafer, W.M., Stephens, D.S., 2005. Cationic antimicrobial peptide resistance in *Neisseria meningitidis*. J. Bacteriol. 187, 5387-5396.

Vakalounakis, D.J., Chalkias, J., 2004. Survival of *Fusarium oxysporum* f. sp. *radicis-cucumerinum* in soil. Crop Prot. 23, 871-873.

Chapter 4
Inhibition of agronomically relevant fungal phytopathogens by the tyrocidines

4.1 Introduction

With approximately one billion undernourished individuals on earth and a global population of seven billion people that is still growing, global food security is under threat. Microbial pathogens, including fungi, augment this predicament by causing a loss of up to 16 % (1) in the annual global food production. Furthermore, some fungal species secrete mycotoxins which can be toxic, as well as mutagenic with long term exposure, when ingested by humans and animals (2, 3).

Conventional chemical fungicides are used to control fungal pathogens (4-7). However, there is increasing evidence of their detrimental effect on the environment and human health (8, 9). In addition, a number of fungal strains have developed resistance against conventional fungicides (7, 10). Therefore alternative, eco-friendly fungicides with a low risk for inducing resistance need to be developed (6, 9).

Antimicrobial peptides (AMPs), with their broad range of activity and rapid antimicrobial action (11, 12), can be considered as potential alternatives to fungicides (5, 13-16). Furthermore, cyclic AMPs are more resistant to degradation by proteases (17), an advantageous property for agricultural application. Unfortunately the antimicrobial activity of AMPs has been shown to be negatively influenced by the presence of cations such as Ca^{2+}, Mg^{2+}, K^{+} and Na^{+} (14, 18) that are prevalent in the biosphere, agricultural and food products. Consequently, to be considered useful for agricultural application, an AMP must be active in the presence of these cations at biologically relevant concentrations.

The bacterium, *Bacillus aneurinolyticus,* produces a group of analogous peptides, namely the tyrocidines, as part of their secondary metabolite complex tyrothricin (19, 20), The tyrocidines are part of a cyclic decapeptide family with conserved sequences forming β-sheets (21-23), only varying in one to three amino acid residues (refer to Tang *et al.* (20) and Chapter 1 for the primary structures of 28 natural tyrocidines). Following their discovery, it was illustrated that tyrocidines have significant antibacterial (24, 25) and anti-malarial (26) activity. However, to date only one study has been conducted on the antifungal activity of tyrothricin (the tyrocidine-gramicidin metabolite complex of *B. aneurinolyticus*) against *Candida albicans* (27) and one report on the activity of tyrocidines against *Neurospora crassa* (28). The potential of tyrocidines to inhibit fungal phytopathogens and subsequently to act as a potential bio-fungicide, thus remains unexplored. The significant activity illustrated by the tyrocidines against bacteria (19, 24, 25) and *Plasmodium falciparum* (26) prompted the investigation into the tyrocidines antifungal activity. The activity of the mixture of tyrocidines (Trc mixture) and eight tyrocidines and analogues (purification described in Chapter 2) were determined against selected agronomically important phytopathogens namely *Fusarium solani*, *F. oxysporum*, *F. verticillioides*, *Cylindrocarpon liriodendri*, *Botrytis cinerea* and *Penicillium digitatum*, *P. glabrum*, *P. expansum*, *Talaromyces mineoluteus*, *T. ramulosus, Asperigellus fumigatis* and *Trichoderma atroviride* isolates. The tyrocidines' effect on fungal membrane integrity and the influence of the cations Ca^{2+}, Mg^{2+}, Na^{+} and K^{+} on their antifungal activity were also investigated.

4.2 Materials

Tyrothricin, bifonazole, trifluoroacetic acid (TFA, >98%), propidium iodide, Coomassie Blue R-250 and gramicidin S (GS) were supplied by Sigma (St Louis, USA). The tyrocidine mixture and purified peptides were prepared as described in Chapter 2. Merck Chemicals (Wadeville, South Africa) supplied the sodium chloride, calcium chloride, magnesium chloride and ethanol (99.9%). Methanol and acetonitrile (HPLC-grade, far UV cut-off) were supplied by Romil Ltd.

(Cambridge, UK). Zymo Research (California, USA) supplied the ZR Fungal/Bacterial DNA Kit while Kapa Biosystems (Woburn, USA) supplied the Kapa Readymix. The Big Dye terminator cycle sequencing premix kit was obtained from Applied Biosystems (California, USA). The Tween 20®, potato dextrose broth (PDB) and potato dextrose agarose (PDA) were obtained from Fluka (St. Louis, USA). Biolab (Wadeville, South Africa) supplied the tryptone soy broth (TSB) powder, yeast extract and agar powder. Potassium chloride was provided by BDH Laboratory Supplies (Poole, England). Nunc (Roskilde, Denmark) supplied the polypropylene plates while Corning Incorporated (Corning, USA) supplied the sterile microtiter plates and culture dishes. The SYTOX green was obtained from Lonza (Walkersville, USA). Analytical quality water was prepared by passing water from a reverse osmoses plant through a Millipore (Milford, USA) Milli Q® water purification system.

Asperigellus fumigatis ATCC 204305 and *Fusarium oxysporum* ATCC 10913 were from the American Type Culture Collection (ATCC) (Manassas, VA, USA). *Fusarium solani* STEU 6188, *Fusarium verticilliodes* CKJ1730, *Botrytis cinerea* CKJ1731, *Cylindrocarpon liriodendri* STEU 6170 were provided by the Department Plant Pathology, University of Stellenbosch. *Penicillium expansum* CKJ1733 and *Penicillium digitatum* CKJ1734 were isolated from infected tangerines (July 2012, Stellenbosch, South Africa); *Talaromyces mineoluteus* CKJ1736 and *Talaromyces ramulosus* CKJ1735 were isolated from infected nectarines (March 2012, Stellenbosch, South Africa); *Penicillium glabrum* CKJ1732 and *Trichoderma atroviride* CKJ1729 were isolated from wood pallets used in the grape industry (February 2012, Wellington, South Africa). The isolated fungal species and strains were subsequently identified by us and placed in the CJK culture collection at department of Microbiology, University of Stellenbosch.

4.3 Methods

4.3.1 Growth and harvesting of fungi

F. solani, *F. oxysporum*, *F. verticilliodes*, *C. liriodendri*, *P. digitatum*, *P. glabrum*, *P. expansum*, *T. mineoluteus*, *T. ramulosus, A. fumigatis* and *Tr. atroviride* were grown at 25 ˚C on PDA until sporulation (± 2 weeks). Spores were harvested with 3 mL 0.1 % Tween-analytical water. *B. cinerea* was grown in culture plates on sterile strawberry halves at 23-25 ˚C until sporulation (± 3 weeks). *B. cinerea* spores were harvested dry using vacuum. Subsequent to harvesting, spores were counted using a counting chamber. Standard practices to ensure sterility were followed.

4.3.2 Identification of isolated fungi

Fungal strains were identified by growing the strains on malt extract agar and Czapek yeast agar for seven days. Based on conidiophore morphology, strains were placed into genera. For species identification, DNA was extracted from strains after growing on PDA for seven days, using the ZR Fungal/Bacterial DNA Kit. The ITS1–5.8S–ITS2 rDNA and β-tubulin gene region was amplified using polymerase chain reaction (PCR). Reaction mixtures (25 µL) consisted of 5 µL Kapa Readymix and 0.250 µM of primers ITS1 and ITS4 (29) for the internal transcribed spacer (ITS) region and primers Bt2a and Bt2b (30) for the β-tubulin gene. PCR products were sequenced using a Big Dye terminator cycle sequencing premix and sequenced with an ABI PRISM 310 automatic sequencer. Sequence contigs were aligned in ClustalX (31) and manually adjusted in Se-Al (32) using a dataset of Visagie & Jacobs (33). The *Trichoderma* strain was identified using the *Trichoderma* database (nt.ars-grin.gov/taxadescriptions/ keys/TrichodermaIndex.cfm), as well as the online key to species of *Trichoderma* (TrichoKey) (34).

4.3.3 Broth microdilution assays in broth media

The activity of the Trc mixture against *F. solani*, *F. oxysporum*, *F. verticillioides*, *C. liriodendri*, *B. cinerea*, *P. digitatum*, *P. glabrum*, *P. expansum*, *T. mineoluteus*, *T. ramulosus, A. fumigatis*

and *Tr. atroviride*, as well as the activity of the eight purified tyrocidines and analogues, against *B. cinerea* and *F. solani*, were determined using broth microdilution assays (25, 35). Standard practices to ensure sterility were followed. The broth microdilution assays were performed in sterile 96-well microtiter plates. Of a 2.5×10^4 spores/mL broth suspension (PDB/water, 1:1, *v*/*v*) 90 µL was added to each well (35). Alternatively, PDB was replaced by yeast supplemented tryptone soy broth (YTSB, TSB containing 20% *m/v* yeast extract). The Trc mixture was dissolved in 15 % ethanol to a concentration of 1.00 mg/mL. Doubling dilution series were made in polypropylene microtiter plates using 15% ethanol. Peptide (10 µL) was then added to the wells containing broth suspension. Growth control received 10 µL of 15% ethanol instead of peptide. Sterility control was a combination of half strength PDB (or YTSB) and 10 µL of 15% ethanol. All wells had a final volume of 100 µL and final ethanol concentration of 1.5%. As control the activity of bifonazole was determined against *F. solani* and *B. cinerea*. Bifonazole was dissolved in 20% ethanol to a concentration of 1.00 mg/mL and doubling dilution series were made using half strength PDB. Subsequent to peptide/fungicide addition, the microtiter plates were incubated at 23-25 ˚C for 48 hours. Light dispersion of each well was determined spectrophotometrically at 595 nm using a BioRad microtiter plate reader.

4.3.4 Micro-gel dilution assays on potato dextrose agarose

Micro-gel dilution assays were used to determine the activity of the Trc mixture on agar medium against *F. solani* and *B. cinerea*. The method as described by Troskie *et al.* (36) was followed. In brief, 96-well microtiter plates containing 70 µl PDA per well were prepared using the reverse pipetting method (36). Of a 1×10^5/mL spore-half strength PDB (PDB/water, 1:1, *v*/*v*) solution, 20 µL were added to each well. The Trc mixture was prepared as described for the broth assays. Following peptide addition, the microtiter plates were incubated at 23-25 ˚C for 48 hours. The plates were subsequently stained with Coomassie Blue (0.063 % Coomassie Blue R-250, 50 % methanol, 10 % acetic acid) for one hour and afterwards destained (12.5 % isopropanol, 10 % acetic acid) for 72 hours. Results were captured with a Canon 600D camera. Image results were

analysed as gels in UN-SCAN-IT *gel*™ (version 6.1 from Silk Scientific Corporation) and the average pixel count for each well used to calculate growth inhibition (36).

4.3.5 Light microscopy of peptide challenged spores and hyphae

For the fungal hyphae studies, half strength PDB suspension containing spores of either *B. cinerea* or *F. solani* were distributed into the wells of sterile 96-well microtiter plates so that each well held a volume of 90 µL and 2000 spores. The plates were incubated for 16 hours at 23-25˚C. The tyrocidines were dissolved and diluted in 15% ethanol using polypropylene plates. The final Trc mixture concentrations were 9 µg/mL (for *F. solani*) and 6 µg/mL (for *B. cinerea*). TrcA and TrcB were respectively added to *F. solani* and *B. cinerea* spores at concentrations of 6 µM and 4.5 µM. Controls received 10 µL of a 15% ethanol solution (final concentration of 1.5%). Each well had an end volume of 100 µL. The microscope studies with *B. cinerea* and *F. solani* spores were performed using the procedures described for the hyphae, leaving out the 16 hour incubation step. Subsequent to the addition of the Trc mixture; events were monitored using a Leica light microscope coupled to a DCM510 digital camera 2 hours, 12 hours and 24 hours after peptide addition.

4.3.6 Fluorescence microscopy

Half strength PDB containing *B. cinerea* spores (2.5×10^4 spores/mL) were added to sterile microtiter plates in order for each well to have a volume of 90 µL. The Trc mixture (10 µL), dissolved in 25% ethanol and diluted in analytical grade water, was subsequently added so that the final peptide concentration was 3 µg/mL (± 2.3 µM) and the final ethanol concentration was less than 0.3%. The growth control had a final ethanol concentration of 0.3%. After incubation at 25 ˚C for 2 hours for spores and 24 hour for hyphae, the cultures were incubated with 0.1 µg/mL propidium iodide for 15 minutes prior to image acquisition. Images were captured with a Nikon Eclipse E600 fluorescence microscope, using ultraviolet filters, fitted with a 100× Apochromat objective and a Media Cybernetics CoolSNAP-Pro monochrome cooled CCD camera.

F. solani hyphae were grown in half strength PDB from a starting concentration of 2.0×10^4 spores/mL for 16 hours at 25˚C. Hyphae were incubated at 25 °C for 1 hour with 25 µM TrcA, TrcB, TrcC, GS and 25 µg/mL Trc mixture. Subsequent to the 1 hour incubation step, the hyphae were incubated for 10 minutes with 0.5 µM SYTOX green (37). SYTOX green uptake was captured with a Carl Zeiss confocal LSM 780 Elyra S1. The laser was set at 488 nm and the filter at 500-676 nm. The collected data was processed using ZEN 2011 software.

4.3.7 Pre-incubation of peptides with chloride salts

Procedures were followed as described for the broth microdilution assays with a few adjustments. Briefly, the Trc mixture, TrcA, TrcB and TrcC were pre-incubated for 60 minutes in NaCl, KCl, $CaCl_2$ or $MgCl_2$ at concentrations ranging from 2.0-100 mM. Each well received 90 µL of the spore-broth suspension followed by the addition of 10 µL tyrocidine-cation suspension so that the wells had a final concentration of 6 µg/mL (Trc mixture) or 5 µM (TrcA, B and C) for *B. cinerea* and 18 µg/mL (Trc mixture) or 12 µM (TrcA, B and C) for *F. solani*. The growth control received 10 µL of 15% ethanol pre-incubated in chloride salts. The activity control received Trc mixture or pure peptides without the chloride salts. Sterility control consisted of half strength PDB and final ethanol and chloride concentration of respectively 1.5% and 10 mM. After the addition of tyrocidine-salt mixture, the microtiter plates were incubated at 25 ˚C for 48 hours. Light dispersion of each well was determined using a BioRad microtiter plate reader set at 595 nm.

4.3.8 Data analysis

In order to calculate the percentage growth inhibition the light dispersion at each concentration (average pixel count for PDA plates) was used as described by Rautenbach *et al* (38). GraphPad Prism® 4.03 (GraphPad Software, San Diego, USA) were used to plot the dose response curves. Non-linear regression and sigmoidal curves (with a slope default setting at <7) were fitted for dose response analysis (38). The point halfway between top and bottom (IC_{50}) represents the

concentration necessary to cause 50% growth inhibition. The minimum inhibition concentration (MIC), calculated as the x-value at the intercept between the slope and the top plateau of a full dose-response curve, was denoted as IC_{max} (38) to make the distinction with MIC values obtained from visual inspection of a dose-response result.

GraphPad Prism® 4.03 was also used for the statistical analysis of data. Analysis included 95% confidence levels, absolute sum of squares, standard error of the mean (SEM), ANOVA analyses, Bonferoni's test and unpaired Student t-test.

4.4 Results and discussion

4.4.1 Antifungal activity of the tyrocidines

The activity of antifungals has been shown to be influenced by the activity test's environment (Chapter 3 and (36)). Agar-based methods have also been proposed to aid in the exposure of resistant microorganisms (39). Therefore both a broth-based assay (25, 35) and a gel-based assay described by Troskie *et al.* (36) was used to evaluate the Trc mixture's activity against *F. solani* and *B. cinerea* on a gelatinous environment (Figure 4.1).

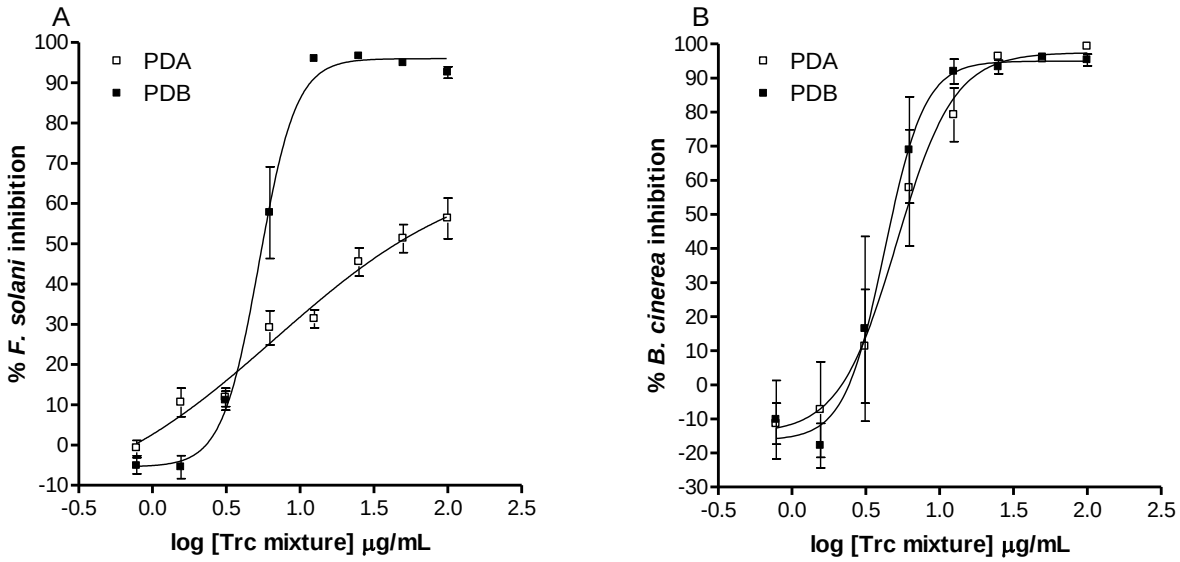

Figure 4.1: Comparison of Trc mixture activity using broth (PDB) and gel-based microdilution assays (PDA) against *F. solani* (**A**) and *B. cinerea* (**B**). Each data point represents the mean ± SEM of duplicate biological repeats with 3-4 technical repeats per biological repeat.

The Trc mixture showed potent activity in the broth media against both target cells and retained its activity on gel media against *B. cinerea* with a slight IC_{max} increase from 4.8 to 7.6 µg/mL. However, the tyrocidine's activity was significantly reduced against *F. solani* on PDA medium relative to the PDB medium (Figure 4.1). The IC_{max} obtained against *F. solani* in PDB was 7.1 µg/mL, while on the PDA, even at a concentration of 100 µg/mL, 100 % inhibition could not be reached. From these results it was, however, evident that the tyrocidines do have potent antifungal activity, particularly in broth media, therefore all the subsequent assays were performed in broth media.

In order to put the Trc mixture's antifungal activity into perspective, its ability to inhibit *F. solani* and *B. cinerea* was compared to that of bifonazole, a known antifungal, and to the purified tyrocidines and analogues (Figure 4.2, also refer to Table 4.1 and Figure 4.3).

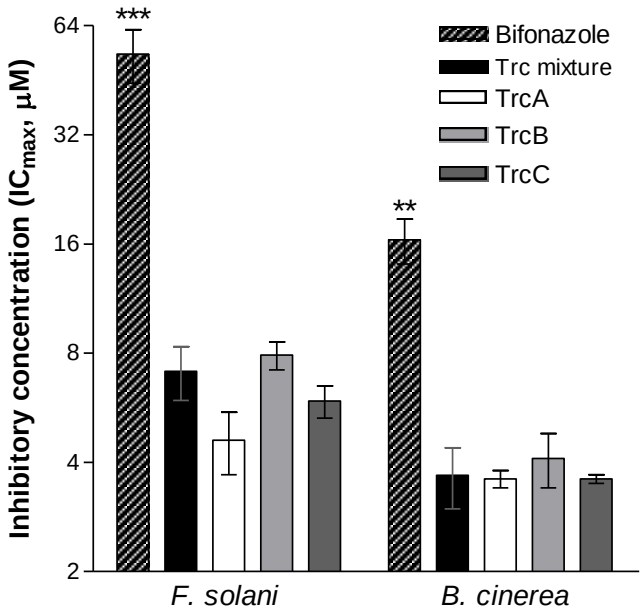

Figure 4.2: Comparison of the antifungal activity of Trc mixture, purified tyrocidines and bifonazole against *B. cinerea* and *F. solani*. The average of at least 5 biological repeats (each with 3-4 technical repeats) with standard error of the mean (SEM) is shown. Significant differences in activity between bifonazole and all the tyrocidines against *F. solani* (***P<0.001) and *B. cinerea* (**P<0.01) were found with One-way ANOVA using Bonferoni's test. The tyrocidines/analogues all had similar activity (P>0.05).

Both the activities of the Trc mixture and purified tyrocidines were significantly higher than that of bifonazole. The Trc mixture's and the purified tyrocidines activities were statistically similar (P>0.05), which substantiates the theorem that the individual tyrocidines contribute similarly to the antifungal activity in the Trc mixture (Figure 4.3). Due to the conserved nature of the tyrocidine structure it is highly probable that they share a similar major mode of action and target. Only the activity of the tryptocidine, TpcC, was significantly lower than that of the other tyrocidines, PhcA as well as that of GS against *B. cinerea* and *F. solani*, in PDB media (which can be considered a low salt media) (Figure 4.3A). Since the environment/culture conditions of fungi may influence their target cell properties, as well as growth and the peptide environment may influence peptide activity, selectivity and peptide mechanism of antimicrobial action (13, 40-42), the activity determinations were also performed in YTSB (considered as a high salt media). When the activities of the individual tyrocidines were determined in YTSB (Figure 4.3B) the phenycidine, PhcA, stood out as the peptide with significantly lower activity compared to the other tyrocidines.

Sequence wise these two analogues differ from some of the tyrocidines in only one residue, namely a Trp^7 or Phe^7 instead of the Tyr^7 of the major tyrocidines. The side chain of Trp contains a bicyclic indole group which makes it structurally larger than Tyr. Tyr only differs from Phe in an additional OH-group. However, this minor difference makes tyrosine amphipathic, dipolar and ionisable (pK_a = 10.07). Phe and Trp are also more hydrophobic than Tyr (Tyr>Trp>>>Phe) (44). The three aromatic amino acids also differ in their hydropathies (Phe = 2.8, Trp = -0.9, Tyr = -1.3) (43). It could be that the Tyr residue has the optimal chemical properties for target interaction and activity in both the low salt (PDB) and high salt (YTSB) media.

Table 4.1: Antifungal activities of the tyrocidine mixture, the eight purified tyrocidines and gramicidin S against *B. cinerea* and *F. solani*

Peptide	***B. cinerea* PDB**		***B. cinerea* YTSB**		***F. solani* PDB**		***F. solani* YTSB**	
	IC_{max} ± SEM (*n*)	IC_{50} ± SEM (*n*)	IC_{max} ± SEM (*n*)	IC_{50} ± SEM (*n*)	IC_{max} ± SEM (*n*)	IC_{50} ± SEM(*n*)	IC_{max} ± SEM (*n*)	IC_{50} ± SEM (*n*)
Trc mix	4.8±0.7 (6)	3.0 ± 0.2 (6)	3.7 ± 0.9 (3)	2.6±0.5 (3)	9.3±1.2 (3)	3.8± 0.4 (3)	5.2 0.4 (3)	3.4±0.1 (3)
TpcC	8.9±1.5 (3)	4.8±0.1 (3)	5.0±0.4 (3)	3.4±0.3 (3)	32±2.8 (3)	18±4.5 (3)	18±5.8 (3)	7.9±1.8 (3)
$TrcC_1$	3.5±0.2 (6)	2.4±0.2 (6)	4.9±0.3 (3)	3.4±0.3 (3)	4.3±0.4 (3)	3.2±0.2 (3)	7.8±1.9 (3)	4.9±0.7 (3)
TrcC	3.6±0.1 (6)	2.3±0.2 (6)	4.5±0.4 (3)	3.0±0.1 (3)	5.9±0.6 (3)	3.5±0.2 (3)	6.7±0.6 (3)	3.7±0.1 (3)
$TrcB_1$	5.1±1.0 (6)	3.3±0.4 (6)	6.3±1.7 (3)	4.1±0.6 (3)	11±4.0 (3)	7.7±2.6 (3)	8.3±1.4 (3)	5.5±1.0 (3)
TrcB	4.1±0.7 (6)	2.6±0.2 (6)	4.4±0.4 (4)	2.5±0.2 (4)	7.9±0.7 (3)	5.7±0.4 (3)	9.1±2.1 (3)	4.6±0.8 (3)
$TrcA_1$	5.2±0.6 (6)	3.5±0.4 (6)	4.7±0.2 (4)	3.3±0.1 (4)	4.0±0.4 (3)	2.9±0.3 (3)	7.5±1.5 (3)	5.5±1.0 (3)
TrcA	3.6±0.2 (6)	2.6±0.1 (6)	3.3±0.3 (3)	2.0±0.1 (3)	4.6±0.9 (3)	3.2±0.4 (3)	5.4±0.5 (3)	3.3±0.2 (3)
PhcA	6.9±1.4 (5)	4.7±1.1 (5)	15±2.4 (3)	10±1.7 (3)	7.2±1.0 (3)	5.2±0.8 (3)	34±7.8 (3)	18 ±1.2 (3)
GS	1.8±0.3 (7)	1.3±0.2 (7)	2.5±0.0 (4)	1.8±0.1 (4)	2.2±0.1 (3)	1.6±0.1 (3)	8.4±1.2 (3)	4.8±0.9 (3)

The values of the tyrocidine mixture are given in µg/mL and those of the purified peptides and gramicidin S in µM. Each value represents the mean of *n* biological repeats, with 3-5 technical repeats per assay±SEM.

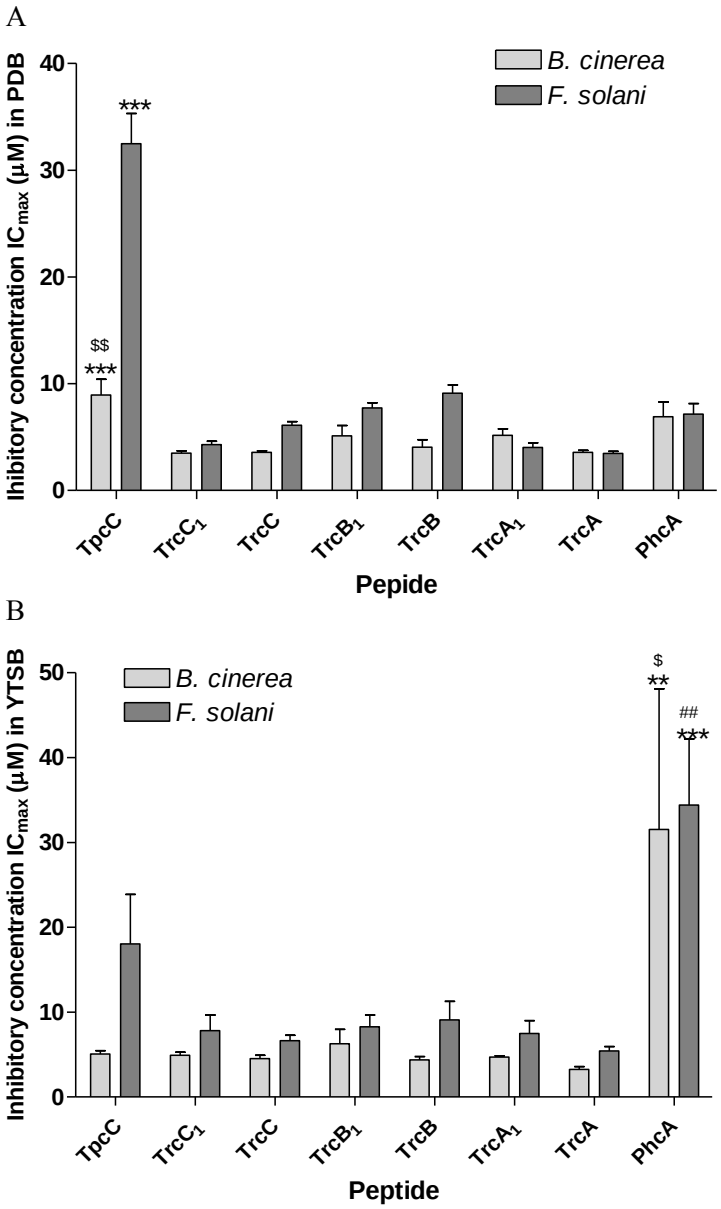

Figure 4.3: The activities of the tyrocidines in PDB (A) and YTSB (B) are compared in terms of their activity parameters (IC_{max}) against both *F. solani* and *B. cinerea*. Activity determinations were performed at least in triplicate. According to the Newman-Keuls multiple comparison test the IC_{max} of TpcC for *F. solani* in PDB was significantly higher (***P<0.001) than all the other peptides and for *B. cinerea* significantly higher than TrcA, TrcB, $TrcC_1$ (***P<0.001), $TrcA_1$, $TrcB_1$, TrcC and PhcA ($^{\$\$}$P<0.01). In YTSB PhcA's IC_{max} against *B. cinerea* was significantly higher than that of $TrcA_1$, $TrcB_1$, $TrcC_1$, TpcC (**P<0.01), TrcA, TrcB and TrcC ($^{\$}$P<0.05). For *F. solani* PhcA's IC_{max} was also significantly higher than that of the major tyrocidines (***P<0.001) and that of TpcC ($^{\#\#}$P<0.01).

Surprisingly no activity-structure relationships regarding the tyrocidines' other structural/chemical parameters could be established. Neither the size of the tyrocidines, their surface area, side chain surface area nor lipophilicity seemed to play a role in the degree of

antifungal activity exhibited by the tyrocidines (results not shown). Minor differences in activity are most probably due to minor differences in peptide aggregation (21, 23), such as different tendencies to form dimers and higher order structures (44) which can potentially influence the initial binding to the fungal target. Furthermore, small differences in amino acid structure can influence the tightness of binding to the targets. For example, tightness of binding of the tyrocidines to membranes could be modulated by the cationic residue (Lys or Orn) and the aromatic amino acid residues (26).

However, it must also be kept in mind that the structure-activity relationships of individual tyrocidines may not give an adequate representation of the true activity events. A hypothesis has also been proposed suggesting that the tyrocidines form higher-order structures for biological activity (44, 45). In this scenario the structural and chemical characteristics of this higher-order structure has to be taken into account and not necessarily that of the individual tyrocidines when comparing activities. The higher antifungal activity observed for the major tyrocidines may imply that the presence of a Tyr^7 may favour the formation of a higher-order structure with high antifungal activity and/or stability in various environments.

With the purpose of determining the spectrum of antifungal activity of the tyrocidines, the growth inhibition by the Trc mixture was assessed using microbroth dilution assays with *F. solani*, *F. oxysporum*, *F. verticillioides*, *C. liriodendri*, *B. cinerea*, *P. digitatum*, *P. glabrum*, *P. expansum*, *T. mineoluteus*, *T. ramulosus Tr. atroviride* and *A. fumigatis* as target organisms. With IC_{50} values between 2.0 and 8.9 µg/mL, the Trc mixture exhibited significant inhibitory activity against all of the fungal pathogens relevant to this study. Refer to Table 4.2 for a summary of inhibitory values in µg/mL and the corresponding values in µM.

In our comparative assays over 48 hours the tyrocidines were found to be 2-4 fold more active towards *C. liriodendri*, *B. cinerea*, *T. mineoluteus*, *T. ramulosus P. digitatum* and *P. expansum*, than toward *A. fumigates, Tr. atroviride P. glabrum*, *F. solani*, *F. oxysporum* and *F.*

verticillioides. This variance in activity can point to the possibility that the nature of the target cell influences/determines the tyrocidines' activity. The different fungal strains may present the same tyrocidine target, such as the fungal cell membrane, but differ in their sensitivity due to target concentration. The difference could also be ascribed to the difference in the growth rate of various fungi species (46), i.e. the growth characteristics of the various fungi species may differ over the test period of 48 hours rendering the fungi less or more susceptible to tyrocidine activity. However, for the case of *F. solani* and *B. cinerea* the differences in activity are probably related to differences in the initial cell wall interaction.

Table 4.2: Summary of activity parameters obtained for the Trc mixture against selected fungal pathogens

Fungal pathogens	**IC_{50}** ± SEM µg/mL (µM)[a]	**IC_{max}** ± SEM µg/mL (µM)[a]
Asperigellus fumigatis ATCC 204305	4.8±0.49 (3.7)	8.6±0.69 (6.6)
Fusarium solani STEU 6188	4.7 ± 0.4 (3.6)	9.3 ± 1.2 (7.1)
Fusarium oxysporum ATCC 10913	6.2 ± 0.5 (4.8)	10 ± 1.1 (7.7)
Fusarium verticilliodes CKJ1730	8.2 ± 1.9 (6.3)	12 ± 2.9 (9.2)
Botrytis cinerea CKJ1731	3.0 ± 0.2 (2.3)	4.8 ± 0.7 (3.7)
Cylindrocarpon liriodendri STEU 6170	2.0 ± 0.1 (1.5)	2.9 ± 0.1 (2.2)
Trichoderma atroviride CKJ1729	7.5 ± 0.0 (5.8)	9.8 ± 0.2 (7.5)
Penicillium glabrum CKJ1732	8.9 ± 0.2 (6.8)	11 ± 0.4 (8.4)
Talaromyces ramulosus CKJ1735	2.7 ± 0.3 (2.1)	3.7 ± 0.4 (2.8)
Talaromyces mineoluteus CKJ1736	2.5 ± 0.1 (1.9)	3.3 ± 0.2 (2.5)
Penicillium expansum CKJ1733	3.8 ± 0.3 (2.9)	5.2 ± 0.3 (4.0)
Penicillium digitatum CKJ1734	2.3 ± 0.1 (1.8)	3.7 ± 0.2 (2.8)

[a] The Trc mixture consists of a group of tyrocidines with relative molar mass (M_r) ranging from 1200-1400. An average M_r of 1303.7 was calculated from the tyrocidine abundances and used to calculate the approximate inhibition parameters in µM. Each value represents the mean of at least three biological repeats with 3-4 technical repeats per assay ± SEM.

4.4.2 Salt tolerance/sensitivity of the tyrocidine's antifungal activity

It has been observed that peptide activity and selectivity are influenced by their environment (13, 41, 42). Cations, for example Na^+, K^+, Mg^{2+} and Ca^{2+}, have been illustrated to decrease the activity of the majority of antimicrobial peptides (47-51). The antibacterial activities of the tyrocidines have been shown to be variably affected by the presence of metal cations (12, 45).

Since the incentive of this research is to explore the potential of an antifungal agent, and the agricultural and food processing environments are exposed to salts, the tyrocidines were tested for the ability to retain activity against fungi in the presence of chloride salts containing biological relevant metal cations. Accordingly their activity against *B. cinerea* and *F. solani* was determined in the presence of 0.2 to 10 mM Ca^{2+}, Mg^{2+}, Na^+ and K^+. The Trc mixture and selected purified tyrocidines proved to be salt tolerant, except in the presence of Ca^{2+} which lead to a significant loss ($P<0.001$) of >70% activity against *F. solani* (Figure 4.4 A). The tyrocidines were slightly more salt tolerant against *B. cinerea* with regards to 5 mM Ca^{2+}, but TrcB showed the highest loss in activity (Figure 4.4 B). This is probably due to the solubility and aggregation differences (44, 45) of the three selected peptides in 5 mM $CaCl_2$.

The loss in activity in the presence of increasing concentrations of $CaCl_2$ was compared for *B. cinerea* and *F. solani*. A significant ($P<0.01$) decrease (±30%) in activity against *B. cinerea* could be observed at a concentration as low as 0.3 mM Ca^{2+} (Figure 4.5 A). From a concentration of 1.3 mM Ca^{2+} and higher, the decrease in activity is more severe ($P<0.001$) and the Trc mixtures' ability to inhibit *B. cinerea* decreased by 50%. However, at ≥5 mM $CaCl_2$, ±40% activity of the Trc mixture against *B. cinerea* was still retained, while the activity against *F. solani* continued to decrease with increasing $CaCl_2$ concentrations (Figure 4.5 A).

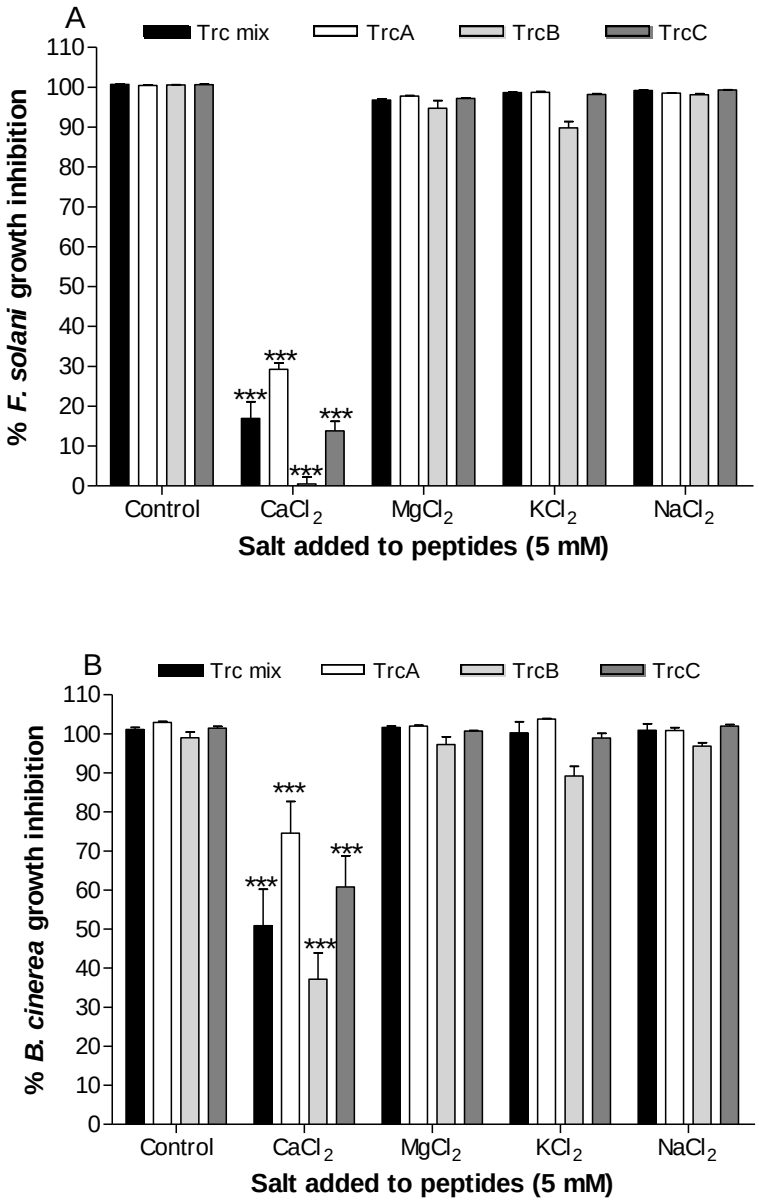

Figure 4.4: Antifungal activity of tyrocidines pre-incubated in chloride salts. The Trc mixture and purified tyrocidines were incubated for 60 minutes in 5 mM $CaCl_2$, $MgCl_2$, NaCl and KCl before *F. solani* **(A)** and *B. cinerea* (**B**) were exposed to the peptide-salt mixtures. According to the unpaired t-test the Trc mixtures, TrcA, B and C's activities in the presence of 5 mM $CaCl_2$ were significantly less (***P<0.001) than in the control and in the presence of the other salts for both target fungi.

The activity of TrcA was much more stable in the presence of Ca^{2+}, especially against *B. cinerea* (Figure 4.5 B). Even at a concentration of 10 mM Ca^{2+} TrcA only lost ±30% of its activity compared to the almost 90% loss in activity of TrcB (Figure 4.5 C) and ±50% loss of TrcC (Figure 4.5 D). This may again be the result of solubility and aggregation differences of the peptides (44, 45).

The Trc mixtures' activity against *F. solani* only started to decrease at a concentration of 1.3 mM Ca^{2+} ($P<0.05$) but at a concentration of 2.5 mM Ca^{2+} 50% activity against *F. solani* was lost ($P<0.001$) (Figure 4.5A). Similar results for *F. solani* as target was found for the purified TrcA, B and C (Figure 4.5 B-D). At Ca^{2+} concentrations higher than 5 mM all the tyrocidines lost most of their activity against *F. solani*.

From these results it is clear that the sensitivity of tyrocidines to Ca^{2+} is target cell and fungal target dependent. There are two likely reasons for a decrease in activity against fungal target cells in the presence of cations. First, the presence of cations can promote peptide aggregation leading to a lowering in the number of available and "active" peptide molecules (50). Second, the decrease in activity can also be the result of interference with a specific peptide target that is dependant on ionic interactions or ion fluctuations in membranes (52). The tyrocidines' activity was only influenced by the presence of Ca^{2+}. If the decrease in tyrocidine activity was as a result of interference by divalent cations in the interaction with the negative phospholipids, one would expect the same decrease in activity for Mg^{2+}. The absence of an effect on activity by the divalent Mg^{2+} indicates that the tyrocidines' target interaction or mode of action is specifically inhibited by Ca^{2+}. This could alternatively imply that the target is protected by exogenous Ca^{2+} or that the tyrocidine complexes with Ca^{2+} is less active, specifically against fungi such as *F. solani.*

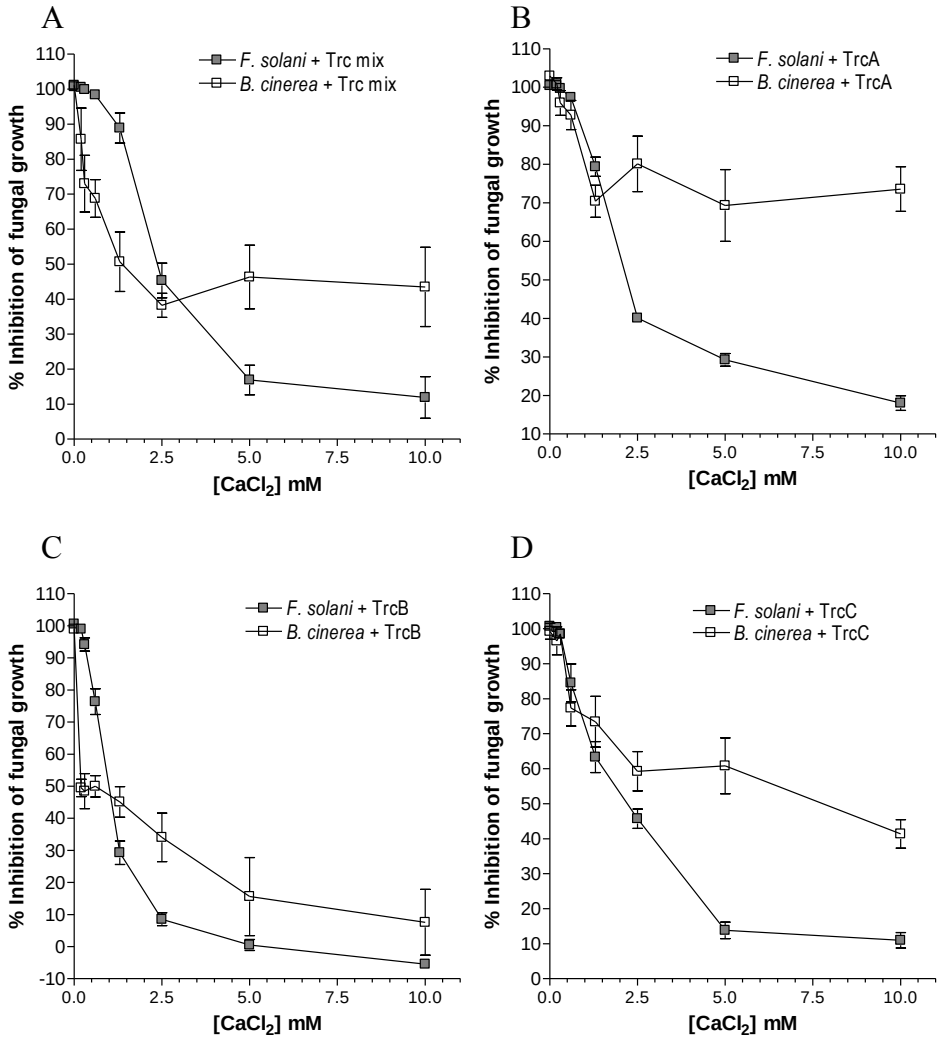

Figure 4.5: The influence of [$CaCl_2$] on the activity of (**A**) 12.5 µg/mL Trc mixture, 12 µM (**B**) TrcA, (**C**) TrcB and (**D**) TrcC against *F. solani* and *B. cinerea.* The average of a minimal of six repeats with SEM is shown in all graphs.

4.4.3 Influence of tyrocidines on fungal morphology

As indicated by the growth inhibition assay results, the tyrocidines exhibit significant antifungal activity. Light microscopy was used to analyse the morphological effect of tyrocidines on the spores and hyphae of fungi. Alterations in fungal morphology as a result of antifungal peptide activity are used to classify the peptides either as morphogenic, peptides that lead to alterations in fungal morphology, or non-morphogenic, although the peptides inhibit fungal growth there are no visible morphological changes. Morphogenic antifungal peptide activity can for instance result in hyperbranching of fungi (53).

The Trc mixture, at 9 µg/mL (double the IC_{50} concentration), was added to 16 hour old *F. solani* cultures. The Trc mixture had a considerable effect on the hyphae of *F. solani* (Figure 4.6). After 12 hours the difference between the control (Figure 4.6 A2) and tyrocidine treated hyphae (Figure 4.6 B2) is significant. There is, in comparison to the control, minimal progress in growth and atypical branching can be observed. The hyphal cells treated with the Trc mixture also appear thicker/swollen compared to the control. The hyperbranching of the tyrocidine treated hyphae is more pronounced after 24 hours (Figure 4.6 B3). In contrast dense, matt-like growth is visible in the control (Figure 4.6 A3).

Similar results were obtained for the Trc mixture on *B. cinerea* hyphae (results not shown). From the microscopy studies it is evident that the tyrocidines do not only inhibit fungal hyphae growth, but also alters the morphology of the hyphae by inducing hyperbranching. The effect of the Trc mixture on *B. cinerea* spores was visualised 2, 12 and 24 hours after peptide addition. Two hours after the addition of 6 µg/mL Trc mixture, there was no visible difference between the control (Figure 4.6 C1) and the tyrocidine treated spores (Figure 4.6 D1). After 12 hours of incubation, germination of the *B. cinerea* spores, with long healthy germination tubes, can be observed in the control (Figure 4.6 C2).

Germination is evidently retarded in the tyrocidine treated spores (Figure 4.6 D2). Germination of individual spores is visible, however, the germination tubes are short compared to that of the control and they appear swollen. After 24 hours of incubation the tyrocidine treated spores appear swollen and multiple germination tubes are visible. On some of the germination tubes dichotomous branching can be seen (Figure 4.6 D3). The Trc mixture had similar effects on the spores of *F. solani*. In Figure 6E the extensive hyperbranching of *F. solani* 5 days post treatment with 3.2 µg/mL Trc mixture can be seen. As expected the purified tyrocidines had a similar effect on fungal morphology. Extensive hyperbranching was observed for *B. cinerea* spores treated with 4.5 µM TrcB (Figure 4.6 F) and retarded germination and multiple germination tubes for *F. solani* spores treated with 3.0 µM TrcA (Figure 4.6 G).

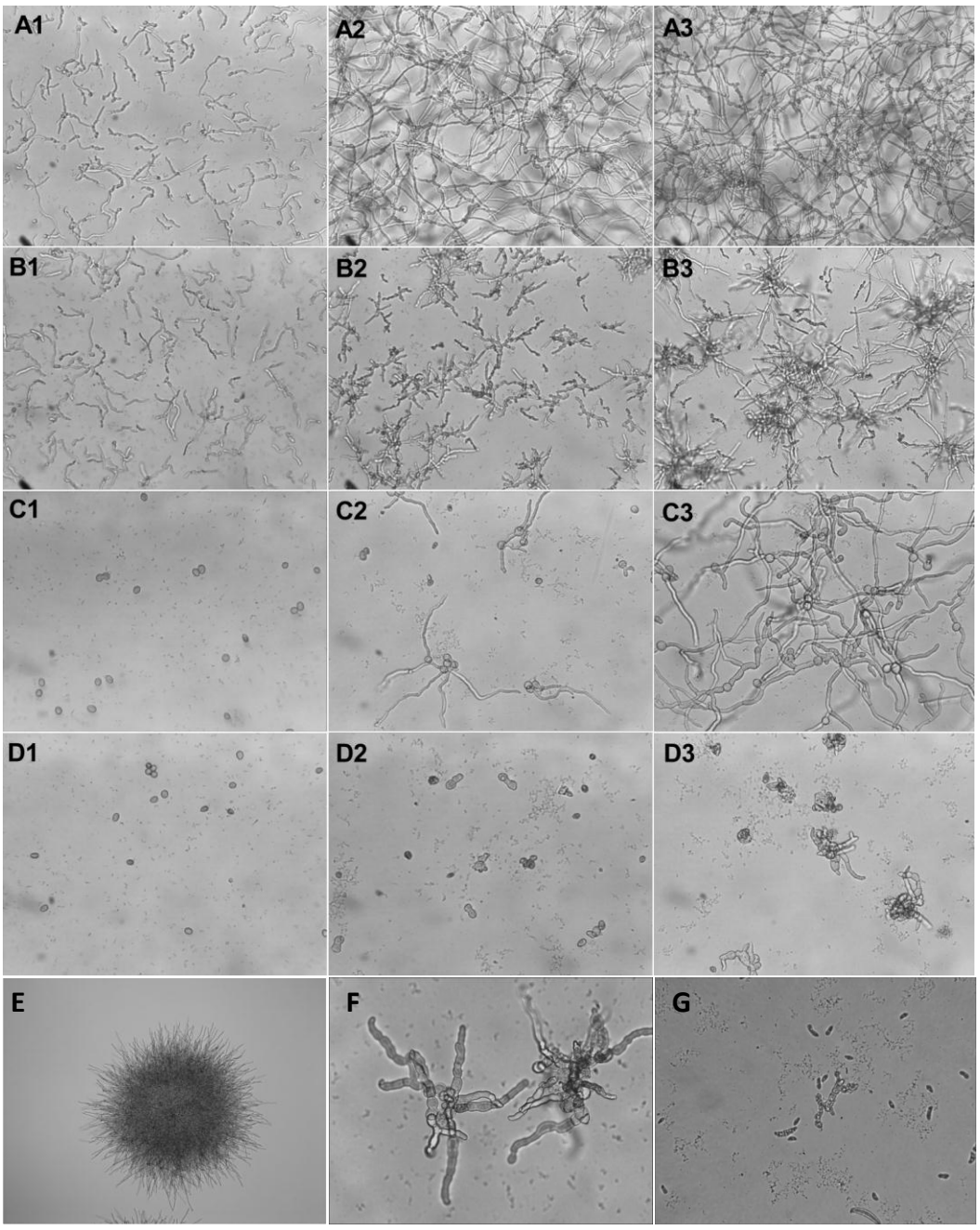

Figure 4.6: *F. solani* hyphae and *B. cinerea* spores treated with tyrocidines. Spores were incubated in half strength PDB and either directly treated or cultured for 16 hours to yield hyphae prior to peptide addition. Trc mixture was added to a final concentration of 9 µg/mL for *F. solani* hyphae (**B**) and 6 µg/mL for *B. cinerea* spores (**D**). *F. solani* hyphae control (**A**) and *B. cinerea* spore control (**C**) had a final ethanol concentration of 1.5%. Events were captured (40x magnification) at 2 hours (**A1-D1**), 12 hours (**A2-D2**) and 24 hours (**A3-D3**) after peptide treatment. Overt morphology changes in *F. solani* spores are shown 5 days post treatment (**E**). Retarded germination and hyperbranching was observed for *B. cinerea* spores treated with 4.5 µM TrcB (**F**) and *F. solani* spores treated with 3 µM TrcA (**G**).

The morphology of fungal hyphae and spores are clearly influenced by the tyrocidines and it is evident that these peptides induce hyperbranching. This hyperbranching can possibly be the result of channel-blocking activity (54), interference with the cell cycle (55, 56) or peptide induced septin mislocalization (57, 58). Morphological abnormalities as a result of peptide action are commonly observed (51) and have been ascribed to the interference with Ca^{2+} signalling (54). It is hypothesised that one aspect of hyphal elongation takes place through a Ca^{2+} regulated process (59) and interference of this process by AMPs may for instance induce hyperbranching (54). The observed hyperbranching as a result of tyrocidine action may, therefore, be due to the tyrocidines targeting Ca^{2+} gradients necessary for hyphal elongation and remains to be elucidated in future studies. Rautenbach *et al.* (26) illustrated that the tyrocidines hamper the life-cycle and development of *Plasmodium falciparum*. The tyrocidines may possibly have a similar effect on the spores of certain fungal species, interfering with the cell cycle and inducing retarded germination and hyperbranching.

Further investigation into the changes in fungal spores and hyphae, show that the mode of action of the tyrocidines is related to cell permeabilisation. Fluorescence imaging with the membrane impermeable dye propridium iodide (PI) showed that after 2 hours 3 µg/mL Trc mixture leads to overt permeabilisation of *B. cinerea* spores and PI uptake (Figure 4.7 A).

Similarly we found pronounced PI uptake in *B. cinerea* hyphae after 24 treatment with the tyrocidines (Figure 4.7 B). The permeabilisation of fungal hyphae was confirmed by SYTOX green uptake after 1 hour treatment of *F. solani* with the Trc mixture and selected purified major tyrocidines. With the tyrocidine concentration at 25 µM, ±100% release of the dye was obtained for *F. solani* hyphae, similar to Triton X-100 and GS. The SYTOX green results for Trc mixture and TrcC are shown in Figure 4.7 C-E. TrcA and B treatment of *F. solani* lead to similar dye uptake (results not shown).

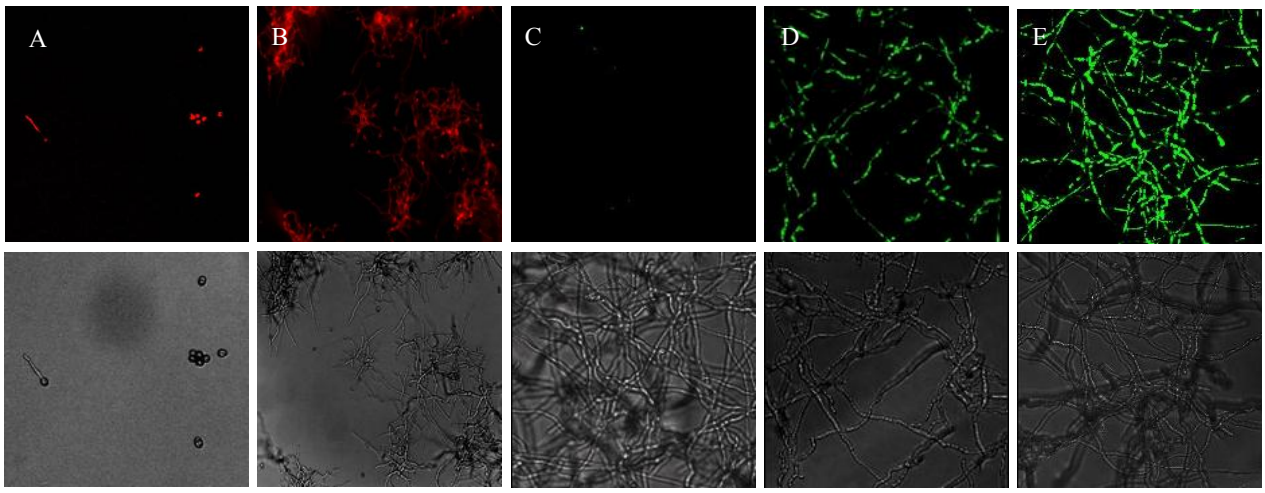

Figure 4.7: Fluorescence microscopy of tyrocidine treated spores and hyphea. *B. cinerea* spores (panel **A**) and hyphae (panel **B**) incubated with 3 μg/mL Trc mixture and propidium iodide mixture at 4x magnification. Panel C-E shows *F. solani* hyphae incubated with SYTOX green alone (**C**), 25 μg/mL Trc mixture (**D**) and 25 μM TrcC. The top panels are fluorescence images while the bottom panels are phase-contrast images, with propidium iodide or SYTOX green.

4.5 Conclusion

Evidently the tyrocidines exhibit significant low micromolar antifungal activity against a range of phytopathogens and their activity remains relatively stable in the presence of biological salts. The absence of overt structural-activity relationships implies that the conserved sequence of tyrocidines - NQYVOLfP - may be important for activity, with the aromatic dipeptide unit - Ff, Wf or Ww - determining the hydrophobicity and putative active dimer formation (Chapter 2, (44, 45)). The tyrocidines' major mode of action involves the disruption of fungal membrane integrity, but they also have morphogenic activity, indicating a non-membrane target or targets. Because of the tyrocidines' broad spectrum and potent antifungal activity, general salt tolerance and possible multiple targets reducing the risk of overt resistance, they are promising candidates that warrant further investigation as potential bio-fungicides.

4.6 References

1. **Chakraborty S, Newton AC.** 2011. Climate change, plant diseases and food security: an overview. Plant Pathology. **60:**2-14.

2. **Smith JE, Solomons G, Lewis C, Anderson JG.** 1995. Role of mycotoxins in human and animal nutrition and health. Natural Toxins. **3:**187-192.

3. **Bennett JW, Klich M.** 2003. Mycotoxins. Clinical Microbiology Reviews. **16:**497-516.

4. **Knight SC, Anthony VM, Brady AM, Greenland AJ, Heaney SP, Murray DC, Powell KA, Schulz MA, Spinks CA, Worthington PA, Youle D.** 1997. Rationale and perspectives on the development of fungicides. Annual Review of Phytopathology. **35:**349-372.

5. **Muñoz A, López-García B, Marcos JF.** 2007. Comparative study of antimicrobial peptides to control citrus postharvest decay caused by *Penicillium digitatum*. Journal of Agricultural and Food Chemistry. **55:**8170-8176.

6. **Narayanasamy P.** 2005. Introduction. *In*, Postharvest Pathogens and Disease Management. John Wiley & Sons, Inc., p. 1-8.

7. **Spadaro D, Gullino ML.** 2004. State of the art and future prospects of the biological control of postharvest fruit diseases. International Journal of Food Microbiology. **91:**185-194.

8. **Klich M, Arthur K, Lax A, Bland J.** 1994. Iturin A: A potential new fungicide for stored grains. Mycopathologia. **127:**123-127.

9. **Janisiewicz WJ, Korsten L.** 2002. Biological control of postharvest diseases of fruits. Annual Review of Phytopathology **40:**411-441.

10. **Diánez F, Santos M, Blanco R, Tello JC.** 2002. Fungicide resistance in *Botrytis cinerea* isolates from strawberry crops in Huelva (southwestern Spain). Phytoparasitica. **30:**529-534.

11. **Blondelle SE, Lohner K.** 2000. Combinatorial libraries: A tool to design antimicrobial and antifungal peptide analogues having lytic specificities for structure-activity relationships studies. Biopolymers. **55:**74-87.

12. **Marques MA, Citron DM, Wang CC.** 2007. Development of tyrocidine A analogues with improved antibacterial activity. Bioorganic & Medicinal Chemistry. **15:**6667-6677.

13. **Zasloff M.** 2002. Antimicrobial peptides of multicellular organisms. Nature. **415:**389-395.

14. **Park S-C, Kim J-Y, Lee J-K, Hwang I, Cheong H, Nah J-W, Hahm K-S, Park Y.** 2009. Antifungal mechanism of a novel antifungal protein from pumpkin rinds against various fungal pathogens. Journal of Agricultural and Food Chemistry. **57:**9299-9304.

15. **Keymanesh K, Soltani S, Sardari S.** 2009. Application of antimicrobial peptides in agriculture and food industry. World Journal of Microbiology & Biotechnology. **25:**933-944.

16. **Rydlo T, Miltz J, Mor A.** 2006. Eukaryotic antimicrobial peptides: Promises and premises in food safety. Journal of Food Science. **71:**R125-R135.

17. **Mantzourani ED, Tselios TV, Grdadolnik SG, Platts JA, Brancale A, Deraos GN, Matsoukas JM, Mavromoustakos TM.** 2006. Comparison of proposed putative active conformations of myelin basic protein epitope 87−99 linear altered peptide ligands by spectroscopic and modelling studies. The role of positions 91 and 96 in T-cell receptor activation. The Journal of Medicinal Chemistry. **49:**6683-6691.

18. **Lehrer R, Ganz T, Szklarek D, Selstedlt ME.** 1988. Modulation of the in vitro candidacidal activity of human neutrophil defensins by target cell metabolism and divalent cations. The Journal of Clinical Investigation. **81:**1829–1835.

19. **Dubos RJ.** 1939. Studies on a bactericidal agent extracted from a soil *Bacillus*: I. Preparation of the agent. Journal of Experimental Medicine. **70:**1-10.

20. **Tang X-J, Thibault P, Boyd RK.** 1992. Characterisation of the tyrocidine and gramicidin fractions of the tyrothricin complex from *Bacillus brevis* using liquid chromatography and mass spectrometry. International Journal of Mass Spectrometry and Ion Processes. **122:**153-179.

21. **Ruttenberg MA, King TP, Craig LC.** 1966. The chemistry of tyrocidine. VII. Studies on association behavior and implications regarding conformation. Biochemistry. **5:**2857-2864.

22. **Kuo M, Gibbons WA.** 1979. Total assignments, including four aromatic residues, and sequence confirmation of the decapeptide tyrocidine A using difference double resonance. Qualitative nuclear overhauser effect criteria for beta turn and antiparallel beta-pleated sheet conformations. Journal of Biological Chemistry. **254:**6278-6287.

23. **Ruttenberg MA, King TP, Craig LC.** 1965. The use of the tyrocidines for the study of conformation and aggregation behavior. Journal of the American Chemical Society. **87:**4196-4198.

24. **Dubos RJ, Hotchkiss RD.** 1941. The production of bactericidal substances by aerobic sporulating bacilli. Journal of Experimental Medicine. **73:**629-640.

25. **Spathelf BM, Rautenbach M.** 2009. Anti-listerial activity and structure–activity relationships of the six major tyrocidines, cyclic decapeptides from *Bacillus aneurinolyticus*. Bioorganic & Medicinal Chemistry. **17:**5541-5548.

26. **Rautenbach M, Vlok NM, Stander M, Hoppe HC.** 2007. Inhibition of malaria parasite blood stages by tyrocidines, membrane-active cyclic peptide antibiotics from *Bacillus brevis*. Biochimica et Biophysica Acta. **1768:**1488-1497.

27. **Kretschmar M, Nichterlein T, Nebe CT, Hof H, Burger KJ.** 1996. Fungicidal effect of tyrothricin on *Candida albicans*. Mycoses. **39:**45-50.

28. **Mach B, Slayman CW.** 1966. Mode of action of tyrocidine on *Neurospora*. Biochimica et Biophysica Acta. **124:**351-361.

29. **White TJ, Bruns T, Lee S, Taylor JW.** 1990. Amplification and direct sequencing of fungal ribosomal RNA genes for phylogenetics. *In* Innis MA, Gelfand DH, Sninsky JJ,

White TJ (ed.), PCR protocols: A guide to methods and applications. Academic Press, San Diego, USA, p. 315-322.

30. **Glass NL, Donaldson GC.** 1995. Development of primer sets designed for use with the PCR to amplify conserved genes from filamentous ascomycetes. Applied and Environmental Microbiology. **61:**1323-1329.

31. **Thompson JD, Gibson TJ, Plewniak F, Jeanmougin F, Higgins DG.** 1997. The ClustalX windows interface: flexible strategies for multiple sequence alignment aided by quality analysis tools. Nucleic Acids Research. **24:**4876-4882.

32. **Rambaut A.** 2007. Se-Al: Sequence Alignment Editor. Available from http://evolve.zoo.ox.ac.uk/.

33. **Visagie CM, Jacobs K.** 2012. Three new additions to the genus Talaromyces isolated from Atlantis sandveld fynbos soils. Persoonia. **28:**14-24.

34. **Druzhinina I, Kopchinskiy AG, Komon M, Bissett J, Szakacs G, Kubicek CP.** 2005. An oligonucleotide barcode for species identification in *Trichoderma* and *Hypocrea*. Fungal Genetics and Biology. **42:**813-828.

35. **Broekaert WF, Terras FRG, Cammue BPA, Vanderleyden J.** 1990. An automated quantitative assay for fungal growth inhibition. FEMS Microbiology Letters. **69:**55-59.

36. **Troskie AM, Vlok NM, Rautenbach M.** 2012. A novel 96-well gel-based assay for determining antifungal activity against filamentous fungi. Journal of Microbiological Methods. **91:**551-558.

37. **van der Weerden NL, Lay FT, Anderson MA.** 2008. The plant defensin, NaD1, enters the cytoplasm of *Fusarium oxysporum* hyphae. Journal of Biological Chemistry. **283:**14445-14452.

38. **Rautenbach M, Gerstner GD, Vlok NM, Kulenkampff J, Westerhoff HV.** 2006. Analyses of dose-response curves to compare the antimicrobial activity of model cationic α-helical peptides highlights the necessity for a minimum of two activity parameters. Analytical Biochemistry. **350:**81-90.

39. **Pfaller MA, Messer SA, Mills K, Bolmström A, Jones RN.** 2001. Evaluation of Etest method for determining caspofungin (MK-0991) susceptibilities of 726 clinical isolates of *Candida* species. Journal of Clinical Microbiology. **39:**4387-4389.

40. **Hwang PM, Vogel HJ.** 1998. Structure-function relationships of antimicrobial peptides. Biochemistry and Cell Biology. **76:**235-246.

41. **Hof WVt, Veerman EC, Helmerhorst EJ, Amerongen AV.** 2001. Antimicrobial peptides: Properties and applicability. Journal of Biological Chemistry. **382:**597-619.

42. **Andreu D, Rivas L.** 1998. Animal antimicrobial peptides: An overview. Journal of Peptide Science. **47:**415-433.

43. **Frecer V.** 2006. QSAR analysis of antimicrobial and haemolytic effects of cyclic cationic antimicrobial peptides derived from protegrin-1. Bioorganic & Medicinal Chemistry. **14:**6065-6074.

44. **Munyuki G, Jackson GE, Venter GA, Kövér KE, Szilágyi L, Rautenbach M, Spathelf BM, Bhattacharya B, Van der Spoel D.** 2013. β-Sheet structures and dimer models of two major tyrocidines, antimicrobial peptides from *Bacillus aneurinolyticus*. Biochemistry. **52:**7798-7806.

45. **Spathelf BM.** 2010. Qualitative structure-actvity relationships of the major tyrocidines, cyclic decapeptides from *Bacillus aneurinolyticus*. PhD Thesis, Department of Biochemistry, University of Stellenbosch, http://scholar.sun.ac.za/handle/10019.1/4001.

46. **Lewis K.** 2001. Riddle of biofilm resistance. Antimicrobial Agents and Chemotherapy. **45:**999-1007.

47. **Skerlavaj B, Romeo D, Gennaro R.** 1990. Rapid membrane permeabilization and inhibition of vital functions of Gram-negative bacteria by bactenecins. Infection and Immunity. **58:**3724-3730.

48. **Montville TJ, Chen Y.** 1998. Mechanistic action of pediocin and nisin: recent progress and unresolved questions. Applied Microbiology and Biotechnology. **50:**511-519.

49. **Bals R, Goldman MJ, Wilson JM.** 1998. Mouse β-Defensin 1 is a salt-sensitive antimicrobial peptide present in epithelia of the lung and urogenital tract. Infection and Immunity **66:**1225-1232.

50. **Cociancich S, Ghazi A, Hetru C, Hoffmann JA, Letellier L.** 1993. Insect defensin, an inducible antibacterial peptide, forms voltage-dependent channels in *Micrococcus luteus*. Journal of Biological Chemistry. **268:**19239-19245.

51. **Broekaert WF, Terras FRG, Cammue BPA, Osborn RW.** 1995. Plant defensins: Novel antimicrobial peptides as components of the host defense system. Plant Physiology. **108:**1353-1358.

52. **Bowman SM, Free SJ.** 2006. The structure and synthesis of the fungal cell wall. BioEssays. **28:**799-808.

53. **Thevissen K, Ghazi A, De Samblanx GW, Brownlee C, Osborn RW, Broekaert WF.** 1996. Fungal membrane responses induced by plant defensins and thionins. Journal of Biological Chemistry. **271:**15018-15025.

54. **Spelbrink RG, Dilmac N, Allen A, Smith TJ, Shah DM, Hockerman GH.** 2004. Differential antifungal and calcium channel-blocking activity among structurally related plant defensins. Plant Physiology. **135:**2055-2067.

55. **Binder U, Oberparleiter C, Meyer V, Marx F.** 2010. The antifungal protein PAF interferes with PKC/MPK and cAMP/PKA signalling of *Aspergillus nidulans*. Molecular Microbiology. **75:**294-307.

56. **Harris SD.** 2008. Branching of fungal hyphae: regulation, mechanisms and comparison with other branching systems. Mycologia. **100:**823-832.

57. **Thevissen K, de Mello Tavares P, Xu D, Blankenship J, Vandenbosch D, Idkowiak-Baldys J, Govaert G, Bink A, Rozental S, de Groot PWJ, Davis TR, Kumamoto CA, Vargas G, Nimrichter L, Coenye T, Mitchell A, Roemer T, Hannun YA, Cammue BPA.** 2012. The plant defensin RsAFP2 induces cell wall stress, septin mislocalization

and accumulation of ceramides in *Candida albicans*. Molecular Microbiology. **84:**166-180.

58. **Terras FR, Schoofs HM, De Bolle MF, Van Leuven F, Rees SB, Vanderleyden J, Cammue BP, Broekaert WF.** 1992. Analysis of two novel classes of plant antifungal proteins from radish (*Raphanus sativus* L.) seeds. Journal of Biological Chemistry. **267:**15301-15309.

59. **Jackson SL, Heath IB.** 1993. Roles of calcium ions in hyphal tip growth. Microbiological Reviews. **57:**367-382.

Chapter 5

Investigation into tyrocidine antifungal mode of action

5.1 Introduction

Antimicrobial peptides (AMPs) are the primary defence system of nearly all organisms on earth (1-3). AMPs show significant activity against various pathogens that include bacteria (4, 5), parasites (6, 7), fungi and even viruses (3, 8). In recent years there has been growing interest in AMPs as novel/alternative antibiotics, mainly as a result of the resistance developing against conventional chemical antibiotics (9, 10). Despite the recent increase in AMP interest and research, there is still a relatively large gap in our understanding of their mode(s) of antimicrobial action. Previously AMP activity was hypothesised to be predominantly as a result of membrane/lytic activity (11). However, there is increasing evidence of alternative/additional modes AMP antimicrobial action (12), including interference with the cell cycle (13), interference with cell wall synthesis (14) and induction of apoptosis (15). Furthermore, it has also been proposed that AMPs may utilise more than one mode of action (MOA) (16).

As is the case with the majority of AMPs, the tyrocidines' MOA has not yet been elucidated. Only lytic activity has been observed for the tyrocidines against Gram-positive bacteria (17), however, a non-lytic mode of action was observed against *Plasmodium falciparum* and it has been proposed that the tyrocidines interfere with cellular development of *P. falciparum via* an unknown mechanism (6).

In Chapter 4 we illustrated that the tyrocidine mixture (Trc mixture), the six major tyrocidines and two tyrocidine analogues, PhcA and TpcC, have significant antifungal activity and that except for the tyrosine (Tyr) residue in position seven, there are no overt structure-activity relationships. Studies with membrane impermeable dyes pointed to the likelihood that tyrocidine

activity leads to disturbances in fungal membrane integrity. Building on the knowledge that the tyrocidines exhibit significant antifungal activities and that they most probably have a membrane related target, a more in depth study was conducted on their potential mode(s) of antifungal action focussing on the fungal membrane as potential target in relation to their antifungal activities (from Chapter 4).

5.2 Materials

The Trc mixture, tyrocidines and gramicidin S (GS) were purified and analysed for purity as described previously in Chapter 2. Merck Chemicals (Wadeville, South Africa) supplied the diethyl ether, acetone, sodium phosphate tris(hydroxymethyl)aminomethane (Tris), sulphuric acid and ethanol (99.9%). *Fusarium solani* STEU 6188 and *Botrytis cinerea* CKJ1731 were provided by the Department Plant Pathology, University of Stellenbosch. The Tween 20® and potato dextrose broth (PDB) were obtained from Fluka (St. Louis, USA). Nunc (Roskilde, Denmark) supplied the polypropylene plates while Corning Incorporated (Corning, USA) supplied the sterile microtiter plates and culture dishes. Sterile petri dishes were obtained from Lasec (Cape Town, South Africa). The SYTOX Green was obtained from Lonza (Walkersville, USA). Analytical quality water was prepared by passing water from a reverse osmoses plant through a Millipore (Milford, USA) Milli Q® water purification system. The lipids 1-palmitoyl-2-oleoylphosphatidylcholine (POPC), 1-palmitoyl-2-stearyl(5-doxyl)-*sn*-glycero-3-phosphatidylcholine (5-DOX), 1-palmitoyl-2-stearyl(12-doxyl)-*sn*-glycero-3-phosphatidylcholine (12-DOX), and 1,2-dioleoyl-*sn*-glycero-3-phosphotempocholine (TEMPO), as well as glycosylceramide (GlcCer) were purchased from Avanti Polar Lipids (Alabaster, USA). Tyrothricin, trifluoroacetic acid (TFA, >98%), ergosterol, EDTA (≥ 99.8%), β-glucanase (from *Aspergillus niger*, Lot# 1407360V, 1.42 U/mg), proteinase K (from *Engyodontium album*) and chloroform were purchased from Sigma (St. Louis, USA). Fluka Chemie (Munich, Germany) provided the calcein and molybdate while tris(hydroxymethyl)aminomethane (Tris), sulphuric acid, sodium phosphate and Triton X-100 was provided by Merck (Darmstadt,

Germany). Sephadex G50 was obtained from Pharmacia Fine Chemicals and the sodium chloride and calcium chloride from J-T. Baker (Deventer, The Netherlands). The 100 nM polycarbonate membranes and extruder were from Averstin. Roth (Karlsruhe, Germany) provided the ascorbic acid. The 5 mL filters were from Roland Vetter Laborbedarf (Ammerbuch, Germany).

5.3 Methods

5.3.1 Culturing of fungi and harvesting of spores

The fungi were cultured and spores harvested as described in Chapters 3 and 4.

5.3.2 Beta-glucanase and proteinase K treatment

The methods described by van der Weerden *et al.* (18) were followed. In brief, *B. cinerea* and *F. solani* hyphae were grown for 16 hours in half strength PDB in sterile microtiter plates from a starting concentration of 2000 spores/well. Hyphae were then treated with 2 mg/mL β-glucanase for 1 hour at 37˚C or 1 mg/mL proteinase K for 40 minutes at 25˚C (18). After washing the fungal hyphae three times with PDB, 90 µL PDB was added to each well followed by the addition of 10 µL peptide to give a final concentration of 6.5 µg/mL Trc mixture, 2.5 µM TrcA and GS, 5.0 µM TrcB and TrcC. After a further incubation step of 36 hours at 23-25˚C, light dispersion at 595 nm was determined using a BioRad microtiter plate reader.

5.3.3 Fluorescence microscopy

F. solani hyphae were grown in half strength PDB from a starting concentration of 2.0×10^4 spores/mL for 16 hours at 25˚C. Hyphae were incubated at 25 ˚C for 1 hour with 3 µM, 6 µM, 12 µM or 25 µM of TrcA, TrcB, TrcC, PhcA, TpcC, and GS. 1% Triton-X 100 served as lytic control. Subsequent to the 1 hour peptide addition step, the hyphae were incubated for 10 minutes with 0.5 µM SYTOX green (19). SYTOX green uptake was quantified with a Carl Zeiss confocal LSM 780 Elyra S1. The laser was set at 488nm and the filter at 500-676nm. The collected data were analysed using ZEN 2011 software.

5.3.4 SYTOX green uptake assays

B. cinerea hyphae were grown in half strength PDB (PDB/water, 1:1, *v*/*v*) in sterile microtiter plates for 24 hours at 23-25˚C from a starting concentration of 2000 spores per well. The hyphae were incubated for 10 minutes with 1.0 µM SYTOX green prior to peptide addition. The Trc mixture, TrcA, TrcB, TrcC and GS were dissolved in 25% ethanol, diluted in analytical grade water and added to the hyphae at 12 µg/mL (Trc mixture), 12 µM (TrcA, TrcB and TrcC) and 8 µM (GS). The final ethanol concentration was less than 0.3%. SYTOX green uptake measurement commenced immediately upon tyrocidine addition using a Varioskan fluorometer at wavelengths 488 nm (excitation) and 538 nm (emission) for 1 hour.

5.3.5 Lipid vesicle preparation

For large unilamellar vesicle (LUV) preparation procedures were followed as described by Dathe *et al.* (20). For preparation of the calcein containing LUVs, dried lipid was vortexed in 80 mM calcein buffer (10 mM Tris, 0.1 mM EDTA, pH 7.4) and extruded 35 times through two stacked 100 nm polycarbonate membranes (85 times for glucosylceramide containing LUVs (21)). Untrapped calcein was removed with Sephadex G50 columns using a minicolumn centrifugation method (22). Subsequent to elution, salt buffer (10 mM Tris, 0.1 mM EDTA, 154 mM NaCl, pH 7.4) were added to the LUVs at a 1:1 ratio. Phosphate analysis was used to determine the lipid concentration (23).

5.3.6 Peptide-induced calcein release

Calcein release from the LUVs as a result of peptide interaction was fluorometrically monitored on a Jasco FP-6500 spectrofluorometer (20). Different concentrations of peptide (ranging from 0.3 µM to 100 µM) in buffer (10 mM Tris, 0.1 mM EDTA, 154 mM NaCl, pH 7.4) were prepared in a quartz cuvette containing a magnetic stirrer. Into these peptide preparations LUV suspension was injected to give a final volume of 2500 µL and LUV concentration of 25 µM. The decrease in self-quenching as a function of time was fluorometrically monitored (excitation

490 nm, emission 520 nm) at 25°C. Leakage of 100% was induced by the addition of 100 µL of a 10% (v/v) Triton X-100 solution. Percentage leakage, *F*(%), after one minute was calculated by the equation $100(\%)(I - I_0)/(I_{100\%} - I_0)$, where I is the intensity observed in the peptide solution and I_0 and $I_{100\%}$ are the fluorescence intensities measured respectively in the absence of peptide and in the presence of Triton X-100 (20). Percentage dye release at each peptide concentration was used to fit dose-response curves from which the EC_{50} (the effective peptide concentration that induces 50% leakage) was determined.

5.3.7 Quenching studies

POPC vesicles with different concentrations of 12-DOX, 5-DOX and TEMPO were prepared by dissolving the lipids in chloroform and combining the appropriate volumes of POPC and labelled lipids followed by drying under nitrogen. TrcB and TrcC were dissolved in ethanol to give a final concentration of 120 µM. A volume of 20 µL peptide was added to each of the lipid-containing tubes and vortexed to dissolve the lipid film. Subsequently 1180 µL buffer (10 mM Tris, 0.1 EDTA, pH 7.4) was added followed by vortexing. A constant end volume of 1200 µL was obtained with a final lipid concentration of 200 µM, peptide concentration of 2 µM and the content of labelled lipid ranged from 0 to 40 mol %. Baseline fluorescence of the labelled lipids was determined in the absence of peptides. Tryptophan fluorescence and quenching was measured with a Perkin Elmer LS 50B Luminescence Spectrometer at excitation of 280 nm, emission of 300 nm and scan range of 300-500 nm. Quenching is given by $F/F_0 = \exp(-\prod(c/70)(R_0^2 - X^2 - z^2))$, where F_0 and F are the fluorescence intensities in respectively the absence and presence of the quencher, R_0 is the critical quenching distance of the W-doxyl pair (12 Å), X is the minimum allowed lateral distance between the fluorophore and quencher, z is the difference in the depth between the quencher and fluorophore, c is the mole fraction of the quencher molecule, and $c/70$ gives the number of quencher molecules per square angstrom assuming that the cross-sectional area of a lipid is 70 $Å^2$. The distance of tryptophan from the bilayer centre, z_{cf}, was calculated using the parallax equation $z_{cf} = L_{cl} + (-70/\prod c(\ln(F_1/F_2) -$

$L_{21}^2))/2L_{21}$), with L_{cl} being the distance of the shallow quencher from the bilayer centre, F_1 and F_2 are respectively the fluorescence intensities in the presence of the shallow and deeper quenchers and L_{21} the difference in depth between the shallow and deeper quenchers. The distances of the applied quenching groups from the bilayer centre have been reported to be 19.5, 12.2 and 5.85 Å for respectively TEMPO, 5-DOX and 12-DOX (22).

5.3.8 Data and statistical analysis

In order to calculate the percentage growth inhibition the light dispersion at each concentration was used as described by Rautenbach *et al*. (24). GraphPad Prism® 4.03 (GraphPad Software, San Diego, USA) were used to plot the dose response curves. Non-linear regression and sigmoidal curves (with a slope default setting at <7) were fitted for dose response analysis (24). The point halfway between top and bottom (IC_{50}) represents the concentration necessary to cause 50% growth inhibition. The minimum inhibition concentration (MIC), calculated as the x-value at the intercept between the slope and the top plateau of a full dose-response curve, was denoted as IC_{max} (24) to make the distinction with MIC values obtained from visual inspection of a dose-response result.

GraphPad Prism® was also used for the statistical analysis of data. Analysis included 95% confidence levels, absolute sum of squares, standard error of the mean, Newman-Keuls multiple comparison test, Student t-test and Bonferroni's post test.

5.4 Results and discussion

The antifungal activities of the individual tyrocidines were previously determined and we found that the purified six tyrocidines, $TrcA_1$, A, B_1, B, C_1 and C, as well as the two analogues, PhcA and TpcC were able to inhibit both *F. solani* and *B. cinerea* (refer to Chapter 4 and Table 5.1). The preliminary studies in Chapter 4 with membrane impermeable dyes also indicated that the fungal membrane may be a target for tyrocidine antifungal action. Therefore we explored the interaction of the tyrocidines with biological fungal membranes, model fungal membranes as

well as any correlation between their antifungal activity parameters (determined in Chapter 4) and their membrane interaction. Since the peptides have to initially traverse the cell wall to interact with the cell membrane, we investigated the effect of the absence of the cell wall on the antifungal activity of the tyrocidines.

5.4.1 Cell wall as target

The cell wall and components of it, for instance proteins, have been illustrated to influence/be targets for AMP antifungal activity (18). With the aim of ascertaining if the tyrocidines' activity is related to a protein target, proteinase K was used to remove proteins from the surface of *B. cinerea* and *F. solani* cell walls prior to the addition of peptide as described by van der Weerden *et al.* (18). Comparison of untreated and β-glucanase treated growth controls did not yield any optical density differences between the growth of treated and untreated *B. cinerea* and *F. solani* cultures (results not shown). The tyrocidines maintained their activity against both *B. cinerea* and *F. solani* after proteinase K treatment (results not shown). A slight increase in activity was observed against *F. solani*. These results indicate that the tyrocidines do not have a protein target sensitive to proteinase K in the cell walls of either *F. solani* or *B. cinerea*. The increase in activity can probably be ascribed to peptides gaining access through a more vulnerable cell wall and/or acting on a more vulnerable cell membrane.

When these two fungi were treated with β-glucanase, the activity of the tyrocidines towards *B. cinerea* remained unaffected by this treatment. However, there was a significant ($P<0.001$) activity loss of ±30% for 6.3 μg/mL Trc mixture towards the β-glucanase treated *F. solani* (Figure 5.1). Similarly, the three purified tyrocidines, 2.5 μM TrcA, 5 μM TrcB and 5 μM TrcC, suffered significant ($P<0.001$) activity loss against β-glucanase treated *F. solani* (Figure 5.1).

The significant ($P<0.001$) activity loss of the Trc mixture, TrcA, TrcB and TrcC against the β-glucanase treated *F. solani* (Figure 5.1), indicates that tyrocidine activity, especially at lower concentration of peptide, could at least in part be determined by a cell wall related target in *F.*

solani. The activity of GS, on the other hand, is not significantly influenced by the presence/absence of *F. solani*'s cell wall. However, the possibility that pre-treatment with β-glucanase could trigger fungal defence and consequently affect tyrocidine activity must also be considered.

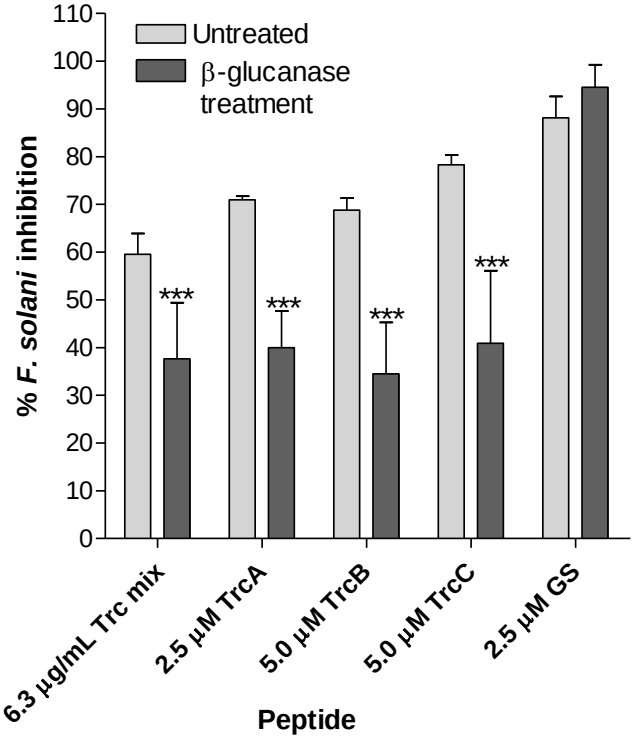

Figure 5.1: Activity of tyrocidines against β-glucanase treated *F. solani*. The Trc mixture's and purified tyrocidines' activities were significantly influenced by the β-glucanase treatment of *F. solani* cell wall (***P<0.001) as determined with the Student t-test (One-tailed). The average of at least 3-8 determinations with standard error of the mean (SEM) is shown.

5.4.2 Cell membrane as target

In terms of their antibacterial activity the tyrocidines are regarded as membrane active lytic peptides (17). Therefore, with regards to their antifungal activity, the fungal membrane may also be a major target. Consequently, the two dyes SYTOX green and propidium iodide - that can only reach the cell interior if the cell plasma membrane is structurally compromised or if membrane potential is dissipated - were used as indicators of cell membrane permeabilisation during initial studies in Chapter 4. The studies showed that the tyrocidine treatment induced dye uptake in both spores and hyphae.

TrcA, TrcB, TrcC, PhcA, TpcC and GS's influence on *F. solani* membrane integrity was further investigated using the membrane impermeable dye SYTOX green (Figure 5.2 and 5.3). Subsequent to one hour incubation period with peptide, SYTOX green fluorescence was observed in the *F. solani* hyphae treated with 3, 6, 12 and 25 µM purified peptide. In Figure 5.2 it can be observed that SYTOX green uptake is induced by all of the peptides at 6 µM compared to that of the control (Figure 5.2 H). Compared to the tyrocidines and analogues, 6 µM GS induced the highest uptake of SYTOX green (Figure 5.2 F) and is comparable to the SYTOX green uptake induced by 1 % TritonX-100 (Figure 5.2 G). In terms of the tyrocidines and their analogues, the activity of TrcA (Figure 5.2 A) and TrcC (Figure 5.2 C) appear to result in the highest SYTOX green uptake. It appears as if initial membrane permeabilisation takes place at the growth tips of hyphae and sites of hyphal branching. This is especially evident with TrcB (Figure 5.2 B), PhcA (Figure 5.2 D) and TpcC (Figure 5.2 E), the peptides which has not yet succeeded to induce overt membrane disruption at a concentration of 6 µM. This could possibly be an indication of the areas of a fungal cell/hyphae and/or fungal cellular processes that the tyrocidines target.

Figure 5.3 depicts the percentage SYTOX green fluorescence induced by the individual peptides in relation to the SYTOX green fluorescence induced by 1% Triton X-100. All of the peptides tested, TrcA, TrcB, TrcC, PhcA, TpcC and the membrane active GS (6) led to a loss in the membrane integrity of *F. solani* (Figure 5.2 and 5.3). However, there was variation in the degree to which they could induce membrane disruption. Only the SYTOX green uptake induced by GS ($P<0.001$), TrcA ($P<0.001$), TrcB ($P<0.01$) and TrcC ($P<0.01$) was significantly higher than that of the untreated hyphae (Figure 5.3A). The SYTOX green uptake observed for PhcA and TpcC cultures did not differ significantly from the untreated cultures. At a higher concentration of peptide (25 µM) there is no significant difference in the SYTOX green uptake induced by the individual peptides (Figure 5.3B).

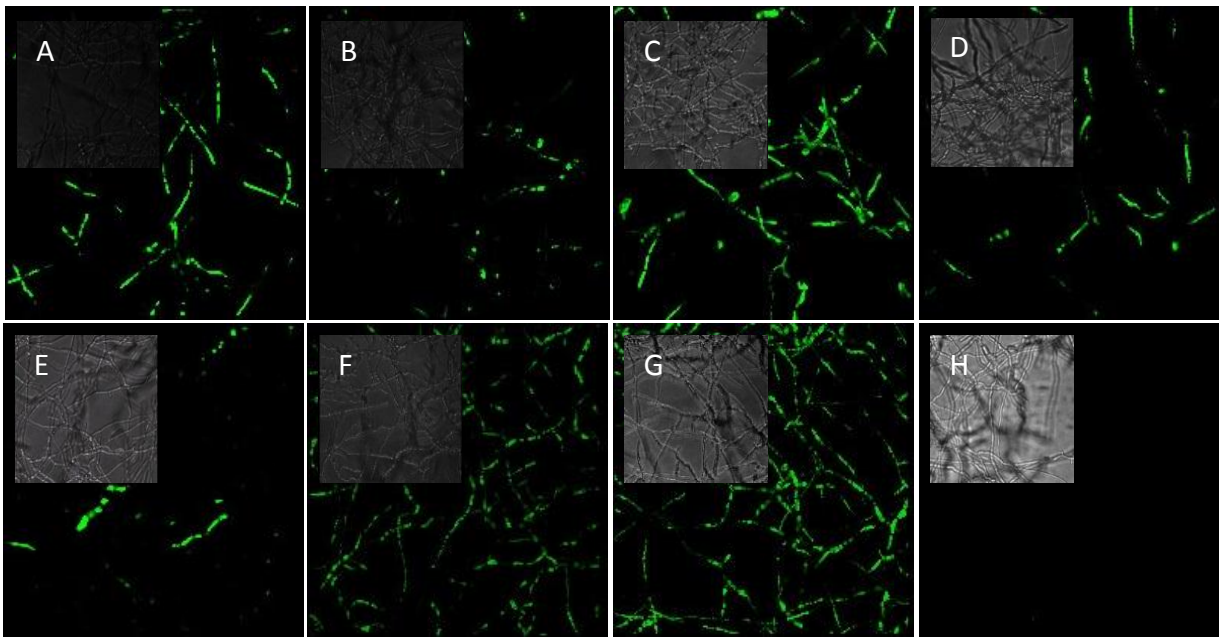

Figure 5.2: Peptide-induced SYTOX green fluorescence in *F. solani* hyphae. 24 hour old *F. solani* hyphae were treated for 1 hour with 6 µM TrcA (**A**), TrcB (**B**), TrcC (**C**), PhcA (**D**), TpcC (**E**) and GS (**F**) prior to staining with 0.5 µM SYTOX green. Hyphae treated with 1% TritonX-100 (**G**) and untreated hyphae (**H**) served as controls.

When the percentage peptide-induced SYTOX green uptake in *F. solani*, at a peptide concentration of 3 µM peptide, are compared to the IC_{max} values obtained for the individual peptides against *F. solani* (refer to Chapter 4), a relationship between high antifungal activity and high membrane activity can be observed (Figure 5.4). GS is clearly the outlier resulting in both the highest antifungal activity and SYTOX green uptake. The importance of the Tyr residue in position seven, highlighted in Chapter 4 as being important for tyrocidine antifungal activity, is again emphasised as being important for the disruption of membrane integrity. The two tyrocidine analogues with respectively a Trp^7 and Phe^7 are clearly grouped as the peptides with the lowest membrane activity (Figure 5.4).

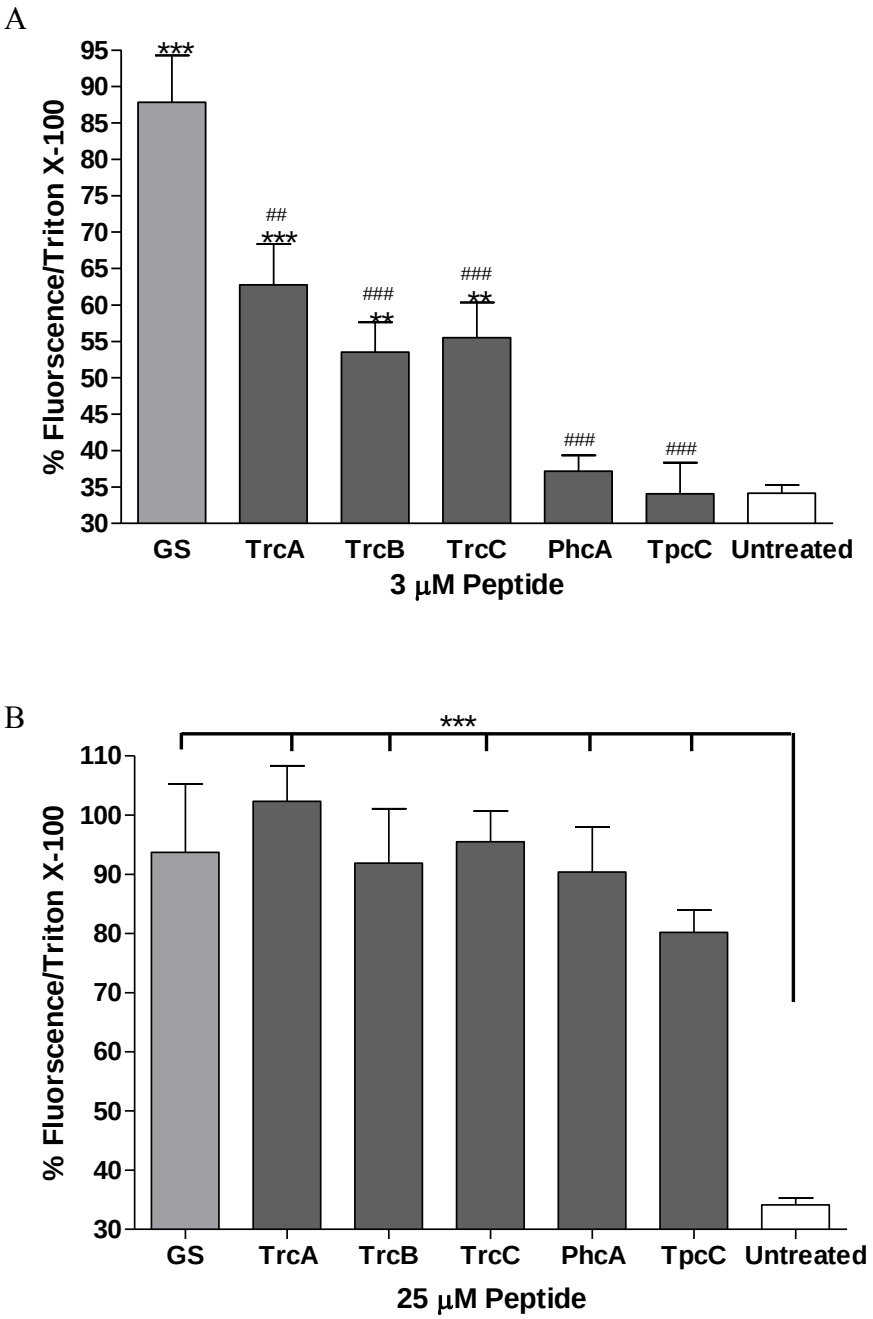

Figure 5.3: Membrane disruptive activities of TrcA, TrcB, TrcC and GS on 24 hour *F. solani* hyphae. Hyphae were incubated for 1 hour with 3 μM (**A**) or 25 μM (**B**) peptide prior to SYTOX green staining. 1% Triton X-100 served as control. Peptide concentration is compared to the percentage peptide-induced SYTOX green fluorescence with regards to the fluorescence induced by 1% TritonX-100. According to One way Anova using Newman-Keuls multiple comparison test the fluorescence induced by the major tyrocidines are significant compared to the untreated hyphae (***$P<0.001$, **$P<0.01$), but some of their activities were significantly lower than that of GS ($^{###}P<0.001$, $^{##}P<0.01$). The average of at least three determinations with SEM is shown.

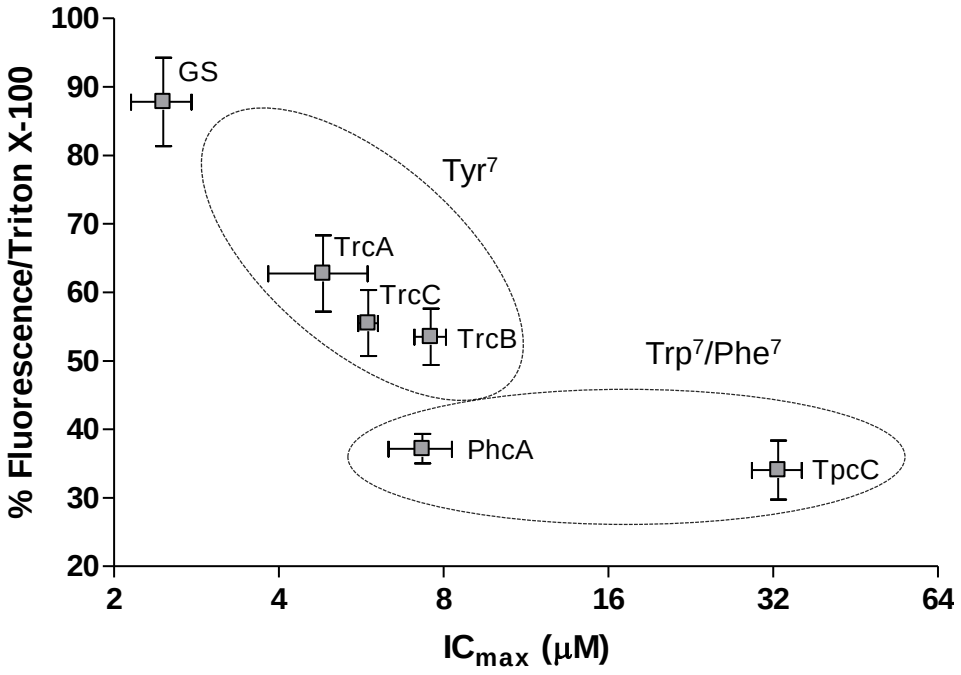

Figure 5.4: The percentage fluorescence induced in *F. solani* hyphae at a concentration of 3 μM peptide are compared to the IC_{max} values obtained for *F. solani* in Chapter 4.

5.4.3 Kinetics of fungal membrane permeabilisation

To assess the kinetics of membrane permeabilisation, 24 hour *B. cinerea* cultures and fresh spores were incubated for 10 minutes with SYTOX green and subsequently treated with peptide (Figure 5.5).

Very fast uptake of SYTOX green in the *B. cinerea* cultures was detected for the Trc mixture and purified tyrocidines, suggesting that tyrocidine activity lead to a loss in the barrier integrity of the fungal cell wall and membranes. This dye uptake was much faster than both Triton X-100 treatment and treatment with 8 μM of the lytic peptide GS. However, the membrane permeabilisation activity of the Trc mixture plateaus after approximately 20 minutes and after 60 minutes does not induce SYTOX green uptake to the same extent as 1% Triton X-100 (Figure 5.5). Similar results were found for the dye uptake in spores (results not shown). Therefore, at tyrocidine concentrations which results in complete fungicidal inhibition of *B. cinerea* growth,

tyrocidine-induced SYTOX green uptake is only half of that observed for 1% Triton X-100, but similar to that of the known membrane active analogous peptide GS.

These results suggest that the tyrocidines do not induce the complete disintegration of fungal membranes at these fungicidal concentrations, as is the case with Triton X-100. Similar results were obtained with purified tyrocidines indicating a shared mode of membrane action for the tyrocidines (Figure 5.5). The tyrocidines could potentially both induce damage to the fungal cell wall and permeabilise membranes to gain entry to internal targets.

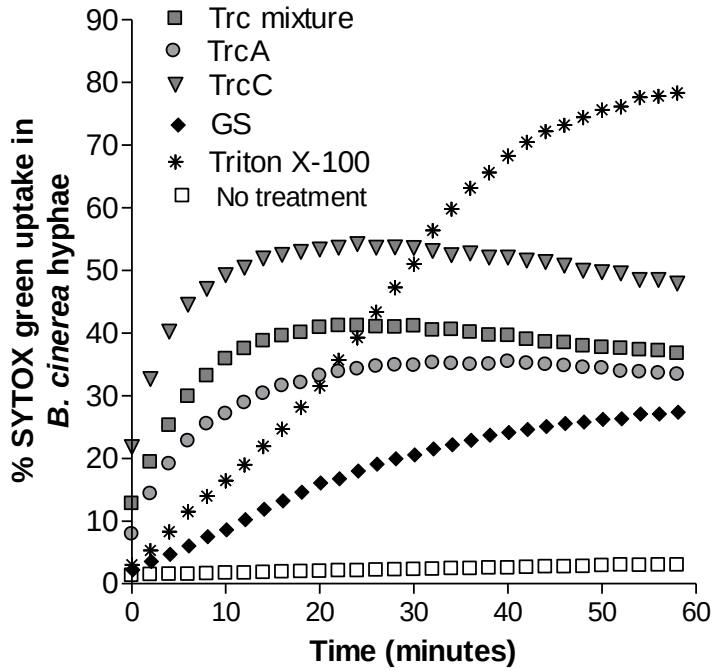

Figure 5.5: SYTOX green uptake by *B. cinerea* hyphae treated with the tyrocidines. *B. cinerea* hyphae were incubated for 10 minutes with SYTOX green, followed by the addition of 12 µg/mL Trc mixture, 12 µM TrcC, 12 µM TrcA, 8 µM GS or 1% Triton X-100. SYTOX green uptake was monitored for 1 hour. Data are the average of two repeats with 1% Triton X-100 serving as lysis control.

When the membrane permeabilisation activities of the three major tyrocidines are compared a strong relationship is again observed between high antifungal activity and membrane activity. TrcA has relatively higher biological activity against *F. solani* and induces a higher percentage SYTOX green uptake in *F. solani* hyphae than TrcC (Figure 5.6). The opposite is true for *B. cinerea*. TrcC, with a lower IC_{50} than TrcA, induces a higher percentage of SYTOX green

fluorescence in *B. cinerea* hyphae after one hour. From Figure 5.6 it is also evident that at 12 μM the tyrocidines are much more lytic toward *F. solani* than *B. cinerea*. This difference is even more pronounced if the IC_{max}/IC_{50} values (Chapter 4) against the two species are taken into account, with the peptides being generally less active against *F. solani*. These results raise the question if the tyrocidines' mode(s) of action against the two fungal species are similar. It would appear as if the action of the tyrocidines is more membrane targeted against *F. solani* than against *B. cinerea*. Previous investigations in our group have indicated that the tyrocidines have an additional mode of antibacterial action to that of membrane activity which is enhanced by the presence of Ca^{2+} (25, 26). In Chapter 4 it was illustrated that although the activity of the tyrocidines against *B. cinerea* were influenced by the presence of Ca^{2+}, it was much less susceptible than their activity against *F. solani*. It could therefore be hypothesised that the membrane activity of the tyrocidines are negatively influenced by the presence of Ca^{2+}, but that their additional mode(s) of action are less susceptible or even enhanced by the presence of Ca^{2+} and that these additional mode(s) of action are employed against *B. cinerea*. An alternative explanation is that *F. solani* and *B. cinerea* have differences in their growth/rates in PDB medium (refer to Chapter 3) which may influence their membrane permeability and sensitivity towards the tyrocidines.

Even though there are conserved sequence differences between the different tyrocidines, they all seem to be membrane active, albeit to different degrees at lower concentrations (Figure 5.3 and 5.4). There is also a strong correlation between high antifungal activity and ability to permeabilise fungal membranes (Figure 5.4 and 5.6). However, it has been observed that if any AMP is present at an adequate concentration the permeability of the cytoplasmic membrane increases (12). The connection between high antifungal activity and membrane permeabilisation may not necessarily be lytic activity, but the ability of the peptides to transverse the membrane and interact with an internal target.

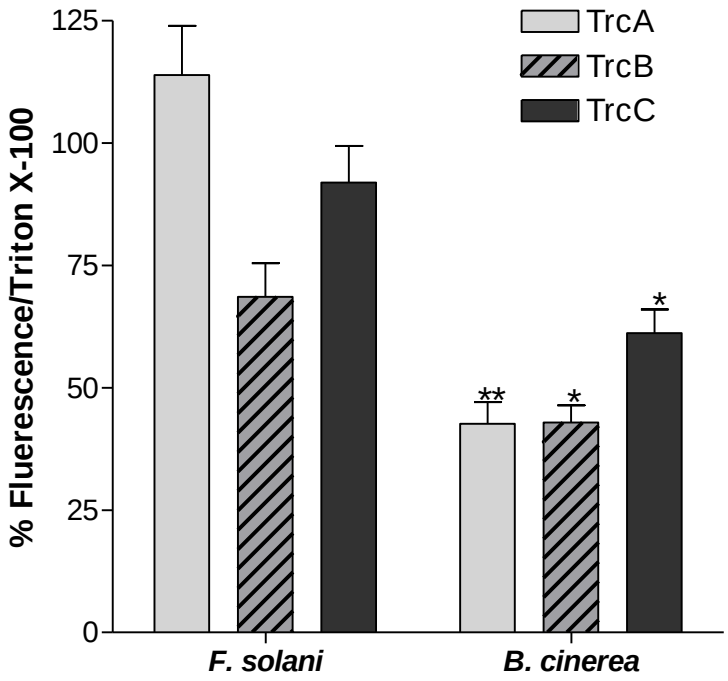

Figure 5.6: Comparison of TrcA, TrcB and TrcC's ability to disturb the integrity of *F. solani* and *B. cinerea* membranes after an incubation period of one hour at a concentration of 12 µM. TrcA, TrcB and TrcC induced SYTOX green uptake was significantly lower in *B. cinerea* than in *F. solani* (**P<0.01, *P<0.05) as determined with the Student t-test (One-tailed).

Therefore it still remains to be elucidated if the tyrocidines have additional or alternative mode(s) of action, especially at lower concentrations. This is of particular interest since we have illustrated in Chapter 4 that tyrocidine activity leads to retarded germination and hyperbranching. Hyperbranching/retarded germination activity can be the result of peptide interference with regulators of spore germination, hyphal elongation and lateral branching such as GTPases (27, 28), cAMP signalling (29, 30), formins and septins (27, 29), the Spitzenkorper, the microtubule cytoskeleton (27, 31), and actin polymerization. In some fungi it also seems as if the cell cycle a regulatory influence has on hyphal branching (27, 32). Therefore there is the possibility that the tyrocidines target any one or more of the above mentioned processes in addition to membrane disruption.

5.4.4 Peptide induced calcein release

In order to further study the tyrocidines' membrane activity, peptide-induced calcein release from model membranes (LUVs), comprising of either POPC:Erg or POPC:GlcCer, was

investigated. Ergosterol (Erg) is the major sterol in filamentous fungal membranes (33) and glucosylceramides (GlcCer) the most common neutral glycosphingolipid found in fungi (21). TrcA, TrcB and TrcC, TpcC, PhcA and GS were investigated for their ability to disturb the integrity of fungal model LUVs composed either of POPC:Erg (70:30) or POPC:GlcCer (70:30). The individual tyrocidines and their analogues resulted in varying degrees of calcein release from the different LUVs (Figure 5.7). Dose-response curves of calcein release after one minute was used to calculate the EC_{50}'s of the peptides (Table 5.1).

The ability to induce calcein release varied both between peptide and LUV identity. With regard to the POPC:Erg LUVs, TrcC exhibited the highest dye release activity (EC_{50} of 0.38 µM). TpcC, PhcA and TrcB followed with comparable EC_{50}'s of respectively 0.57, 0.59 and 0.64 µM. In terms of the other tyrocidines, TrcA had the lowest lytic activity with an EC_{50} of 0.75 µM. With an EC_{50} of 2.38 µM, GS exhibited the lowest calcein release and therefore lytic activity. A decrease in calcein release and larger diffrences between the activities of the individual peptides were observed for POPC:GlcCer LUVs. Although the membrane activity of TrcC decreased by a factor of two, TrcC still exhibited the highest activity. TrcB and PhcA exhibited the second highest activity, followed by TpcC. TrcA, with an EC_{50} of 3.07 µM, and GS, with an EC_{50} of 7.83 µM, again exhibited the lowest calcein release activity.

Comparing the peptide structures with their membrane activities it could be observed that TrcC, with two Trp residues, displayed the highest calcein release activity. This activity is followed by TrcB, a peptide with one Trp residue. The lowest dye release activity is exhibited by TrcA whose sequence does not contain any Trp residues. These results are consistent with results from Schmidtchen *et al.* (34) who found that end-tagging short AMPs with Trp increases their membrane activity and selectivity for ergosterol-containing model fungal membranes. Conversely, this observed trend for increased membrane activity and selectivity for Trp containing peptides are not applicable to the two tyrocidine analogues. TpcC, with three Trp

residues, exhibited lower dye release activity than PhcA, whose sequence does not have any Trp residues. TpcC also exhibited lower or similar lytic activity against the model membranes than that of TrcC and TrcB, respectively possessing only two and one Trp residue. These results could possibly imply that a Trp residue increases membrane activity and selectivity, but that other factors, such as the importance of the Tyr residue in the major tyrocidines, also plays a role in the membrane disruptive activity of the tyrocidines.

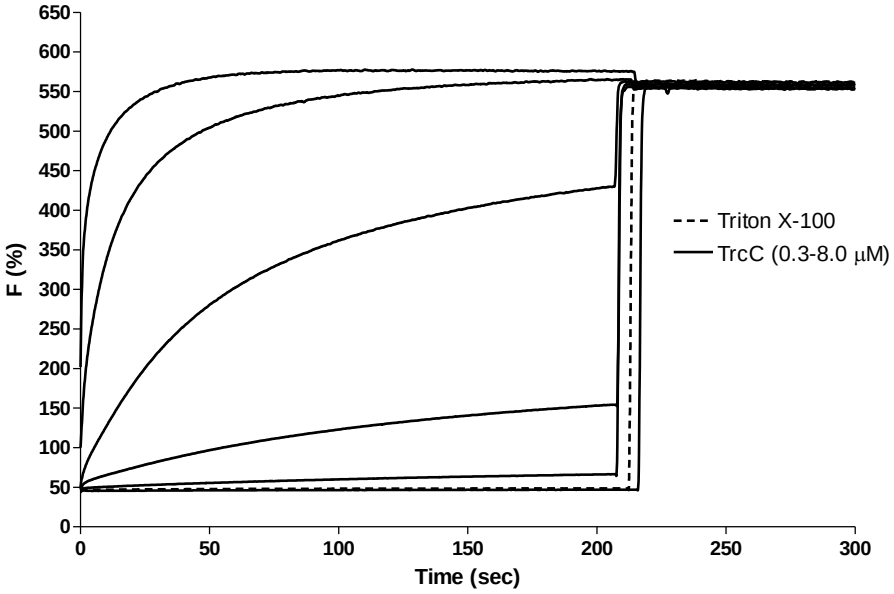

Figure 5.7: Kinetics of large unilamillar vesicle (LUV) permeabilisation. Representative dequenching of calcein fluorescence (F) induced by TrcC from POPC:GlcCer (70:30) LUVs as a function of time. The lipid concentration was 25 μM and the concentration of TrcC ranged from 0.32 μM to 8 μM in buffer (10 mM Tris, 0.1 mM EDTA, 154 mM NaCl, pH 7.4). After approximately 4 minutes, total dequencing was induced by the addition of Triton X-100.

GS exhibited lower dye release activity than all of the tyrocidines and their analogues. The tyrocidines significant decrease (up to four fold) against membranes consisting of POPC:GlcCer indicate that these peptides are sensitive to the presence of glucosylceramides. These results could be noteworthy since the $GlcCer_{soybean}$ used in this study to prepare the POPC:GlcCer is structurally very similar to $GlcCer_{F.solani}$, the main neutral glycolipid in *F. solani* (35). $GlcCer_{F.solani}$ differs from $GlcCer_{soybean}$ in only two positions. $GlcCer_{F.solani}$ has a methyl group on its ninth carbon and a double bond on its third carbon which is not present in $GlcCer_{soybean}$ (21).

This could possibly explain the relatively lower activity of the tyrocidines against *F. solani* compared to *B. cinerea*.

Table 5.1 Comparison of antifungal and LUV permeabilisation activity parameters for selected tyrocidines

	B. cinerea	*F. solani*	POPC:Erg (70:30)	POPC:GlcCer (70:30)
	IC_{50}[1]	IC_{50}[1]	EC_{50}[2]	EC_{50}[2]
Trc mix	2.72 ± 0.39	3.88 ± 0.34	-	-
$TrcA_1$	2.73 ± 0.20	2.92 ± 0.33	-	-
TrcA	2.25 ± 0.40	3.17 ± 0.39	0.75 ± 0.60	3.07 ± 0.29
$TrcB_1$	2.59 ± 0.20	6.62 ± 1.76	-	-
TrcB	2.11 ± 0.25	5.68 ± 0.44	0.64 ± 0.05	1.23 ± 0.00
$TrcC_1$	2.34 ± 0.33	3.21 ± 0.19	-	-
TrcC	2.03 ± 0.29	3.33 ± 0.22	0.38 ± 0.02	0.61 ± 0.06
PhcA	3.20 ± 0.23	5.19 ± 0.82	0.59 ± 0.10	1.26 ± 0.14
TpcC	4.33 ± 0.63	17.7 ± 4.49	0.57 ± 0.15	2.02 ± 0.12
GS	1.06 ± 0.03	1.62 ± 0.05	2.38 ± 0.03	7.83 ± 0.30

[1]The IC_{50} values determined in Chapter 4 are included for comparison.
[2] The LUV permeabilisation activity values represent the average of duplicate repeats ±SEM.

Comparing the calcein release results with both biological activity and SYTOX green fluorescence results, a few inconsistencies in the activity order of the individual peptides can be observed. First inconsistency is the high antifungal but generally low lytic activity of GS. The antifungal activity of GS is potent against both *F. solani* and *B. cinerea* and is generally higher than that of the tyrocidines. Furthermore, in contrast to the calcein release activity, the SYTOX green uptake induced by GS was significant (Figure 5.2 and 5.3). However, in the model membranes GS's calcein release activity is considerably lower than that of the tyrocidines. For the POPC:GlcCer LUVs, GS's calcein release activity is almost 13-fold lower than that of TrcC and for the POPC:Erg LUVs 6-fold lower (Table 5.1). This may indicate that the permeabilisation of the fungal hyphae may depend on alternative factors, other than membrane permeabilisation, such as self-promoted uptake *via* lesions in the cell wall (36). The hypothesis that AMP interaction with other cellular structures (such as cell wall components) may enhance/influence AMP membrane disruptive activity, has also been offered (37).

TrcA exhibited antifungal activity (Chapter 4 and Table 5.1) and induction of SYTOX green fluorescence (Figure 5.3) equal to that of TrcC. However, the calcein release activity of TrcA was considerably lower than that of TrcC. TrcA's calcein release activity is even lower than that of TpcC, the tyrocidine with the lowest antifungal activity (Table 5.1 and Chapter 4). TrcB, PhcA and TpcC were expected to exhibit lower calcein release activity than TrcC since they in general exhibited lower antifungal activity and SYTOX green uptake in *F. solani*. This discrepancy between model membrane results and that of the biological results could indicate that other factors in the cell membrane influence biological membrane activity and/or other cellular parameters/targets influence the antifungal activity of the tyrocidines, for instance the composition of the cell wall. In addition the differences between a biological system (i.e. growing fungal cells) and a model system (i.e. static liposomes) must be considered. While only the interaction of the peptides with the model membrane is measured in the liposome model, various factors contribute to the interaction of peptides with living cells. The growth rate, the cell metabolism, the cell cycle as well as defence mechanisms are just some of the factors which may influence the peptide activity in a biological system.

The lower lytic activity of the tyrocidines and analogues against the liposomes containing GlcCer and the loss of activity towards glucanase treated *F. solani* may indicate that the peptides interact with carbohydrate moieties that could either enhance or inhibit their antifungal activity. This is not the case for GS, which was only less lytic in the presence of GlcCer, indicating a difference in mode of action. These results could also support the theory that the tyrocidines have additional targets to that of the cell membrane, for instance depending on the composition of the cell wall, and that other cellular parameters and events may determine their antifungal activity, especially at lower tyrocidine concentrations.

5.4.5 Tryptophan quenching studies

In order to further understand tyrocidine interaction with model membranes tryptophan fluorescence quenching experiments using *n*-doxyl phosphatidylcholines (TEMPO-, 5-DOX- and 12-DOX) were used to determine if and how deep the tyrocidines insert into POPC:Erg and POPC:GlcCer model membranes (Figure 5.8). Two tryptophan containing peptides, TrcB and TrcC, were used as representative tyrocidines. According to results using the parallax method (22, 38) the distance of TrcB from the bilayer centre for POPC:Erg and POPC:GlcCer was respectively 10.9 Å and 11.3 Å. For both the POPC:Erg and POPC:GlcCer membranes TrcC's distance from the bilayer centre was 11.9 Å (Table 5.2).

The parallax analysis is most accurate when the Trp residue is close to the quencher (39). From Figure 5.8 it is evident that the POPC:GlcCer bound TrcC was the most affected by 5-DOX and 12-DOX compared to TEMPO. The tryptophan fluorescence of TrcC and TrcB, bound to POPC:Erg and POPC:GlcCer was the most strongly quenched by 5-DOX and 12-DOX (Table 5.2). The calculated distances for Trp (z_{cf}) from the bilayer centre show that TrcC and TrcB insert into the membrane bilayer and are positioned close to the phosphate head groups. Furthermore, the tryptophan's of both peptides have relatively the same position in the bilayer and that their positions are not significantly influenced by the composition of the membrane. These results indicate that the tyrocidines interact with and insert into fungal model membranes.

The depths of insertion for TrcB and TrcC are comparable for both the POPC:Erg and POPC:GlcCer membranes, contrary to what one would expect from the calcein release, SYTOX uptake and biological activity results. It would therefore seem as if it is not necessarily the depth of membrane insertion that determines the membrane permeabilisation and biological activity of the tyrocidines. The variance in biological/membrane activity observed for TrcB and TrcC can either be related to a non-membrane related target/mode of action or to other/additional parameters that determine the activities of the tyrocidines.

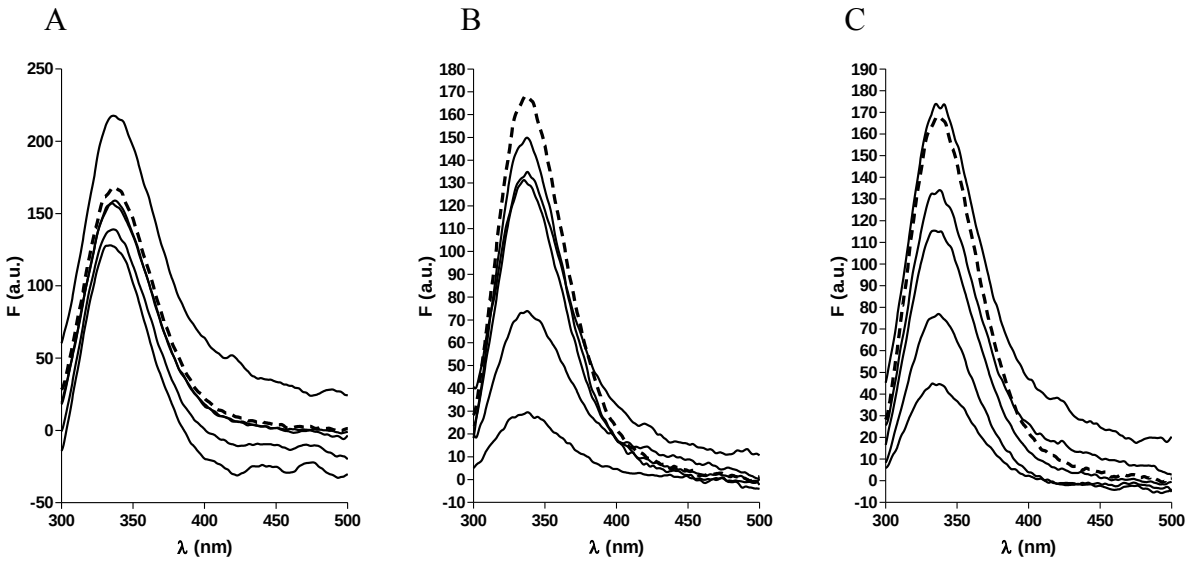

Figure 5.8: Representative fluorescence spectra of TrcC bound to POPC:GlcCer vesicles containing (**A**) TEMPO, (**B**) 5-DOX and (**C**) 12-DOX-labelled lipids. The lipid concentration (c_l) was 200 μM while the concentration of peptide (c_p) was 2 μM. The fraction of the spin-labelled lipids was 10, 15, 20, 30 and 40 mol %. The dotted line represents vesicles without spin-labelled lipids.

Table 5.2 Quenching of tryptophan fluorescence by nitroxide-labeled lipids and distances between tryptophan and bilayer centre

	POPC:Erg (70:30 mol/mol)				POPC:GlcCer (70:30 mol/mol)			
	TrcB		TrcC		TrcB		TrcC	
	S	z_{cf}(Å)	*S*	z_{cf}(Å)	*S*	z_{cf}(Å)	*S*	z_{cf}(Å)
Tempo	-1.1503	11.4	0.3004	9.2	-0.0014	9.8	0.0048	8.9
5-DOX	-4.0804	10.9	-4.0842	11.9	-3.9633	11.3	-4.5665	11.9
12-DOX	-3.0129	11.2	-0.0246	10.4	-2.6895	10.5	-2.9581	10.3

S is the slope of the plot F/F_o vs the mole fraction of lipids carrying spin labels 19.5 Å (TEMPO) 12.2 Å (5-DOX) and 5.85 Å (12-DOX) (30) from the bilayer centre . F/F_o is the ratio of W fluorescence intensity in vesicles containing quencher to that of vesicles without.

As we mentioned above, there is the suggestion that the tyrocidines may form higher-order structures necessary for activity, in particular dimers which displays an amphipathic structure (25, 40). The interaction of these higher-order structures with the target membrane bilayer of fungi may be different to the model membranes as these biological membranes have much more complex structures.

5.5 Conclusion

Studies with the membrane impermeable dye SYTOX green and calcein release studies with model membranes indicate that the tyrocidines are active against fungal membranes. Although induction of high SYTOX green fluorescence could be related to high biological activity and the importance of the Tyr^7 residue, high calcein release activity did not necessarily correlate to high biological membrane activity or high antifungal activity. Kinetics of fungal membrane permeabilisation indicated that although higher antifungal activity could be related to increased membrane activity, tyrocidine concentrations that led to 100 % fungal death did not result in complete disintegration of the fungal membrane. Furthermore, tryptophan quenching studies indicate that tyrocidines insert into fungal model membranes, but depth of insertion does not appear to determine either high calcein release or biological activity. These results suggest that other factor(s) in addition to membrane composition influences/determines the tyrocidines ability to permeabilise the fungal membrane; and/or the tyrocidines act on additional target(s) or lead to cellular events causing cell death that is not only due to membrane permeabilisation. The decrease in tyrocidine antifungal activity in the absence of the fungal cell wall supports the hypothesis that additional factors influence/determines tyrocidine antifungal activity.

5.6 References

1. **Nakatsuji T, Gallo RL.** 2012. Antimicrobial peptides: Old molecules with new ideas. Journal of Investigative Dermatology. **132:**887-895.

2. **Andreu D, Rivas L.** 1998. Animal antimicrobial peptides: An overview. J. Pept. Sci. **47:**415-433.

3. **Zasloff M.** 2002. Antimicrobial peptides of multicellular organisms. Nature. **415:**389-395.

4. **Augustin R, Anton-Erxleben F, Jungnickel S, Hemmrich G, Spudy B, Podschun R, Bosch TCG.** 2009. Activity of the novel peptide arminin against multiresistant human pathogens shows the considerable potential of phylogenetically ancient organisms as drug sources. Antimicrobial Agents and Chemotherapy. **53:**5245-5250.

5. **Godballe T, Nilsson LL, Petersen PD, Jenssen H.** 2011. Antimicrobial β-peptides and α-peptoids. Chemical Biology & Drug Design. **77:**107-116.

6. **Rautenbach M, Vlok NM, Stander M, Hoppe HC.** 2007. Inhibition of malaria parasite blood stages by tyrocidines, membrane-active cyclic peptide antibiotics from *Bacillus brevis*. Biochim. Biophys. Acta. **1768:**1488-1497.

7. **Ullal AJ, Noga EJ.** 2010. Antiparasitic activity of the antimicrobial peptide HbβP-1, a member of the β-haemoglobin peptide family. Journal of Fish Diseases. **33:**657-664.

8. **Albiol Matanic VC, Castilla V.** 2004. Antiviral activity of antimicrobial cationic peptides against Junin virus and herpes simplex virus. International Journal of Antimicrobial Agents. **23:**382-389.

9. **Spadaro D, Gullino ML.** 2004. State of the art and future prospects of the biological control of postharvest fruit diseases. Int. J.Food Micrbiol. **91:**185-194.

10. **Bouchra C, Achouri M, Hassani ILM, Hmamouchi M.** 2003. Chemical composition and antifungal activity of essential oils of seven Moroccan Labiatae against *Botrytis cinerea* Pers: Fr. Journal of Ethnopharmacology. **89:**165-169.

11. **Hancock REW, Patrzykat A.** 2002. Clinical development of cationic antimicrobial peptides: from natural to novel antibiotics. Current Drug Targets - Infectious Disorders. **2:**79-83.

12. **Zhang L, Rozek A, Hancock REW.** 2001. Interaction of cationic antimicrobial peptides with model membranes. Journal of Biological Chemistry. **276:**35714-35722.

13. **Lobo DS, Pereira IB, Fragel-Madeira L, Medeiros LN, Cabral LM, Faria J, Bellio M, Campos RC, Linden R, Kurtenbach E.** 2007. Antifungal *Pisum sativum* defensin 1 interacts with *Neurospora crassa* Cyclin F related to the cell cycle. Biochemistry. **46:**987-996.

14. **De Lucca AJ, Walsh TJ.** 1999. Antifungal peptides: Novel therapeutic compounds against emerging pathogens. Antimicrobial Agents and Chemotherapy. **43:**1-11.

15. **Helmerhorst EJ, Troxler RF, Oppenheim FG.** 2001. The human salivary peptide histatin 5 exerts its antifungal activity through the formation of reactive oxygen species. Proceedings of the National Academy of Sciences USA. **98:**14637–14642.

16. **Jenssen H, Hamill P, Hancock REW.** 2006. Peptide antimicrobial agents. Clinical Microbiology Reviews. **19:**491-511.

17. **Spathelf BM, Rautenbach M.** 2009. Anti-listerial activity and structure–activity relationships of the six major tyrocidines, cyclic decapeptides from *Bacillus aneurinolyticus*. Bioorg. Med. Chem. **17:**5541-5548.

18. **van der Weerden NL, Hancock REW, Anderson MA.** 2010. Permeabilization of fungal hyphae by the plant defensin NaD1 occurs through a cell wall-dependent process. Journal of Biological Chemistry. **285:**37513-37520.

19. **van der Weerden NL, Lay FT, Anderson MA.** 2008. The plant defensin, NaD1, enters the cytoplasm of *Fusarium oxysporum* hyphae. J. Biol. Chem. **283:**14445-14452.

20. **Dathe M, Schümann M, Wieprecht T, Winkler A, Beyermann M, Krause E, Matsuzaki K, Murase O, Bienert M.** 1996. Peptide helicity and membrane surface

charge modulate the balance of electrostatic and hydrophobic interactions with lipid bilayers and biological membranes. Biochemistry. **35:**12612-12622.

21. **Gonçalves S, Teixeira A, Abade J, de Medeiros LN, Kurtenbach E, Santos NC.** 2012. Evaluation of the membrane lipid selectivity of the pea defensin Psd1. Biochimica et Biophysica Acta (BBA) - Biomembranes. **1818:**1420-1426.

22. **Dathe M, Nikolenko H, Klose J, Bienert M.** 2004. Cyclization increases the antimicrobial activity and selectivity of arginine- and tryptophan-containing hexapeptides. Biochemistry. **43:**9140-9150.

23. **Böttcher CJF, Van gent CM, Pries C.** 1961. A rapid and sensitive sub-micro phosphorus determination. Analytica Chimica Acta. **24:**203-204.

24. **Rautenbach M, Gerstner GD, Vlok NM, Kulenkampff J, Westerhoff HV.** 2006. Analyses of dose-response curves to compare the antimicrobial activity of model cationic α-helical peptides highlights the necessity for a minimum of two activity parameters. Anal. Biochem. **350:**81-90.

25. **Spathelf BM.** 2010. Qualitative structure-actvity relationships of the major tyrocidines, cyclic decapeptides from *Bacillus aneurinolyticus*. PhD Thesis, Department of Biochemistry, University of Stellenbosch, http://scholar.sun.ac.za/handle/10019.1/4001.

26. **Leussa AN-N.** 2013. Characterisation of small cyclic peptides with antimalarial and antilisterial activity, Department of Biochemistry, University of Stellenbosch, PhD Thesis in progress, completion March 2014. Personal communication.

27. **Harris SD.** 2008. Branching of fungal hyphae: regulation, mechanisms and comparison with other branching systems. Mycologia. **100:**823-832.

28. **Nesher I, Minz A, Kokkelink L, Tudzynski P, Sharon A.** 2011. Regulation of pathogenic spore germination by CgRac1 in the fungal plant pathogen *Colletotrichum gloeosporioides*. Eukaryotic Cell. **10:**1122-1130.

29. **Boyce KJ, Chang H, D'Souza CA, Kronstad JW.** 2005. An *Ustilago maydis* septin is required for filamentous growth in culture and for full symptom development on maize. Eukaryotic Cell. **4:**2044-2056.

30. **Fillinger S, Chaveroche M-K, Shimizu K, Keller N, D'Enfert C.** 2002. cAMP and Ras signalling independently control spore germination in the filamentous fungus *Aspergillus nidulans*. Molecular Microbiology. **44:**1001-1016.

31. **Kaiserer L, Oberparleiter C, Weiler-Görz R, Burgstaller W, Leiter E, Marx F.** 2003. Characterization of the *Penicillium chrysogenum* antifungal protein PAF. Archives of Microbiology. **180:**204-210.

32. **Binder U, Oberparleiter C, Meyer V, Marx F.** 2010. The antifungal protein PAF interferes with PKC/MPK and cAMP/PKA signalling of *Aspergillus nidulans*. Mol. Microbiol. **75:**294-307.

33. **Pasanen A-L, Yli-Pietilä K, Pasanen P, Kalliokoski P, Tarhanen J.** 1999. Ergosterol content in various fungal species and biocontaminated building materials. Applied and Environmental Microbiology. **65:**138-142.

34. **Schmidtchen A, Ringstad L, Kasetty G, Mizuno H, Rutland MW, Malmsten M.** 2011. Membrane selectivity by W-tagging of antimicrobial peptides. Biochimica et Biophysica Acta. **1808:**11-11.

35. **Duarte RS, Polycarpo CR, Wait R, Hartmann R, Barreto Bergter E.** 1998. Structural characterization of neutral glycosphingolipids from Fusarium species. Biochimica et Biophysica Acta (BBA) - Lipids and Lipid Metabolism. **1390:**186-196.

36. **Meincken M, Holroyd DL, Rautenbach M.** 2005. Atomic force microscopy study of the effect of antimicrobial peptides on the cell envelope of *Escherichia coli*. Antimicrob. Agents Chemother. **49:**4085-4092.

37. **Marcos JF, Gandía M.** 2009. Antimicrobial peptides: to membranes and beyond. Expert Opinion on Drug Discovery. **4:**659-671.

38. **Chung LA, Lear JD, DeGrado WF.** 1992. Fluorescence studies of the secondary structure and orientation of a model ion channel peptide in phospholipid vesicles. Biochemistry. **31:**6608-6616.

39. **Ladokhin AS, Holloway PW.** 1995. Fluorescence of membrane-bound tryptophan octyl ester: a model for studying intrinsic fluorescence of protein-membrane interactions. Biophysical Journal. **69:**506-517.

40. **Munyuki G, Jackson GE, Venter GA, Kövér KE, Szilágyi L, Rautenbach M, Spathelf BM, Bhattacharya B, Van der Spoel D.** 2013. β-Sheet structures and dimer models of two major tyrocidines, antimicrobial peptides from *Bacillus aneurinolyticus*. Biochemistry. **52:**7798-7806.

Chapter 6

Synergistic activity of the tyrocidines, antimicrobial cyclodecapeptides from *Bacillus aneurinolyticus*, with amphotericin B and caspofungin against *Candida albicans* biofilms

6.1 Introduction

In recent years a rise in the frequency and variety of human fungal infections has been observed (1) with growing resistance against conventional antifungal drugs (1-4). The widespread use of broad spectrum antibiotics together with the growth in immune compromised individuals (1-3), immune-suppression, chemotherapy and radiotherapy (1, 4) are just some of the factors that have led to this increase in the occurrence of resistant fungal pathogens. *Candida* species in particular lead to serious infections and are recognised as one of the major causative agents of nosocomial infections (5, 6). *Candida albicans* is the most commonly isolated species, which predominantly forms biofilms on biotic and abiotic surfaces. Biofilms are microbial communities embedded in a polymeric matrix (4-7). Biofilm formation on biological and/or inert surfaces is usually the culprit behind the instigation of candidiasis (5, 8, 9). Furthermore, *C. albicans* biofilms have been shown to be particularly resistant to antifungal agents commonly used to control fungal infections, including amphotericin B and fluconazole (5, 8, 10-12).

Amphotericin B (AmB) and caspofungin (CAS) are currently two key drugs in the treatment of fungal infections (13, 14). AmB acts through the binding of its hydrophobic moiety to the fungal sterol ergosterol, resulting in the formation of transmembrane channels and cytoplasmic leakage (14-16). However, AmB's severe nephro- and renal toxicity in some cases necessitates the premature termination of AmB treatment (14). Furthermore, there is a rise in isolates resistant to AmB treatment (17-19). CAS, a semi-synthetic lipopeptide from the echinocandin family,

inhibits the synthesis of the major structural component in fungal cell walls, 1,3-β-D-glucan (1, 8, 20). Although CAS has a very good track record regarding side-effects with limited development of microbial resistance, resistance against CAS has been observed (1, 20). Strains of *C. albicans* with mutations in their (1,3)-D-glucan synthase show *in vitro* resistance against caspofungin (1).

The rise in fungal pathogens resistant to conventional treatments (6, 21) has driven the search for novel antifungal compounds and treatments that simultaneously exhibit specificity toward fungal cells and low risk for inducing pathogen resistance. Combinatorial treatment is considered as a solution to the development of resistance against an individual compound. Combining compounds that act synergistically in general allows for lower drug dosage with concurrent decrease in toxicity (6).

Antimicrobial peptides (AMPs) are the first line of defence in most organisms (22) and in recent years have been considered as potential alternatives/supplements to traditional antifungal compounds (6). The tyrothricin complex (the tyrocidine-gramicidin metabolite complex from *Bacillus aneurinolyticus*) was one of the first antibiotic preparations to be used as a topical antibiotic (23, 24) The tyrocidine component of the tyrothricin complex has been illustrated to have significant anti-bacterial (24, 25) and anti-malarial (26) activity. So far only tyrothricin (the tyrocidine-gramicidin complex) has been observed to have activity against *C. albicans* (27).

To our knowledge this is the first investigation on the activity of the tyrocidines against planktonic and biofilm *C. albicans* cells. We report the antiyeast and antibiofilm activity of the three major tyrocidines (tyrocidine A, B and C) and two of their analogues (phenycidine A and tryptocidine C) against *C. albicans*. The membrane impermeable dye propidium iodide was used to investigate the tyrocidines effect on the integrity of biofilm cell membranes. With combinatorial treatment in mind the tyrocidines were also evaluated for potential enhancing effect on the *in vitro* biofilm eradication activity of AmB and CAS. A *Caenorhabditis elegans*

infection model was used to assess the *in vivo* efficacy and toxicity of tyrocidine A in combination with CAS.

6.2 Materials

6.2.1 Strain and media

The *Candida albicans* SC5314 known to form biofilms was used in this study as target organism (28). Overnight cultures were grown in YPD (1% yeast extract, 2% peptone and 2% glucose) or on YPD agar (1% yeast extract, 2% peptone, 2% glucose and 1.5% agar). PBS (pH 7.4) was prepared with NaCl (8 g/L), KCl (0.2 g/L), Na_2HPO_4 (1.44 g/L) and KH_2PO_4 (0.24 g/L). *C. albicans* was grown in RPMI 1640 medium with $_L$-glutamine and without bicarbonate (pH 7.0) purchased from Sigma (St. Louis, USA).

6.2.2 Peptides

The tyrocidines were purified and analysed for purity as described in Chapter 2. *De novo* sequencing using electrospray mass spectrometry by Vosloo *et al.* (29) and Spathelf (30) confirmed the identity of the tyrocidines and analogues. All the tyrocidines (TrcA, TrcB, TrcC, TpcC and PhcA) used in this study had purities >90% according to ultra-performance liquid chromatography linked to high resolution electrospray mass spectrometry (refer to Chapter 2). Gramicidin S (GS) (97.5 % purity according to manufacturers, 94% purity according to UPLC-MS, Chapter 2) was supplied by Sigma (St Louis, USA).

6.3 Methods

6.3.1 Anti-planktonic yeast assays

The anti-yeast activity of the Trc mixture (group of tyrocidines isolated from commercial tyrothricin (26)), selected tyrocidines, tyrocidine analogues and gramicidin S (GS) was determined using the standard NCLLS M27-A protocol (31).

6.3.2 Biofilm prevention activity assays

The ability of the tyrocidines and analogous peptides to prevent the formation of *C. albicans* biofilms was determined using micro-dilution assays in 96-well tissue culture microtiter plates as optimised by the Plant-Fingus Interaction group (PFI) at the Centre of Microbial and Plant Genetics (CMPG) at the KU Leuven in Belgium (32). *C. albicans* cells in RPMI 1640 medium (1 × 10 cells/mL) were incubated with 0.78-100.0 μM tyrocidines (final ethanol concentration of 1%) for 24 hours at 37°C. One percent ethanol in RPMI 1640 medium was the control treatment. The biofilms were washed with PBS and biofilm formation was determined using CellTiterBlue™ (Promega, Madison,WI) staining. After 1 hour incubation at 37°C, fluorescence was measured with a Multimode Microplate Reader, Synergy MX, BioTek, at wavelengths 535 nm (excitation) and 617 nm (emission).

6.3.3 **In vitro *biofilm eradication assay***

In vitro eradication activity was determined using 96-well microtiter as optimised by the PFI at the CMPG at the KU Leuven in Belgium (32). *C. albicans* biofilms were grown in 96-well microtiter plates in RPMI 1640 medium at 37°C. Subsequent to a PBS wash step, the biofilms were incubated with tyrocidine (concentration range 1.6-200.0 μM) in RPMI 1640 medium (final ethanol concentration of 1%) for 24 hours at 37°C. One percent ethanol in RPMI 1640 medium served as control treatment. The combined eradication activity of the tyrocidines and CAS/AmB was determined by incubating 24 hour old biofilms with 0.04-5.0 μM of either AmB (Sigma-Aldrich, St Louis, USA) or CAS (Merck, United Kingdom), in the absence or presence of either 1.8, 3.0 or 6.2 μM TrcA, TrcB or TrcC (final ethanol concentration of 0.05% and DMSO of 0.05%), for 24 hours at 37°C. Biofilm survival was measured using CellTiterBlue™ assays and the BEC_{50} was defined as the concentration that resulted in 50% eradication of 24 hour old *C. albicans* biofilms. Combinatorial activity of AmB/CAS and the tyrocidines were assessed by statistically comparing the BEC_{50} values of AmB/CAS alone, and in combination with tyrocidines, using the Bonferroni's multiple comparison test, as well as determining the

fractional inhibitory concentration index (FICI) (33). The FICI was calculated using the following equation:

$$FICI = [C_{A+B}/ C_A] + [C_{B+A}/C_B]$$

where C_A and C_B are the BEC_{50}'s of the antifungal compounds alone and C_{A+B} and C_{B+A} are the BEC_{50}'s of the antifungal compounds in combination. A FICI ≤0.5 was interpreted as synergistic, a FICI between 0.5-4.0 as indifferent and a FICI ≥4.0 as antagonistic (33).

6.3.4 Membrane-permeability assay

The membrane disruptive activity of the tyrocidines on 24 hour old *C. albicans* biofilms was determined using the membrane impermeable dye propidium iodide from Sigma-Aldrich (St. Louis, USA). Twenty-four hour old *C. albicans* biofilms were prepared as described for the biofilm eradication experiments. Subsequent to 24 hour treatment with tyrocidines (0.78-100.0 µM) at 37°C, the biofilms were washed with PBS and incubated with 1.5% propidium iodide in the dark for a further 20 minutes. Propidium iodide fluorescence was measured as described by Bink *et al.* (33) and fluorescence values of samples were corrected with values obtained for untreated biofilms. Triton X-100 (1%) served as the lytic control.

6.3.5 Assay for determination of endogenous reactive oxygen species

The induction of endogenous reactive oxygen species (ROS) was determined using the fluorescent dye 2',7'-dichlorodihydrofluorescein diacetate (H_2DCFDA) (Molecular Probes®, Eugene, USA). *C. albicans* biofilms were grown in 96-well microtiter plates in RPMI 1640 medium for 24 hours and treated for 24 hours with 0.78-100.0 µM tyrocidines. Biofilms were washed with PBS and incubated for 1 hour with 10.0 µM H_2DCFDA shaking at 37°C. Fluorescence was measured with a Multimode Microplate Reader, Synergy MX, BioTek, at excitation wavelength of 492 nm and emission of 525 nm (2). The relationship between endogenous ROS generation in *C. albicans* and tyrocidine antifungal activity was investigated using the antioxidant ascorbic acid. The influence of 10 mM ascorbic acid on the biofilm

eradication and ROS induction activity of 100 µM TrcA, TrcB and TrcC was determined (34, 35). Citric acid served as the pH control.

6.3.6 In vivo studies using Caenorhabditis elegans *model system*

The toxicity of TrcA and its combined effect on the *in vivo* activity of CAS was evaluated using the *C. elegans* model system described by Breger *et al.* (36). The efficacy of CAS alone, or in combination with TrcA, to increase survival of *C. albicans* infected nematodes, was evaluated over a period of seven days. The temperature sensitive *C. elegans* Δ*glp*-4Δ*sek*-1 mutants were stored on *Escherichia coli* OP50 covered NGM (0.25% Bacto Peptone, 0.3% NaCl, 1.7% Agar) plates at 16°C. Prior to infection, the nematodes were collected and treated with bleach in order to collect the eggs which were then incubated at 25°C so that all the nematodes reached the same growth phase (L3-L4) four days later for *C. albicans* infection and treatment studies. Nematodes were infected for two hours with *C. albicans* and subsequent to transfer to pathogen-free media, treated with 0.095/0.19 µM CAS, 3.0 µM TrcA, 0.095/0.19 µM CAS in combination with 3.0 µM TrcA or a combination of 0.5% ethanol and 0.5% DMSO as control. For the toxicity test the nematodes were treated with 3.0 and 6.0 µM TrcA and nematode survival was monitored for seven days. The control group received 0.5% ethanol. For both experiments survival was calculated relative to the survival on day 0.

6.3.7 Data analysis

Analyses of dose-response assay data were done with GraphPad Prism® 4.03 (GraphPad Software, San Diego, USA) using non-linear regression to generate sigmoidal curves and the data normalisation function (range 0-100%) if required (37). The IC_{50}, BEC_{50} and BIC_{50} represent the concentration necessary to cause 50% growth inhibition, biofilm eradication and biofilm prevention, respectively. The inhibition/eradication/prevention concentration, calculated as the x-value at the intercept between the slope and the top plateau of a full dose-response curve, was denoted as IC_{max} (37), to make the distinction with minimal inhibition concentration

(MIC) values obtained from visual inspection of a dose-response result. The values calculated from the full dose-response curves were used for statistical analyses. MIC and minimum biofilm prevention concentration (BIC) was defined as the lowest concentration that induced ≥ 95% inhibition compared to the growth control.

GraphPad Prism® 4.03 (GraphPad Software, San Diego, USA) was used for the statistical analysis of data. Analysis included 95% confidence levels, absolute sum of squares, standard error of the mean (SEM), Student t-tests and One-way ANOVA analyses using Bonferroni's multiple comparison test.

6.4 Results and discussion

6.4.1 Antifungal activity against Candida albicans *planktonic cells*

The Trc mixture, the three pure major tyrocidines (TrcA, TrcB and TrcC) and their analogues (PhcA and TpcC) showed noteworthy activity against planktonic *C. albicans* cells. Although their activity was not as high as that of AmB and CAS, the activities of the tyrocidines were still in the low micromolar range (Table 6.1). The Trc mixture exhibited high antifungal activity against *C. albicans* characterised by a MIC (minimal inhibitory concentration) of 6 µg/mL (Table 6.1). Purified tyrocidines and TpcC, as well as the analogous peptide gramicidin S (GS) were characterised by antifungal activity with MIC values of 6.25 µM (IC_{50s} ranging from 3.1-4.6 µM), whereas the phenycidine (PhcA) had a significantly higher MIC of 12.5 µM (IC_{50} of 7.9 µM) (Table 6.1 and Figure 6.1).

Tyrocidines have a highly conserved sequence, differing in some cases in only one amino acid residue. The major tyrocidines have the basic sequence of *cyclo*[$f^1P^2X^3x^4N^5Q^6Y^7V^8X^9L^{10}$] and the relevant tyrocidines only vary in one or two residue positions, $Trp^{3,4}$ or $Phe^{3,4}$ in the aromatic dipeptide unit. The two tyrocidine analogues in this study, PhcA (a phenycidine) and TpcC (a tryptocidines), respectively have a Phe^7 and Trp^7 instead of the Tyr^7 that is found in the major

tyrocidines (refer to Chapter 2). Except for PhcA, the minor differences in their sequences did not appear to significantly influence their fungicidal activity. Since PhcA has the highest hydrophobicity, the lower activity observed for PhcA could possibly be ascribed to peptide aggregation or alternatively point to the role of a residue with hydrogen bonding character such as Tyr a or Trp in residue position 7.

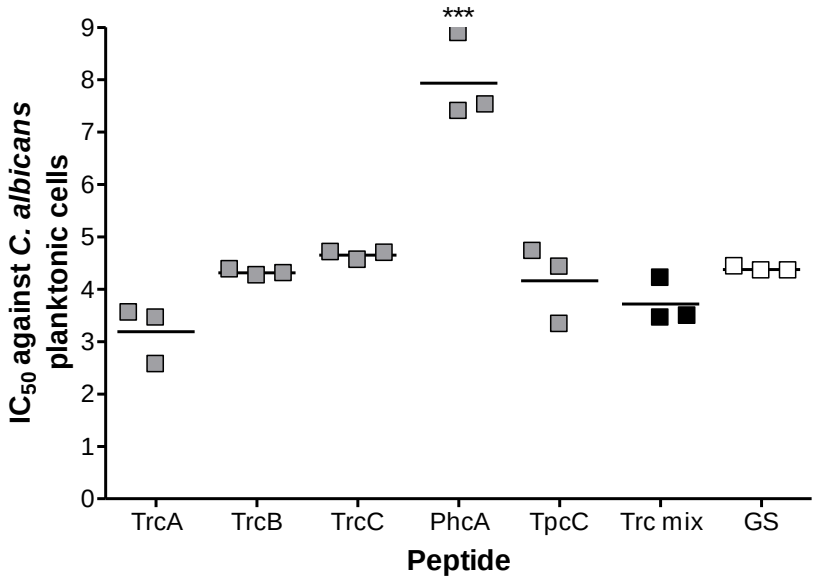

Figure 6.1: The activity parameters (IC_{50} values in µM, expect Trc mixture in µg/mL) of the individual peptides against planktonic *C. albicans* cells. Each data point represents the value of an individual biological activity determination (with three technical repeats per assay) with the line representing the mean of the individual data points. According to One-way ANOVA with Bonferroni's multiple comparison test the IC_{50} values of PhcA are significantly (***P<0.001) higher than the values for the other tyrocidines, TpcC and GS.

6.4.2 Activity against Candida albicans *biofilm cells*

Apart from their activity against planktonic cells, the tyrocidines and analogues were also able to prevent the formation of *C. albicans* biofilms *in vitro* (Table 6.1). However, greater variation in the biofilm prevention activity of the individual peptides could be observed compared to their activity against planktonic cells. In terms of their BIC values TrcA, TrcB and GS exhibited equal biofilm prevention activity, all characterised by BIC values of 12.5 µM, whereas the BIC values of PhcA, TpcC and TrcC were two-fold higher (Table 6.1). Similar to their activities against the planktonic cells, the tyrocidines' activities were again lower than that of AmB and CAS.

However, bearing in mind that the AmB and CAS formulations have both been optimised for pharmaceutical use, in comparison the tyrocidines show good potential for further optimisation for use against *C. albicans* infections.

The tyrocidines and analogues failed to fully eradicate mature biofilms and only the analogous GS could achieve 100% eradication of 24 hour old *C. albicans* biofilms (Table 6.1). Although TrcC exhibited lower fungicidal activity and biofilm preventive activity than the other two tyrocidines, it was characterised by the highest biofilm eradication activity: at 200 μM, TrcC resulted in 74±3 % eradication of the biofilms, whereas TrcA and TrcB treatment of biofilms resulted respectively in 64±5 % and 55±7 % eradication. Treatment of the biofilms with 200 μM PhcA or TpcC did not induce 50% eradication of the biofilms.

Compared to the planktonic activity of the tyrocidines, greater variance in the activities of the individual peptides was observed with regards to their ability to prevent biofilm formation. It seems that, in terms of their biofilm prevention activity, a Phe^4 instead of a Trp^4 as aromatic amino acid residue is preferred. These aromatic amino acid residues have a substantial influence on the hydrophobicity of tyrocidines and concurrently contribute to the tyrocidines' ability for membrane partitioning (38). It has been illustrated that Phe has a greater propensity to insert deeper into the membrane (39, 40). The presence of a Tyr^7 (as in tyrocidines) instead of for example a Phe^7 (as in PhcA) or Trp^7 (as in TpcC) also appears to be advantageous for the biofilm eradication activity of the tyrocidines. As has been proposed in Chapter 5, a higher order structure may be the active conformation of the tyrocidines and consequently it could be that the more hydrophobic TrcA and TrcB with Phe^4 instead of a Trp^4 favours the formation of more active higher order structures, such as dimers (30, 41).

Table 6.1: Summary of activity parameters obtained for tyrocidines against *C. albicans*.

Compound	Inhibition of planktonic cells IC_{max} (MIC)[a]	Inhibition of planktonic cells IC_{50}	Biofilm prevention BIC_{max} (BIC)[b]	Biofilm prevention BIC_{50}	Biofilm eradication BEC_{50}	% Biofilm eradication at 200 µM
Trc mix	6.0 ± 0.26 (6.25) *	3.7 ± 0.25*	11.3 ± 0.67 (12.5) *	8.3 ± 0.43*	107 ± 20*	81 ± 3.3*
TrcA	5.2 ± 0.44 (6.25)	3.2 ± 0.31	8.01 ± 1.77 (12.5)	5.7 ± 0.71	145 ± 23	64 ± 4.8
TrcB	6.3 ± 0.0 (6.25)	4.3 ± 0.03	10.6 ± 0.32 (12.5)	8.3 ± 0.11	164 ± 18	55 ± 7.3
TrcC	7.8 ± 0.81 (6.25)	4.7 ± 0.05	24.3 ± 1.44 (25.0)	17.4 ± 0.20	133 ± 6.3	74 ± 3.3
PhcA	12.5 ± 0.0 (12.5)	7.9 ± 0.48	11.2 ± 1.78 (25.0)	12.2 ± 2.5	> 200	41 ± 3.5
TpcC	6.0 ± 0.26 (6.25)	4.2± 0.42	18.4 ± 3.33 (25.0)	15.5 ± 0.91	> 200	28 ± 5.4
GS	6.8 ± 0.52 (6.25)	4.4 ± 0.03	8.55 ± 0.57 (12.5)	5.7 ± 0.29	40.9 ± 6.2	100 ± 0.04
CAS	0.05[c]	0.03[c]	0.13[c]	0.05[c]	0.35 ± 0.03	-
AmB	1.73[c]	0.79[c]	1.35[c]	0.37[c]	0.56 ± 0.02	-

Each value represents the mean of at least 3 biological repeats, with 2-3 technical repeats per assay. Values are given in µM except for µg/mL where indicated with *.
[a]Minimal concentration that results in ≥ 95% yeast death; [b]minimal concentration that prevents ≥ 95% biofilm formation;
[c]Inhibition values supplied by N. Delattin, Centre of Microbial and Plant Genetics, CMPG, KU Leuven, Heverlee, Belgium.

In terms of their biofilm eradication activity it would seem as if the Tyr^7 amino acid residue of the major tyrocidines is key to higher activity. Sequence wise PhcA and TpcC respectively differ from TrcA and TrcC in only one residue, namely a Phe^7 or Trp^7 instead of a Tyr^7 (90% sequence identity). Tyr differs from Phe in only an OH-group, but this difference makes Tyr amphipathic, dipolar and ionisable (pK_a = 10.07). Phe and Trp are more hydrophobic than Tyr (Tyr>Trp>>Phe) (42). The three aromatic amino acids also differ in their hydropathies (Phe = 2.8, Trp = -0.9, Tyr = -1.3) (42). It could be that the Tyr residue has just the right chemical properties for target interaction and activity. As was mentioned above it has been hypothesised that in order to form amphipathic structures for activity, the tyrocidines require the formation of higher order structures such as dimers (30, 41). From our handling of the peptides we found that PhcA exhibits a high tendency to aggregate in solution, while TpcC's tendency to aggregate is lower than that of the major tyrocidines, leading either to loss of activity due to solubility or less formation of active amphipathic structures. The significantly higher activity of GS (Table 6.1),

point out the importance of the VOLfP pentapeptide moiety in terms of biofilm eradication activity. This pentapeptide moiety, shared by the tyrocidines relevant to this study, has also been linked to an increase in membrane activity (26).

6.4.3 Tyrocidines disrupt membrane integrity of biofilm cells

The membrane disruptive activities of TrcA, TrcB and TrcC on *in vitro* grown *C. albicans* biofilm cells were assessed using the fluorescent membrane impermeable dye propidium iodide (Figure 6.2). As GS is known to disrupt microbial membranes, it was included in the study. GS induced membrane permeabilisation at concentrations starting from 6.25 µM, whereas the tyrocidines induced membrane permeabilisation at two- to fourfold higher concentration (Figure 6.2). The decrease in peptide-induced propidium iodide fluorescence at higher GS concentrations corresponds with the biofilm eradication activity of GS (compare Figure 6.2 and Table 6.1).

These data indicate that the tyrocidines disrupt the membrane integrity of mature *C. albicans* biofilm cells, albeit not to the same extent as GS. If they also target an internal target subsequent to membrane permeabilisation, especially at lower concentrations, remains to be further investigated. The significant membrane activity of GS (which contains two VOLfP pentapeptide moieties) compared to that of the tyrocidines, again highlights the association between the VOLfP sequence and membrane activity (26).

6.4.4 Induction of endogenous reactive species (ROS) by tyrocidines

Various antifungal molecules are known to induce accumulation of ROS in susceptible yeast and fungal species (2, 34, 35). Significant accumulation of endogenous ROS - indicated by the fluorescent dye H_2DCFDA - in *C. albicans* biofilm cells was observed subsequent to 24 hour treatment with TrcA, TrcB and TrcC compared to untreated cells (Figure 6.3 A). In order to determine if this induction of endogenous ROS in *C. albicans* biofilm cells is linked to tyrocidine activity, the influence of ascorbic acid on the biofilm eradication activity of 100 µM TrcA, TrcB and TrcC was determined (35, 43).

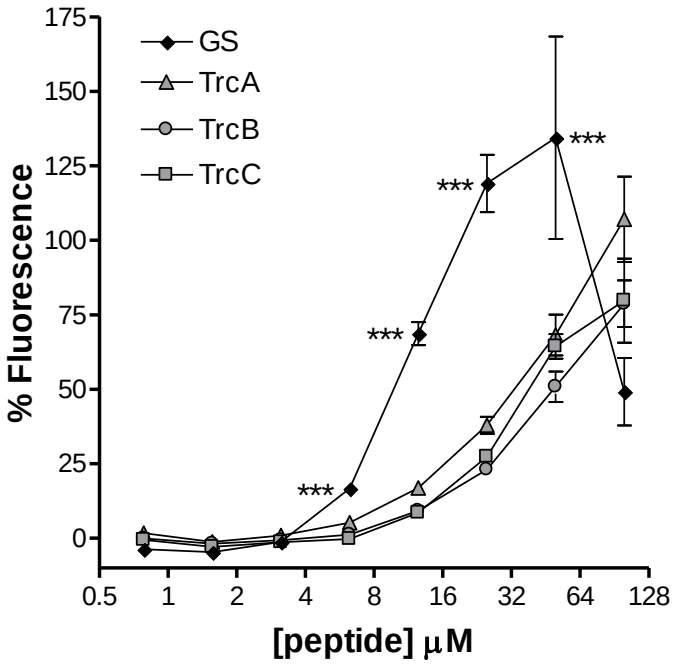

Figure 6.2: Percentage propidium iodide (PI) fluorescence induced by TrcA, TrcB, TrcC and GS on 24 hour *C. albicans* biofilms with 1% Triton X-100 as reference for 100% lysis. Biofilms were incubated for 24 hours with peptide prior to PI staining. Fluorescence values were corrected with those obtained from untreated cells. Each data point represents the mean of at least 8-10 repeats ±SEM. According to One-way ANOVA with Bonferroni's multiple comparison test the fluorescence induced by GS is significantly higher than that of TrcA, TrcB and TrcC from concentrations of 6.2 μM and up (***P<0.001). There were no significant differences between the fluorescence induced by TrcA, TrcB and TrcC.

Although the addition of 10 mM ascorbic acid significantly decreased the presence of endogenous ROS in *C. albicans* biofilm cells, no significant decrease in the biofilm eradication activity of the peptides was observed (Figure 6.3 B). Therefore it would seem as if tyrocidine-induced ROS is a secondary result of tyrocidine activity and not essential for their antifungal activity. A clear correlation can be observed between the propidium iodide and ROS fluorescence induced by the tyrocidines (compare Figure 6.2 and Figure 6.3 A) which could point to the possibility that the observed ROS induction is a result of the membrane disruptive activity of the tyrocidines. However, it must also be kept in mind that ascorbic acid is specific to certain ROS species. Although the total ROS is reduced in the presence of 10 mM ascorbic acid,

a small percentage of ROS still remains (Figure 6.3 B). It could therefore be that these remaining ROS species are responsible for the activity of the tyrocidines. However, surprisingly ascorbic acid significantly (P<0.01) enhanced the activity of the two less active peptides TrcA and TrcB. The reason for this is unclear, but could point to a difference in activity between TrcC and the less bulky and more hydrophobic TrcA and TrcB. It is possible that the formulation of the two more hydrophobic cationic tyrocidines with the high concentration ascorbic acid (as possible chaotropic agent) lead to less detrimental aggregation and stabilise more active structures.

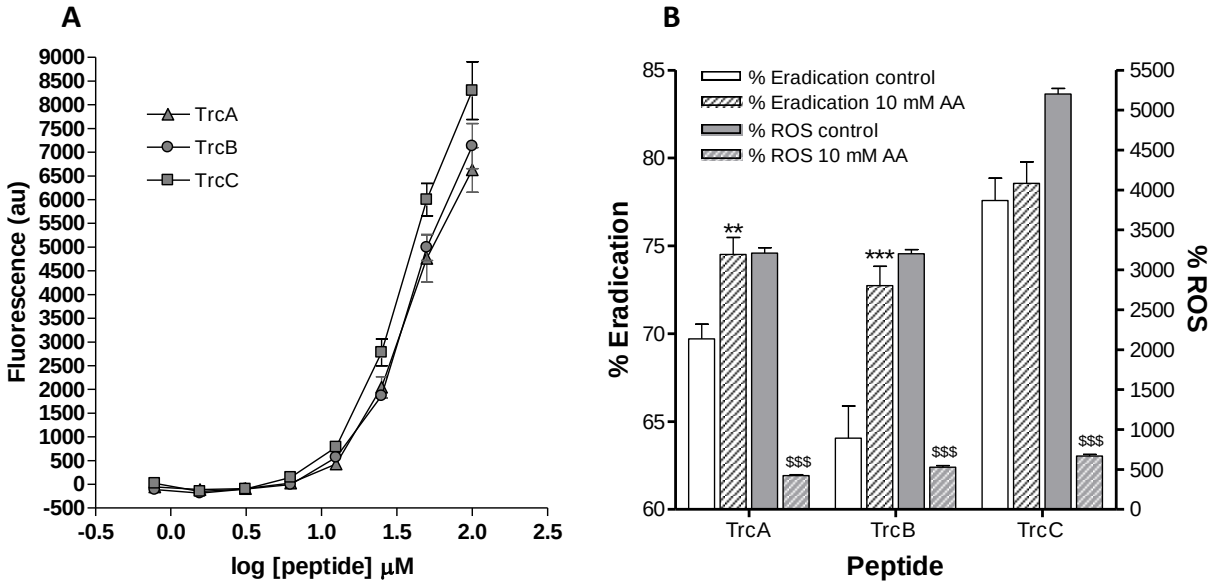

Figure 6.3: **A.** Dose response curves of ROS induction in 24 hour old *C. albicans* biofilms treated with peptides in relation to untreated cells. Biofilms were incubated for 24 hours with TrcA, TrcB or TrcC prior to staining with H_2DCFDA. Each data point represents the mean of triplicate biological repeats ± SEM, with triplicate technical repeats per assay. **B.** ROS induction in mature *C. albicans* biofilms treated for 24 hours with 100 µM TrcA, TrcB and TrcC prior to staining with H_2DCFDA. The influence of 10 mM ascorbic acid (AA) on the tyrocidines' ability to eradicate biofilms and induce endogenous ROS was determined. According to the Student t-test the ROS induced in the presence of 10 mM ascorbic acid is significantly less ($^{\$\$\$}$P<0.001) than in the absence of it. There is significant increase in the biofilm eradication activity in the presence of ascorbic acid for TrcA (**P<0.01) and TrcB (***P<0.001). The experiment was performed in quadruplicate and citric acid served as pH control.

6.4.5 Potentiating of antibiofilm activity of caspofungin and amphotericin B by the tyrocidines

Combination drug therapy is currently preferred to limit resistance, therefore we assessed combinations of the three major tyrocidines (TrcA, TrcB and TrcC) with commonly used antimycotics namely caspofungin (CAS) and amphotericin B (AmB) in biofilm eradication assays. In combination TrcA, TrcB and TrcC significantly increased the biofilm eradication activity of both CAS (Figure 6.4) and AmB (Figure 6.5).

The presence of 1.8-6.3 µM of TrcA, TrcB or TrcC decreased the BEC_{50} of CAS (0.35 µM) and AmB (0.56 µM) up to 25- and 16-fold, respectively. Furthermore, our results show that, although the tyrocidines alone have only minor biofilm eradicating activity (BEC_{50} >100 µM, Table 2), 1.8-6.3 µM of TrcA, TrcB or TrcC in combination with CAS or AmB displayed synergistic activity with regard to eradication of mature biofilms (Table 6.2). The calculated FICI values of both AmB and CAS, in combination with the tyrocidines, were well below 0.5 at values of 0.10-0.42, pointing toward pronounced synergistic activity (33) (Table 6.2). From the FICI values it is also observed that the tyrocidines have a slightly greater effect on the activity of CAS (FICI=0.10-0.35) than on the activity of AmB (FICI=0.14-0.42) (Table 6.2). These data indicate that combination therapy using co-administration of the tyrocidines and CAS or AmB could be effective in curing biofilm-associated infections. The results of the propidium iodide studies indicate that the tyrocidines disrupt the membrane integrity of *C. albicans* biofilm cells. Therefore one could hypothesise that the synergistic activity could be the result of increased accumulation of the antifungal drug into the cell by the increased membrane permeability.

Since AmB and the tyrocidines both target the fungal cell membrane (14-16), competition for this target could possibly explain why higher synergism was observed for CAS (Figure 6.4) than for AmB (Figure 6.5). Nevertheless, further studies will need to be conducted to draw definite conclusions regarding the mode of synergism between the tyrocidines and CAS/AmB.

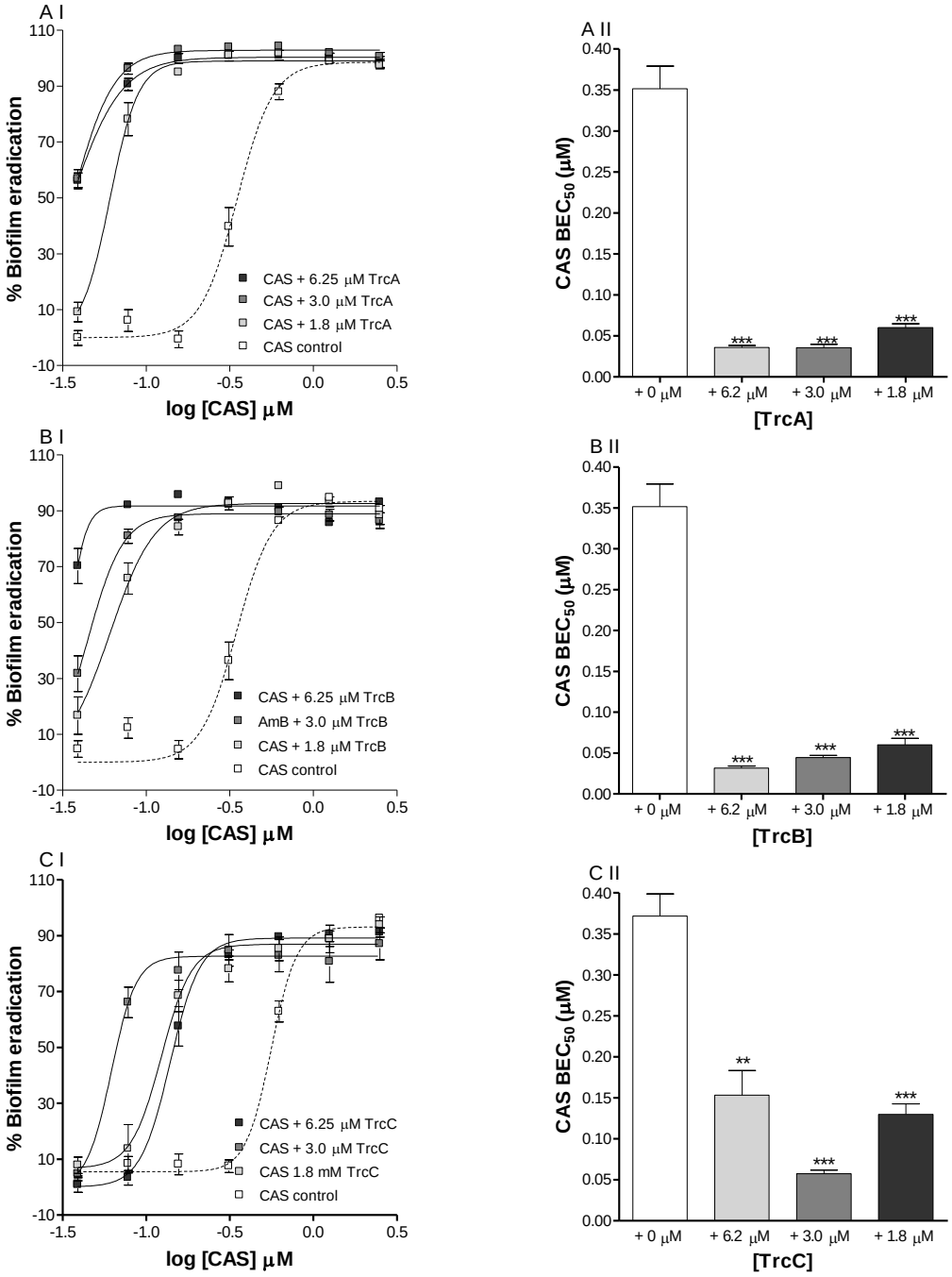

Figure 6.4: Dose response curves of CAS biofilm eradication activity (I) and comparison of BEC_{50}'s of CAS (II) in the absence and presence of TrcA (**A**), TrcB (**B**) and TrcC (**C**). Each data point represents the mean of triplicate biological repeats ± SEM, with triplicate technical repeats per assay. According to One-way ANOVA with the Bonferroni's multiple comparison test the BEC_{50}'s of CAS was significantly (***P<0.001, **P<0.01) lower in the presence of 1.8, 3.0 and 6.2 µM TrcA, TrcB and TrcC.

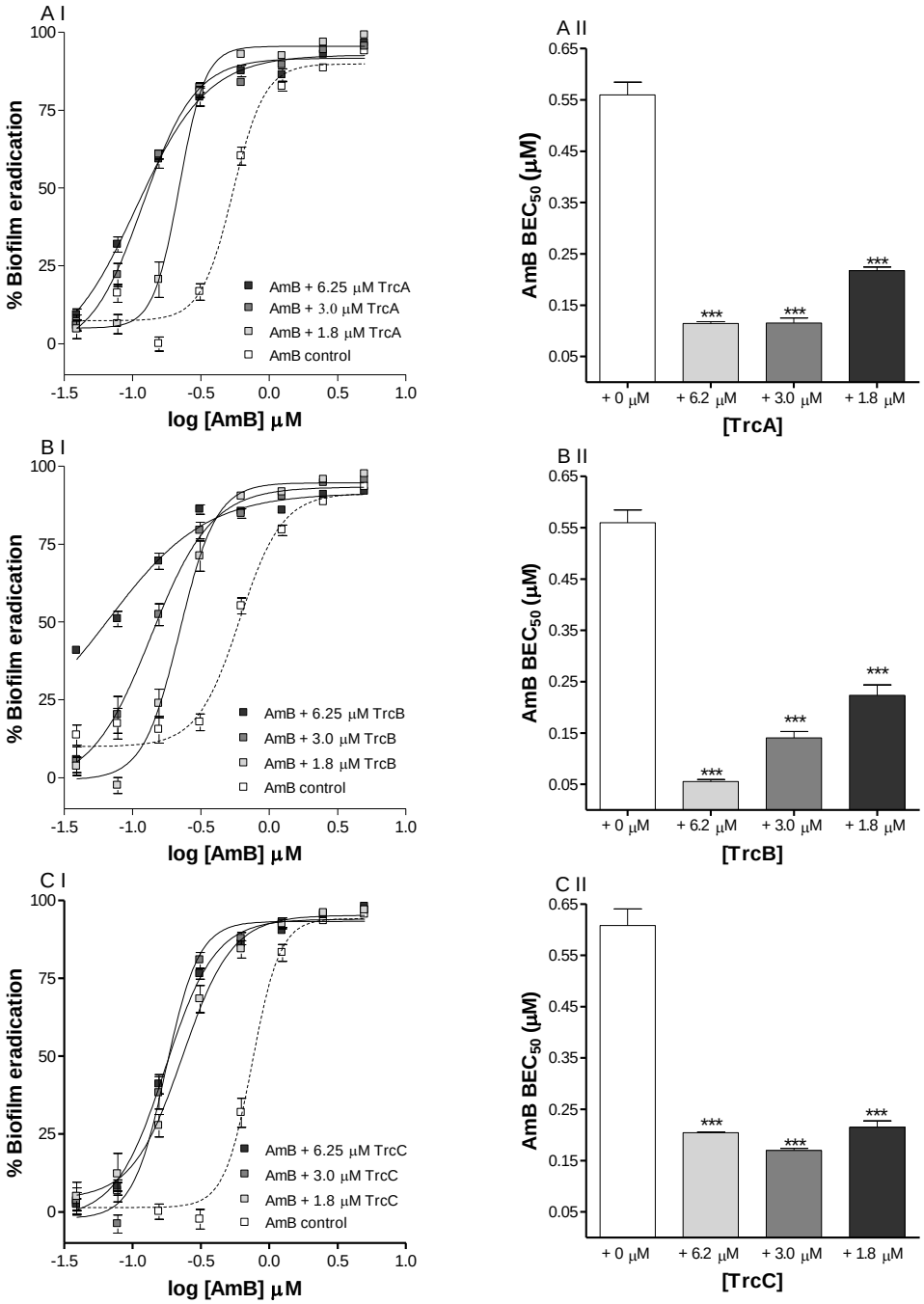

Figure 6.5: Dose response curves of AmB biofilm eradication activity (I) and comparison of BEC_{50}'s of AmB (II) in the absence and presence of TrcA (**A**), TrcB (**B**) and TrcC (**C**). Each data point represents the mean of triplicate biological repeats ± SEM, each with triplicate technical repeats per assay. According to One-way ANOVA with the Bonferroni's multiple comparison test the BEC_{50}'s of CAS was significantly (***P<0.001) lower in the presence of 1.8, 3.0 and 6.2 µM TrcA, TrcB and TrcC.

Table 6.2: Summary of activity parameters for AmB and CAS in combination with TrcA, TrcB and TrcC, against 24 hour old *C. albicans* biofilms.

	TrcA				TrcB				TrcC			
	+AmB		+ CAS		+AmB		+ CAS		+ AmB		+ CAS	
[Tyrocidine]	BEC_{50} (μM)	FICI	BEC_{50} (μM)	FICI	BEC_{50} (μM)	FICI	BEC_{50} (μM)	FICI	BEC_{50} (μM)	FICI	BEC_{50} (μM)	FICI
6.2 μM	0.11	0.25	0.04	0.11	0.06	0.14	0.03	0.15	0.21	0.34	0.15	0.12
3.0 μM	0.12	0.23	0.04	0.10	0.14	0.27	0.04	0.12	0.17	0.28	0.06	0.15
1.8 μM	0.22	0.41	0.06	0.18	0.22	0.42	0.06	0.19	0.22	0.35	0.13	0.35

Each value represents the mean of at least 3 biological repeats, with 2-3 technical repeats per assay ± SEM.
The BEC_{50} value represents the concentration AmB/CAS at which 50% eradication was achieved in the presence of the tyrocidines.
The FICI (fractional inhibitory concentration index) was calculated using the BEC_{50} obtained for combinatorial treatment and the BEC_{50} values for the individual compounds (Table 6.1).

6.4.6 In vivo *activity of tyrocidine A with caspofungin*

TrcA and CAS were chosen from their promising FICI values (Table 6.2) to evaluate their combined antibiofilm activity *in vivo* using the *C. elegans*-*C. albicans* infection model system as described by Breger *et al.* (36). We performed dose-response experiments with TrcA and CAS to determine the TrcA and CAS concentrations ineffective (<10% survival) in curing *C. elegans* infected with *C. albicans* compared to the control treatment (data not shown). Five days after infection with *C. albicans,* only 4±2 % of the *C. albicans* infected nematodes survived. The survival of nematodes treated with 3.0 µM TrcA (3±1 % survival) or 0.095 µM CAS (10±5 % survival) were similar to the survival of untreated nematodes (Figure 6.6).

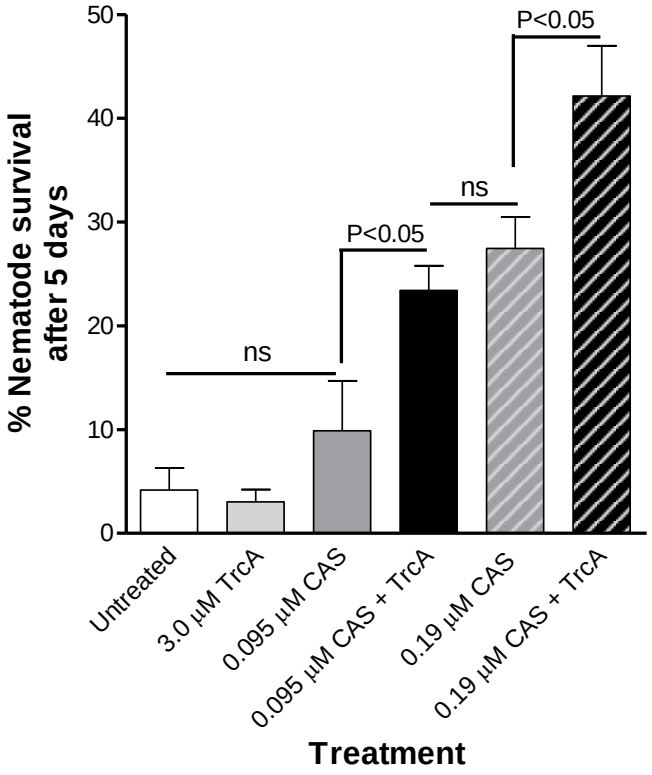

Figure 6.6: Comparison of *C. albicans* infected nematode survival 5 days post treatment with either 3 µM TrcA, 0.095 µM / 0.19 µM CAS or a combination of 3 µM TrcA and 0.095/ 0.19 µM µM CAS. Statistical analysis was done using One-way ANOVA with Bonferroni's multiple comparison test. Each bar represents the average of 3-6 repeats ±SEM. Note: There was no toxicity observed for 6.0 µM TrcA five days post treatment and the MC_{50} (concentration at which 50% of the nematodes died) was determined as 25 µM TrcA.

A single treatment of infected nematodes with a combination of 3.0 µM TrcA and 0.095 µM CAS significantly increased the survival of the nematodes to 23±2 % five days post infection and treatment, compared to treatment with 3.0 µM TrcA or 0.095 µM CAS alone or control treatment (0.6% DMSO). This combination gave similar nematode survival as treatment with double the CAS dose, namely 0.19 µM, CAS which led to 27±3% survival. Although 0.19 µM CAS led to significant nematode survival, a single treatment with the combination of 3.0 µM TrcA and 0.19 µM CAS almost doubled the survival to 42±3% nematodes after five days (Figure 6.6). These data indicate that TrcA also enhances the activity of CAS *in vivo* in the *C. elegans* infection model. Furthermore, there was no toxicity observed for the nematodes for TrcA up to 6 µM. These results reveal the potential of tyrocidines to act as candidates for further studies as antifungal drugs, especially as potentiating factors to be used in combination with other antifungal drugs, such as AmB and CAS.

6.5 Conclusion

The significant fungicidal and biofilm prevention activities indicate that the tyrocidines have the potential to serve as lead compounds for novel antifungal compounds. Although the tyrocidines activity is probably not connected to the induction of ROS, propidium iodide fluorescence as a result of tyrocidine activity reveals that the tyrocidines disturb the integrity of *C. albicans* cell membranes in biofilms. If there is an alternative/additional target to the membrane target remains to be discovered in future studies. The significant synergistic effect of the tyrocidines on the *in vitro* biofilm eradication activity of AmB and CAS, as well as the potentiating effect of TrcA on the *in vivo* remediating activity of CAS, are promising evidence for the potential of combinatorial treatment that will not only decrease the toxicity of the individual compounds, but which will also decrease the likelihood of resistance developing against the individual compounds.

6.6 References

1. **Letscher-Bru V, Herbrecht R.** 2003. Caspofungin: the first representative of a new antifungal class. J. Antimicrob. Chemother. **51:**513-521.

2. **Bink A, Vandenbosch D, Coenye T, Nelis H, Cammue BPA, Thevissen K.** 2011. Superoxide dismutases are involved in *Candida albicans* biofilm persistence against miconazole. Antimicrob. Agents Chemother. **55:**4033-4037.

3. **Tobudic S, Lassnigg A, Kratzer C, Graninger W, Presterl E.** 2010. Antifungal activity of amphotericin B, caspofungin and posaconazole on *Candida albicans* biofilms in intermediate and mature development phases. Mycoses. **53:**208-214.

4. **Ramage G, Mowat E, Jones B, Williams C, Lopez-Ribot J.** 2009. Our current understanding of fungal biofilms. Crit. Rev. Microbiol. **35:**340-355.

5. **Ferreira JAG, Carr JH, Starling CEF, de Resende MA, Donlan RM.** 2009. Biofilm formation and effect of caspofungin on biofilm structure of *Candida* species bloodstream isolates. Antimicrob. Agents Chemother. **53:**4377-4384.

6. **Bink A, Pellens K, Cammue BPA, Thevissen K.** 2011. Anti-biofilm strategies: How to eradicate *Candida* biofilms? Open Mycol. J. **5:**29-38.

7. **Chandra J, Kuhn DM, Mukherjee PK, Hoyer LL, McCormick T, Ghannoum MA.** 2001. Biofilm formation by the fungal pathogen *Candida albicans*: Development, architecture, and drug resistance. J. Bacteriol. **183:**5385-5394.

8. **Bachmann SP, VandeWalle K, Ramage G, Patterson TF, Wickes BL, Graybill JR, López-Ribot JL.** 2002. *In vitro* activity of caspofungin against *Candida albicans* biofilms. Antimicrob. Agents Chemother. **46:**3591-3596.

9. **Crump JA, Collignon PJ.** 2000. Intravascular catheter-associated infections. Eur. J. Clin. Microbiol. Infect. Dis. **19:**1-8.

10. **Baillie GS, Douglas LJ.** 1999. *Candida* biofilms and their susceptibilty to antifungal agents. Methods Enzymol. **310:**644-656.

11. **Hawser SP, Douglas LJ.** 1995. Resistance of *Candida albicans* biofilms to antifungal agents in vitro. Antimicrob. Agents Chemother. **39:**2128-2131.

12. **Ramage G, Wickes BL, Lopez-Ribot JL.** 2001. Biofilms of *Candida albicans* and their associated reistance to antifungal agents. Am. Clin. Lab. **20:**42-44.

13. **DiDone L, Oga D, Krysan DJ.** 2011. A novel assay of biofilm antifungal activity reveals that amphotericin B and caspofungin lyse *Candida albicans* cells in biofilms. Yeast. **28:**561-568.

14. **Laniado-Laborın R, Cabrales-Vargas MN.** 2009. Amphotericin B: side effects and toxicity. Rev. Iberoam. Micol. **26:**223–227.

15. **Brajtburg J, Bolard J.** 1996. Carrier effects on biological activity of amphotericin B. Clin. Microbiol. Rev. **9:**512-531.

16. **Johnson RH, Einstein HE.** 2007. Amphotericin B and coccidioidomycosis. Ann. N. Y. Acad. Sci. **1111:**434-441.

17. **Kelly SL, Lamb DC, Kelly DE, Manning NJ, Loeffler J, Hebart H, Schumacher U, Einsele H.** 1997. Resistance to fluconazole and cross-resistance to amphotericin B in *Candida albicans* from AIDS patients caused by defective sterol Δ5,6-desaturation. FEBS Lett. **400:**80-82.

18. **Nolte FS, Parkinson T, Falconer DJ, DIX D, S., Williams J, Gilmore C, Geller R, Wingard JR.** 1997. Isolation and characterization of fluconazole- and amphotericin B-resistant *Candida albicans* from blood of two patients with leukemia. Antimicrob. Agents Chemother. **44:**196-199.

19. **Conly J, R. R, Johnson J, Farah S, Hellman L.** 1992 Disseminated candidiasis due to amphotericin B-resistant *Candida albicans*. J. Infect. Dis. **165:**761-764.

20. **Deresinski SC, Stevens DA.** 2003. Caspofungin. Clin. Infect. Dis. **36:**1445-1457.

21. **Klepser ME.** 2006. *Candida* resistance and its clinical relevance. Pharmacotherapy. **26:**68S-75S.

22. **Onaizi SA, Leong SSJ.** 2011. Tethering antimicrobial peptides: Current status and potential challenges. Biotechnol. Adv. **29:**67-74.

23. **Van Epps HL.** 2006. René Dubos: unearthing antibiotics. J. Exp. Med. **203:**259.

24. **Spathelf BM, Rautenbach M.** 2009. Anti-listerial activity and structure–activity relationships of the six major tyrocidines, cyclic decapeptides from *Bacillus aneurinolyticus*. Bioorg. Med. Chem. **17:**5541-5548.

25. **Hotchkiss RD, Dubos RJ.** 1941. The isolation of bactericidal substances from cultures of *Bacillus brevis*. J. Biol. Chem. **141:**155-162.

26. **Rautenbach M, Vlok NM, Stander M, Hoppe HC.** 2007. Inhibition of malaria parasite blood stages by tyrocidines, membrane-active cyclic peptide antibiotics from *Bacillus brevis*. Biochim. Biophys. Acta. **1768:**1488-1497.

27. **Kretschmar M, Nichterlein T, Nebe CT, Hof H, Burger KJ.** 1996. Fungicidal effect of tyrothricin on *Candida albicans*. Mycoses. **39:**45-50.

28. **Fonzi WA, Irwin MY.** 1993. Isogenic strain construction and gene mapping in *Candida albicans*. Genetics. **134:**717-728.

29. **Vosloo JA, Stander M, Leussa AN-N, Spathelf BM, Rautenbach M.** 2013. Manipulation of the tyrothricin production profile of *Bacillus aneurinolyticus*. Microbiology. **159:**2200-2211.

30. **Spathelf BM.** 2010. Qualitative structure-actvity relationships of the major tyrocidines, cyclic decapeptides from *Bacillus aneurinolyticus*. PhD Thesis, Department of Biochemistry, University of Stellenbosch, http://scholar.sun.ac.za/handle/10019.1/4001.

31. **Institute CaLS.** 2008. Reference method for broth dilution antifungal susceptibility testing of filamentous fungi, 2nd ed. CLSI, Wayne, Pa, USA.

32. **Delattin N, De Brucker K, David J. Craik2, Cheneval O, Fröhlich M, Veber M, Girandon L, Davis TR, A.E. W, Kumamoto CA, Cos P, Coenye T, De Coninck B, Cammue BPA, Thevissen K.** 2014. The plant-derived decapeptide OSIP108 interferes with *Candida albicans* biofilm formation without affecting cell viability. Antimicrobial Agents and Chemotherapy. **Accepted for publication**.

33. **Bink A, Kucharikova S, Neirinck B, Vleugels J, Van Dijck P, Cammue BPA, Thevissen K.** 2012. The nonsteroidal anti-inflammatory drug diclofenac potentiates the in vivo activity of caspofungin against *Candida albicans* biofilms. J. Infect. Dis. **206:**1790-1797.

34. **Aerts AM, François IEJA, Meert EMK, Li Q-t, Cammue BPA, Thevissen K.** 2007. The antifungal activity of RsAFP2, a plant defensin from *Raphanus sativus*, involves the induction of reactive oxygen species in *Candida albicans*. J. Mol. Microbiol. Biotechnol. **13:**243-247.

35. **François IE, Thevissen K, Pellens K, Meert EM, Heeres J, Freyne E, Coesemans E, Viellevoye M, Deroose F, Martinez Gonzalez S, Pastor J, Corens D, Meerpoel L, Borgers M, Ausma J, Dispersyn GD, Cammue BP.** 2009. Design and synthesis of a series of piperazine-1-carboxamidine derivatives with antifungal activity resulting from accumulation of endogenous reactive oxygen species. ChemMedChem. **4:**1714-1721.

36. **Breger J, Fuchs BB, Aperis G, Moy TI, Ausubel FM, Mylonakis E.** 2007. Antifungal chemical compounds identified using a *C. elegans* pathogenicity assay. PLoS Pathog. **3:**e18.

37. **Rautenbach M, Gerstner GD, Vlok NM, Kulenkampff J, Westerhoff HV.** 2006. Analyses of dose-response curves to compare the antimicrobial activity of model cationic α-helical peptides highlights the necessity for a minimum of two activity parameters. Anal. Biochem. **350:**81-90.

38. **Dubos RJ, Hotchkiss RD.** 1941. The production of bactericidal substances by aerobic sporulating bacilli. J. Exp. Med. **73:**629-640.

39. **Kelkar DA, Chattopadhyay A.** 2006. Membrane interfacial localization of aromatic amino acids and membrane protein function. J. Biosci. **31:**297–302.

40. **Wymore T, Wong TC.** 1999. Molecular dynamics study of substance P peptides in a biphasic membrane mimic. Biophys. J. **76:**1199–1212.

41. **Munyuki G, Jackson GE, Venter GA, Kövér KE, Szilágyi L, Rautenbach M, Spathelf BM, Bhattacharya B, Van der Spoel D.** 2013. β-Sheet structures and dimer models of two major tyrocidines, antimicrobial peptides from *Bacillus aneurinolyticus*. Biochemistry. **52:**7798-7806.

42. **Frecer V.** 2006. QSAR analysis of antimicrobial and haemolytic effects of cyclic cationic antimicrobial peptides derived from protegrin-1. Bioorg. Med. Chem. **14:**6065-6074.

43. **Bink A, Govaert G, François IEJA, Pellens K, Meerpoel L, Borgers M, Van Minnebruggen G, Vroome V, Cammue BPA, Thevissen K.** 2010. A fungicidal piperazine-1-carboxamidine induces mitochondrial fission-dependent apoptosis in yeast. FEMS Yeast Res. **10:**812-818

Chapter 7

Conclusions and recommendations for future studies

7.1 Introduction

The main goal of this study was to provide novel information and insights regarding the antifungal activity of the tyrocidines and their potential to serve as bio-control agents in the agricultural sector and therapeutic agents in the medical industry. To realise this goal the major tyrocidines and natural analogues had to be purified from the commercial *Bacillus aneurinolyticus* tyrothricin complex and the culture medium of *Brevibacillus aneurinolyticus* ATCC 8185 and subsequently analysed for peptide identity and purity; antifungal activity test parameters optimal for fungal growth and peptide activity had to be determined; the biological activity of the tyrocidines and any structure-activity parameters had to be elucidated; and the potential mode(s) of action investigated.

This is the first study to give a detailed report on the antifungal activities of the purified tyrocidines and their analogues against agronomic important pathogens (Chapter 4-5) and medically relevant pathogens (Chapter 6) using the tyrocidines and natural analogues purified and analysed in Chapter 2 and the activity test parameters determined in Chapter 3.

7.2 Experimental conclusions

7.2.1 Influence of the environment on fungal growth and peptide activity

In Chapter 3 it was illustrated that the assay medium and peptide solvent composition influences the growth of both *F. solani* and *B. cinerea*. *F. solani* flourished in the nitrogen rich yeast supplemented tryptone soy broth (YTSB) while *B. cinerea* preferred the potato dextrose broth (PDB). Both species exhibited improved growth on the gel-based media, yeast supplemented

tryptone soy agar (YTSA) and potato dextrose agarose (PDA), compared to the broth media. Similar to previous observations made from tyrocidine studies (1), the activities of the tyrocidines were also influenced by the environment and solvent conditions. With increasing ethanol concentrations in the peptide solvent a concurrent increase in tyrocidine activity was observed. The amphipathic tyrocidines have a tendency to aggregate in aqueous environments (1-6) and with increased ethanol to water ratio the extent of their initial aggregation is reduced. Unfortunately ethanol also influences the growth of fungi which meant a midway ethanol concentration (15 %) was chosen for subsequent activity determinations. Compared to their activity in broth media, the tyrocidines activity was significantly lower on the agar media (Chapter 4). As was mentioned above, the tyrocidines are extremely sensitive to their environment and tend to oligomerise which is hypothesised to influence their activity. The significant loss in tyrocidine activity on an agar-based assay environment could be the result of variation in peptide assembly compared to that in a broth-based environment. An alternative explanation for the loss in activity may be that the altered environment influences the growth of the fungal target cell which could lead to adjustments to the target(s) of the tyrocidines in the fungal cell. Last mentioned is supported by the observation that the loss in tyrocidine activity is much more significant against *F. solani* than *B. cinerea*.

In contrast to the majority of antimicrobial peptides (AMPs) (7-9), the activities of the tyrocidines were relatively salt stable and were only negatively influenced by the presence of Ca^{2+} (Chapter 4). The loss of tyrocidine activity in the presence of Ca^{2+} can either be the result of cation-induced peptide aggregation leading to a lowering in the number of available and "active" peptides (10) or it can be the result of interference with a specific peptide target that is dependant on ionic interactions or ion fluctuations in membranes (11). Because the tyrocidines' activities against *B cinerea* were in general more stable in the presence of Ca^{2+} than against *F. solani*, we theorised that the tyrocidines have additional/alternative targets in *B. cinerea* which are not sensitive to the presence of Ca^{2+}. Of all the tyrocidines tested, tyrocidine A (TrcA) was the most

successful in maintaining its activity in the presence of Ca^{2+}. These theorised additional target(s) may therefore be more effectively targeted by TrcA than the other tyrocidines.

7.2.2 Biological activity

The activity of the tyrocidines, a complex of analogous cyclic decapeptides produced by *Bacillus aneurinolyticus*, was determined using broth microdilution assays against a range of phytopathogenic fungi, namely *F. solani*, *F. oxysporum*, *F. verticillioides*, *Cylindrocarpon liriodendri*, *B. cinerea* and *Penicillium digitatum*, *P. glabrum*, *P. expansum*, *Talaromyces mineoluteus*, *T. ramulosus, Asperigellus fumigatis* and *Trichoderma atroviride* isolates (Chapter 4). The activity of the tyrocidine peptide complex (Trc mixture) was significant, minimum inhibition concentrations below 13 µg/mL (~10 µM) were obtained and the Trc mixture's activity was significantly more potent than that of the commercial imidazole fungicide, bifonazole. However, the activity of the Trc mixture varied between the different fungal species indicating that the fungal target cell a role plays in tyrocidine activity. A significant loss in tyrocidine activity was observed on the agar compared to the activity in a broth environment, especially against *F. solani*. The activities of the purified six major tyrocidines and two of their natural analogues, phenycidine A (PhcA) and tryptocidine C (TpcC), were investigated against *F. solani* and *B. cinerea*, in either YTSB or PDB. Each one of the peptides had the ability to inhibit both *F. solani* and *B. cinerea* in both the broth mediums. However, the activities of the individual peptides were influenced by the identity of the target organism and the specific medium used. Especially the two tyrocidine analogues, with respectively a Phe and Trp in amino acid position 7, were susceptible to changes in the media environment. These results highlight the importance of the Tyr^7 residue for consistent high activity against different organisms and in various environments. It could be that the Tyr residue has the optimal chemical properties for target interaction in both PDB and YTSB media or/and the Tyr residue leads to the right amount of self-assembly to yield the most active/stable higher-order structure. Surprisingly, in contrast to the tyrocidines' antibacterial (12) and antiplasmodial (13) activity, no other overt structure-

activity correlations could be uncovered. The minor differences in the activities of the peptides may possibly be the result of minor differences in their propensities to aggregate (3, 4).

The activities of the Trc mixture, three major tyrocidines, TrcA, TrcB and TrcC, as well as the two analogues, PhcA and TpcC, were also determined against the medically relevant pathogen *Candida albicans* and its biofilms (Chapter 6). The selected tyrocidines had significant antiyeast activity against planktonic *C. albicans* cells in the low micromolar range and, except for PhcA, their activities were comparable. The tyrocidines were also able to prevent *in vitro C. albicans* biofilm formation, but with more variation in their individual activities. Even though the tyrocidines failed to achieve full eradication of mature biofilms, they exhibited pronounced synergistic activity with the *in vitro* biofilm eradication activities of two key antifungal drugs, amphotericin B and caspofungin. Using a *Caenorhabditis elegans* infection model, TrcA was also illustrated to have a potentiating effect on the *in vivo* activity of caspofungin. Tyrocidines therefore present promising candidates for further research as antifungal drugs and as agents for combinatorial treatment.

To summarise, the tyrocidines exhibit significant antifungal activity which is influenced/determined by the identity of the target cell and which is sensitive to environmental conditions. The absence of overt structure-activity relationships, besides the apparent significance of the Tyr^7 residue, could point to the possibility that higher-order structures are the biologically active structures of tyrocidines, a hypothesis that has also been proposed in previous studies (1, 2).

7.2.3 Mode of action studies

Studies with the membrane impermeable dyes SYTOX green and propidium iodide illustrated that the tyrocidines disrupt the integrity of fungal spore membranes (Chapter 4), fungal hyphae membranes (Chapter 4 and 5) and the integrity of the membranes of *C. albicans* biofilm cells (Chapter 6). Fluorescence microscopy images revealed that initial membrane permeabilisation

takes place at hyphal growth tips and sites of hyphal branching. Therefore it can be concluded that at least one of the tyrocidines' mode(s) of action (MOA) is membrane targeted. However, concentrations that resulted in maximum inhibition of filamentous fungi did not lead to complete membrane disintegration (compared to 1 % TritonX-100 as 100 % lysis control). Therefore it would seem as if membrane interaction is not the only mode of tyrocidine antifungal action, but that there are additional target(s) subsequent to membrane interaction, especially at lower concentrations of peptide. Furthermore, the membrane disruptive activity of the tyrocidines, in terms of their activity parameters, appeared to be much lower against *B. cinerea* than *F. solani* (Chapter 5). Tyrocidine activity against *B. cinerea* was also more stable in increasing Ca^{2+} concentrations than against *F. solani* (Chapter 4). The presence of Ca^{2+} may therefore influence the membrane activity of the tyrocidines and since tyrocidine activity against *B. cinerea* appears to be less dependent on membrane interaction, their activities are more stable against *B. cinerea* in the presence of Ca^{2+}. Similar observations was made in terms of the tyrocidines' antibacterial activity (1, 14).

Experimental evidence also suggests that tyrocidine interaction with the fungal cell membrane is not solely determined by the composition of the cell membrane. Individual tyrocidines that had high membrane disruptive action toward fungal model membranes [comprising of 1-palmitoyl-2-oleoylphosphatidylcholine:ergosterol (70:30) and 1-palmitoyl-2-oleoylphosphatidylcholine: glucosylceramide (70:30)] did not necessarily have high biological membrane disruptive activity (that results in SYTOX green uptake in *F. solani* hyphae) and *vice versa* (Chapter 5). This may indicate that the permeabilisation of the fungal hyphae may depend on alternative factors, other than membrane permeabilisation, such as self-promoted uptake *via* lesions in the cell wall (15). It has also been hypothesised that even though AMPs may act through membrane permeabilisation, additional elements such as their interaction with specific components, for instance chitins and phosphomannans of the cell wall, may regulate or enhance their membrane activity (16). The observance that the tyrocidines lose activity against *F. solani* subsequent to

treatment with β-glucanase (to remove the cell wall) may indicate that a cell wall related component modulates the activity (probably membrane related) of the tyrocidines against *F. solani* (Chapter 5).

Microscopic analysis revealed that the tyrocidines have a significant impact on the morphology of *F. solani* and *B. cinerea* which includes retarded germination and hyperbranching of hyphae (Chapter 4). Tyrocidine action may therefore target the various processes and regulators believed to be involved in spore germination and hyphal branching. These processes include establishment of a polar axis (17) which is believed to be regulated by Rho-type GTPases (17) and cAMP signalling.(18, 19); hyphal elongation believed to be controlled by GTPases (17, 20), formins and septins (18, 20), the Spitzenkorper, the microtubule cytoskeleton (20, 21), actin polymerization (21) and Ca^{2+} gradient regulated process (22); and subsequent hyphal branching which is thought to be determined by septa location, GTPases activity (20) and localized spikes in Ca^{2+} (23, 24) and ROS (20) and the cell cycle (20, 25). In Chapter 4 it was illustrated that only Ca^{2+} - and none of the other cations - inhibit tyrocidine activity. These results suggests that Ca^{2+} inhibition of tyrocidine activity is not the result of electrostatic interference, but a more specific inhibition of tyrocidine-target interaction. Tyrocidine activity could "mimic" the Ca^{2+} spikes, believed to be involved in the regulation of hyphal branching (23, 24), or interfere with Ca^{2+} gradients believed to be involved with hyphal elongation (22), leading to abnormal hyphal branching and hyphal growth. The presence of high concentrations Ca^{2+} may counter/neutralise this effect leading to a loss in tyrocidine activity. Tyrocidine activity also induces reactive oxygen species (ROS) in *C. albicans* biofilm cells (Chapter 6). It is therefore possible that tyrocidine activity may similarly lead to the formation of ROS in filamentous fungi which could induce hyperbarnching. Tyrocidine interference with the cell cycle of *Plasmodium falciparum* has also been hypothesised (13). The tyrocidines may likewise interfere with the cell cycle of filamentous fungi leading to retarded germination and hyperbranching.

Although tyrocidine activity results in the production of endogenous ROS species in *C. albicans* biofilm cells (which has been linked to the candidacidal activity of antifungal compounds (26-28)), the addition of the antioxidant ascorbic acid did not decrease tyrocidine activity which could indicate that ROS production is not essential for tyrocidine activity. However, since a range of ROS species can be produced and the scavenger ascorbic acid acts against specific ROS species, this deduction is not absolute and the involvement of ROS in tyrocidine activity remains to be further investigated.

To summarise, the tyrocidines exhibit membrane activity but there are additional MOA(s) which results in morphological abnormalities. Ca^{2+} inhibits at least one of the tyrocidines MOA. The tyrocidines induce ROS in *C. albicans* cells but it still remains to be elucidated if this is linked to tyrocidine antifungal effect.

7.3 Hypothesis

The tyrocidines have a broad range of antifungal activity which is influenced by the assay environment and the properties of the target cell. The strong evidence of tyrocidine oligomerisation from the results in Chapter 2, together with the structure-activity results from Chapter 3, implies that the biologically active structures of the tyrocidines are most probably higher-order structures formed *via* peptide self-assembly. Munyuki *et al.* (2) illustrated the tendency of TrcA and TrcC to form dimers in aqueous environments through hydrogen bonding or hydrophobic interactions. The investigators also hypothesised that the tyrocidines may also easily form higher aggregates (2). Investigations by Spathelf (1) yielded strong evidence of tyrocidine self-assembly and it was hypothesised that the tyrocidines form higher-order structure(s) for membrane activity (1). However, there is a fine line between the formation of the active oligomer(s) and excessive tyrocidine aggregation which leads to a decrease in available active peptide structures and a concurrent decrease in peptide activity. The variance in peptide

activity in and on different mediums may therefore be the result of variances in tyrocidine self-assembly in the different media, either not allowing for adequate oligomerisation to form the active higher-order structure or promoting excessive aggregation that leads to loss in peptide activity.

The tyrocidines in all probability have more than one mode of action (MOA) of which one is undoubtedly fungal membrane disruption. It is most likely that their membrane activity, especially at lower concentrations, is regulated by other cellular components and which is probably cell wall related for *F. solani*. In addition to their interaction with the fungal membrane, the tyrocidines have an additional effect on fungal spores and hyphae that result in retarded germination and hyperbranching. The processes of spore germination, hyphal elongation and hyphal branching is complex and not yet fully understood and consequently it is difficult to pinpoint what action(s) of AMP action will result in these morphological alterations. Nonetheless, some of the processes/regulators proposed to be involved in spore germination and hyphal development include Ca^{2+} concentrations (22-24), ROS production (20), septin mislocalisation (18, 20), nuclear division and the cell cycle (20, 25). The inhibition of tyrocidine activity by the presence of Ca^{2+} points to one possible way the tyrocidines can influence these cellular processes in fungi. Furthermore, although it appears that the induction of ROS by tyrocidine activity is not essential for their antifungal effect, ROS species not affected by the antioxidant ascorbic acid may still be involved in tyrocidine action. Interference with the cell cycle is another possibility since cellular interference with a target cell's cell cycle has been proposed for the tyrocidines (13). However, these findings do not exclude possible tyrocidine interaction with any of the other processes/regulators proposed for fungal germination and hyphae development. Furthermore, there is the possibility that the tyrocidines have, to some extent, different modes of action to different fungal species. Last mentioned theory is partly supported by the results that the influence of assay environment and the presence of Ca^{2+} have a more pronounced effect on tyrocidine activity against *F. solani* than *B. cinerea*. Furthermore, in

contrast to *F. solani*, tyrocidine concentrations higher than the minimal inhibition concentration were needed to achieve only 70% of the membrane disruption induced by the membrane lytic control (1% TritonX-100) in *B. cinerea*, and tyrocidine action against *F. solani* was more severely influenced by the presence of Ca^{2+} than their activity against *B. cinerea*.

7.4 Recommendations for future studies

During the course of this study only the *in vitro* activity of the tyrocidines against phytopathogens and the medically relevant *C. albicans* was investigated. Considering the significant activity exhibited by the tyrocidines and their relative stability in various environments as well as in the presence of cations, it would be feasible to investigate the *in vivo* activity of the tyrocidines on agricultural crops. Since the activities of the tyrocidines are influenced by their solvent composition and environment, it would be advisable to experiment with different solvents and treatment conditions. Furthermore, a more in depth study of the nature and spectrum of the tyrocidines enhancing effect on caspofungin and amphotericin B can be conducted and expanded to include *in vivo* studies.

The absence of overt structural-activity relationships implies that the conserved sequence of tyrocidines, namely NQYVOLfP, may be important for activity with the aromatic dipeptide unit (Ff, Wf or Ww) determining the hydrophobicity and putative active dimer formation (Chapter 2, (1, 2)). However, extreme tyrocidine aggregation leads to a decrease in peptide activity. It would therefore be of interest to investigate different tyrocidine self-assembly states and how the different levels of self-assembly influences tyrocidine antifungal activity, as well as how tyrocidine self-assembly is influenced by various environments.

During the MOA studies differences in peptide activity between the biological and model membranes were observed. This may be the result of differences between the activity of a particular Trc in a static system such as model membranes and a complex and dynamic

biological system, such as growing fungal cells. The model membrane system is limited to measuring the peptides direct interaction with the artificial membranes and other factors that may complicate peptide activity on biological membranes, such as the fungal cell wall, fungal growth and fungal defence mechanisms, in not included in the evaluation of activity. The biological system also has its drawbacks. Peptide activity on fungal target cells is only measured by their ability to inhibit fungal growth, while viability of the residual fungi, such as hyper branched fungi is not assessed in most assays. Future studies can explore the options on how to overcome the drawbacks/pitfalls of these experimental systems.

The presence of Ca^{2+} inhibits at least one of the tyrocidines MOA(s). Greater insight regarding the tyrocidines MOA may be gained if a more in depth study is conducted on the effect of Ca^{2+} on tyrocidine activity. Fluorescence microscopy could be utilised to study the effect of Ca^{2+} on the membrane activity of the tyrocidines. Likewise, using light microscopy, the effect of Ca^{2+} on the morphological effect of the tyrocidines could be investigated. Likewise further insight into the tyrocidnes' MOA will be gained by investigating the influence of Ca^{2+} presence on the tyrocidines' morphogenic effect on target fungi cells.

The role of ROS in tyrocidine activity against *C. albicans* may be further investigated. Additional ROS stains to that of 2′,7′-dichlorodihydrofluorescein diacetate and additional ROS scavengers to that of ascorbic acid can be used to evaluate the effect of ROS production and the absence of ROS, on tyrocidine activity.

Future studies should also include an investigation into the effect the tyrocidines have on fungal cells that leads to germination and hyperbranching. ROS stains can be used to see if the tyrocidines also induce ROS in filamentous fungi and if this ROS production is limited to certain areas in the hyphae. Calcium stains (such as Fura-2) can also be used to assess if the tyrocidines influence Ca^{2+} gradients. Furthermore, stains specific for structural components such as the

cytoskeleton network (CellLight Tubulin-GFP) or septa (Solophenyl Flavine 7GFE) of fungi can be used to visualize any effect the tyrocidines may have on these structures.

The tyrothricin complex has been approved for oral use and is the active substance in Tyrozets throat lozenges. Preliminary studies conducted in our group showed that the tyrocidines are not toxic to bees (personal communication with J.A. Vosloo, BIOPEP peptide group, Biochemistry, University of Stellenbosch). However, future studies should include a variety of studies of tyrocidine impact on human health and the environment. Furthermore, even though the likelihood of AMPs to induce *de novo* resistance against them is low, considerable care should be taken to avoid such a scenario. This can be achieved by limiting the use of tyrocidine-biocide and not to encourage widespread use as a broad-spectrum biocide. The tyrocidines can also be formulated with other antifungal AMPs of antifungals for combinatorial use, thereby decreasing the chance of developing resistance.

7.5 Last word

Because of the tyrocidines' broad spectrum and potent antifungal activity, their membrane activity and the possibility of more than one MOA - which reduces the risk of resistance developing against them - they are promising candidates for bio-fungicides in the agricultural sector and combinatorial treatment in the medical industry. The tyrocidines or derivatives could be the answer to resistant fungal pathogens in both the agricultural and medical sector.

7.6 References

1. **Spathelf BM.** 2010. Qualitative structure-actvity relationships of the major tyrocidines, cyclic decapeptides from *Bacillus aneurinolyticus*. PhD Thesis, Department of Biochemistry, University of Stellenbosch, http://scholar.sun.ac.za/handle/10019.1/4001.

2. **Munyuki G, Jackson GE, Venter GA, Kövér KE, Szilágyi L, Rautenbach M, Spathelf BM, Bhattacharya B, Van der Spoel D.** 2013. β-Sheet structures and dimer models of two major tyrocidines, antimicrobial peptides from *Bacillus aneurinolyticus*. Biochemistry. **52:**7798-7806.

3. **Ruttenberg MA, King TP, Craig LC.** 1965. The use of the tyrocidines for the study of conformation and aggregation behavior. Journal of the American Chemical Society. **87:**4196-4198.

4. **Ruttenberg MA, King TP, Craig LC.** 1966. The chemistry of tyrocidine. VII. Studies on association behavior and implications regarding conformation. Biochemistry. **5:**2857-2864.

5. **Laiken SL, Printz MP, Craig LC.** 1971. Studies on the mode of self-assocation of tyrocidin B. Biochemical and Biophysical Research Communications. **43:**595-600.

6. **Paradies HH.** 1979. Aggregation of tyrocidine in aqueous solutions. Biochemical and Biophysical Research Communications. **88:**810-817.

7. **Hof WVt, Veerman EC, Helmerhorst EJ, Amerongen AV.** 2001. Antimicrobial peptides: Properties and applicability. Journal of Biological Chemistry. **382:**597-619.

8. **Zasloff M.** 2002. Antimicrobial peptides of multicellular organisms. Nature. **415:**389-395.

9. **Andreu D, Rivas L.** 1998. Animal antimicrobial peptides: An overview. Journal of Peptide Science. **47:**415-433.

10. **Cociancich S, Ghazi A, Hetru C, Hoffmann JA, Letellier L.** 1993. Insect defensin, an inducible antibacterial peptide, forms voltage-dependent channels in *Micrococcus luteus*. Journal of Biological Chemistry. **268:**19239-19245.

11. **Bowman SM, Free SJ.** 2006. The structure and synthesis of the fungal cell wall. BioEssays. **28:**799-808.

12. **Spathelf BM, Rautenbach M.** 2009. Anti-listerial activity and structure–activity relationships of the six major tyrocidines, cyclic decapeptides from *Bacillus aneurinolyticus*. Bioorganic & Medicinal Chemistry. **17:**5541-5548.

13. **Rautenbach M, Vlok NM, Stander M, Hoppe HC.** 2007. Inhibition of malaria parasite blood stages by tyrocidines, membrane-active cyclic peptide antibiotics from *Bacillus brevis*. Biochimica et Biophysica Acta. **1768:**1488-1497.

14. **Leussa AN-N.** 2013. Characterisation of small cyclic peptides with antimalarial and antilisterial activity, Department of Biochemistry, University of Stellenbosch, PhD Thesis in progress, completion March 2014. Personal communication.

15. **Meincken M, Holroyd DL, Rautenbach M.** 2005. Atomic force microscopy study of the effect of antimicrobial peptides on the cell envelope of *Escherichia coli*. Antimicrobial Agents and Chemotherapy. **49:**4085-4092.

16. **Marcos JF, Gandía M.** 2009. Antimicrobial peptides: to membranes and beyond. Expert Opinion on Drug Discovery. **4:**659-671.

17. **Nesher I, Minz A, Kokkelink L, Tudzynski P, Sharon A.** 2011. Regulation of pathogenic spore germination by CgRac1 in the fungal plant pathogen *Colletotrichum gloeosporioides*. Eukaryotic Cell. **10:**1122-1130.

18. **Boyce KJ, Chang H, D'Souza CA, Kronstad JW.** 2005. An *Ustilago maydis* septin is required for filamentous growth in culture and for full symptom development on maize. Eukaryotic Cell. **4:**2044-2056.

19. **Fillinger S, Chaveroche M-K, Shimizu K, Keller N, D'Enfert C.** 2002. cAMP and Ras signalling independently control spore germination in the filamentous fungus *Aspergillus nidulans*. Molecular Microbiology. **44:**1001-1016.

20. **Harris SD.** 2008. Branching of fungal hyphae: regulation, mechanisms and comparison with other branching systems. Mycologia. **100:**823-832.

21. **Kaiserer L, Oberparleiter C, Weiler-Görz R, Burgstaller W, Leiter E, Marx F.** 2003. Characterization of the *Penicillium chrysogenum* antifungal protein PAF. Archives of Microbiology. **180:**204-210.

22. **Jackson SL, Heath IB.** 1993. Roles of calcium ions in hyphal tip growth. Microbiological Reviews. **57:**367-382.

23. **Dicker JW, Turian G.** 1990. Calcium deficiencies and apical hyperbranching in wild-type and the "frost" and "spray" morphological mutants of *Neurospora crassa*. Journal of General Microbiology. **136:**1413-1420.

24. **Spelbrink RG, Dilmac N, Allen A, Smith TJ, Shah DM, Hockerman GH.** 2004. Differential antifungal and calcium channel-blocking activity among structurally related plant defensins. Plant Physiology. **135:**2055-2067.

25. **Binder U, Oberparleiter C, Meyer V, Marx F.** 2010. The antifungal protein PAF interferes with PKC/MPK and cAMP/PKA signalling of *Aspergillus nidulans*. Molecular Microbiology. **75:**294-307.

26. **Bink A, Vandenbosch D, Coenye T, Nelis H, Cammue BPA, Thevissen K.** 2011. Superoxide dismutases are involved in *Candida albicans* biofilm persistence against miconazole. Antimicrobial Agents and Chemotherapy. **55:**4033-4037.

27. **Aerts AM, François IEJA, Meert EMK, Li Q-t, Cammue BPA, Thevissen K.** 2007. The antifungal activity of RsAFP2, a plant defensin from *Raphanus sativus*, involves the induction of reactive oxygen species in *Candida albicans*. Journal of Molecular Microbiology and Biotechnology. **13:**243-247.

28. **François IE, Thevissen K, Pellens K, Meert EM, Heeres J, Freyne E, Coesemans E, Viellevoye M, Deroose F, Martinez Gonzalez S, Pastor J, Corens D, Meerpoel L, Borgers M, Ausma J, Dispersyn GD, Cammue BP.** 2009. Design and synthesis of a series of piperazine-1-carboxamidine derivatives with antifungal activity resulting from accumulation of endogenous reactive oxygen species. ChemMedChem. **4:**1714-1721.